# Synthesis and Chemistry of Novel Ambiphilic Phosphorus Based Ligands and Complexes

A thesis submitted to the University of Sussex for the degree of Doctor of Philosophy

August 2016
Victoria Greenacre
Department of Chemistry

## Declaration

I hereby declare that this thesis has not been and will not be, submitted in whole or in part to another University for the award of any other degree.

Signed …….....

Victoria Greenacre

## Acknowledgments

Firstly, the important thanks should go to my supervisor Dr. Ian Crossley - for his continuing support and for remaining seemingly omniscient, despite the lending of many brain cells.

Thanks are also due to Mark Roe for crystal magic, to Ali Abdul-Sada for MassSpec superpowers, to Iain Day, the master of NMR and to Mick Henry - the provider of both chemicals and glassware.

Thank you to the doctors of Lab14 who have come before, especially the ladies of the lab (Drs Rachel Kahan, Jessica Frey, Amy Saunders and Nikki Trathen) for leading the way.

Thank you to all the MChem's for their distraction, enthusiasm and innocence, especially to Pete Winrow - my washing-up fairy. More importantly, to the current inhabitants of Lab14 for their friendship; Dr Nikos Tsoureas, for his experience and wisdom, Chris Inman and Matt Molloy for their inexperience and related hilarity, Dr Samantha Furfari for her timely arrival and calming presence and to Matt Leech for all of the above and even more.

Finally, thank you to those who stayed friends through the years, to Gavin and Jess for providing the non-inorganic viewpoints, and to the extended nanite family, especially to JK, Giac and Tom for the distractions, support and friendship through the blood, sweat, scars and tears...

And to my family - its ok, you can stop reading now - I won't think any less of you. I promise!

## Summary

The chemistry of ambiphilic molecules, such as phosphine-boranes, has experienced a resurgence in interest, in part due to the emergence of Frustrated Lewis Pairs (FLPs).

With a 2-atom bridge to separate the phosphine and borane units, the unsaturated, 1-borata-4-phosphoniacyclobut-2-enes $R_2BC(R)=C(Ph)PPh_2$ have been investigated. Their solid state data has been complemented by DFT studies, with a view towards controlling the geometry around a metal centre in order to position the Lewis acid unit over the Lewis basic metal centre without forming an adduct.

The reactivity of the saturated and unsaturated phosphine-boranes has been also probed with a series of Lewis-basic metals. It was found that while the saturated systems readily coordinate to group 9 and 10 metals, the phosphorus-boron bond of the unsaturated systems remains too strong for coordination. Therefore, attempts to disrupt the strong P-B bond were made using pyridine.

Phosphaalkynes of the type $RMe_2SiC{\equiv}P$ have been prepared from $RSiMe_2CH_2Cl$, by converting the '$CH_2Cl$' unit into '$CH_2PCl_2$', before dehydrochlorination. The ruthenaphosphaalkenyls $[Ru\{P=CH(SiMe_2R)\}Cl(CO)(PPh_3)_2]$ are then prepared in high yield from the corresponding phosphaalkynes ($P{\equiv}CSiMe_2R$, R = Ph, tolyl, $^{n}$Bu, *p*-$CF_3$-$C_6H_4$) through hydroruthenation with $[RuHCl(CO)(PPh_3)_3]$. The first solid-state structural data of these ruthenaphosphaalkenyls is described and complemented by DFT studies of the precedent $[Ru(P=CH^{t}Bu)Cl(CO)(PPh_3)_2)]$ alongside silyl based systems, allowing the visualisation of molecular orbitals and calculated NMR data.

The silyl systems mimic the previously reported propensity toward electrophilic addition shown by $Ru\{P=CH(^{t}Bu)\}Cl(CO)(PPh_3)_2]$. However, the presence of the silyl group also appears to modify the reactivity compared to that previously published for $[Ru\{P=CH(^{t}Bu)\}Cl(CO)(PPh_3)_2]$; demonstrated by the addition of HCl to form the saturated P-C linkage shown in $[RuCl_2(CO)(PPh_3)_2\{P(HCl)CH_2SiMe_2R\}]$. The ruthenaphosphaalkenes also exhibit reactivity with nucleophiles (pyrazolates) to form novel bridging pyrazolyl $\eta^2$–phosphaalkenic compounds of the type $[Ru(CO)\{\kappa^3\text{-}N,C,P\text{-}P(Pz^{R',R''})CH(SiMe_2R)\}(PPh_3)_2]$, building on earlier work within the group.

## List of abbreviations

| | |
|---|---|
| δ | Chemical shift |
| 9-BBN | 9-Borabicyclo[3.3.1]nonane ($C_{16}H_{30}B_2$) |
| Ad | Adamantyl ($C_{10}H_{15}$) |
| AgOTf | Silver triflate ($AgCF_3SO_3$) |
| AIM | Atoms in Molecules |
| Ar | Aryl |
| br | broad |
| Bu | Butyl ($C_4H_9$) |
| $^t$Bu | Tertiary butyl ($C_4H_9$) |
| COD | 1,5-Cyclooctadiene ($C_8H_{12}$) |
| COT | 1,3,5,7-cyclooctatetraene ($C_8H_8$) |
| Cp | Cyclopentadienyl ($C_5H_5$) |
| Cp* | $(1,2,3,4,5\text{-}Me)_5$-Cyclopentadientyl ($C_{10}H_{15}$) |
| Cy | Cyclohexane ($C_6H_{12}$) |
| DABCO | 1,4-Diazabicyclo[2.2.2]octane ($C_6H_{12}N_2$) |
| DBU | 1,8-Diazabicyclo[5.4.0]undec-7-ene ($C_9H_{16}N_2$) |
| DCM | Dichloromethane ($CH_2Cl_2$) |
| dcpp | 1,3-Bis (dicyclohexylphosphino)propane ($Cy_2P(CH_2)_3PCy_2$) |
| depe | 1,2-bis(diethylphosphino)ethane ($Et_2PCH_2CH_2PEt_2$) |
| DFT | Density Functional Theory |
| dme | 1,2-Dimethoxyethane ($C_4H_{10}O_2$) |

| | |
|---|---|
| DMF | Dimethylformamide ($(CH_3)_2NC(O)H$) |
| dmpe | 1,2-Bis(dimethylphosphino)ethane ($Me_2PCH_2CH_2PMe_2$) |
| DMSO | Dimethyl sulfoxide ($(CH_3)_2SO$) |
| dppe | 1,2-Bis(diphenylphosphino)ethane ($Ph_2PCH_2CH_2PPh_2$) |
| EI | Electron Impact |
| Elem. Anal. | Elemental Analysis |
| ESI-MS | Electrospray Ionization Mass Spectrometry |
| Et | Ethyl ($C_2H_5$) |
| Fc | Ferrocenyl ($\eta^5$-$C_5H_5$)Fe($\eta^5$-$C_5H_4$) |
| FLP | Frustrated Lewis Pair |
| Fu | Furyl ($C_4H_3O$) |
| IR | Infrared |
| HBcat | Catecholborane ($C_6H_5BO_2$) |
| HMBC | Heteronuclear Multiple Bond Correlation |
| HOMO | Highest Occupied Molecular Orbital |
| HSQC | Heteronuclear Single Quantum Coherence |
| Hz | Hertz |
| K(Bm) | Dihydrobis(methimazolyl)borate [$H_2B(mt)_2$] |
| K(Tp*) | Hydrotris(3,5-dimethylpyrazole)borate $[HB(C_5N_2H_{11})_3]^-$ $K^+$ |
| K(Tp) | Hydrotrispyrazolylborate $K^+[HB(C_3N_2H_3)_3]^-$ |
| LUMO | Lowest Unoccupied Molecular Orbital |
| lut | 2,6-Lutidine |
| M | Molar |

| | |
|---|---|
| m | Multiplet |
| mbar | Millibar |
| Me | Methyl ($CH_3$) |
| Mes | 1,3,5-Trimethylbenzene ($C_6H_3Me_3$) |
| Mes* | 2,4,6-Tri-*tert*-butyl phenyl ($C_6H_3(^tBu)_3$) |
| mol | Moles |
| MS | Mass Spectrometry |
| mt | Methimazole |
| NBO | Natural Bond Orbital |
| NMR | Nuclear Magnetic Resonance |
| Np | Neopentyl |
| OTf | Trifluoromethanesulfonate |
| PBB | Tris(2,2‘,2‘‘-nonafluorobiphenyl)borane |
| Ph | Phenyl ($C_6H_5$) |
| $PPh_3$ | Triphenylphosphine ($P(C_6H_5)_3$) |
| ppm | Parts per million |
| Pz | Pyrazolyl |
| Pz* | 3,5-Dimethylpyrazolyl |
| $Pz^{(CF3)}$ | 3-(Trifluoromethyl)pyrazolyl |
| $Pz^{(Me,CF3)}$ | 3-Methyl-5-(trifluoromethyl)pyrazolyl |
| $Pz^{(CF3)2}$ | 3,5-Bis(trifluoromethyl)pyrazolyl |
| $Pz^{(tBu)}$ | 3-*Tert*-butyl-1H-pyrazolyl |
| RT | Room Temperature |

| | |
|---|---|
| $Sia_2BH$ | Disiamylborane ($C_{10}H_{23}B$) |
| TBAF | Tetra-*n*-butylammonium fluoride ($(C_4H_9)_4NF$) |
| TBAT | $[NBu_4][Ph_3SiF_2]$ |
| THF | Tetrahydrofuran ($C_4H_8O$) |
| Tip | 2,4,6-Triisopropylphenyl |
| Tol | Toluene ($CH_3Ph$) |
| TMP | 2,2,6,6-Tetramethylpiperidine |
| Xyl | 2,6-Dimethylphenyl ($(CH_3)_2C_6H_3$) |

## Compound Numbers

1. $Bu_2B(Bu)C=C(Ph)PPh_2$
2. $Ph_2B(Ph)C=C(Ph)PPh_2$
3. $Et_2B(Et)C=C(Ph)PPh_2$
4. $Ph_2PC{\equiv}CPh$
5. $Bu_2B(Bu)C=C(Ph)P^iPr_2$
6. $Et_2B(Et)C=C(Ph)P^iPr_2$
7. $^tBu_2PC{\equiv}CPh$
8. $^iPr_2PC{\equiv}CPh$
9. $Ph_2PC{\equiv}CSiMe_3$
10. $Me_2B(Me)C=C(Me)PMe_2$
11. $Bu_2B(Bu)C=C(SiMe_3)PPh_2$
12. $(C_6F_5)_2B(C_6F_5)C=C(Ph)PPh_2$
13. $^iPr_3SiC{\equiv}CCH_2Cl$
14. $^nPr_3SiC{\equiv}CCH_2Cl$
15. $^nBu_3SiC{\equiv}CCH_2Cl$
16. $Me_2PhSiC{\equiv}CCH_2Cl$
17. $Me_2PhSiC{\equiv}CCH_2PPh_2$
18. $Ph_2PCH_2CH_2BBN$
19. $Ph_2PCH_2CH_2CH_2BBN$
20. $Fu_2PC(H)=CH_2$
21. $Fu_2PCH_2CH_2BBN$
22. $[Rh(CO)Cl(Fu_2PCH_2CH_2BBN)_2]$
23. $[^tBu(Ph)P]_2$
24. $[Rh(CO)Cl(Ph_2PCH_2CH_2BBN)_2]$
25. $[Rh(CO)Cl(Ph_2PCH_2CH_2CH_2BBN)_2]$
26. *cis*-$[PtCl_2(Fu_2PCH_2CH_2BBN)_2]$
27. *cis*/*trans*-$[PdCl_2(Fu_2PCH_2CH_2BBN)_2]$
28. $[(C_8H_{12})RhCl(Ph_2PCH_2CH_2CH_2BBN)]$
29. $[(C_8H_{12})RhCl(Ph_2PCH_2CH_2BBN)]$
30. $[(C_8H_{12})RhCl(Fu_2PCH_2CH_2BBN)]$
31. $[Cp^*IrCl_2(Fu_2PCH_2CH_2BBN)]$

32. $[PtCl_2(Ph_2PCH_2CH_2BBN)_2]$
33. $^{t}BuC{\equiv}P$
34. $[RuCl(CO)(PPh_3)_2(P{=}CH^{t}Bu)]$
35. $[RuCl_2(CO)(PPh_3)_2\{PH{=}CH^{t}Bu\})]$
36. $Me_3SiC{\equiv}P$
37. $Me_2PhSiC{\equiv}P$
38. $[RuCl(CO)(PPh_3)_2\{P{=}CH(SiMe_3)\}]$
39. $[RuCl(CO)(PPh_3)_2\{P{=}CH(SiPhMe_2)\}]$
40. $[Ru(CO)\{\kappa^3\text{-}N,C,P\text{-}P(Pz)CH(SiMe_3)\}(PPh_3)_2]$
41. $[Ru(CO)\{\kappa^3\text{-}N,C,P\text{-}P(Pz^*)CH(SiMe_3)\}(PPh_3)_2]$
42. $^{i}PrMe_2SiCH_2Cl$
43. *p*-$tolylMe_2SiCH_2Cl$
44. $(C_6F_5)Me_2SiCH_2Cl$
45. *p*-$CF_3\text{-}C_6H_4Me_2SiCH_2Cl$
46. $2,5\text{-}((CF_3)_2C_6H_3)Me_2SiCH_2Cl$
47. $PhC{\equiv}CSi(Me_2)CH_2Cl$
48. $Me_3SiC{\equiv}CSi(Me_2)CH_2Cl$
49. $^{n}BuMe_2SiCH_2Cl$
50. $Me_3SiCH_2PCl_2$
51. $PhMe_2SiCH_2Cl$
52. *p*-$tolylMe_2SiCH_2Cl$
53. *p*-$CF_3\text{-}C_6H_4SiMe_2CH_2PCl_2$
54. $^{n}BuMe_2SiCH_2PCl_2$
55. *p*-$tolylMe_2SiC{\equiv}P$
56. *p*-$CF_3\text{-}C_6H_4Me_2SiC{\equiv}P$
57. $^{n}BuMe_2SiC{\equiv}P$
58. $[RuHCl(CO)(PPh_3)_3]$
59. $[RuCl(CO)(PPh_3)_2(P{=}CHSiMe_2p\text{-tolyl})]$
60. $[RuCl(CO)(PPh_3)_2(P{=}CHSiMe_2p\text{-}CF_3\text{-}C_6H_4)]$
61. $[RuCl(CO)(PPh_3)_2(P{=}CHSiMe_2{}^{n}Bu)]$
62. $[Ru(CO)\{\kappa^3\text{-}N,C,P\text{-}P(Pz^*)CH^{t}Bu\}(PPh_3)_2]$
63. $[Ru(CO)\{\kappa^3\text{-}N,C,P\text{-}P(Pz^*)CH(SiMe_2Ph)\}(PPh_3)_2]$
64. $[Ru(CO)\{\kappa^3\text{-}N,C,P\text{-}P(Pz^*)CH(SiMe_2p\text{-tolyl})\}(PPh_3)_2]$
65. $[Ru(CO)\{\kappa^3\text{-}N,C,P\text{-}P(Pz^*)CH(SiMe_2p\text{-}CF_3\text{-}C_6H_4)\}(PPh_3)_2]$
66. $[Ru(CO)\{\kappa^3\text{-}N,C,P\text{-}P(Pz^*)CH(SiMe_2{}^{n}Bu)\}(PPh_3)_2]$

67. [Ru(CO){κ$^3$-N,C,P-P(Pz$^{tBu}$)CH(SiMe$_3$)}(PPh$_3$)$_2$]
68. [Ru(CO){κ$^3$-N,C,P-P(Pz$^{CF3}$)CH(SiMe$_2$*p*-tolyl)}(PPh$_3$)$_2$]
69. [Ru(CO){κ$^3$-N,C,P-P(Pz$^{CF3}$)CH(SiMe$_2$*p*-CF$_3$-C$_6$H$_4$)}(PPh$_3$)$_2$]
70. [Ru(CO){κ$^3$-N,C,P-P(Pz$^{CF3}$)CH(SiMe$_2$$^n$Bu)}(PPh$_3$)$_2$]
71. [Ru(CO){κ$^3$-N,C,P-P(Pz$^{Me,CF3}$)CH(SiMe$_2$*p*-tolyl)}(PPh$_3$)$_2$]
72. [Ru(CO){κ$^3$-N,C,P-P(Pz$^{Me,CF3}$)CH(SiMe$_2$*p*-CF$_3$-C$_6$H$_4$)}(PPh$_3$)$_2$]
73. [Ru(CO){κ$^3$-N,C,P-P(Pz$^{Me,CF3}$)CH(SiMe$_2$$^n$Bu)}(PPh$_3$)$_2$]
74. [Ru(CO){κ$^3$-N,C,P-P(Pz$^{Ph}$)CH(SiMe$_3$)}(PPh$_3$)$_2$]
75. [Ru(CO){κ$^3$-N,C,P-P(Pz$^{Ph}$)CH(SiMe$_2$Ph)}(PPh$_3$)$_2$]
76. [Ru(CO){κ$^3$-N,C,P-P(Pz$^{Ph}$)CH(SiMe$_2$*p*-tolyl)}(PPh$_3$)$_2$]
77. [Ru(CO){κ$^3$-N,C,P-P(Pz$^{Ph}$)CH(SiMe$_2$*p*-CF$_3$-C$_6$H$_4$)}(PPh$_3$)$_2$]
78. [Ru(CO){κ$^3$-N,C,P-P(Pz$^{Ph}$)CH(SiMe$_2$$^n$Bu)}(PPh$_3$)$_2$]
79. Result of addition of LiPz$^{(CF3)2}$ to **61** [RuCl(CO)(PPh$_3$)$_2$(P=CHSiMe$_2$$^n$Bu)]
80. [RuHCl(CO)(PPh$_3$)$_2$(PMe$_3$)]
81. [RuCl(CO)(HC=CHPh)(PPh$_3$)$_2$]
82. [RuCl(CO)H(HPz*)(PPh$_3$)$_2$]
83. [RuCl(CO) H(HPz)(PPh$_3$)$_2$]
84. [RuCl(CO)(HC=CH$^t$Bu)(PPh$_3$)$_2$]
85. [RuCl(CO)(HC=CHSiMe$_3$)(PPh$_3$)$_2$]
86. [RuCl(CO)(HC=CSiMe$_3$)(PPh$_3$)$_2$(HPz*)]
87. [RuCl(CO)(HC=CSiMe$_3$)(PPh$_3$)$_2$(HPz)]
88. [RuCl$_2$(P(H)ClCH$_2$SiMe$_3$)(CO)(PPh$_3$)$_2$]
89. [RuCl$_2$(P(H)ClCH$_2$SiMe$_2$Ph)(CO)(PPh$_3$)$_2$]
90. [RuCl$_2$(P(H)ClCH$_2$SiMe$_2$*p*-tolyl)(CO)(PPh$_3$)$_2$]
91. [RuCl$_2$(P(H)ClCH$_2$SiMe$_2$*p*-CF$_3$-C$_6$H$_4$)(CO)(PPh$_3$)$_2$]
92. [RuCl$_2$(P(H)ClCH$_2$SiMe$_2$$^n$Bu)(CO)(PPh$_3$)$_2$]
93. [RuCl(P(H)FCH$_2$$^t$Bu)(CNXyl)(CO)(PPh$_3$)$_2$]
94. [RuCl$_2$(P(H)ClCH$_2$$^t$Bu)(CO)(PPh$_3$)$_2$]

# Contents

# 1. Introduction

Ambiphilic molecules are compounds that can act as a nucleophile as well as an electrophile. Ambiphilic ligands combine donor and acceptor coordination sites and their use is widespread while their study represents a very active field in main-group chemistry.[1] **Figure 1.1** shows four possible coordination modes depending on the way the Lewis acid moiety interacts with the coordination sphere of the transition metal. The incorporation of Lewis acid moieties in ligands for transition metals has been extensively studied, and these ambiphilic ligands have been described as possessing rich and unusual coordination properties. The reactivity of complexes deriving from ambiphilic ligands has been recently reviewed by Bouhadir and Bourissou, who describe how the presence of a Lewis acid moiety in the first coordination sphere of transition metals opens new reactivity paths, both at the stoichiometric and catalytic level.[1]

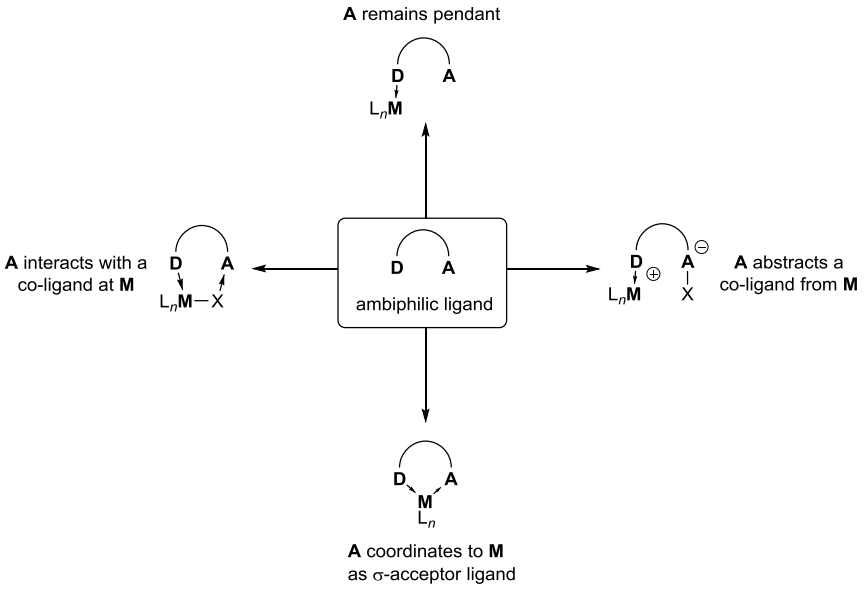


**Figure 1.1**: Schematic representation of the four coordination modes of ambiphilic ligands (**D** = electron donor, **A** = electron acceptor, Lewis acid, **M** = metal).

Ambiphilic ligands with the ability to activate both the metal centre and a substrate molecule in a cooperative manner have found application in catalysis. For example, Labinger and Miller reported the use of the phosphorus containing ambiphilic ligand $Ph_2PN^tBuAlR$ (R = Et, Me), with $[HMn(CO)_5]$ to install C-H bonds.[2] More recently the ambiphilic ligand $Me_2PCH_2AlMe_2$[3] has been employed as a co-catalyst in the nickel(II)-catalysed dehydrogenative oligimiseration of

$PhSiH_3$,[4] and has been shown to coordinate to [Cp*$RhMe_2$(dmso)] (dmso = dimethylsulfoxide) to afford [Cp*$RhMe_2$($PMe_2CH_2AlMe_2$·dmso)].[5]

The factors controlling the unique ability of these ambiphilic molecules to play key roles using metal-ligand cooperation or to modulate the reactivity of the metal center[6] and therefore the properties of transition metal complexes, have been summarised in several recent reviews,[7,8] alongside the different coordination modes of polyfunctional phosphine-borane ligands.[9]

This work is concerned with two distinct classes of ambiphilic molecules - frustrated Lewis pairs and organometallic phosphacarbons - the relevant background to which is summarised in the following sections.

## 1.1 Introduction to Frustrated Lewis Pairs

In 1923 Gilbert Lewis, described 'Lewis acids' as electron pair acceptors and 'Lewis bases' as electron pair donors.[10] Lewis acids have low-lying LUMOs which can interact with the HOMO of a Lewis base; the combination of these results in neutralisation, and the formation of a Lewis adduct (or Lewis pair) (**Figure 1.2**). A common example of this type of interaction is $H_3N \rightarrow BH_3$.

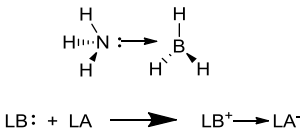


**Figure 1.2**: Typical Lewis adduct formation.

While the formation of adducts is prevalent, there are instances where this does not occur. Brown documented the first example of this phenomenon in 1942, where it was found that lutidine and $BF_3$ formed a Lewis adduct, but lutidine and $BMe_3$ did not. This was attributed to the increased steric bulk of the methyl groups on the borane, but was not investigated further (**Scheme 1.1a**).[11,12] In 1950, Wittig reported that $Ph_3CNa$ reacting with $BPh_3$·thf did not result in the displacement of tetrahydrofuran by the trityl anion, but rather the trityl anion effected the opening of tetrahydrofuran (**Scheme 1.1b**), affording the anion $[Ph_3C(CH_2)_4OBPh_3]^-$.[13] Similarly, Wittig and Benz demonstrated that *o*-fluorobromobenzene reacts with magnesium to generate a benzyne intermediate, which then reacts with $BPh_3$ and $PPh_3$ to from the *o*-phenylene-bridged phosphonium-borate as shown in **Scheme 1.1c**.[14] Furthermore, Tochtermann investigated a series of bulky Lewis pairs (such as $Ph_3CNa/BPh_3$) which do not form adducts. However, in the presence of a suitable substrate, $Ph_3CNa$ has been shown to form a new "organosodium compound" which can then be trapped out using $BPh_3$ or $AlPh_3$ (**Scheme 1.1d**).[15] He described such systems, that didn't form adducts, using the German phrase "antagonistisches Paare".

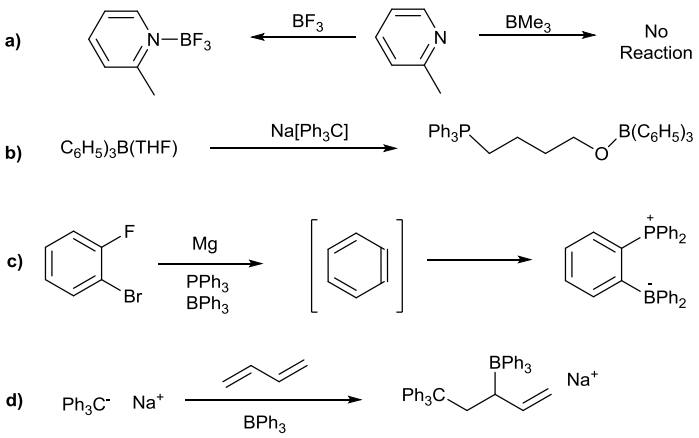


**Scheme 1.1**: Early systems which do not form the expected Lewis adducts.[11–15]

In 1998, Erker investigated the combination of the Lewis acid $B(C_6F_5)_3$ and several sterically encumbered phosphorus based ylides and found that $Ph_3P$=CHPh and $B(C_6F_5)_3$ do form the adduct $Ph_3P^+$-CHPh-$B(C_6F_5)_3^-$ at room temperature. However, this was shown to undergo thermal rearrangement to yield the zwitterionic phosphonium borate salt, $Ph_3PCHPh(C_6F_4)BF(C_6F_5)_2$ (**Scheme 1.2**).[16]

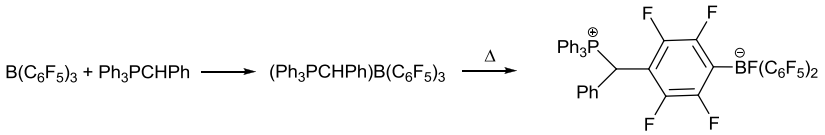


**Scheme 1.2**: Non-classical Acid-Base reaction of $B(C_6F_5)_3$ with an ylide.[16]

The curious reactions illustrated in **Scheme 1.1** and **Scheme 1.2**, were suggested to result from the steric bulk within the Lewis pair. More recently Stephan reported the combination of $B(C_6F_5)_3$ and $Mes_2PH$ (Mes = 1,3,5-trimethylbenzene), followed by the addition of $Me_2SiClH$. This resulted in the formation of the phosphonium-borate $Mes_2HP^{\delta+}$-$C_6F_4$-$^{\delta-}BH(C_6F_5)_2$, which is the first example of a main group compound that allows for the reversible activation of $H_2$. Although this activation only occurred in small concentrations,[17] it caused a resurgence of interest in this odd behaviour. Stephan described this lack of adduct formation as a 'frustrated Lewis pair' (FLP). This was defined as a system where sterically hindered Lewis donors and acceptors are combined, but their steric bulk precludes formation of Lewis acid–base adducts. These Lewis acids and bases also need to retain appreciable acidity and basicity, and this unquenched reactivity of such systems, can then be utilised to effect reactivity.

### 1.1.1 Commonly used boranes - $B(C_6F_5)_3$ and $HB(C_6F_5)_2$

FLPs typically involve N/B or P/B frustration; the archetypal boranes for most known FLP systems are $B(C_6F_5)_3$ and $HB(C_6F_5)_2$ due to their strong Lewis acidity and steric bulk.[18–20]

Tris(pentafluorophenyl)borane was first prepared in 1963 by Massey and co-workers, and was shown to form strong adducts with a variety of Lewis bases.[21] The Lewis acidity of $B(C_6F_5)$ was later measured and was found to lie between those of $BF_3$ and $BCl_3$.[22] However, $B(C_6F_5)_3$ is advantageous in that it is thermally stable, with good resistance to hydrolysis, and is therefore easier to handle. It has been referred to as "the ideal boron-based Lewis acid" by Piers and Chivers.[23] It provides activation of catalysts for many synthetic organic transformations and olefin polymerisation. The related borane, $HB(C_6F_5)_2$ (known as Piers' borane) was synthesised by the group of Piers in 1995,[24] and quickly became a standard hydroborating agent[23] as it is just as selective as previously used secondary boranes (9-BBN[25] or $Sia_2BH$[26]) (**Figure 1.3**), but is more reactive, allowing for higher reaction rates.[27]

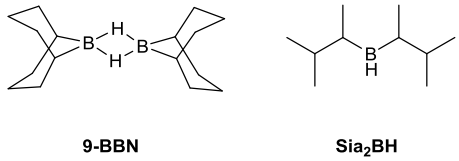


**Figure 1.3**: Secondary boranes - 9-BBN dimer and Disiamylborane ($Sia_2BH$).

Hydroboration is an established method for the functionalisation of C≡C and C=C bonds. More recently, the chemistry of the resulting boranes is becoming of increasing interest. For example, the hydroboration of the vinyl phosphine, $Mes_2PCH_2{=}CH_2$ and the alkynes, $^tBu_2PC{\equiv}CR$ (R = Me, Ph) and $Mes_2PC{\equiv}CMe$ results in intramolecular FLPs that have been shown to activate $H_2$ in analogous fashion to the FLP's featured in Stephan's seminal report (**Scheme 1.3**).[28]

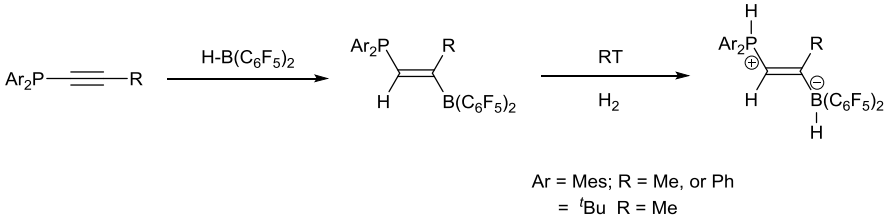


**Scheme 1.3**: Intramolecular FLPs have been shown to activate $H_2$.[28]

## 1.1.2 Alternative boranes used in FLPs

The boranes $B(C_6F_5)_3$ and $HB(C_6F_5)_2$ are by no means the only ones known to form FLPs. The borane $B(p\text{-}C_6F_4H)_3$, is prepared in a similar fashion to $B(C_6F_5)_3$ (**Scheme 1.4**), but still effects $H_2$ activation when combined with $Mes_3P$, $^tBu_3P$ and $(2\text{-}MeC_6H_4)_3P$, despite being 5% less acidic than $B(C_6F_5)_3$. In particular, the combination of $B(p\text{-}C_6F_4H)_3$ and $(2\text{-}MeC_6H_4)_3P$ activates $H_2$ to form $[(o\text{-}C_6H_4Me)_3PH][HB(p\text{-}C_6F_4H)_3$, the process being reversible at 25 ˚C under static vacuum (**Scheme 1.5**).[29]

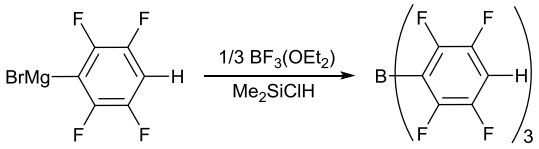


**Scheme 1.4**: Synthesis of $B(p\text{-}C_6F_4H)_3$.[29]

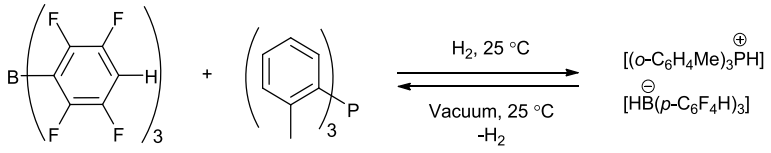


**Scheme 1.5**: Reversible $H_2$ activation using $B(p\text{-}C_6F_4H)_3$.

Chen *et al.* have produced tris(2,2‘,2‘‘-nonafluorobiphenyl)borane (PBB), which is marginally more acidic than $B(C_6F_5)_3$. They assert the enhanced acidity to be due to the larger inductive withdrawing effect of $C_6F_5$ *vs* F, in the *ortho* position.[30] PBB was also investigated by O’Hare and co-workers for FLP-type behaviour with a series of nitrogen bases (**Scheme 1.6**). Equimolar amounts of 2,2,6,6-tetramethylpiperidine (TMP), 1,4-diazobicyclo[2.2.2]octane (DABCO) and 2,6-lutidine (lut) with PBB in toluene were monitored by $^1H$, $^{19}F$ and $^{11}B$ NMR spectroscopy. This revealed a lack of adduct formation, exhibiting only the characteristic resonances associated with the free components. It was thought that the increased bulk from the PBB could compensate for the reduced bulk of the nitrogen bases and still lead to frustrated reactivity. After the addition of 1 atm of $H_2$ to the systems at room temperature, $^{19}F$ NMR data showed an immediate reaction, the observation of nine additional $^{19}F$ resonances suggesting the formation of $[HPBB]^-$. From this, the formation of the corresponding salts $[2,2,6,6\text{-}Me_4C_5H_6NH_2][HB(C_{12}F_9)_3]$ and $[N(C_2H_4)_3NH][HB(C_{12}F_9)_3]$, and lutidinium borate [2,6-

$Me_2C_5H_3NH][HB(C_{12}F_9)_3]$ was concluded. However, none of the systems shown in **Scheme 1.6** activated $H_2$ in high yields, which was attributed to the greater bulk of PBB relative to $B(C_6F_5)_3$.[31] This implies that while significant steric bulk is required to generate an active FLP, too much bulk can impede activity.

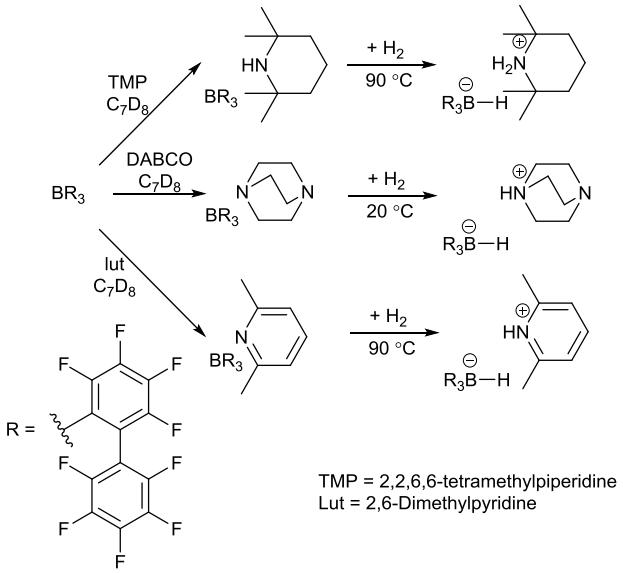


**Scheme 1.6**: Formation of new boron-nitrogen based FLPs, PBB/TMP, PBB/DABCO and PBB/lut.[31]

## 1.1.3 Aluminium based Acids

Aluminium is inherently Lewis acidic and dialkylaluminium groups are ideal for the generation of active FLP's. Al/P based FLPs are often made through hydroalumination of alkynylphosphines with dialkylaluminium hydrides, as exemplified in **Scheme 1.7**. $Mes_2PC{\equiv}C^tBu$ and $Mes_2PC{\equiv}CPh$ were treated with $[AlH(CH_2{}^tBu)_2]$ and $[AlH(^tBu)_2]$ respectively, and the structures of the resulting adducts were confirmed by X-ray diffraction studies; these show long Al-P separations (3.153 and 3.287 Å, respectively) that prove a lack of any Al-P bonding interaction. The unquenched reactivity of the *trans*-isomer ($Mes_2P(H)C{=}C(R)AlR'_2$) was also shown to activate terminal alkynes, such as $PhC{\equiv}CH$ and $^tBuC{\equiv}CH$, and to reversibly bind $CO_2$. Appelt *et al.* bubbled $CO_2$ through a toluene solution of $[Mes_2PC(Al^tBu_2){=}C(H)Ph]$ for 30 seconds at ambient temperature to form a $CO_2$ adduct (shown in **Scheme 1.7**) in 74% yield. Heating this adduct in the solid state to 135 ˚C for 2 minutes under vacuum removed the $CO_2$, regenerating the FLP. Initial results from the group show that $[Mes_2P(H)C{=}C(R)AlR'_2]$ is unreactive towards $H_2$. The small calculated endothermicity of the FLP ($\Delta E$ = 5.9 kcal $mol^{-1}$) can

be used to suggest that enhancing the acidity and basicity of the aluminium hydrides and phosphine respectively could lead to $H_2$ activation.[32]

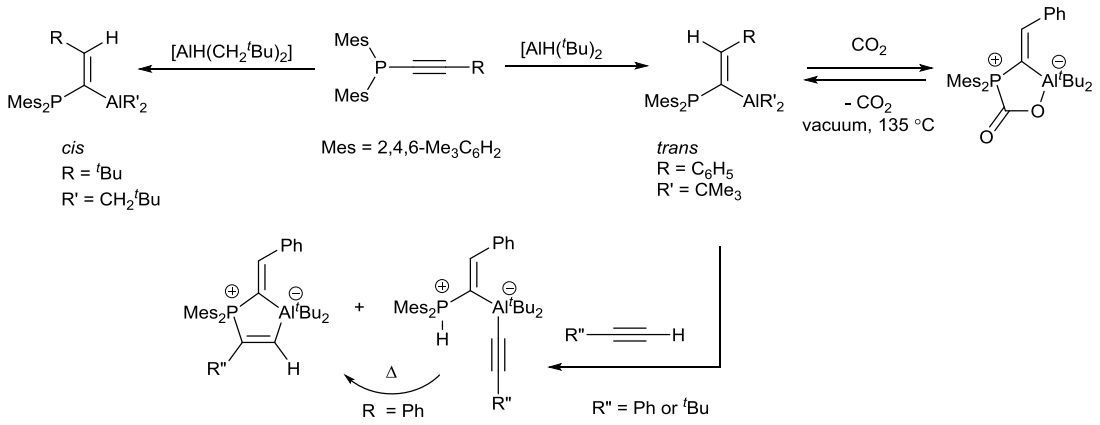


**Scheme 1.7**: Hydroalumination of $Mes_2PC{\equiv}CR$ can form the *cis*, or *trans* isomer (dependant on R groups), the *trans* product shown effects activation of terminal alkynes and reversible activation of $CO_2$. Note: R"=$^t$Bu does not rearrange into the cyclic product because of steric crowding in the transition state.[32]

## 1.1.4 Applications of FLPs

Traditionally, transition-metal complexes are common catalysts for a large number of organic reactions and transformations, used in both industry and academic laboratories; frustrated Lewis pairs are being investigated as greener and more cost-effective alternatives to these. The activation of small molecules, notably $H_2$, $H_2O$ and $CO_2$ has been achieved using main-group FLPs, this area has been comprehensively reviewed by Stephan and Erker.[18,33,34]

### 1.1.4.1 $H_2$ Activation

Hydrogenation reactions are a particularly important class of reaction for forming plastics, specialty chemicals and pharmaceuticals, which are commonly mediated by transition metal complexes.[35,36] The inherent toxicity and cost of these complexes make such industrially important reactions of both environmental and economic concern. Investigations towards finding a suitable replacement for transition metal complexes in these reactions are limited, however, main group compounds of aluminium and germanium have shown some success in the activation of $H_2$ (**Scheme 1.8**). For example, germanium compounds have been shown to

react with $H_2$ under ambient conditions,[37] and AlCp* has also been shown to react with $H_2$, however, harsh reaction conditions and irradiation ($\lambda_{max}$ = 254 nm) are required.[38] More recently, frustrated Lewis pairs have been proposed as an alternative to transition metals and a possible improvement upon current main group systems.

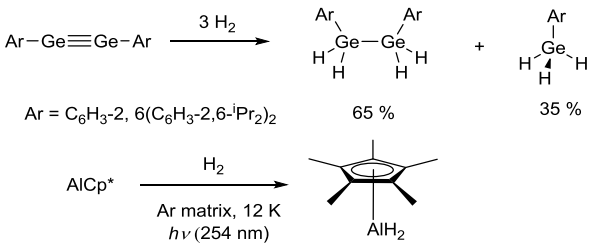


**Scheme 1.8**: Addition of $H_2$ to main-group compounds.[37,38]

### 1.1.4.1.1 Main group activation of $H_2$

While the activation of $H_2$ using transition metal systems is a well-documented reaction,[39] comparable reactions with main group elements were virtually unheard of until 2006 when Stephan observed the reversible activation of $H_2$ using $Mes_2P(C_6F_4)B(C_6F_5)_2$ (**Scheme 1.9**). The resulting compound was air and moisture stable and exhibited the stoichiometric loss of $H_2$ at 100 °C in toluene, as monitored by $^1H$, $^{31}P\{^1H\}$ and $^{19}F$ NMR spectroscopy, and visually by the formation of the orange-red phosphine-borane species.[40]

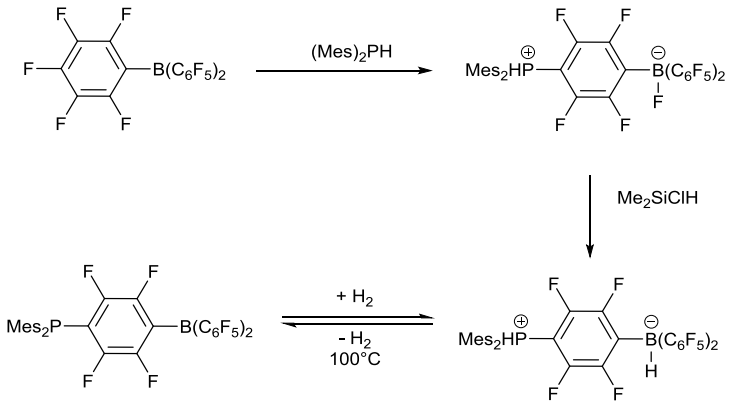


**Scheme 1.9**: The heterolytic cleavage of dihydrogen.[40]

Stephan is careful to point out that the system shows reversible binding of less than 0.25% weight $H_2$, considerably less than the targets of 6 - 9% for hydrogen storage applications.[40] However, this key example of metal-free $H_2$-activation rekindled interest in frustrated Lewis pairs, and started a whole new concept for small molecule activation. Since then, numerous simple molecular phosphine-borane Lewis pairs (e.g. $^tBu_3P$, or $Mes_3P$ and $B(C_6F_5)_3$) have been shown to heterolytically cleave dihydrogen.[17,19,29,41]

### 1.1.4.1.2 More Recent Developments in $H_2$ Activation

Erker and co-workers developed a new FLP based on 1,8 diphosphino-naphthalene, which, in combination with $B(C_6F_5)_3$, has been shown to activate $H_2$ which is liberated on heating to 60 ˚C with regeneration of the FLP (**Scheme 1.10**). The same FLP, under 2 bar of $H_2$, has been demonstrated to catalytically reduce silyl-enol ethers, this reaction displays an unprecedented small temperature gap between absorption and release of $H_2$.[42]

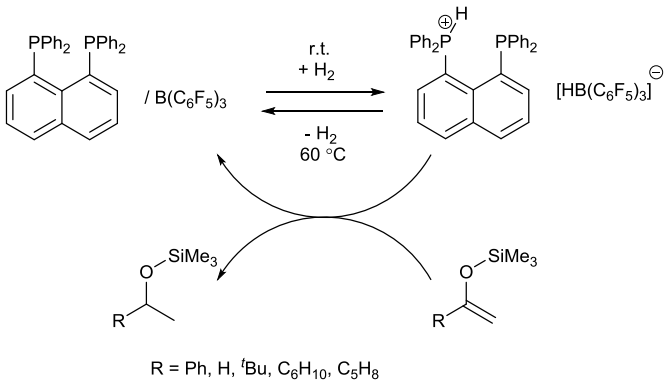


**Scheme 1.10**: 1,8 diphosphino-naphthalene phosphine / $B(C_6F_5)_3$ based FLP.[42]

While $B(C_6F_5)_3$ is by far the most commonly used Lewis acid, $Ph_3B$ has also been shown to activate $H_2$ when combined with $^tBu_3P$ to yield the salt $[^tBu_3PH][HBPh_3]$, albeit over longer times and in lower yields (**Scheme 1.11**) when compared to $B(C_6F_5)_3$.[43] This longer reaction time is attributed to the reduced Lewis acidity of the boron in $BPh_3$ compared to $B(C_6F_5)_3$.

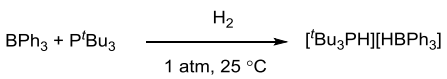


**Scheme 1.11**: $H_2$ cleavage reaction with an alternative borane gave a 33% yield.[43]

The activation of $H_2$ was also observed in the reaction of $H_2$ with 2,2,6,6-tetramethylpiperidine (TMP) and $B(C_6F_5)_3$ by the group of Rieger.[44] Furthermore, they reported preliminary data indicating that the resulting species stoichiometrically reduces benzaldehyde under mild conditions (**Scheme 1.12**), the NMR spectra of the product are consistent with the structural formula $[R_2NH_2][PhCH_2OB(C_6F_5)_3]$.

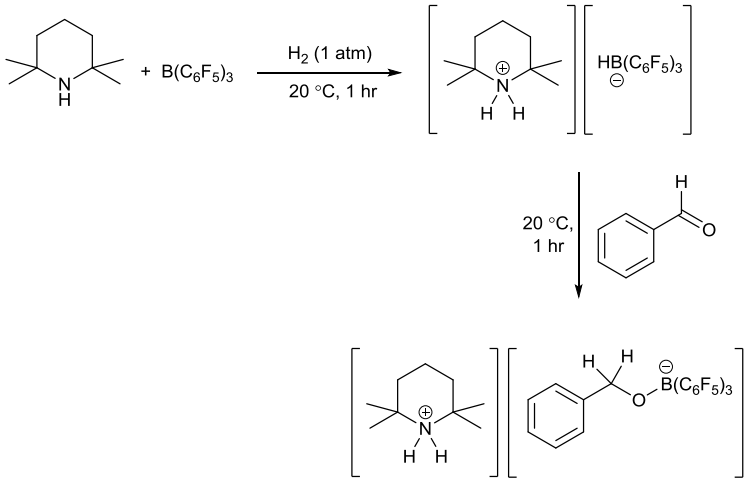


**Scheme 1.12**: $H_2$ activation of an amine based FLP.[44]

The hydrogenation of nitriles and imines, to primary and secondary amines respectively, is synthetically vital to the fine chemical and the pharmaceutical industries;[45] low cost reaction conditions and catalysts are therefore necessary. Currently, many of the industrial processes, such as the hydrogenation of ketones, use costly transition metal complexes, while many of those that do not require forcing conditions. The first example of a transition metal-free hydrogenation was observed 40 years ago when Walling and Bollyky reported the hydrogenation of benzophenone, with $KO^tBu$ as a catalyst, to form benzhydrol. This non-FLP reactivity required harsh conditions (200 °C, 100 atm $H_2$) which limits possible substrates.[46] Berkessel and co-workers are using structural variation to experimentally investigate the mechanism of the base-catalysed hydrogenation of ketones, in order to be able to modify the reaction to proceed under milder conditions.[47] This investigation has been complimented using DFT (Density Functional Theory) from Chen and Radom.[48] Despite the above requiring up to ten times more base-catalyst than the analogous ruthenium based catalysts, using main group FLPs instead is still likely to be more economically viable and more efficient, due to the milder reaction conditions required.

Catalytic hydrogenation using an FLP was demonstrated by Stephan in 2008. The combination of bulky imines with $B(C_6F_5)_3$ activates $H_2$, facilitating the catalytic hydrogenation of the imine (**Scheme 1.13**).[49] This same set of imines can also be hydrogenated using the phosphorus/borane FLP $[(C_6H_2Me_3)_2PH][(C_6F_4)BH(C_6F_5)_2]$.[50] Less bulky nitriles can also be reduced if stoichiometric $B(C_6F_5)_3$ is added, before reduction with $(C_6H_2Me_3)_2PH(C_6F_4)BH(C_6F_5)_2$, however, given the cost of stoichiometric $B(C_6F_5)_3$ there isn't an industrial saving relative to the forcing conditions and transition metals otherwise used. It has also been shown that other molecules such as carbenes[51,52] and amines[44] also activate $H_2$ when combined with $B(C_6F_5)_3$ or related fluoroaryl boranes.[49]

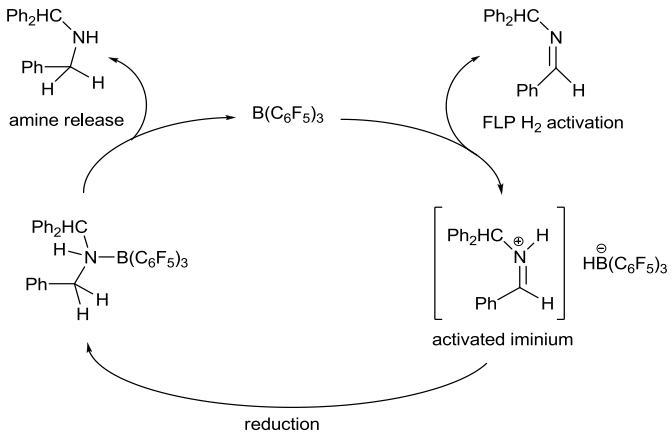


**Scheme 1.13**: Proposed mechanism for the hydrogenation of imines.[49]

### 1.1.4.2 Activation of other small molecules by Metal-Free compounds

#### 1.1.4.2.1 $CO_2$ Activation

The activation of $CO_2$ has been widely explored by organometallic chemists using a variety of approaches, including photochemical reduction, electrochemical reduction, thermal heterogeneous and homogeneous reductions, or any combination of these. These methods all involve the coordination of $CO_2$ to a transition metal complex to effect its activation; this first step is necessary to lower the activation energy required for subsequent reactions. These reactions were comprehensively reviewed by Yin and Moss in 1999.[53] More recently, O'Hare and co-workers have shown the reduction of $CO_2$ with $H_2$ using $B(C_6F_5)_3$ /(TMP) (TMP = 2,2,6,6-tetramethylpiperidine) metal free-FLP systems (**Scheme 1.14**),[54] subsequent work has focussed on improving the catalytic stability without reducing the effectiveness.[31,55]

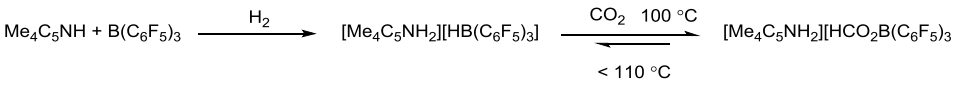


**Scheme 1.14**: Reversible reduction of $CO_2$ to formate with $H_2$, activated by a frustrated Lewis acid–base pair.[54]

Other FLPs have been used to demonstrate the metal-free activation of syn-gas ($CO/H_2$), such as $^tBu_3P/B(C_6F_5)_3$ (**Scheme 1.15)**, which reduces CO to form a formyl-borate species **(a)**, this upon heating forms the epoxy-borate anion **(b)**. The addition of syn-gas at ambient temperature leads to the formation of **(c)** from a second equivalent of $H_2$, and **(d)** from a second equivalent of CO.[56]

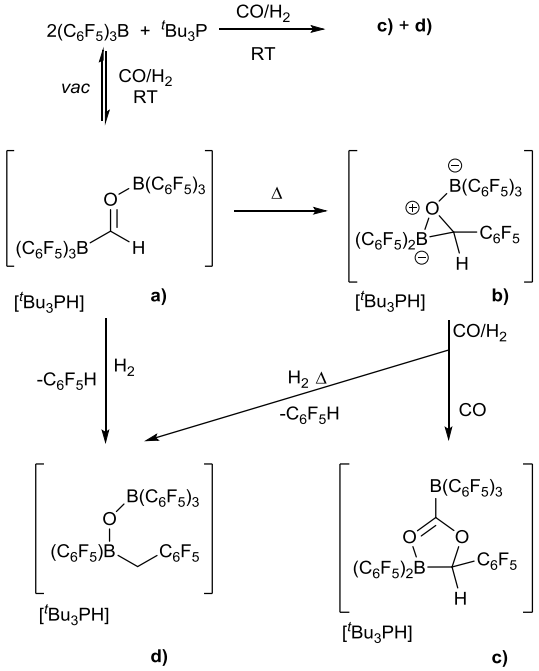


**Scheme 1.15:** Reaction products from $^tBu_3P/B(C_6F_5)_3$ with $CO/H_2$.[56]

The activation of $CO_2$ has also been demonstrated for aluminium based FLPs.[57–60,61] Stephan *et al.* used an aluminium based FLP with $H_2$ to reduce $CO_2$ to methanol at room temperature,[60] and to reduce $CO_2$ to CO stoichiometrically (**Scheme 1.16**).[59]

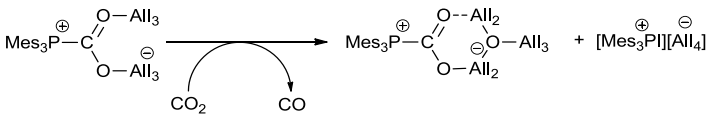

**Scheme 1.16**: Reduction of $CO_2$ to CO using Al-P based FLP.[59]

### 1.1.4.2.2 CO Activation

Transition metal complexes have been widely used in the activation of CO, however, a number of reactions are also known with main group compounds. Dureen and Stephan activated carbon monoxide using the boron amidinate complex, $HC(RN)_2B(C_6F_5)_2$ [R = $^{i}$Pr, $^{t}$Bu], to yield new boron heterocycles through the insertion of CO into the B−N bond, as illustrated in **Scheme 1.17**.[62]

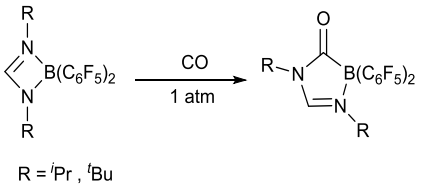

**Scheme 1.17**: Insertion of CO into a weak N-B adduct.[62]

Carbon monoxide is generally considered too stable to be reduced by primary boranes,[63] but it is reported to react with $B_2H_6$ to form an equilibrium with the "borine carbonyl" gas [$H_3B$-CO], sealed in a bomb with excess CO heated to 100 °C.[64] However, recent reports suggest secondary borane reduction of CO, using a borane-phosphine FLP, proceeds under the much milder conditions of 2 bar and ambient temperature (**Scheme 1.18a**). The intramolecular ethlyene bridged FLP shown in **Scheme 1.18**, with its weak internal P---B interaction also reacts with CO and $HB(C_6F_5)_2$ (**Scheme 1.18b**) under mild conditions.[65]

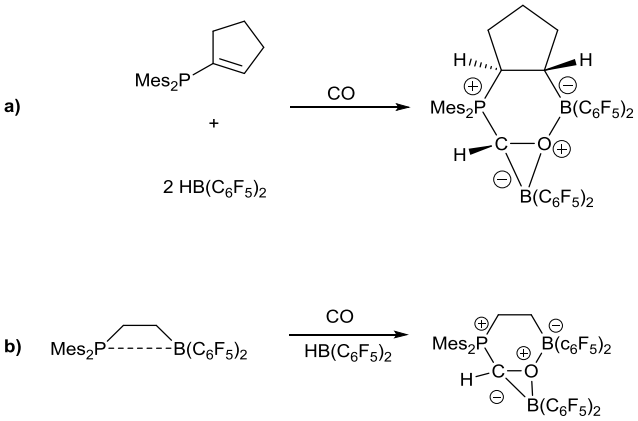


**Scheme 1.18**: Cyclopentenylphosphine with [$HB(C_6F_5)_2$], and the intramolecular ethylene bridged FLP, both reduce CO under mild conditions.[65]

## 1.1.5 FLPs containing Lewis acidic Transition Metals

While main-group FLP systems have demonstrated activity towards small molecules, there are very few cases where this process is catalytic. Notable examples include, imine or enamine hydrogention[66] and deoxygenative hydrogenation of $CO_2$.[67] Combining the innate ability of transition metal complexes to engage in catalysis, with the activation capabilities of FLPs is one potential method of addressing this deficit. Metal-based FLPs are also ideal for exploring activation pathways and reactivity patterns; a greater understanding of the role of the metal in these reactions might eventually lead to the replacement of the metal by a main group fragment to allow the creation of metal-free FLP systems.

### 1.1.5.1 Zirconium centred FLPs

The use of zirconocenes in this manner, was extensively reviewed by Erker in 2011.[68] The first example of the use of zirconium was in 2009 by Erker and co-workers, who showed the catalytic hydrogenation of bulky imine functionalities with the ammonium salt shown in **Scheme 1.19**.[69]

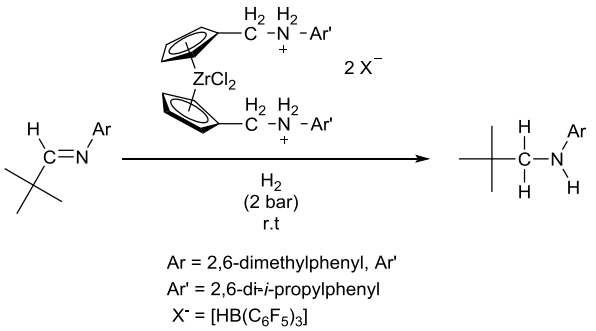


**Scheme 1.19**: Catalytic hydrogenation of bulky imines.[69]

Examples since this date include Wass' report of cationic zirconocene-phosphinoaryloxide complexes as analogues of main group FLPs. These feature an electrophilic transition metal centre with an phosphinoaryloxide which results in an FLP, which was shown to mirror the reactivity of main group systems in the activation of $CO_2$, alkenes, alkynes and aldehydes, and the ring-opening of THF (**Scheme 1.20**).[57] Furthermore, this FLP, and the Cp* analogue, were both found to catalytically activate amine-boranes (**Scheme 1.21**), which had only previously been observed to occur stoichiometrically with main group systems.[70] In 2016, Wass and co-workers expanded the range of reactions of their Zr-based FLP systems with the catalytic hydrogenation of $^{t}$Bu-substituted imines under mild conditions (1 bar $H_2$, ambient temperature), which compare favourably to those conditions (5 atm $H_2$, 120 °C) utilised previously for main-group FLP systems.[49]

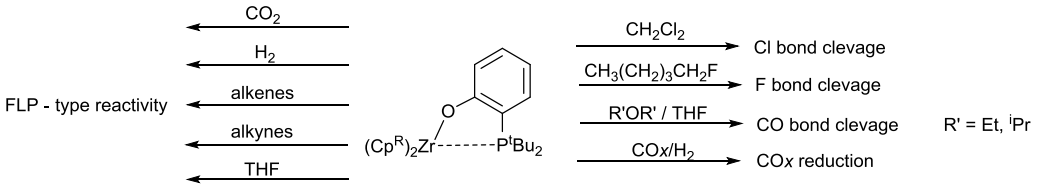


**Scheme 1.20**: Comparison of Zr-based FLP system reactivity to main group FLP reactivity.[57]

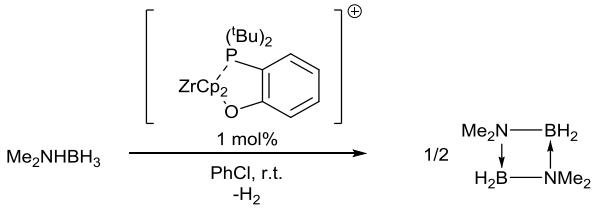


**Scheme 1.21**: Amine-borane dehydrogenation. Counter ion: $[B(C_6F_5)_4]^-$.[70]

Wass and co-workers have also expanded the range of intermolecular Zr-P FLPs by using a range of phosphines ($PCy_3$, $PEt_3$, $PPh_3$, $PMes_3$, $P(C_6F_5)_3$) alongside zirconocene aryloxide, these FLPs demonstrate reactivity analogous to the intramolecular counterparts.[71] These systems have been shown to mediate the activation of small molecules ($D_2$, $CO_2$, THF, PhC≡CH), the facility of which is dependent on the steric and electronic properties of the phosphine. The weakly basic $P(C_6F_5)_3$ showed no reactivity towards small molecules, suggesting that for activation to occur, the phosphine must be sufficiently basic to promote the reactivity. This is seemingly of more importance than the bulk, as the relatively unencumbered $PEt_3$ provided the cleanest results/activations. The bulk of the base also has an effect on the reaction mode as illustrated in **Scheme 1.22**, where the change in base from $PPh_3$ to the more bulky $PMes_3$ changes the reactivity with phenylacetylene from a 1,2 addition to deprotonation.[71]

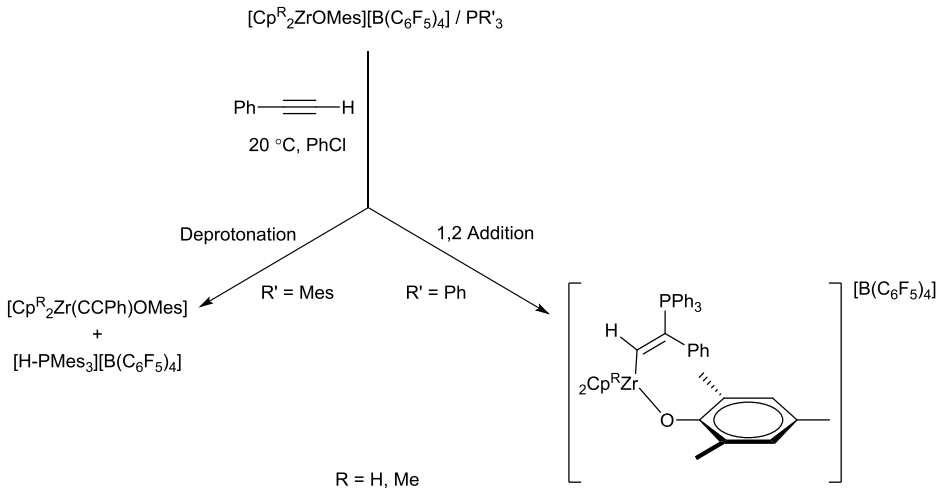


**Scheme 1.22**: Reactivity of Zr-P FLP systems with phenylacetylene.[71]

Another example of a Zr-based FLP with phosphorus as the basic component (**Scheme 1.23**) was published in 2015, and prepared by formal [2+2] cycloaddition of diphenylacetylene to $Cp_2Zr(Me)PCy_2$.[72] The Zr-P interaction was apparent from the Cp protons coupling to phosphorus ($J_{H\text{-}P}$ = 0.7 Hz) in the NMR spectra. This FLP system was made *in situ* in order to explore its reactivity with benzaldehyde or ferrocene carboxaldehyde, and 1,3-diphenyl-2-propen-1-one to give the 1,2 addition, and 1,4 addition products respectively. This FLP was also found to cleanly react with $CO_2$, but this was re-released upon workup or under vacuum.[72] The authors suggest that as the synthesis for the Zr-based FLP uses commercially available precursors, such as secondary phosphines and alkynes, it could be used to expand the range of FLPs with controlled steric and electronic properties.[72]

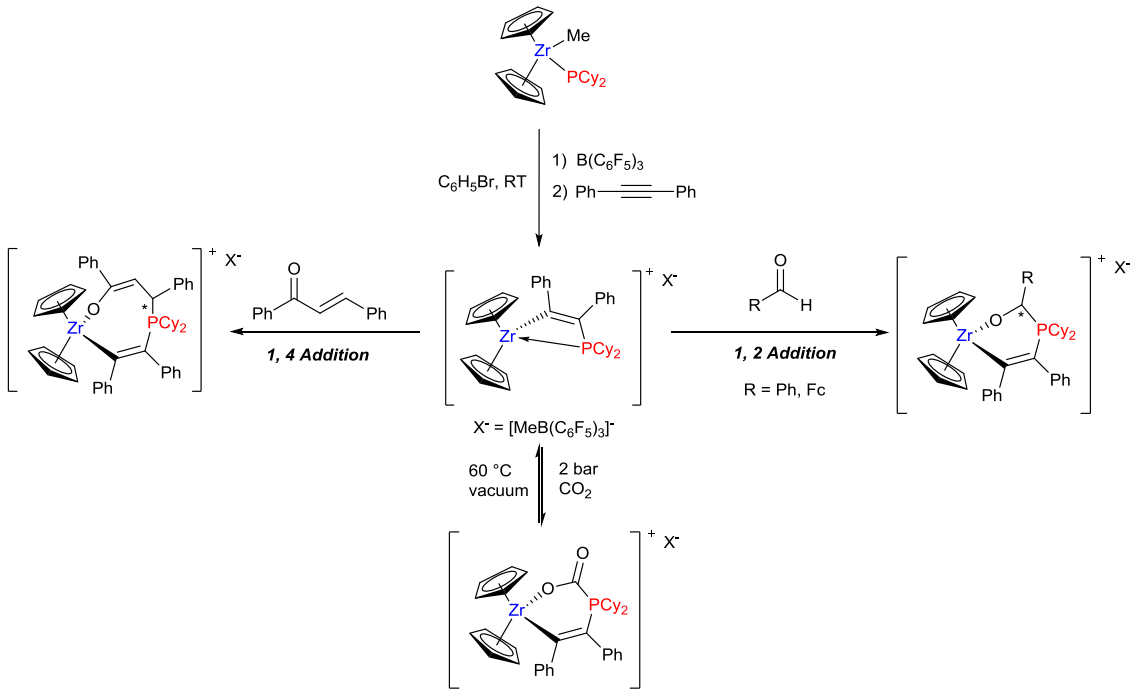


**Scheme 1.23:** Synthesis and reactivity of some $Zr^{+}$/P FLPs.[72]

A similar FLP is formed from $[Cp_2ZrPCy_2Me]$ with $B(C_6F_5)_3$, and has been shown to activate the N=N bond of aromatic azo compounds (PhN=NPh). The 'NHPh' moiety was then deprotonated with $KN(SiMe_3)_2$ to form a neutral Zr(IV) complex featuring a dianionic PNN ligand as shown in **Scheme 1.24**.[73]

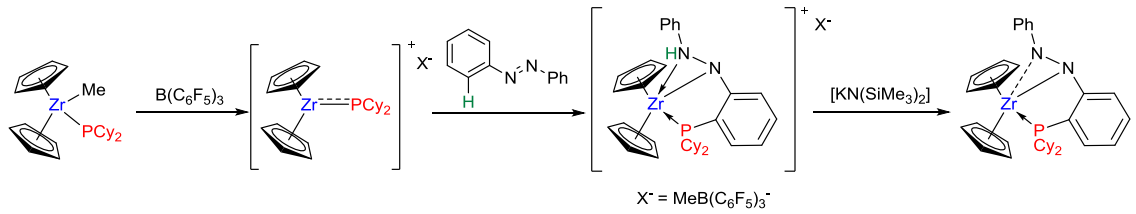


**Scheme 1.24**: P-functionalisation of azobenzene.[73]

### 1.1.5.2 Titanium centred FLPs

Titanium-based FLPs have also been investigated both by Wass[74] and Kehr.[75] Wass synthesised $[Cp_2TiOC_6H_4P(^tBu)_2][B(C_6F_5)_4]$, which was shown to effect $H_2$ activation at low pressure (1-3 bar) over 20 hours at ambient temperature, to afford the cationic Ti(III) complex

$[Cp_2TiOC_6H_4PH(^tBu)_2][B(C_6F_5)_4]$. The Ti-H bond then undergoes homolysis to form a hydrogen radical, which then dimerizes to $H_2$.[74]

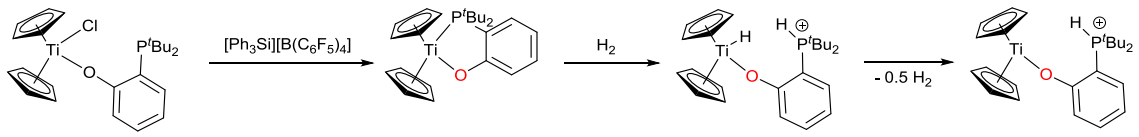


**Scheme 1.25**: Synthesis and $H_2$ activation of titanium based FLP.[74]

### 1.1.5.3 FLPs containing other transition metals

Harmen and Peters prepared a nickel-FLP, $[MesB(o\text{-}Ph_2PC_6H_4)_2]Ni$, which has been used to catalyse olefin hydrogenation.[76] While the heterolysis of $H_2$ with Ni(II) typically invoke nickel as a Lewis acid,[77] in this case, it is the Lewis basic nickel centre which accepts $H^+$ and the Lewis acidic borane that accepts $H^-$.

Berkefeld and co-workers demonstrated the stoichiometric functionalisation of carbon monoxide using an 'ionic frustrated Lewis pair'. The Lewis acidic site $[Sc(Cp^*)_2]^+$ is accessible to the incoming CO ligand, and activated by the weakly coordinating anion $[B(C_6F_5)_3]^-$.[78]

Activation of $CO_2$ has been achieved by hafnium-phosphinomide complexes, which behave as metal-based FLPs and have recently been shown to coordinate one or two equivalents of $CO_2$, leading to a bimetallic, pseudo-tetrahedral $P_2CO_2$ fragment between two hafnium centres (**Scheme 1.26**).[79]

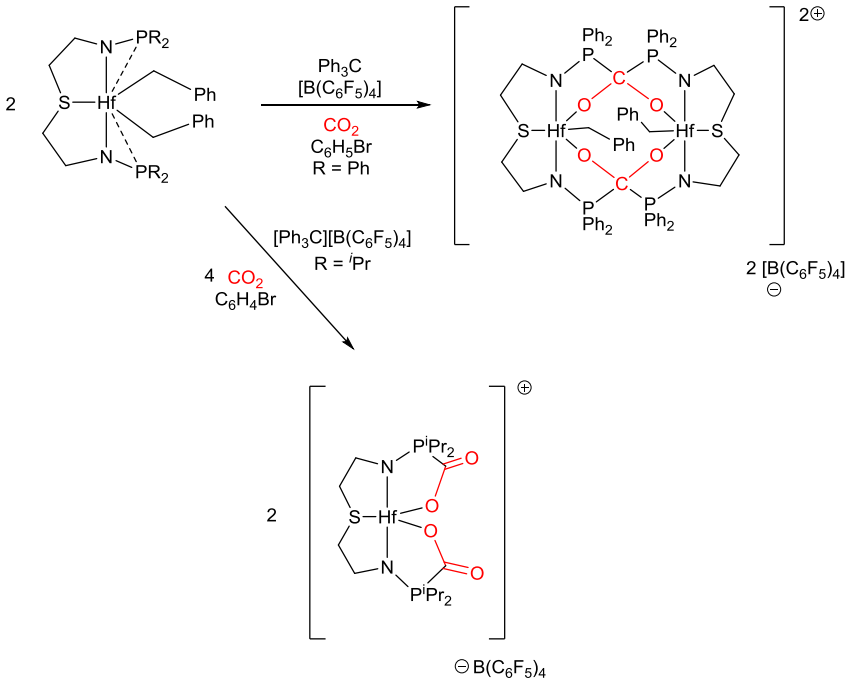


**Scheme 1.26**: Hafnium-based FLP $CO_2$ activation.[79]

## 1.1.6 Mechanism of small molecule activation by Frustrated Lewis Pairs

Owing to the fact that FLP chemistry is a very recent area of study, the finer details of the mechanism of activation remain an on-going topic of investigation. Stephan first suggested a mechanism in 2007 for the heterolytic cleavage of dihydrogen by the combination of $BPh_3$ and $P^tBu_3$ (**Scheme 1.11**).[43] Due to the analogous nature of FLP chemistry to transition metal chemistry, it is logical to propose the mechanism as an interaction of $H_2$ with the Lewis acidic $BR_3$ which polarises the dihydrogen molecule, facilitating the protonation of the approaching Lewis base, in this case phosphine, as shown in **Scheme 1.27**.[43] This idea was supported by Kubas in 2006,[80] who suggested that $H_2$ could initially form a side-on interaction with the ($\delta^+$) borane, before the proton migrates from $H_2$ to the ($\delta^-$) phosphorus atom. Kubas notes that this could occur stepwise through the bridging arene, or be assisted by solvent. It has been established by the computational work of Andrews and co-workers that the species $BH_5$ can essentially be described as a weak ($\eta^2$-$H_2$)$BH_3$ adduct,[81] however, no evidence of $H_2$-$B(C_6F_5)_3$ was found by Stephan in related experiments.[43]

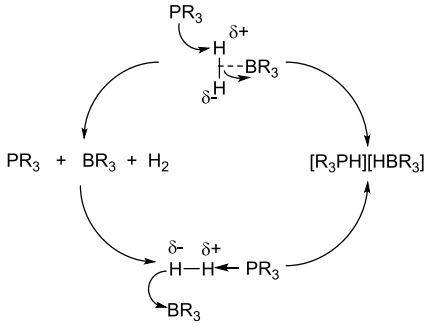


**Scheme 1.27**: First suggested mechanism for the heterolytic cleavage of $H_2$ by phosphine and borane.[43]

Pápai notes that computational studies have shown that delocalisation of the π-electrons into the *p*-orbitals on boron prevent the σ-electrons of $H_2$ from binding. Additionally $B(C_6F_5)_3$---$H_2$ was found to be unstable at low temperature.[82] He goes on to suggest the mechanism proceeds by the end-on addition of $H_2$ to $PR_3$. This is based upon previous investigations by Moroz *et al*., who demonstrate the formation of a Van der Waals complex, on the basis of IR spectroscopic data, for several Lewis bases (including water, acetone, amines, phosphines, pyridine and ammonia) with $H_2$ in an argon matrix. This leads to the polarisation of $H_2$ *via* an end-on-base-$H_2$ interaction.[83]

However, more recent computational studies of the mechanism found that the binary reactions of $H_2$ with either phosphine or borane are unfavourable, and suggest pre-association of the Lewis acid and base as an initial step.[84] Calculations on the $[^tBu_3P][B(C_6F_5)_3]$ system revealed a frustrated complex with the acid-base pair held together by multiple C–H---F hydrogen bonds. After this, the small molecule inserts into the flexible FLP. This is followed by the heterolytic cleavage of the H-H bond, yielding phosphonium and hydridoborate ions in a single concerted step as shown in **Scheme 1.28**.[84]

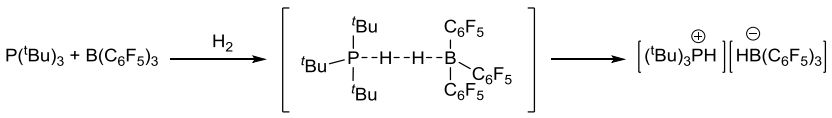


**Scheme 1.28**: Mechanism for bond cleavage through a synchronous transition state.[84]

Grimme *et al*. doubted the "PH--HB" linear arrangement in the transition state, because they did not take into account the interaction between the large substituents which are typically used in FLP's. They argue a more 'realistic' description of the transition states suggest that the polarisation of $H_2$ is induced by the electrical field on the FLP interaction inside the cavity, (or "reactive pocket") which is held together by dispersive forces between the Lewis acid and base. The insertion of $H_2$ into this cavity is the key step, and after this, the reaction proceeds in an essentially barrier-less process.[85] Wang *et al*. designed a theoretical FLP, in order to enlarge the active pocket and lower the activation barrier (**Figure 1.4**).[86] Ponec and Beran used computational methodologies to study the electron reorganisation occurring during the heterolytic splitting of $H_2$ within the pre-organised cavity of a FLP catalyst. Their calculations indicated that the field strength in the FLP designed computationally by Wang *et al*., is not sufficient to reduce the barrier for the splitting of the H-H bond.[87]

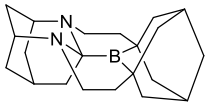


**Figure 1.4**: Metal-free $H_2$ activation catalyst, designed by Wang *et al.*, with two basic nitrogen centres joined to the acidic boron.[86]

Using the model system $H_3N{\bullet}BCl_3$, the activation of $H_2$ has been found to accompany the pyramidal distortion of the $BCl_3$ to accept $H^-$, and the activated complex is then stabilised by charge-transfer interactions. Camaioni *et al*. noted that while the electric field in the cavity plays a part towards the polarizing of $H_2$, the orbital interactions ultimately play a greater role in the product formation.[88]

Tibor Soós also investigated the energetics of the heterolytic cleavage of dihydrogen, using the reaction shown in **Scheme 1.11**, and determined that the energy of frustration ($\Delta E_f$) lowered the activation barrier. This resulted in a more exothermic reaction when compared to a hypothetical classical Lewis pair displaying the same intrinsic acid–base properties (**Figure 1.5**). The presence of bulky substituents not only enabled the formation of the frustrated complexes, but also stabilised the transition state and the product. Expanding the calculations to other sterically demanding $PR_3$ and $BR'_3$ molecules, $[(C_6H_2Me_3)_3P][B(C_6F_5)_3]$ and $[(C_6F_5)_2B$-

$C_6F_4$-P($^t$Bu)$_2$][($C_6F_5$)$_2$B-$C_6F_4$-P($^t$Bu)$_2$], indicates that the present model may have general validity for reactions initiated by frustrated Lewis pairs.[89]

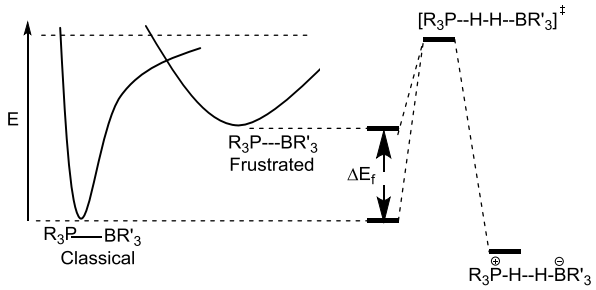


**Figure 1.5**: Energy diagram of the activation barrier and transition states of the heterolytic cleavage of $H_2$ by a frustrated Lewis pair.[89]

## 1.1.7 Ambiphilic Ligands

As noted in earlier sections, many examples of FLPs encompass both acidic and basic components within the same molecule. These systems fall into the class of ambiphilic ligands, also known as amphoteric ligands. Containing both electron donor and acceptor sites within a single ligand enables the molecule to engage in coordination modes where the participation, or otherwise, of the Lewis acid varies, as illustrated in **Scheme 1.29**. The first example is where the Lewis acid remains pendant **(a)**. Other examples include the Lewis acid interacting with the metal itself (as an σ-acceptor) **(b)** or, interacting with a co-ligand **(c)** and the more extreme zwitterionic complexes **(d)**.

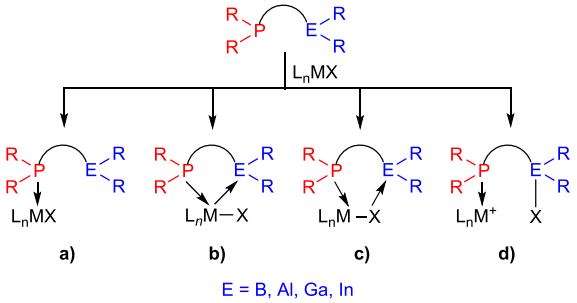


**Scheme 1.29**: Bonding modes of ambiphilic ligands to metal complexes.

### 1.1.7.1 Ambiphilic ligands as Intramolecular FLPs

Intramolecular FLPs have been shown to engage in a variety of activation reactions, including the heterolytic cleavage of $H_2$. The majority of these intramolecular FLPs are ambiphilic molecules, featuring both Lewis acidic and Lewis basic sites, the first example of these (**Scheme 1.30**), was shown to reversibly incorporate $H_2$.[40]

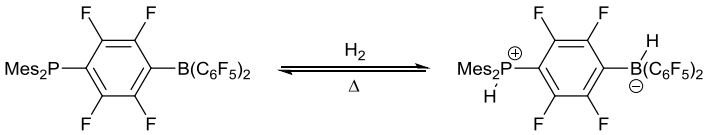


**Scheme 1.30:** Stephan's FLP system showing reactivity with $H_2$.[40]

### 1.1.7.2 Synthesis of Ambiphilic ligands

Erker and co-workers are largely credited with the development of intramolecular FLPs, based on the research of Tilley and co-workers, who developed the synthesis of phosphine-boranes of the form ($Ph_2PCH_2CH_2BR_2$).[90] Two equivalents of diphenylvinylphosphine were allowed to react with either 9-BBN (9-BBN = 9-Borabicyclo[3.3.1]nonane) or $[Cy_2B(\mu\text{-}H)]_2$ to produce the *trans*-hydroboration products shown in **Scheme 1.31.** Both reactions were near quantitative when monitored by NMR spectroscopy, but they claimed the 9-BBN analogue, $Ph_2PCH_2CH_2BBN$, was more difficult to isolate due to the high solubility of the compounds.[90]

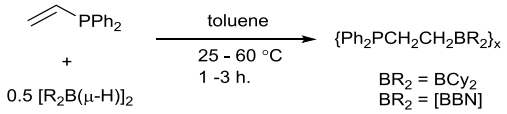


**Scheme 1.31**: Synthesis of phosphine-borane adducts *via* hydroboration.[90]

The authors suggest aromatic solvents such as toluene, rather than THF, which had previously been the standard for hydroboration reactions, was found to allow the preparation of the phosphine-borane (**Scheme 1.31**), and avoid the loss of ethylene which results in the formation of the boraphosphetane (**Scheme 1.32**) in tetrahydrofuran.[91]

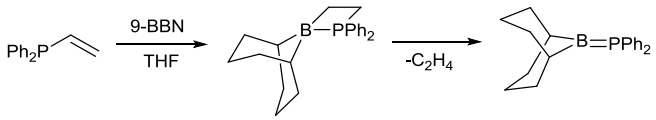


**Scheme 1.32**: Suspected side reaction occurring when hydroboration is attempted in THF.[91]

Spies *et al.* investigated related compounds, incorporating more electrophilic boron fragments into ambiphilic ligands to increase reactivity. They used Piers' borane, $HB(C_6F_5)_2$, with $R_2P$(allyl) or $R_2P$(butynyl) as shown in **Scheme 1.33**. The phosphine underwent clean hydroboration to form a species with strong intramolecular phosphorus-boron bond, by heating to reflux for two hours in toluene before drying the mixture and extracting the product with pentane.[92]

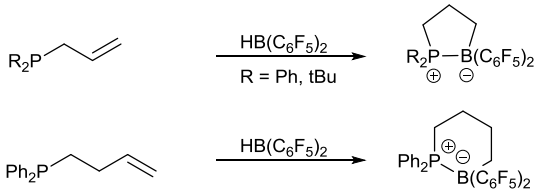


**Scheme 1.33**: Hydroboration of alkenyl phosphines with $HB(C_6F_5)_2$.[92]

Similarly, $Mes_2PHC{=}CH_2$, undergoes hydroboration with Piers' borane to form the phosphine-borane $Mes_2PCH_2CH_2B(C_6F_5)_2$ which, when exposed to 1.5 bar $H_2$, effected activation of $H_2$ to afford a zwitterion as shown in **Scheme 1.34**.[93] Moreover, the adduct undergoes 'H for $C_6F_5$' exchange at boron upon the addition of 9-BBN to form a new FLP, though this could not be separated from remaining dimesitylvinylphosphine; however, the pyridine adduct was able to be isolated and crystallographically characterised to prove its identity.[94]

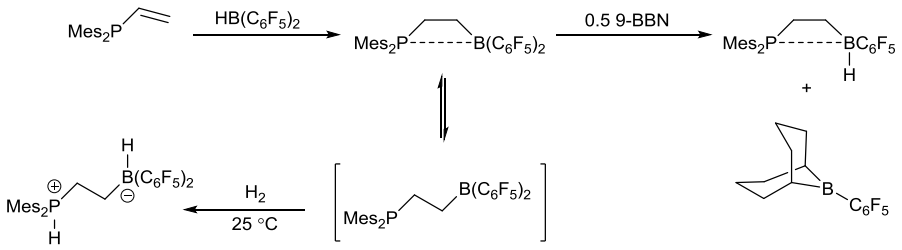


**Scheme 1.34**: Spies *et al.* demonstrated a new FLP which can heterolytically cleave $H_2$ in addition to undergo an H-for-$C_6F_5$ exchange at boron.[95]

Similarly Erker and co-workers observed the activation of $H_2$ by an ethylene linked phosphine-borane (**Scheme 1.35**).[96] This intramolecular FLP has since been used in the hydrogenation of a variety of molecules, including enamines and imines.[28,93]

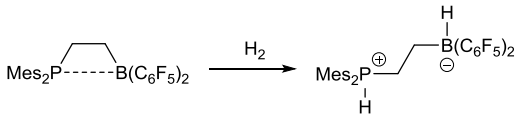


**Scheme 1.35**: Rapid, intramolecular, heterolytic dihydrogen activation by a four-membered heterocyclic phosphine–borane adduct.[28,93]

Binger and Koster quoted high yields for the series of ambiphilic phosphine-borane ligands shown in **Scheme 1.36**. The borate salt reacts with the chlorophosphine, to form the borylphosphinoethenes, upon the loss of NaCl.[97]

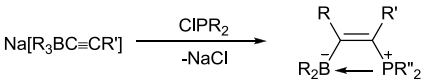


R, R' = Me, R" = $C_6H_5$
R = Et, R = Me, R" = $C_6H_5$
R, R"= Et, R' = Me
R = Et, R' = Me, R" = $C_6H_{11}$

**Scheme 1.36**: Synthesis of borylphosphinoethenes using Na-compounds.[97]

These borylphosphinoethenes undergo further reactivity with $H^+$, which results in the loss of the borane moiety. They also form a ketone of the type RCO-CHR'R" in the presence of oxidising agents or react with Grignard reagents (RMgX) to yield molecules of the type RMg(R)C=CR'R". The addition of $AlR_3$ to $R_2B(R)C=CP(R')R"_2$, results in the displacement of the borane to form the aluminium phosphinoethene, $R_2A(R)C=CP(R')R"_2$, (R = Et, R' =Me, R" = $C_6H_5$).[97]

## 1.1.8 Lewis basic Metal-based FLPs

### 1.1.8.1 Heterometallic FLP system

Chapman and Wass more recently published the heterobimetallic complex shown in **Scheme 1.37.** This was formed through the reaction of the FLP system, $[Cp_2Zr(Me)(OC(CF_3)_2CH_2P^tBu_2)]$ with $[Pt(norbornene)_3]$ *via* the clean insertion of a Pt(0) fragment into a Zr-C bond.[98] Phosphorus NMR ($\delta_P$ = 77 ($^1J_{P\text{-}Pt}$ = 2172 Hz)) and X-ray crystallography confirm the presence of the P-Pt bond. The geometry is shown to include a T-shaped platinum fragment (illustrated in **Figure 1.6**) with no evidence for any agostic interactions between the $^t$Bu groups and platinum; this is confirmed in the solution state by spectroscopic data. DFT calculations confirm the stability of the T-shaped geometry, and found it to be more stable (by approximately 78 kcal/mol) than a structure with the Zr-Pt interaction removed. The unusual T-shape could be rationalised by the Zr-fragment behaving as a *Z*-type ligand - in a similar manner to borane-based fragments in metalloboratranes (**Section 1.9.4**).

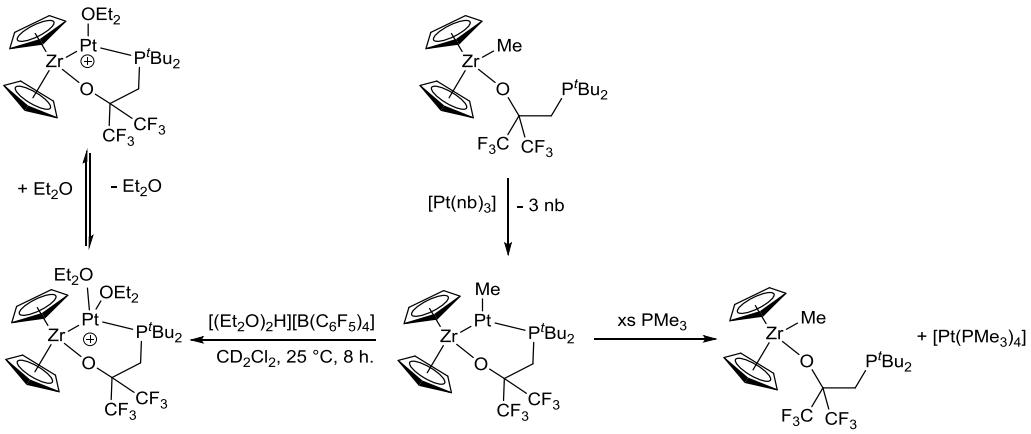


**Scheme 1.37**: Synthesis and reactivity of a bimetallic complex from Wass and co-workers.[98]

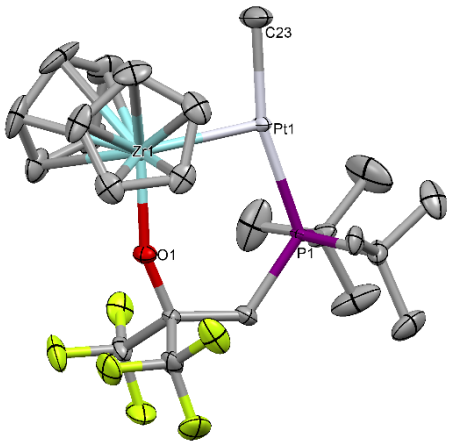


**Figure 1.6**: Molecular structure of Zr-Pt bimetallic complex displaying 'T-shaped' fragment.[98]

The DFT studies also showed that the HOMO is located primarily on the platinum centre, while the LUMO is centred on both platinum and zirconium, and could therefore be favourable for nucleophilic attack due to the large, sterically unhindered orbitals on platinum. While the Zr-Pt complex does not react with $H_2$, $CO_2$ or $H_2C{=}CH_2$, it does react cleanly with $PMe_3$ to afford $[Pt(PMe_3)_4]$, regenerating the zirconium precursor. Using $[(Et_2O)_2H][B(C_6F_5)_4]$ as a proton source, resulted in the removal of the methyl ligand and afforded a diethyl ether adduct on the now oxidised, platinum centre, shown in **Scheme 1.37**.[98]

#### 1.1.8.2 Group 10 centred FLPs

Investigations into the interactions of Lewis acidic fluoroboranes with Lewis basic platinum complexes have been undertaken by the group of Braunschweig.[99] They were not able to isolate the predicted adducts, the first of which, $[(Et_3P)_3Pt{\rightarrow}BF_2(C_6F_5)]$ was detected in solution, and the structure suggested on the basis of spectroscopic evidence. Boron-11 NMR data revealed a 6 ppm shift towards lower frequency relative to the precursor, $BF_2(C_6F_5)$; no starting material was observed in the phosphorus NMR spectrum, instead the spectrum shows two signals (a doublet and a multiplet) exhibiting coupling to platinum. However, this compound quickly degraded and the new product was postulated to be the zwitterionic compound resulting from the activation of an aromatic C-F bond *i.e*. $[(Et_3P)_3Pt(C_6F_4\text{-}2\text{-}BF_3)]$ (**Scheme 1.38a**). The second Lewis adduct proposed (*trans*-$[(Cy_3P)_2Pt{\rightarrow}BF_2Ar^F]$) existed as an intractable equilibrium mixture at ambient temperature (**Scheme 1.38b**), though was observed spectroscopically at -80 °C. The only signal in the $^{31}P$ NMR spectrum ($\delta_P$ = 49.7) displayed platinum satellites ($^1J_{P-Pt}$ = 3760 Hz) and appeared as a triplet ($^3J_{P-F}$ = 18 Hz). While attempting to shift the equilibrium in favour of this Lewis adduct, an additional $^{19}F$ NMR resonance was observed, which they suspected to result from an oxidative addition taking place (**Scheme 1.38c**).[99]

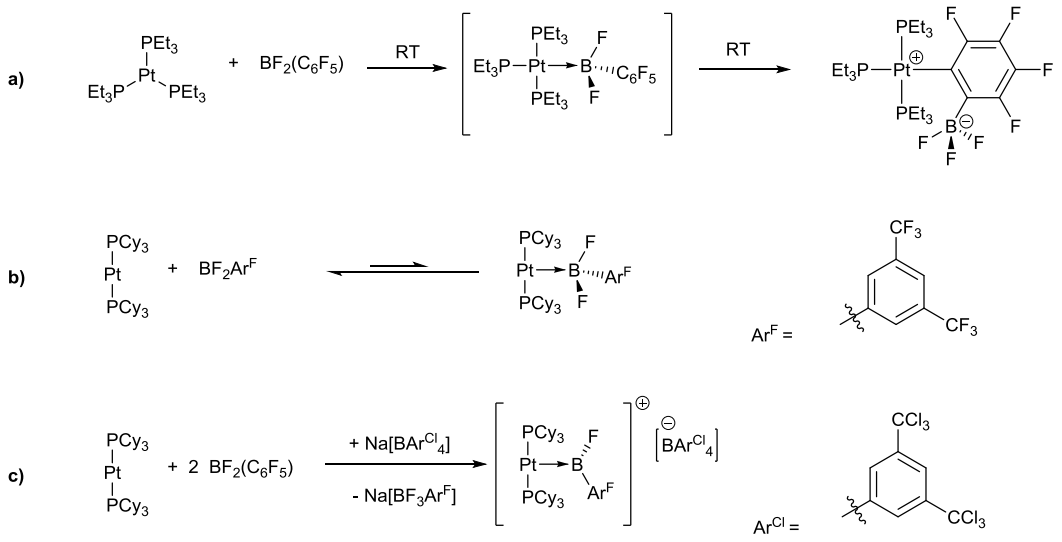


**Scheme 1.38**: Lewis adducts of Lewis acidic fluoroboranes with Lewis basic platinum complexes.[99]

A platinum-based FLP featuring a pre-coordinated small molecule, [(dcpp)Pt($C_2H_4$)] (dcpp = 1,3-bis(dicyclohexylphosphino)propane) and $B(C_6F_5)_3$ was reported in 2013. The addition of $B(C_6F_5)_3$ immediately formed an adduct (**Scheme 1.39**), the structure of which was confirmed by crystallographic data. The structure suggested the activation of ethane within [dcpp)Pt($B(C_6F_5)_3$)($CH_2CH_2$)], by the presence of an agostic interaction between the ethene and platinum centre.[99]

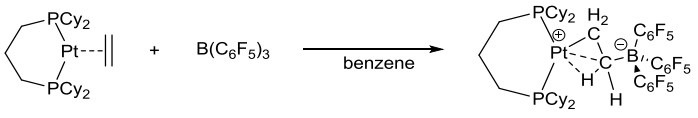


**Scheme 1.39**: Platinium-based FLP system suggesting activation of ethane.

As the concept of donor–acceptor adducts form the basis of transition metal coordination chemistry, it is only fitting that the absence of this adduct formation is also investigated with respect to transition metal coordination chemistry.

Organometallic complexes are often used to probe the reactivity of ambiphilic ligands. After coordination, the Lewis acidic component can either interact directly with the metal centre or interact with an anionic ligand from the metal coordination sphere. *Trans*-phosphine-borane adducts of the form $Ph_2PCH_2CH_2BR_2$ were reacted with [(dmpe)$NiMe_2$] (dmpe = 1,2-bis(dimethylphosphino)ethane) at ambient temperature. This led to the formation of

zwitterionic Ni-Me complexes (**Scheme 1.40**). The reaction proceeded by a methyl-abstraction from the nickel centre, however, adding a second equivalent of ligand did not result in the abstraction of the second methyl group. Adding a single equivalent of the strongly Lewis acidic $B(C_6F_5)_3$, in an NMR scale reaction, resulted in methide abstraction from the cyclohexylborate moiety to $B(C_6F_5)_3$.[90] These reactions highlight the ambiphilic nature of the β-phosphinoethylboranes as simultaneous donors and acceptors.

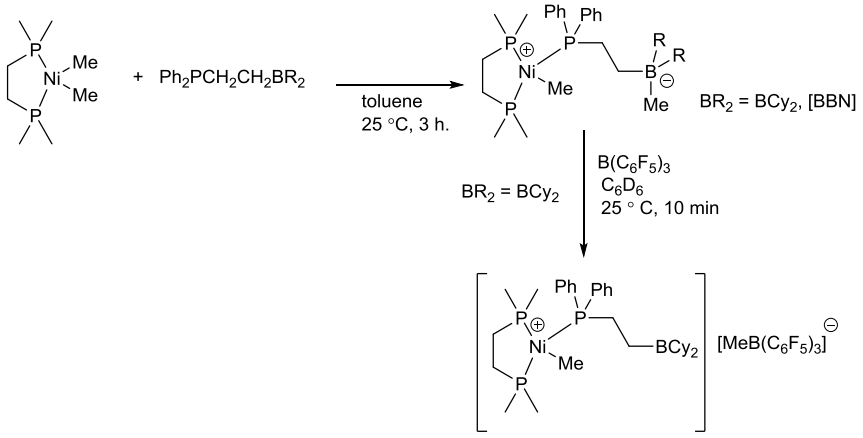


**Scheme 1.40**: Methyl abstractions of β-phosphinoethylboranes from $[(dmpe)NiMe_2]$.[90]

An excess of the tripodal ligand $B(CH_2CH_2PMe_2)_3$ was shown to react with $[Pd(PPh_3)_4]$, when stirred for 24 hours in an NMR scale reaction. The $^{31}P\{^1H\}$ NMR spectrum confirmed the presence of the cage complex shown in **Scheme 1.41**, alongside free $PPh_3$, in addition to the mononuclear product $[B(CH_2CH_2PMe_2)_3Pd]$ and the adduct $Ph_3P\rightarrow B(CH_2CH_2PMe_2)_3$.[100]

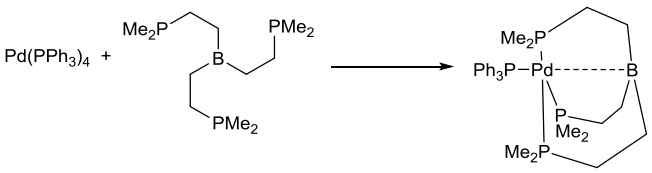


**Scheme 1.41**: The cage structure shows Pd-B interaction of $Ph_3P\rightarrow PdB(CH_2CH_2PMe_2)_3$.[100]

### 1.1.8.3 Rhodium centred FLPs

Only one published example of a coordinated borylphosphinoethene ligand has been found within the literature (**Scheme 1.42**). The rhodium-complex $[RhCl(CO)(L)_2]$ (L =

$Me_2B(Me)C=C(Me)PMe_2$) was confirmed by spectroscopic evidence of a donor/acceptor interaction between rhodium and boron. A resonance was observed at $\delta$ = 22.3 ppm in the $^{31}P\{^1H\}$ NMR spectrum, which was at a higher frequency than that of any other previously studied Rh(I)-phosphine complexes. This was thought to be a result of the Rh → B interaction causing electron density to move towards the boron, away from rhodium, leading to additional deshielding of the phosphorus atom. Further evidence of the interaction was provided by IR spectroscopy, the $^1J_{Rh\text{-}P}$ coupling constant and bond lengths.[100]

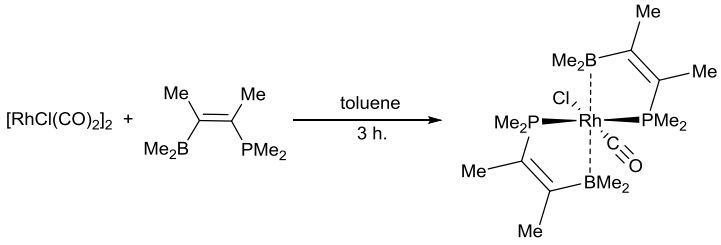


**Scheme 1.42**: Synthesis of the first borylphosphinoethene coordinated to rhodium.[100]

Investigations into the coordination of borylphosphinoethene to $[Cp^*Rh(CO)_2]$, indicated that the coordination does not result in a single product. It was found that both mono and di-substituted complexes were formed (**Scheme 1.43**).[100] The $^{31}P\{^1H\}$ NMR spectra of the di-substituted product proved that the ligands were no longer magnetically and chemically equivalent, as evidenced by two mutually coupling doublet resonances, which was proposed to be caused by rotational hindrance of the Cp* ligand on the Rh Cp *-axis-oriented methyl group.

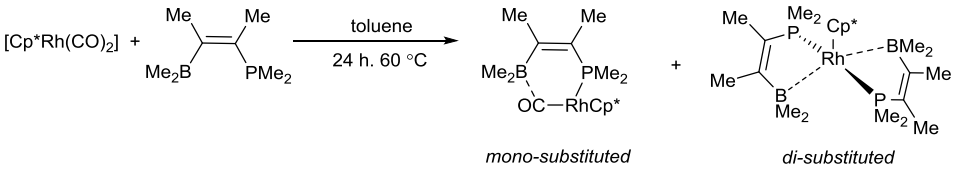


**Scheme 1.43**: The coordination of $Me_2BC(Me)=C(Me)PMe_2$ to $[Cp^*Rh(CO)_2]$ is complicated by the mixture of mono- and di-substituted complexes.[100]

### 1.1.8.4 Metalloboratranes

The coordination chemistry of poly(pyrazolyl)borate complexes is well reviewed in the literature.[101–107] These 'metalloboratranes' (**Figure 1.7a**) are named by analogy to the traditional 'boratrane' moiety shown in **Figure 1.7b**, with the first example of a metallaboratrane, $[Ru\{B(mt)_3\}(CO)(PPh_3)]$ shown in **Figure 1.7c** (mt = methimazole). X-ray diffraction studies of this complex, published in 1999, prove the Ru-B interaction in the solid state through the bond distance (2.161(5) Å). There was no precedent for a ruthenium-boron bond in the literature, but the bond length was similar to those found in a range of osmium-σ-boryl complexes This interaction was confirmed in the solution state by the broadness of the resonance in the phosphorus NMR spectrum ($\delta_P$ = 26.6), indicating proximity to quadrupolar boron.[108]

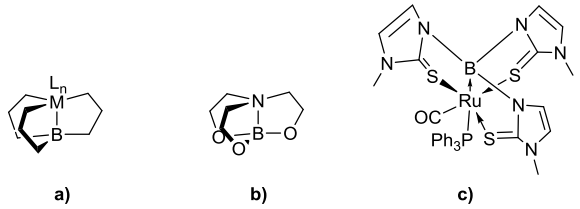


**Figure 1.7**: General motif of **a)** metallaboratrane, and **b)** boratrane cages and **c)** the first metalloboratrane.[108]

In 2008, the first examples of reversible M-B bond formation in relation to these metalloboratranes were published.[109] This is significant because it demonstrates that metallaboratranes are not simply inert cage structures featuring an unreactive M→B bond. A hydride was transferred between the metal centre and the boron, raising the question as to what other ligands might show similar behaviour. In 2011, the first example of the addition of $H_2$ across a transition metal-borane bond was reported, Owen and co-workers suggested the possible use of this and similar systems as hydrogenation catalysts.[110]

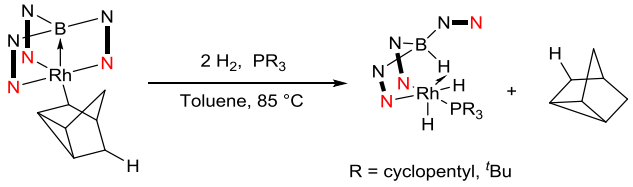


**Scheme 1.44**: Reaction of metallaboratrane with $H_2$ and $PR_3$ R = cyclopentyl, $^t$Bu.[110]

The activation of C≡S has also been reported in 2007, illustrated in **Scheme 1.45**. It is notable that no discrete metallaboratrane bond was observed, therefore the activation of C≡S might indicate FLP type reactivity.[111]


**Scheme 1.45**: Activation of C≡S by a metallaboratrane system.[111]

The reaction of C≡S, in addition to the established metal-acidic FLP systems and the combination of [(dcpp)Pt($C_2H_4$)], and $B(C_6F_5)_3$ revealing a FLP interaction with the Lewis basic metal centre, suggests the real possibility of designing intramolecular metal-basic systems for explicit FLP reactivity. Indeed, frustration should also be possible with a weaker acid than derivatives of $B(C_6F_5)_3$ or $HB(C_6F_5)_2$, as a weaker acid should still retain adequate acidity.[112]

Herein, (chapters 2 and 3) attempts to synthesise a range of phosphine-boranes featuring a saturated 2- or 3-atom bridge, or an unsaturated 2-atom bridge alongside their coordination chemistry are described. The strength of the P-B interaction present in the unsaturated systems has been additionally explored through solid state and computational data.

## 1.2 Overview of organophosphorus chemistry

Phosphorus was one of the first elements to be discovered, it has been known since 1669 and has only one stable isotope, $^{31}P$, which is therefore 100% naturally abundant and has a half integer nuclear spin.

When scientists began looking for heavier analogues to carbon-carbon bonds, the logical step was to investigate silicon-carbon bonds, as silicon lies in the same group as carbon, and therefore has the same number of valence electrons. It became apparent that multiple bonds of this type are difficult to form, and are very reactive, as shown by Brook (C=Si) and West (Si=Si), due to poorer orbital overlap.[113,114] Phosphorus-carbon bonds were found to be a better target, as phosphorus is isolobal and isoelectronic with the 'CH' fragment. This means they possess similar frontier molecular orbitals, which are identical in both shape and energy with a similar electronic configuration. Phosphorus and carbon have also been shown to have similar values of Pauling electronegativities (2.5 for carbon, and 2.1 for phosphorus) as was demonstrated by Michl and co-workers using UV absorption spectroscopy and magnetic circular dichroism spectroscopy.[115]

It is well established that nitrogen can also form multiple covalent bonds with carbon to afford moieties such as cyanides (-C≡N) and imines (RC=N-). Chemists would therefore expect that phosphorus, being in the same group as nitrogen, should also be able to form analogous compounds. In order to categorise the organophosphorus compounds, the phosphorus atom can be described by the number of atoms directly attached (coordination number-σ) or the number of bonds to phosphorus (its valency-λ) (**Figure 1.8**). For example, a pentavalent phosphorus atom can be found in both phosphoranes ($\lambda^5$-$\sigma^5$) (**Figure 1.8A**) and phosphine oxides ($\lambda^5$-$\sigma^4$) (**Figure 1.8B**), while phosphonium salts ($\lambda^4$-$\sigma^4$) (**Figure 1.8C**) have a positive charge on the phosphorus. Phosphines (($\lambda^3$-$\sigma^3$) (**Figure 1.8D**) are often further divided into primary ($PRH_2$) secondary ($PR_2H$) and tertiary, ($PR_3$). The remaining of these organophosphorus types, (phosphaalkenes ($\lambda^3$-$\sigma^2$) (**Figure 1.8E**) and phosphaalkynes ($\lambda^3$-$\sigma^1$) (**Figure 1.8F**)) have a low coordination number, with two reactive sites, the π-system and the phosphorus lone pair.

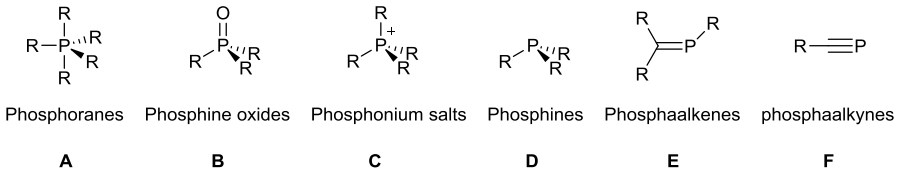


**Figure 1.8**: Types of organophosphorus compounds.

The diagonal relationship between phosphorus and carbon is derived from the general ability of phosphorus to accept or release electrons in a similar manner to carbon. Phosphorus also has the ability to mimic the varying oxidation states of silicon and nitrogen.[116,117] Due to this, the chemistry of low coordinate phosphorus molecules mimics their all-carbon analogues to such an extent that a new term was coined for the study of the analogy between the chemistry of low coordinate carbon and phosphorus species, 'phospha-organic chemistry'. It is now well documented that replacing a carbon atom with a phosphorus atom in a C=C bond results in analogous products with similar reactivity, despite P=C being a (slightly) weaker, and thus more reactive bond than C=C.[118]

The 'double bond rule' suggested that multiple bonding involving the heavier elements of the periodic table would not occur due to the poor overlap of the differently sized $p_z$ orbitals, resulting in weak $p_\pi$-$p_\pi$ bonding.[119] This was first disproven in 1961 when Gier reported the synthesis of HC≡P, formed from the pyrolysis of $PH_3$ in a rotating arc between carbon electrodes. This novel phosphaalkyne is unstable at temperatures exceeding −124 °C and above this polymerises to a black solid. Microanalysis of the polymeric species $(HC{\equiv}P)_n$ supported the formation of HC≡P, and this was further confirmed through the addition of excess anhydrous HCl to HC≡P at −110 °C, which afforded a pure sample of $CH_3PCl_2$.[120] The breaking of the 'double bond rule' as demonstrated during the synthesis of the phosphorus analogue of hydrogen cyanide, has led to increased research activity in the field.

Further studies into the synthesis of phosphacarbon compounds were started by a series of experiments led by Kroto and Nixon.[121] Through the use of gas-phase microwave spectroscopy, their pioneering work allowed the detection and isolation of a whole new family of molecules featuring the highly unusual carbon-phosphorus double bond. These and subsequent studies on multiply bonded phosphorus (featuring both homo- and hetero-atom bonding), have been largely responsible for the rapid expansion of interest into organophosphorus chemistry.

## 1.2.1 Phosphaalkynes

### 1.2.1.1 General Overview

Comparison of the energies of C≡P and C≡C bonds shows the similarity of the π-systems ($\pi_{C\equiv C}$ = -11.40 eV and $\pi_{P\equiv C}$ = -10.79 eV respectively).[122,123] However, due to the presence of the lone pair on the phosphorus atom, comparison can also be drawn between the electronic structures of phosphaalkynes (RC≡P:) and nitriles (RC≡N:). The frontier orbitals are similar for both systems with the HOMO being the π-system, and the HOMO-1 encompassing the lone

pair (**Figure 1.9**), however, the HOMO/HOMO-1 energy gap is much smaller for HC≡N than for HC≡P. The phosphorus lone pair has a higher *s*-character and is therefore less reactive than the nitrogen lone pair.[117] Nitrogen is also more electronegative (N; 3.0 v. P; 2.2)[124] and thus nitriles have the opposite polarity to phosphaalkynes.

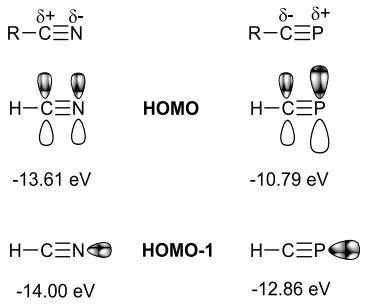


**Figure 1.9**: Polarisation and bonding energies of HC≡N and HC≡P.[123]

### 1.2.1.2 Synthetic routes towards phosphaalkynes

In the years following the discovery of HC≡P, the groups of Kroto and Nixon made vast progress in generating and characterising short-lived phosphaalkynes.[121,125] The first kinetically stable phosphaalkyne was published by Becker in 1981, prepared from the NaOH catalysed β-elimination of hexamethyldisiloxane from $Me_3SiOC(^tBu)=PSiMe_3$ to afford $^tBuC{\equiv}P$ (*tert*-butyl-phosphaethyne).[126] The colourless liquid boils at 60 °C (ambient pressure) and is relatively stable, it has a P≡C bond length of 1.548(1) Å[127] (*cf*. typical C=C bond length 1.34 Å)[128] while UV photoelectron spectroscopy shows a large difference in energy between the π-systems (-9.61 eV) and the lone pair (-11.44 eV).[129]

The Becker synthesis of phosphaalkynes (**Scheme 1.46**) was expanded upon by Regitz, increasing the number of known phosphaalkynes to include RC≡P where R = $^t$Bu, $Me_2EtC$, $Me_2BuC$, $Et_2CH$, Ad, $C_6H_2Me_3$, $C_6H_2{}^tBu_3$.[130]

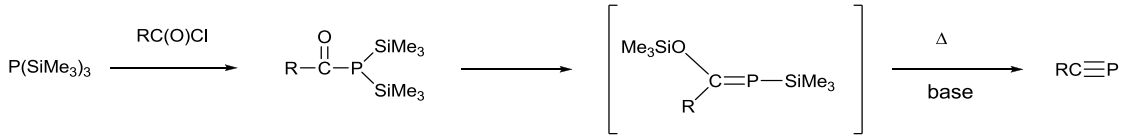


**Scheme 1.46:** The Becker synthesis of phosphaalkynes.[126]

### 1.2.1.3 Double dehydrohalogenation

Approximately 20 years after Gier's synthesis of HC≡P, Kroto, Nixon and co-workers found an alternative route to HC≡P and other phosphaalkynes, using flash pyrolysis of $CH_3PCl_2$ as shown in **Scheme 1.47a**.[131] This double dehydrohalogenation methodology was also found to apply to other phosphaalkynes, *e.g.* MeC≡P[132,133] and FC≡P[134,135] (**Scheme 1.47b** and **c**).

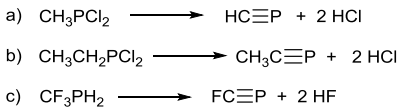


**Scheme 1.47:** General double dehydrohalogenation reactions.[131–135]

More recently, double-dehydrohalogenation reactions have been routinely performed in solution with either DBU (1,8−Diazabicyclo[5.4.0]undec-7-ene) (**Scheme 1.48a**)[136] or AgOTf/DABCO (DABCO = 1,4−diazabicyclo[2.2.2]octane) (**Scheme 1.48b**).[137,138] It is noteworthy that the use of DBU does not allow the isolation of the more unstable derivatives ClC≡P and PhC≡P, however, they have been prepared by Denis using "vacuum gas-solid HCl elimination."[139]

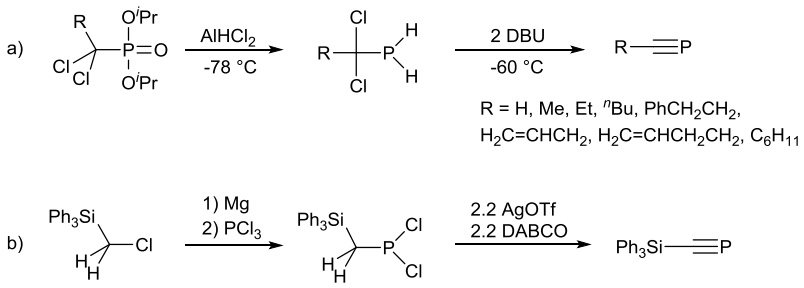


**Scheme 1.48**: Synthesis of RC≡P[136] and $Ph_3SiC{\equiv}P$.[137]

### 1.2.1.4 Alternative synthetic routes

An alternative method for the synthesis of phosphaalkynes involves the elimination of chlorotrimethylsilane, without the need for base (**Scheme 1.49a**).[140] Other methods involve a low-temperature, Lewis base catalysed, rearrangement of primary ethyn-1-ylphosphanes, involving an intermediate such as RCH=C=PH (**Scheme 1.49b**)[141] and the use of vacuum gas-solid HCl elimination reactions of $RCl_2CPH_2$ and freshly ground $K_2CO_3$ to form RC≡P, where R = Me, Et, Bu, $SiMe_3$ (**Scheme 1.49c**).[139] Thermolysis of 1-vinyl phosphirane has been shown to afford the phosphapropyne, $CH_3C{\equiv}P$, through the elimination of ethane (**Scheme 1.49d**).[142] These synthetic pathways typically involve high temperatures or pressures, and produce simple phosphaalkynes that are typically thermodynamically unstable under ambient conditions.

While HC≡P can be kept for months in diethyl ether at temperatures lower than −20 °C, alkyl-substituted phosphaalkynes are stable at room temperature if they are free from impurities. While PhC≡P and $Me_3SiC{\equiv}P$ degrade over time at ambient temperature, $Me_3SiC{\equiv}P$ has been estimated (using quantitative $^{31}P\{^1H\}$ NMR spectroscopy) to have a half-life of 246 hours (>10 days) in toluene,[143] but can be preserved for longer at colder temperatures, and has been shown to be indefinitely stable at -78 °C.[144]

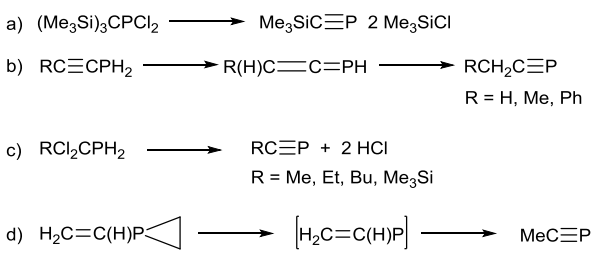


**Scheme 1.49**: Alternative synthesis of phosphaalkynes.[139–142]

### 1.2.1.5 Conjugated systems

Other conjugated systems that have been observed in the gas phase, and identified by their microwave spectrum, feature 'N' and 'CH' units (**Scheme 1.50**). Cyanophosphaethyne, N≡C-C≡P was synthesised from the copyrolysis of HC≡P with $NCN_3$, while phosphabutadiyne, H≡C-C≡P, was made similarly from the pyrolysis of $HC{\equiv}C\text{-}CH_2Cl$ with $PCl_3$, via the proposed intermediate $HC{\equiv}CCH_2PCl_2$.[131]

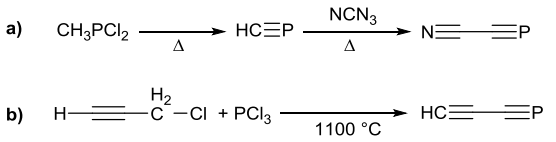


**Scheme 1.50**: Synthesis of conjugated phosphaalkynes **a)** N≡C-C≡P and **b)** HC≡C-$CH_2$Cl.[131]

#### 1.2.1.5.1 Aryl-phosphaalkynes

Few examples of phosphaalkynes with extended π-conjugation are found in the literature. The aryl systems, MesC≡P[130] **(Figure 1.10a**), Mes*C≡P[145] (**Figure 1.10b**) and (2,6-Mes)$_2$C$_6$H$_3$C≡P[146] (**Figure 1.10c**) are all relatively stable due to their bulk and can be accessed *via* the Becker synthesis along with the less stable PhC≡P (**Figure 1.10d**), which is reported to have a half-life of 7 minutes at 0 °C.[140] Little further work has been undertaken to expand upon the range of these phosphaalkynes.

An alternative synthesis for phosphaalkynes, reported by Toyota *et al.*, uses [$NiBr_2(PPh_3)_2$] as a catalyst with a series of dibromomethylenephosphines, to generate the highly air sensitive (2,6-$^t$Bu)$_2$(4-R)C$_6$H$_2$C≡P, where R = H, OMe, $NMe_3$ (**Figure 1.10e**).[147]

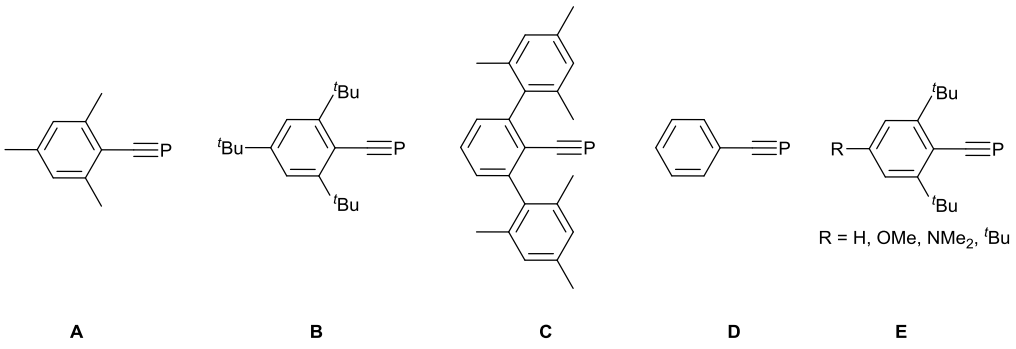


**Figure 1.10**: Selection of aryl-phosphaalkynes.[130,140,145–147]

#### 1.2.1.5.2 Diphosphaalkynes

Diphosphaalkynes are rare, but have potential as building blocks for a variety of phosphorus containing functionalities such as organophosphorus polymers, heterocycles, cages and coordination polymers. Notable examples in the literature include the radical P≡C-C≡$P^+$, reported in 2000 and shown to exist on at least a microsecond timescale. It was synthesised through the EI (Electron Impact) ionisation of $Cl_2PC≡CPCl_2$ or $Cl_2PCH_2P(Cl)CH_3$ in a mass

spectrometer, and this radical was converted to the diphosphaalkyne with $Xe/O_2$ through neutralisation-reionisation (**Figure 1.11a**) but was not isolated.[148]

Various metal-bis(2-phosphaethynolate) (*vide infra*) complexes $[M(dme)_3(OC{\equiv}P)_2]$, where M = Mg, Ca, Sr or Ba (dme = 1,2-dimethoxyethane) (**Figure 1.11b**), were formed upon reaction of $M\{P(SiMe_3)_2\}_2$ with $(MeO)_2C{=}O$, but were found to be unstable upon removal of solvent.[149] While the air/moisture stable system bis(phosphaethynyl)triptycene (**Figure 1.11c**) was synthesised *via* the Becker condensation with catalytic KOH.[150] More recently, Jones and co-workers published the related diphosphaalkyne $(P{\equiv}C\{C(C_2H_4)_3C\}C{\equiv}P)$ with a bridging norbornyl unit. This phosphaalkyne (**Figure 1.11d**) was formed *via* the base catalysed elimination of hexamethyldisiloxane from *Z*,*Z*-$(Me_3Si)P{=}C(OSiMe_3)\text{-}\{C(C_2H_4)_3C\}C(OSiMe_3){=}P(SiMe_3)$.[151]

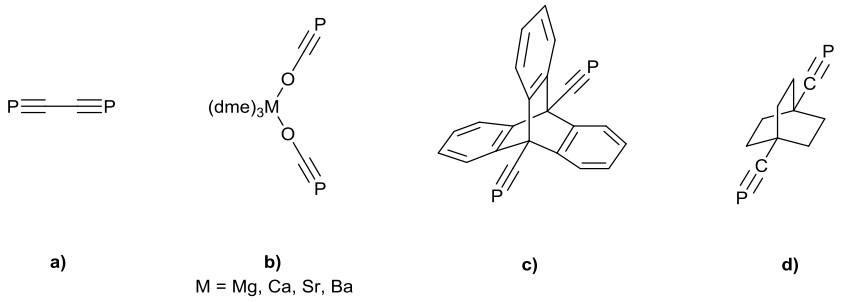


**Figure 1.11**: Diphosphaalkynes – **a)** $P{\equiv}C\text{-}C{\equiv}P$,[148] **b)** $[M(dme)_3(OC{\equiv}P)_2]$,[149] **c)** bis(phosphaethynyl)triptycene,[150] and **d)** $P{\equiv}C\{C(C_2H_4)_3C\}C{\equiv}P$.[151]

#### 1.2.1.5.3 The phosphacyanate anion, $(O\text{-}C{\equiv}P)^-$

The sterically unprotected phosphorus cyanate ion, $(O\text{-}C{\equiv}P)^-$ can be isolated, despite the lack of steric shielding, it was first synthesised by Becker as the lithium salt, $[Li(O\text{-}C{\equiv}P){\bullet}(dme)_2]$, through the reaction of $LiP(SiMe_3)_2$ with dimethylcarbonate in 1,2-dimethoxyethane, very little work followed to investigate its reactivity.[152]

Sodium phosphacyanate, Na(OC≡P), is made readily from $NaPH_2$ and up to 110 bar of CO at temperatures between 50-120 °C. This allows the clean isolation of the DME-adduct, $[Na(OCP)(dme)_2]_2$, or by addition of dioxane, $[\{Na(O\text{-}C{\equiv}P)(dioxane)_{2.5}\}_\infty]$. Both of these sodium salts can be handled in air and only slowly hydrolyse in deoxygenated water.[153] An alternative synthesis of $[Na(OC{\equiv}P)(dme)_2]_2$ was later published by Krummenacher and Cummins using $[Na(Et_2O)][(C_6F_5)_3BPNb(N[Np](3,5\text{-}C_6H_3Me_2)_3]$ (Np = neopentyl) and $CO_2$ before the

resulting complex, $[Na(OC{\equiv}P)(dme)_2]_2$, was crystallised from 1,2-dimethoxyethane and pentane (**Scheme 1.51**).[154]

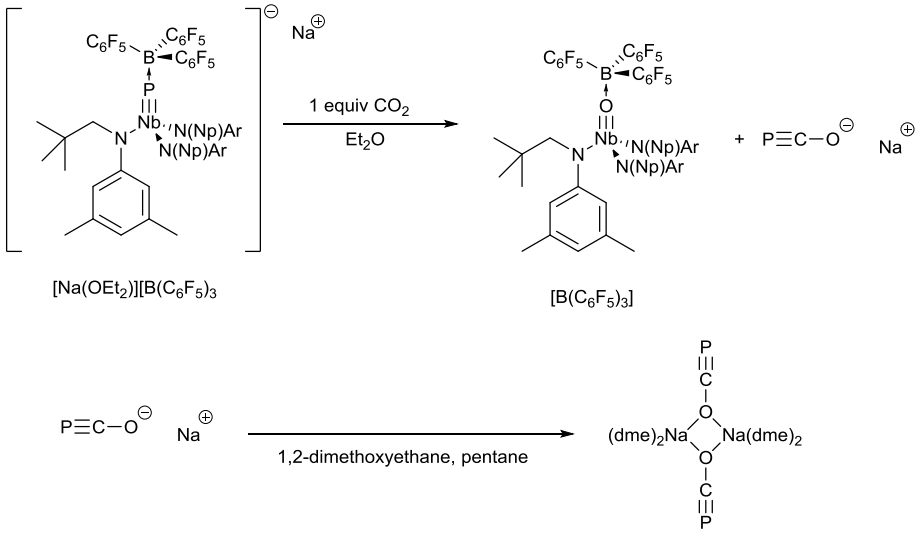


**Scheme 1.51**: Synthesis of $[Na(OC{\equiv}P)(dme)_2]_2$.[154]

An additional method for the synthesis of $^{-}OC{\equiv}P$ uses a dimethylformamide solution of $K_3P_7$ and [18]crown-6 with one atmosphere of CO, which is heated to 150 °C for 24 hours to afford [K(18crown-6)][OC≡P]. This formation was confirmed by $^{31}P\{^1H\}$, ($\delta_P$ = −396.8) and $^{13}C\{^1H\}$ ($\delta_C$ = 170.3, $^1J_{P\text{-}C}$ = 62 Hz) spectroscopy, alongside X-ray diffraction and the presence of the P≡C stretching mode at 1730 $cm^{-1}$ in the IR spectrum. The 2-phosphaethylyl anion readily undergoes cycloaddition reactions in a similar manner to other phosphaalkynes.[155] The reactivity of $O\text{-}C{\equiv}P^-$ has also been explored, firstly by Grützmacher who notes that the anion can be used as a phosphide transfer agent to yield an *N*-heterocyclic carbene stabilised phosphinidene (**Scheme 1.52a**).[156] Secondly by Goicoechea who reported that the reaction of $O\text{-}C{\equiv}P^-$ with cyclotrisilenes leads to the addition of CO and P across the Si=Si bond, and that the resulting $[P(CO)Si_3(Tip)_4]$- (Tip = 2,4,6- triisopropylphenyl) can undergo pyrolysis to remove the carbonyl group and generate $[PSi_3(Tip)_4]^-$, directly incorporating the phosphide into an unsaturated ring system (**Scheme 1.52b**).[157]

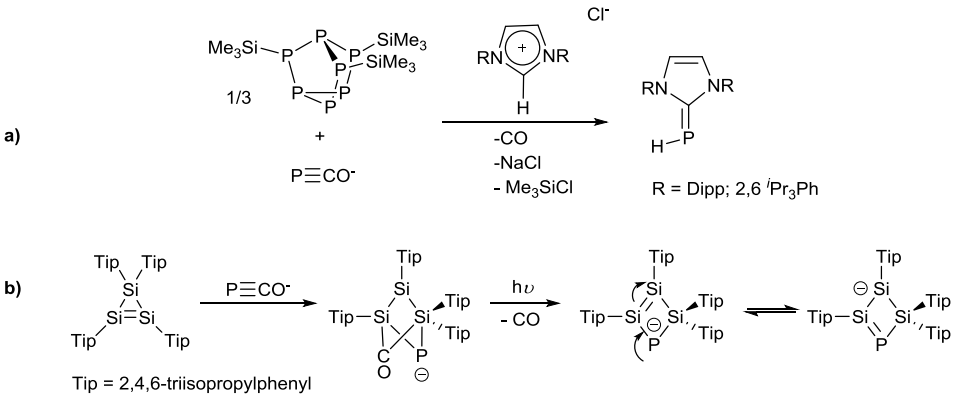


**Scheme 1.52**: Reactivity of $^{-}$OC≡P.[156, 157]

### 1.2.1.6 Reactivity of phosphaalkynes

The reactivity of the P≡C triple bond is primarily based on its addition behaviour, specifically the facile conversion of phosphaalkynes ($\lambda^3$-$\sigma^1$) into phosphaalkenes ($\lambda^3$-$\sigma^2$). This reaction often results in phosphacyclic compounds which contain the reactive doubly bonded unit 'P=C'.

#### 1.2.1.6.1 Cycloaddition reactions

Like alkynes, phosphaalkynes can readily undergo a range of cycloadditions with transition-metal and main group fragments resulting in a variety of heterocyclic compounds.[158] Indeed, [2+1] cycloadditions of phosphaalkynes have been shown to occur with a variety of reagents including carbenes,[159] silylenes[160] and germylenes.[161] These give three membered heterocycles containing P=C bonds which then show further reactivity; for example AdC≡P (Ad = Adamantyl) or 2-$CH_3(C_6H_{10})$C≡P undergo a double cycloaddition with $Mes_2Si(SiMe_3)_2$ to afford phosphadisilacyclobutenes (**Scheme 1.53a**), while Wagner showed that cycloadditions with 1-chlorocarbenes allow access to 1-chlorophosphirenes (**Scheme 1.53b**).[162]

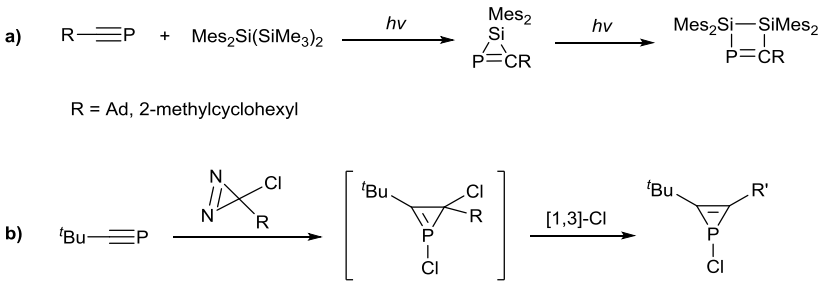


**Scheme 1.53:** Examples of [2+1] additions to give **a)** phosphadisilacyclobutene,[160] and **b)** 1-chlorophosphirenes.[162]

In contrast, [2+2] cycloadditions remain rare for phosphaalkynes, and it is unknown if the mechanism proceeds in a stepwise, or concerted fashion. For instance, when reacting $^{t}$BuC≡P with a Schrock carbene [(RfO)$_2$NArMo=CH$^{t}$Bu] (RfO = O-C(Me)CF$_3$)$_2$), the expected [2+2] cycloadduct undergoes a spontaneous [1,3] migration of an alkoxy group from the molybdenum centre to phosphorus to afford the phosphametallacycle shown in **Scheme 1.54a**.[163] The phosphaalkyne, $^{t}$BuC≡P has also been shown to react with one equivalent of the stannylidene [Sn{CH(SiMe$_3$)$_2$}$_2$]$_2$ to form a distannaphosphacyclobutene (**Scheme 1.54b**).[164]

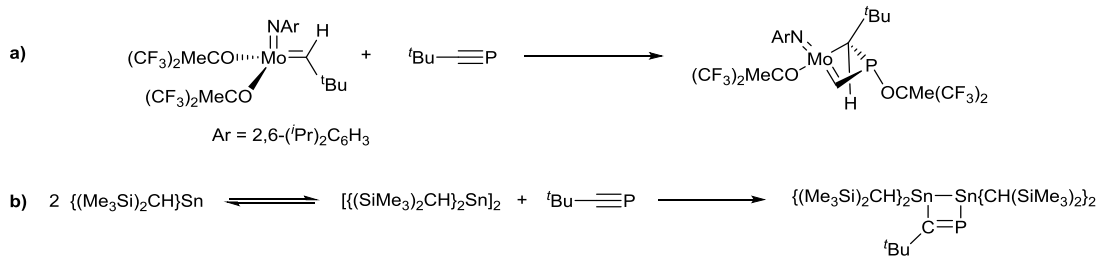


**Scheme 1.54:** [2+2] addition of $^{t}$BuC≡P to **a)** a carbene,[163] and **b)** a stannylidene.[164]

The [4+2] cycloaddition reaction of phosphaalkynes is also well studied, the initial cycloadduct tends to be unstable and can react further to give either an aromatic phosphinine[165] or react with an additional molecule of phosphaalkyne in an 'ene' type reaction to give the diphosphiranes shown in **Scheme 1.55**.[166] Further variations of cycloaddition reactions, such as [3+2] and [8+2] additions, have been discussed by Mathey[167] and Regitz in 2003,[158] along with Homo-Diels-Alder reactions and oligermisation reactions, which lead to complex cage compounds.

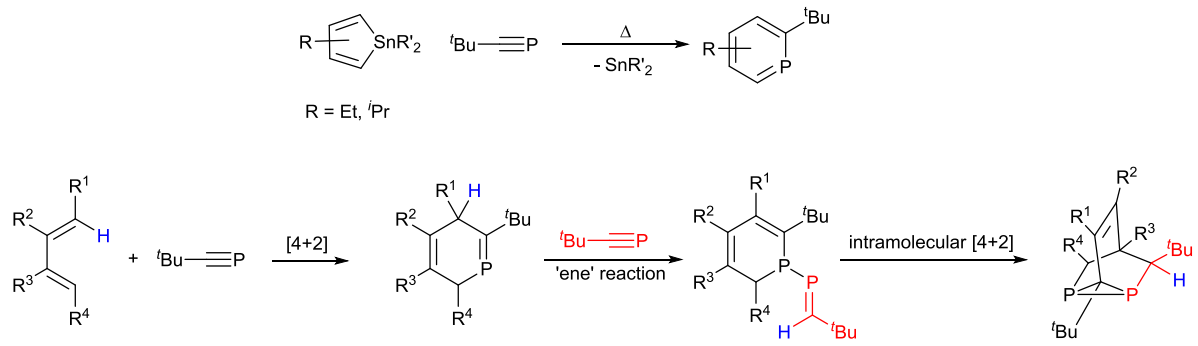


**Scheme 1.55:** Single [2+4] cycloaddition to give an aromatic phosphinine,[165] and the product of a further [4+2] addition.[166]

### 1.2.1.6.2 Formation and reactivity of aromatic rings

Phosphaalkynes are also commonly used as building blocks for carbon analogues of $\eta^4$, $\eta^5$ and $\eta^6$ ring systems. The most common precursor for these reactions is $^t$BuC≡P, although AdC≡P is also frequently used.[168]

In 1986, two papers independently described the cyclodimerisation of a phosphaalkyne by transition metal complexes[169,170] whereby two equivalents of $^t$BuC≡P were added to $[CpCo(C_2H_4)_2]$ to initiate a head-to-tail dimerization. This results in a 4-membered ring with alternating phosphorus and carbon atoms. Nixon *et al.* expanded upon this with various metal and Cp*analogues shown in **Scheme 1.56**.

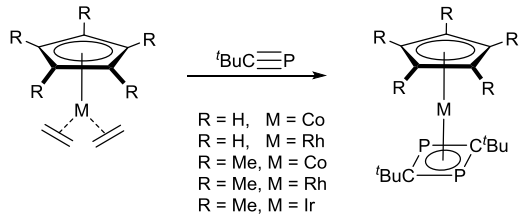


**Scheme 1.56:** First example of cyclodimerisation of a phospha-alkyne to a 1,3-diphosphacyclobutadiene.[169,170]

Diphosphacyclobutadienes can exhibit both $\eta^1$ and $\eta^4$ coordination modes. Nixon and co-workers describe the use of $[Rh(\eta^5\text{-}C_5H_5)(P_2C_2{}^tBu_2)]$ to displace the $C_2H_4$ units from $[RhCl(C_2H_4)_2]_2$ to give the hexa-rhodium complex shown in **Figure 1.12a**. This complex features both $\eta^1$ coordination of the phosphorus lone pair towards the $[RhCl]_2$ fragment, and $\eta^4$ coordination of the heterocycle towards $Rh(\eta^5\text{-}C_5H_5)$. The heterometallic system shown in **Figure 1.12b** results from the salt metathesis using $[K(thf)_4\{Co(P_2C_2R_2)_2\}]$ (R = Ad or $^t$pent) which was added to a THF solution of silver, gold or copper salts, the resulting products also display both $\eta^1$ and $\eta^4$ coordination modes.

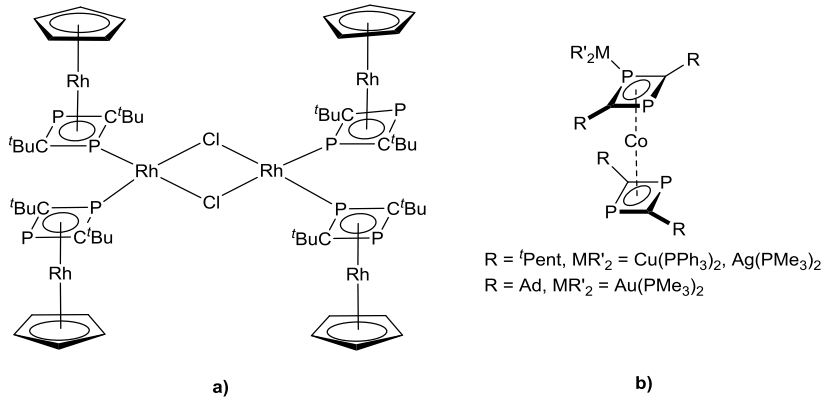


**Figure 1.12**: Product from the reaction of [Rh(η$^5$-$C_5H_5$)($P_2C_2{}^tBu_2$)] and [RhCl($C_2H_4$)$_2$] (**a**) and [M{Co($P_2C_2R_2$)$_2$}($PR_3$)$_2$] (**b**) exemplifies two types of phosphorus coordination modes in the same heterocycle.[171,172]

Bigger phosphorus-containing (5 and 6 membered) rings are also present in the literature, a notable example being 2,4,6-tri-tert-butyl-1,3,5-triphosphabenzene, which was first synthesised by Binger and co-workers in 1995, using a hafnium butadiene complex. A non-substituted COT (COT = 1,3,5,7-cyclooctatetraene) ring provides bulk to the hafnium complex. This reacts with three equivalents of $^t$BuC≡P to afford a phosphaalkyne trimer coordinated to the hafnium centre. The addition of $C_2Cl_6$ to this hafnium complex results in the liberation of free 1,3,5-triphosphabenzene shown in **Scheme 1.57a**. Conversely, the presence of a substituted COT ring (e.g. 1,4-bis(trimethylsilyl)cyclooctatetraene) on hafnium leads to the formation of a cyclic trimer upon addition of $^t$BuC≡P, the subsequent removal of the metal fragment with $C_2Cl_6$ affording triphosphadewar-benzene (**Scheme 1.57b**).[173]

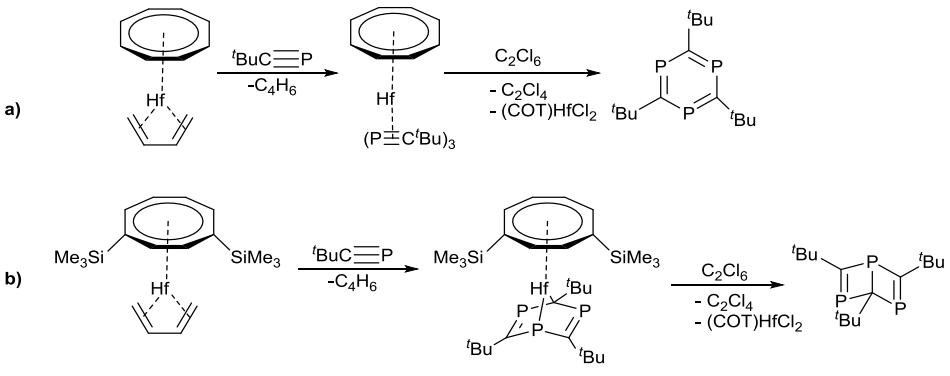


**Scheme 1.57:** Synthesis of triphosphabenzene using hafnium complexes.[173]

A more facile synthesis, reported in 1998 (**Scheme 1.58**) uses the vanadium imide $^{t}$BuN=VCl$_3$, which reacts with a variety of phosphaalkynes to form 1,3,5-triphosphabenzenes; in contrast, the 1,2-dimethoxyethane adduct of the vanadium complex leads instead to the formation of azatetraphosphaquadricyclanes.[174]

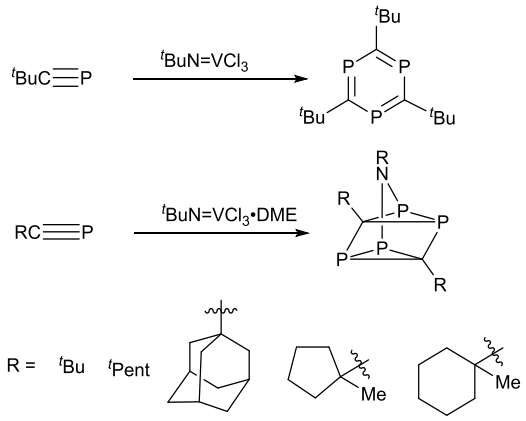


**Scheme 1.58:** Use of vanadium complexes with phosphaalkynes.[174]

The first example of coordination of these phosphabenzenes was documented by Nixon and co-workers, and afforded *trans*-[PtCl$_2$(PEt$_3$)(η$^1$-PC$_5$$^{t}$Bu$_3$)] as the kinetic product, which was characterised by $^{31}$P{$^1$H} NMR spectroscopic data. The platinum-phosphorus coupling of the phosphabenzene ($^1J_{P\text{-}Pt}$ = 2418 Hz), compared to that for PMe$_3$ ($^1J_{P\text{-}Pt}$ = 2901 Hz) implies a weaker σ-donation to the metal, this in turn indicates a tightly held lone pair, consistent with the high *s*-character.[175] Over time, the product isomerised to the thermodynamic *cis*-complex as shown in **Scheme 1.59**.[176] In 1996 Cloke, Nixon and co-workers reported the first η$^6$-coordinated complex, the scandium triple sandwhich shown in **Scheme 1.59b**, was characterised by X-ray crystallography. The planar 2,4,6-*tert*-butyl-1,3,5-triphosphabenzene is coordinated on each side by a scandium atom with a 1,3-diphospholide anion using metal vapour synthesis.[177] Cycloadditions with alkynes and alkenes are also known.[178]

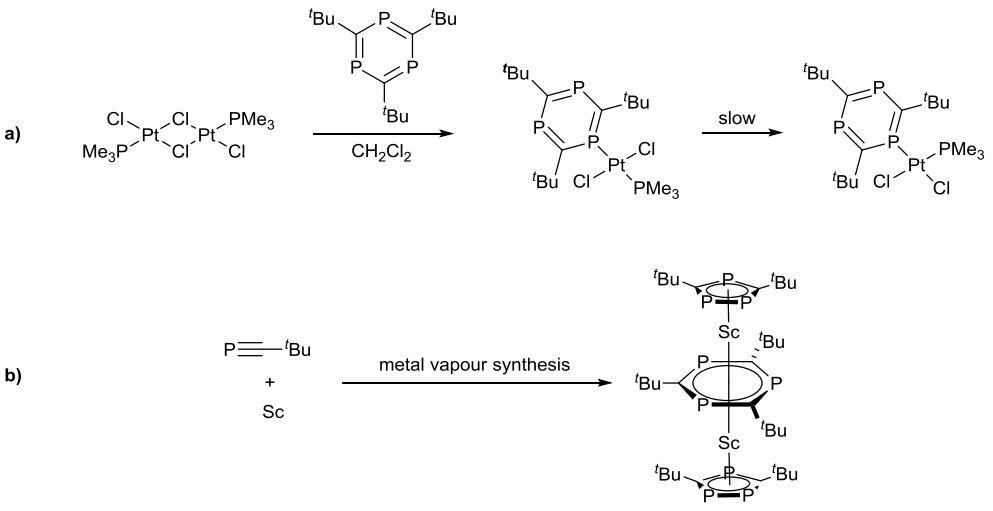


**Scheme 1.59**: The first examples of triphosphabenzene as a $\eta^1$ coordinated (**a**) and $\eta^6$ coordinated fashion (**b**) by Cloke, Nixon and coworkers.[175,177]

### 1.2.1.7 Coordination chemistry

Phosphaalkynes can coordinate to metal centres either through the lone pair ($\eta^1$) or, as a result of the higher energy of the π-system, through the P≡C bond ($\eta^2$) and even as a combination of both. The first reported metal-phosphaalkyne complex [Pt($\eta^2$-$^t$BuC≡P)($PPh_3$)$_2$] was reported in 1981 and exemplifies the $\eta^2$ side-on interaction between the triple bond and the platinum.[179] Since this first example, all the bonding modes shown in **Figure 1.13** have been demonstrated.[167]

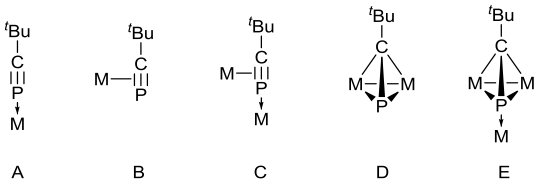


**Figure 1.13**: Coordination modes of phosphaalkynes: using RC≡P moiety as $\eta^2$ bridging and/ or P lone pair donor ligands.

A single crystal X-ray diffraction study of the first example of the $\eta^2$-bonding mode, revealed a significant change in C≡P bond length (1.672(17) Å)[179] compared to free $^t$BuC≡P (1.548(1) Å)[127] due to back-bonding from the platinum centre. Other mononuclear complexes with $\eta^2$-bonded

phosphaalkynes have been demonstrated with platinum, titanium and zirconium as shown in **Scheme 1.60**.

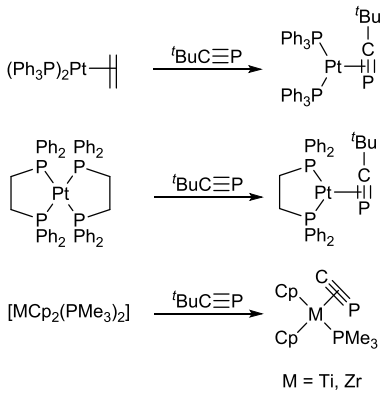


**Scheme 1.60:** Examples of side-on coordinated C≡P complexes.[179–181]

While the lone pair is energetically accessible, $\eta^1$-coordination can only be achieved with a suitable ligand system that impedes $\eta^2$ coordination to allow the end on coordination of RC≡P. The first examples of this were reported by Nixon in 1987 using $[M(dppe)_2(N_2)_2]$ (M = Mo, W) (dppe = 1,2-bis(diphenylphosphino)ethane) or $[Mo(depe)_2(N_2)_2]$ (depe = 1,2-bis(diethylphosphino)ethane) with $^t$BuC≡P.[182] Other examples include iron and rhenium-based dppe complexes (**Scheme 1.61**).

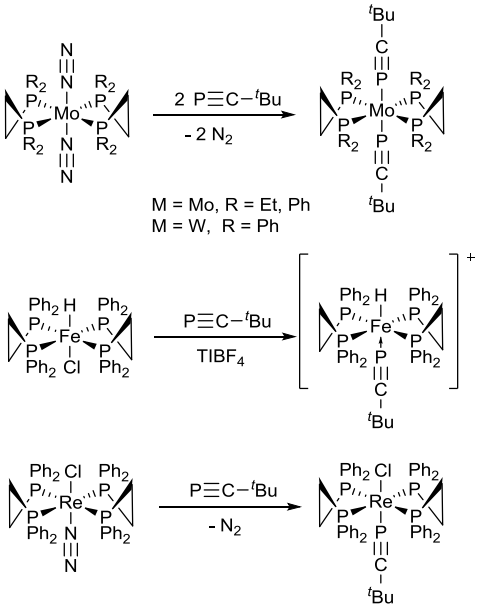


**Scheme 1.61:** Molybdenum, tungsten, iron and rhenium complexes of $^t$BuC≡P.[171,183]

The $\eta^1$, $\eta^2$ coordination mode remains rare, though Carmichael reported three examples in 1993,[184] and the bridging complexes where $^t$BuC≡P acts as both a 4 and a 6 electron donor ($\eta^2$:$\eta^2$ and $\eta^2$:$\eta^2$:$\eta^1$ respectively, **Scheme 1.62**) were reported by Nixon and co-workers in 1981 and 1982.

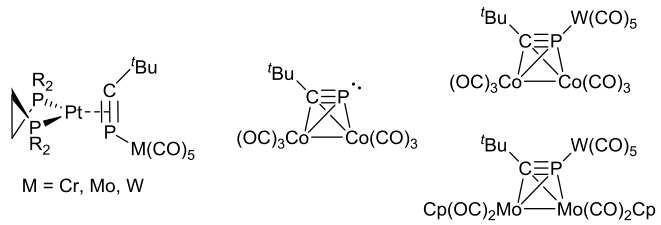


**Scheme 1.62:** Multi-metallic complexes of $^t$BuC≡P.[179,184,185]

### 1.2.1.7.1 Cyaphide complexes

The phosphorus analogue of cyanide, the cyaphide ligand (-C≡P) is a desirable system which has not yet been widely studied. The first suggested complex of a terminal cyaphide ligand "$Cl(Et_3P)_2Pt(C{\equiv}P)$"was observed *in situ* by Angelici in 1992 (**Scheme 1.63**).[186] The cyaphide unit was later trapped by addition of $[Pt(PEt_3)_4]$ to form $[Cl(Et_3P)_2Pt(\mu\text{–}\eta^1\text{:}\eta^2\text{-}C{\equiv}P)Pt(PEt_3)_2]$, the structure of which was confirmed in the solid state by X-ray diffraction studies.[187] The $^{31}P\{^1H\}$ NMR spectroscopic data of a solution phase species were considered consistent with a cyaphide unit, as the resonance at 68.0 ppm ($^3J_{P\text{-}P}$ = 9.13, $^1J_{Pt\text{-}P}$ = 303 Hz) displays a lower magnitude coupling to the platinum centre, when compared to the *trans*-$PEt_3$ groups (δ = 7.3, $^2J_{P\text{-}P}$ = 9.16, $^2J_{Pt\text{-}P}$ = 2871 Hz). This platinum coupling is consistent with greater separation of metal and phosphorus in the cyaphide unit, especially when compared with the additional $Pt(PEt_3)_2$ unit of the trapped system (δ = 18.6 ($^1J_{Pt\text{-}P}$ = 3619, $^3J_{P\text{-}Pt}$ = 137 Hz, $PEt_3$)).[186,187]

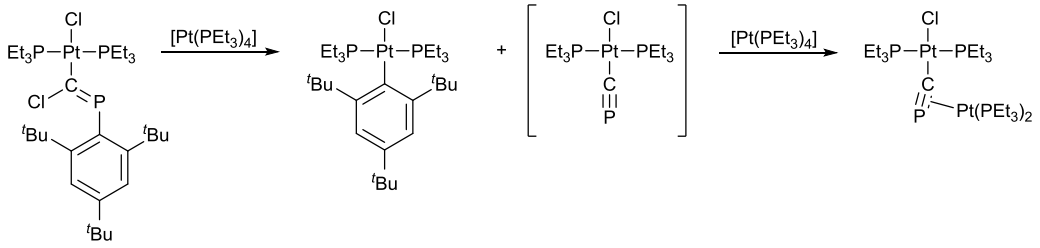

**Scheme 1.63**: Synthesis of platinum-cyaphide complex and subsequent trapping with $[Pt(PEt_3)_4]$.[186,187]

Fourteen years later, Grützmacher published the first irrefutable, crystallographically characterised example of a terminal cyaphide complex *i.e.* [Ru{C≡P}(H)(dppe)$_2$]. This was formed by a reaction of the η$^1$ dppe complex [Ru(H)(dppe)$_2${P≡CSiPh$_3$}], with NaOPh, which converted the phosphaalkyne into the terminal cyaphide ligand, affording [Ru(H)(dppe)$_2$(C≡P)] (**Scheme 1.64**).

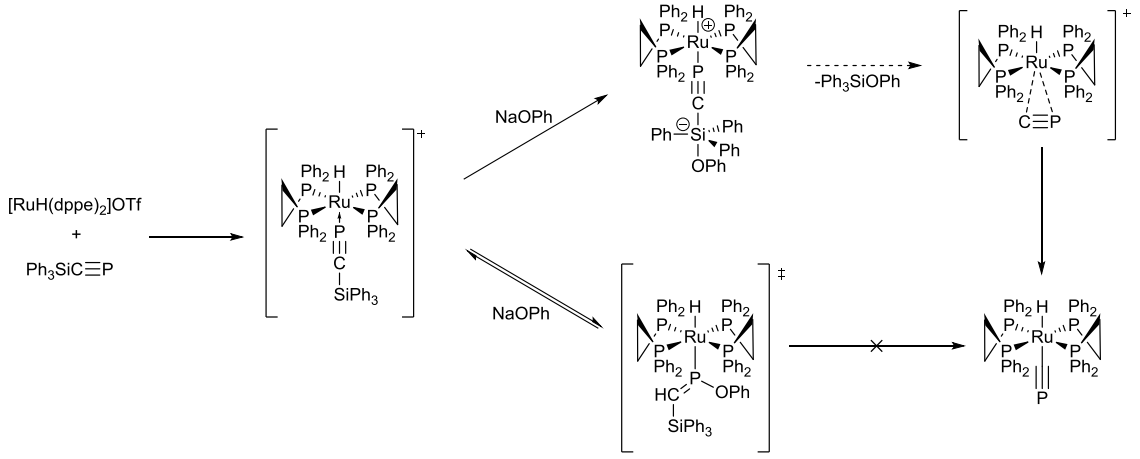


**Scheme 1.64:** Suggested conversion from η$^1$-phosphaalkyne to cyaphide *via* isocyaphide intermediate.[137,188]

Grützmacher suggested the mechanism for the formation of the cyaphide complex proceeds *via* nucleophilic attack of the PhO$^-$ ion on the silicon, to give PhOSiPh$_3$ and the isocyaphide intermediate [Ru(H)(dppe)$_2$(P≡C)], which rearranges to bond through the carbon to give [Ru(H)(dppe)$_2$ (C≡P)]. A second species was observed *in situ*, *via* $^{31}$P{$^1$H} NMR spectroscopy and based upon computational studies, it was assumed to be formed from the reversible nucleophilic attack on phosphorus, instead of silicon.[137,188]

Russell has suggested the synthesis of a mixed phosphaalkyne-cyaphide complex [Mo(Me$_3$SiC≡P)(C≡P)(dppe)$_2$]$^-$ through the addition of TBAT (TBAT = [NBu$_4$][Ph$_3$SiF$_2$]) to the solution of [Mo(P≡CSiMe$_3$)$_2$(dppe)$_2$].[189] The soluble fluoride anion source was more successful than reaction with NaOPh, which led to either no reaction, or complete decomposition. After heating with TBAT in THF, $^{31}$P{$^1$H} NMR spectroscopy showed the disappearance of the quintet and triplet resonances from the η$^1$-complex, and showed instead a doublet of doublets ($\delta_P$ = 65.6) and two complex multiplets ($\delta_P$ = 197.8 and 183.0). This shows the non-dppe phosphorus atoms are now inequivalent, and with similar changes in chemical shift to that from the transformation of [RuH(dppe)$_2$(P≡CSiPh$_3$)]$^+$ into [RuH(dppe)$_2$(C≡P)] shown by Grützmacher

(**Scheme 1.64**).[137,188] The case for an isolated mixed-cyaphide complex is further evidenced by $^{19}F$ NMR data showing the presence of $SiMe_3F$, further suggesting the removal of one $SiMe_3$ group from the complex and therefore a mixed phosphaalkyne-cyaphide complex of type $[Mo(Me_3SiC{\equiv}P)(C{\equiv}P)(dppe)_2]^-$ (**Scheme 1.65**) is the likely product of this reaction. Further characterisation has not yet been reported.[189]

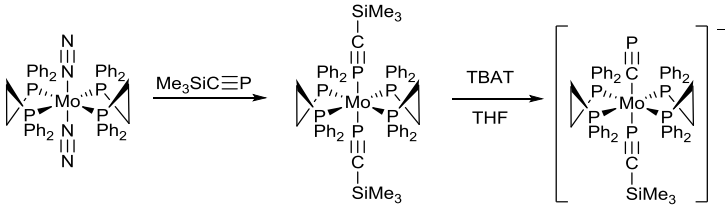


**Scheme 1.65**: Coordination of $Me_3SiC{\equiv}P$ to molybdenum complex, with possible conversion to a cyaphide complex.[189]

More recently, Crossley and co-workers have furnished a number of other cyaphide complexes shown in **Scheme 1.66**, using the phosphaalkyne $Me_3SiC{\equiv}P$ in a similar method to that employed by Grützmacher. These new cyaphide complexes include a *trans*-alkynyl ligand, and the conjugated cyaphide-alkynyl systems have been studied by both computational and electrochemical methods.[190,191]

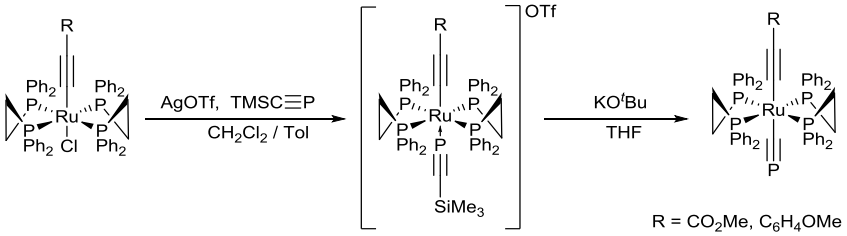


**Scheme 1.66:** Synthetic route to conjugated phosphaalkynes.[191]

## 1.2.2 Phosphaalkenes

### 1.2.2.1 General details

Phosphaalkenes are tervalent phosphorus derivatives featuring a double bond between carbon and phosphorus. As generally highly reactive species, they cannot be observed under standard

conditions unless they are stabilised by conjugation, steric hindrance or within the coordination sphere of a metal. In the absence of these stabilising effects, phosphaalkenes have a tendency to oligomerize, with head-to-head and head-to-tail dimers having been observed.[192,193]

As with their triply-bonded counterpart, comparisons between C=C, C=P and C=N reveal that P=C bond is more similar in nature to the C=C bond, rather than the C=N bond. This is in part due to the difference in nature of the frontier molecular orbitals of C=N and C=P systems (**Figure 1.14**). The HOMO of $H_2C$=NH is heavily associated with, and therefore the compound reacts almost exclusively through, the lone-pair on nitrogen. In contrast the HOMO of $H_2C$=PH is associated with its π-system, (which is closer in energy to that of ethene (−10.51 eV), than to $H_2C$=NH (−10.62 eV)) though the lone pair is close in energy to the HOMO. Since the energies of the π-system and the lone pair are similar, the P=C moiety is able to react at both sites. In cases where a desired reaction at the lone pair is impeded by the competition from the lone pair, the reactivity can be directed to the π-system, by first occupying the lone pair (*via* $\eta^1$ coordination to a metal centre).

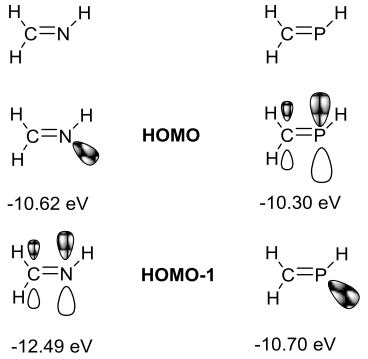


**Figure 1.14**: Frontier orbitals of imine and phosphaethylene.[194]

The electronegativity of phosphorus (χ = 2.2) lies closer to that of carbon (χ = 2.5) than nitrogen (χ = 3.0) on the Pauling scale, yet phosphorus is still slightly electropositive and this causes the P=C bond to have some polarity.[117] The charge distribution on the 'P=C' unit consists of a slight positive charge on phosphorus due to polarisation of the sigma bond shown in **Figure 1.15**, however, the 'inverse' charge distribution has been observed on select examples of phosphaalkenes, and depends on the substituents on carbon. These 'inverse' phosphaalkenes resonate at much lower frequencies, for example the $^{31}P\{^1H\}$ NMR resonance for $HP^{\delta-}=C^{\delta+}(NMe_2)_2$ is −62.6 ppm,[195] compared to simple phosphaalkenes typically displaying a

resonance of $\delta_P$ = 200−300.[196] The difference in charge between inverse and standard phosphaalkenes is very small, such that 'P=C' itself is considered essentially apolar until you consider the substituents. Regitz and co-workers synthesised the first examples of an inverse π-electron distribution at the exocyclic P=C double bond, in a series of phosphatriafulvenes shown in **(Figure 1.16a)**.[197] This was followed by other examples such as those by Gröbe where the $^{31}P\{^1H\}$ NMR spectra of $F_3CP{=}C(F)NR_2$ (**Figure 1.16b**) gave resonances at an unusually low frequency ($\delta_P$ ~ −9).[198,199] The polarisation is even more pronounced in phosphaalkenes with two amino substituents on the carbon atom such as those shown in **Figure 1.16c**.[200]

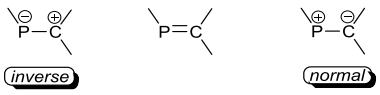


**Figure 1.15**: 'Normal' phosphaalkenes with an electrophilic phosphorus and nucleophilic carbon atoms, and the opposite ('inverse') distribution.

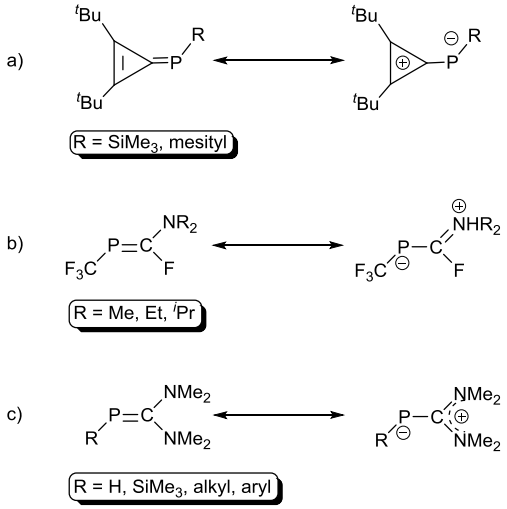


**Figure 1.16**: A series of phosphatriafulvenes, Zwitterionic structure of **a)** 2,3-di-tert-butylcyclopropylidene phosphanes. [197] **b)** $F_3CP{=}C(F)NR_2$ **c)** $RP{=}C(NMe_2)_2$.[195,197–199]

#### 1.2.2.1.1 Isomerisations

The stereochemistry of phosphaalkenes and their complexes is important because the orientation for the substituents around the P=C moiety dictates the coordination mode.

Phosphaalkenes exist as both *E*- and *Z*- isomers due to lack of rotation around the double bond. The atom bound directly to the phosphaalkenic carbon determines the *E*/*Z* assignment on the basis of its molecular mass (the greater the mass, the higher the priority), the lone pair on the phosphorus is always the lowest priority, due to its negligible mass. In situations where both isomers are present, general trends suggest that the *Z*-isomer is identifiable in both the $^{13}C\{^{1}H\}$ and $^{31}P\{^{1}H\}$ NMR spectroscopic data as it tends to exhibit a chemical shift to lower frequencies, and a larger carbon-phosphorus coupling constant when compared to the *E*-isomer.[201] The compound *E*/*Z*-{$C_6H_2$(2,6-Mes)$_2$(4−Br)}P=C(H){$C_6H_4$(4-Br)} represents the only reported example whereby both the *E*- and *Z*-isomer have been crystallographically characterised. These data demonstrate a longer C=P bond in the *E*-configuration, which is consistent with the reduced magnitude observed for the smaller one bond carbon phosphorus coupling constant.[202]

### 1.2.2.2 Synthetic routes towards phosphaalkenes

#### 1.2.2.2.1 Using [1,3] silatropic shifts

The majority of syntheses towards phosphaalkenes involve 'The Becker's condensation', which features a 1,3 silatropic rearrangement (**Scheme 1.67**).[203] The reaction is driven by the oxophilicity of silicon and the resulting phosphaalkene is stabilised by the bulk of the groups on carbon. In the case of the first synthesis of the phosphaalkene PhP=C$^{t}$Bu(OSiMe$_3$), stabilisation is achieved by the bulk of the $^{t}$Bu and silyoxy groups on carbon (**Scheme 1.67a**). However, disadvantages of this method include the expense and sensitive nature of the precursor, RP(SiMe$_3$)$_2$.

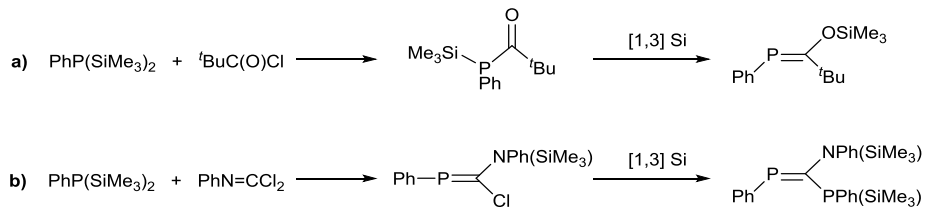


**Scheme 1.67**: 1,3 sigmatropic rearrangement for the formation of phosphaalkenes, **a)** with carbonyl functionality, **b)** using nitride.[203,204]

Appel and co-workers continued to investigate using this method, and synthesised the first phosphaketene upon the addition of phosgene to $^{t}$BuPR(SiMe$_3$) (R=H, SiMe$_3$) to furnish $^{t}$BuP=C=O.[205] They also demonstrated that the carbonyl functionality (**Scheme 1.67a**) can be replaced with nitride (**Scheme 1.67b**).[204] Schmidt later extended this work to a range of other nitrides to include carbodiimides (RN=C=NR')[206] and iminoyl chlorides (ClR'C=NR").[207]

#### 1.2.2.2.2 Using dehydrohalogenation

The classic 1,2 elimination reaction for the formation of phosphaalkenes uses precursors of the form RP(Cl)-CHR'$_2$ with a base such as DBU, to liberate HX. This was first employed by Bickelhaupt in the synthesis of *P*-mesityldiphenylmethylenephosphine, which was described as "the first thermally stable phosphaalkene with a localised, all carbon subsituted phosphorus-carbon double bond."[208] The precursor alkylphosphane was prepared by the addition of the lithium reagent LiCHPh$_2$ to MesPCl$_2$. The alkylphosphane undergoes dehydrohalogation upon addition of DBU in THF to afford the aryl-conjugated phosphaalkene almost quantitatively (**Scheme 1.68**).

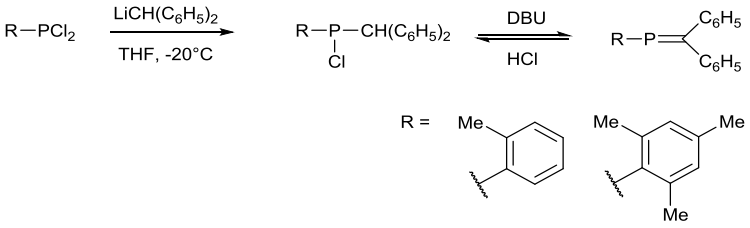


**Scheme 1.68**: Synthesis of RP=CPh$_2$ *via* dehydrohalogenation.[208]

#### 1.2.2.2.3 Alternative Methods

The Phospha-Peterson reaction (**Scheme 1.69**) features condensation of primary phosphines with suitable carbonyl derivatives to form highly stabilised phosphaalkenes.

**Scheme 1.69a** demonstrates the formation of the P=C bond through the reaction of ArP(Li)SiMe$_2$$^{t}$Bu with pyridinecarboxaldehyde. The *E*-isomer of the resulting product has been shown to act as a chelating ligand upon addition to Cu(NCCH$_3$)$_4$•PF$_6$.[209] Yoshifuji *et al.* have also reacted ArP(Li)SiMe$_2$$^{t}$Bu with benzaldehyde to afford *E*-[ArP=C(H)Ph], which interconverts to the *Z*-isomer using UV irradiation.[210]

**Scheme 1.69b** demonstrates that similar reactivity is observed with $PhPH_2$ and carboxylic acid amide acetals.[211]

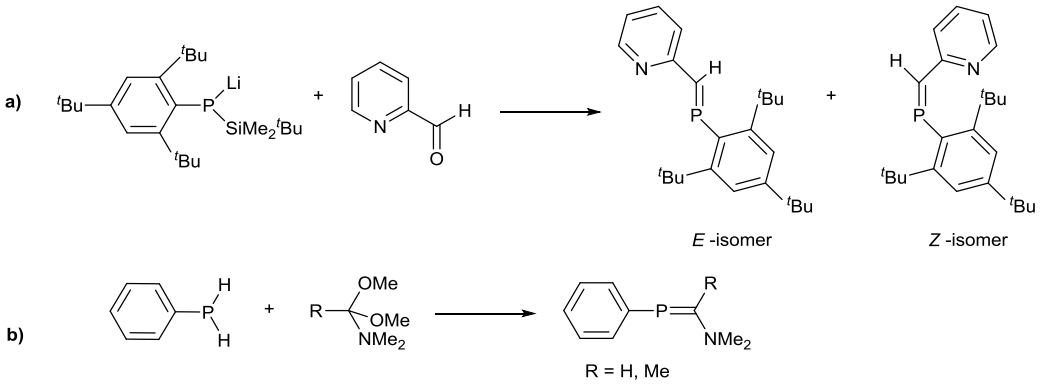


**Scheme 1.69**: Phospha-Peterson reactivity using carbonyl compounds; pyridinecarboxaldehyde (**a**) and carboxylic acid amide acetals (**b**).[209,211]

Phosphaylids (**Scheme 1.70**) are "reasonably stable" when bulky groups are present at the two-coordinate phosphorus atom. These are readily obtained from dichlorophosphanes, trialkylphosphanes and zinc in THF, and react with aldehydes to afford the corresponding phosphaalkenes.[212] The reliance on bulky groups for stability around phosphorus can be removed through coordination of phosphorus, for example in **Scheme 1.70c**, the use of $[W(CO)_5]$ stabilises the starting phospha-ylide and the resulting phosphaalkene.[213] More recently Mathey and co-workers expanded upon this reaction, and inserted $[RP\text{-}W(CO)_5]$ into the P-H bond of $Ph_2P(O)H$, the resulting Phospha-Wittig reagent and its reactivity with PhCHO, and excess 2,3-dimethyl-1,3-butadiene are shown in **Scheme 1.70d**.

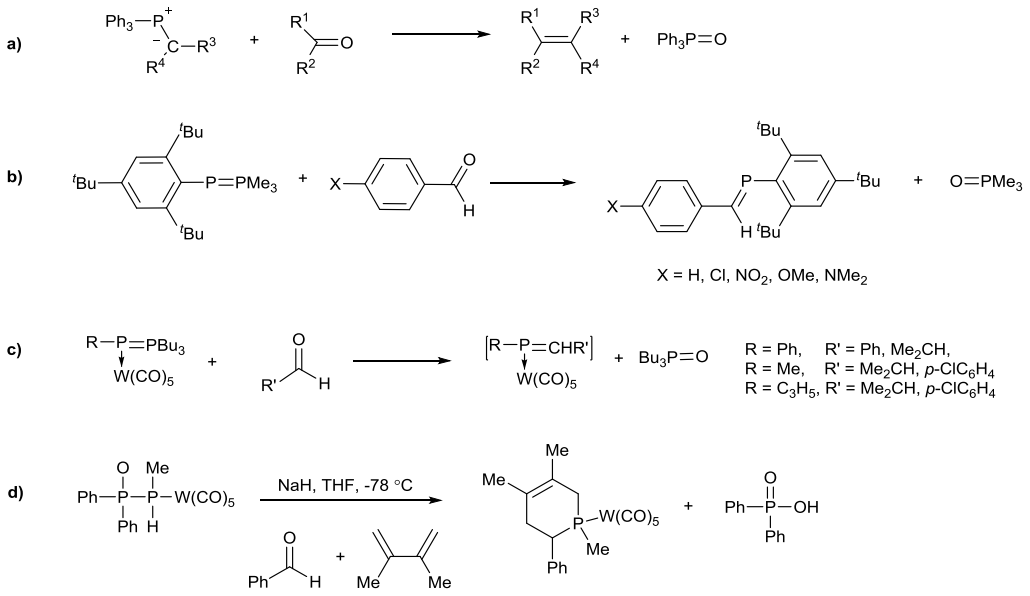


**Scheme 1.70**: Generic Wittig reaction (**a**) compared to the Phospha-Wittig reaction as presented by Shah, (**b**)[212] and Mathey (**c** and **d**).[213]

The synthesis of phosphaalkenes using Wittig type chemistry has also been demonstrated using transition metal terminal phosphinidene complexes, with a number of carbonyl compounds and organohalides (**Scheme 1.71**). In 1993, Schrock used a bulky aldehyde to form a phosphaalkene from C=O addition to the Ta=P bond, *via* a 4-membered metallacyclic intermediate.[214] In 1995 Breen and Stephan showed that halogenated compounds such as $CH_2Cl_2$ and chloroform react with [$Cp_2Zr(PMe_3)$=PMes*] to form the phosphaalkene ($H_2C$=PMes), alongside [$Cp_2ZrCl_2$] and $PMe_3$.[215]

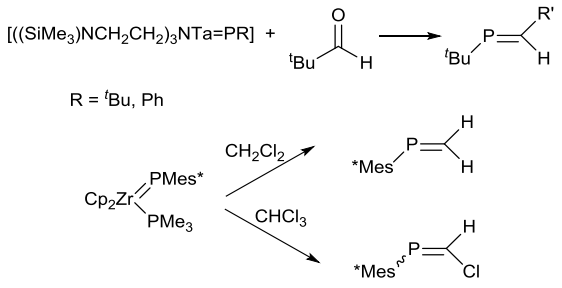


**Scheme 1.71**: Metal-mediated synthesis of phosphaalkenes from bulky aldehydes and organohalides.[214,215]

### 1.2.2.3 Reactivity

The small energy gap between the π-system and the lone pair of phosphaalkenes means electrophilic reagents do not always discriminate between the two, but commonly reactions tend to invoke the P=C π-system. **Scheme 1.72** illustrates the addition of MeOH across the P=C bond of 'normal' polarity phosphaalkenes (to form a 'CH' unit) and 'inverse' phosphaalkenes (to form a PH unit).

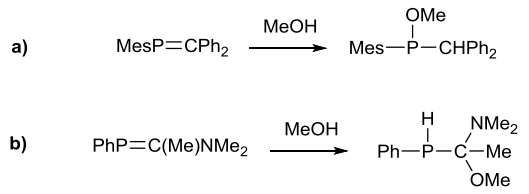


**Scheme 1.72**: Phosphaalkenes with **a)** 'normal' polarity, and **b)** 'inverse' polarity.

#### 1.2.2.3.1 Coordination chemistry

Coordination chemistry of low coordinate phosphorus species became more than just academic curiosity when applications of phosphaalkene complexes in homogeneous catalysis were discovered.[216] Five coordination modes are known for phosphaalkene complexes which are illustrated in **Figure 1.17**. Type **A** shows the coordination of the lone pair of phosphorus, which still allows the practically unaffected structure of the P=C bond to be accessible for reactions. An increase in coordination number from three to four is demonstrated by type **B**, whereas in type **C**, the P=C bond is elongated due to ligand-to-metal electron donation from the occupied π-orbital, and metal to ligand back-donation into the π* orbital. Types **D** and **E** are 4-electron complexes which show π-coordination in addition to the involvement of the phosphorus lone pair. These types are identified by the characteristic shift to lower frequency in the $^{31}P\{^{1}H\}$ NMR spectrum,[217] which is accompanied by a sharp decrease in $^{1}J_{(P\text{-}M)}$ coupling.

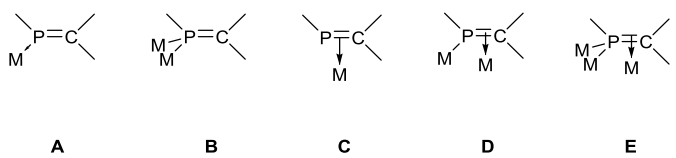


**Figure 1.17: A**-**E** show different coordination numbers and geometries for the known types of phosphaalkene coordination complexes.

The most common coordination mode is **A**, first reported independently in 1981 by the groups of Nixon and Bickelhaupt; both group utilised $MesP{=}CPh_2$ to form a complex with chromium by displacing CO from $[Cr(CO)_5(thf)]$ to form *cis*-$[M(CO)_4(P(Mes){=}CPh_2)_2]$.[218,219] Nixon *et al.* also expanded the range of metal centres to include various molybdenum, tungsten, rhodium and platinum complexes featuring the $\eta^1$ coordination of $MesP{=}CPh_2$ to the metal centre. The crystallographic data reported by Bickelhaupt confirmed the geometry, and shows the P=C bond length (1.65 Å) is similar to the free phosphaalkene (1.67(4) Å). [85]

The alternative coordination mode **C**, involves interaction of the π-system of the phosphaalkene with the metal centre. The first instance of a proven solid state $\eta^2$-coordination mode was reported in 1983. Al-Resayes *et al*. describe the synthesis of $[Pt(PPh_2CH_2)_3CMe\{P(Mes){=}CPh_2\}]$. The $^{31}P\{^1H\}$ NMR data reveal weaker coupling to platinum ($J_{Pt\text{-}P}$ = 467 and 455 Hz for the different isomers) than would otherwise be expected when compared to the $\eta^1$ coordinated $[Pt\{P(Mes){=}CPh_2\}_3]$ ($^1J_{Pt\text{-}P}$ = 4946 Hz). This weaker coupling implies that the phosphorus lone pair is not involved in bonding, this is suggested to be primarily due to its high *s*-character, and is therefore directed away from platinum.[220]

An equilibrium between type **A** and type **C** can sometimes occur. For example the platinum complex, $[Pt(PPh_3)_2\{(Mes)P{=}CPh_2]$, exists with an $\eta^1$-coordination mode in the solid state, which was unambiguously established by X-ray crystallography. However, low temperature (−55 °C) solution state $^{31}P\{^1H\}$ NMR data show inequivalent $PPh_3$ ligands and that the phosphaalkene phosphorus ($\delta_P$ = −33.5) is shifted to significantly lower frequency compared to the free phosphaalkene ($\delta_P$ = 233), which appears to be unusually large. This, when combined with the phosphorus-platinum coupling ($J_{Pt\text{-}P}$ = 505 Hz) being significantly weaker than expected led to Bickelhaupt and co-workers to suggest that the complex might exist in the $\eta^2$ coordination mode in the solution state, and $\eta^1$ in the solid state.[221] An alternative explanation could be that the complex exists in both coordination modes in the solution state under ambient conditions, and one of these preferentially crystallises.

The first phosphaalkene complex featuring both $\eta^1$ and $\eta^2$ coordination modes was synthesised by Mathey and co-workers.[222] Lithium(3,4-dimethylphospholyl) was reacted with $[W(CO)_5(thf)]$ before protonating the resulting anion, to generate the phospholyl with two $[W(CO)_5]$ units coordinated. The novel complex featuring both $\eta^1$ and $\eta^2$ coordination was exemplified by X-ray diffraction data (**Scheme 1.73**).[222]

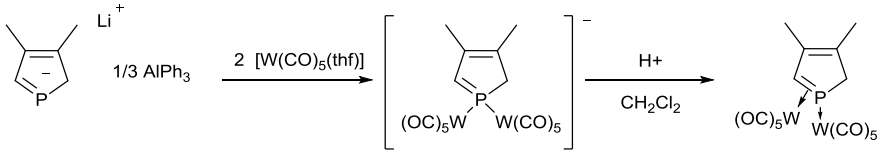


**Scheme 1.73**: Synthesis of the first metal phosphaalkene complex with $\eta^1$ and $\eta^2$ bonding.[222]

### 1.2.2.3.2 Cycloaddition reactions

Cycloaddition reactions with phosphaalkenes can yield 1-chlorophosphiranes, *via* a [2+1] cycloaddition with chlorocarbenes,[223] (**Figure 1.18a**), and aromatic heterophospholes using a [2+3] cycloaddition with 1,3-dipole compounds (**Figure 1.18b**).[224] Diels-Alder [4+2] reactions are also common as well as [2+4] and [2+8] addition reactions. In addition to 'ene' reactions, [1,5] and [3,3] sigmatropic shifts, 4π and 6π electrocyclisations, which further demonstrate the analogy between C=C and P=C bonds, have been explored and are reviewed extensively by Nixon, Dillon and Mathey.[117] Conjugated or cumulated phosphapolyenes also demonstrate comparable chemistry to their all-carbon analogues.[117]

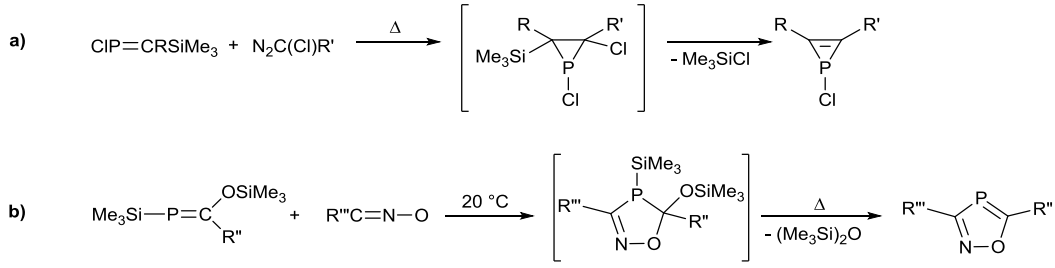


**Figure 1.18:** Cycloaddition reactions **a**) [2+1] cycloaddition **b**) [2+3] cycloaddition.[223,224]

### 1.2.2.3.3 Phosphinines

Monophosphinines are considered the phosphorus analogues of pyridines, these planar aromatic 6-membered rings include a phosphorus atom and are also analogues of benzene. The first example was isolated from the reaction of $[C_5H_6Sn(^nBu)_2]$ with $PBr_3$, to furnish $C_5H_5P$ as an air sensitive solid.[225] Derivatives have been more recently synthesised from phospholides with acyl chlorides,[226] while other phosphinines such as triphosphabenzenes are generated from corresponding phosphaalkynes, as indicated from **Scheme 1.74**.[174] These aromatic phosphorus heterocycles are ambidentate ligands, with two potential coordination sites, either the lone pair on the phosphorus atom, or the aromatic π-system. The various

coordination modes of phosphinenes and a discussion of their development in homogenous catalysis have been reported in reviews by Müller.[227,228]

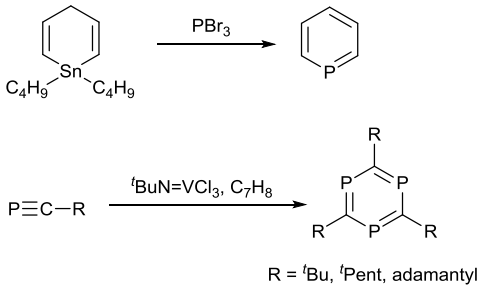


**Scheme 1.74**: Synthesis of phosphabenzenes.[174,225]

### 1.2.2.4 Metallaphosphaalkenes

It should be possible to replace any of the 'R' groups on a phosphaalkene unit with a metal fragment; this gives five possible motifs which are shown in **Figure 1.19**, the first four of which (**A**-**D**) have already been realised. The majority of metallophosphaalkenes published are either types **A** or **B**, referred to as *C*- or *P*-metallaphosphaalkenes respectively.

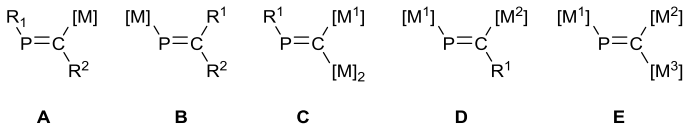


**Figure 1.19**: Proposed geometries of metallaphosphaalkenes.

#### 1.2.2.4.1 *C*-Metallaphosphaalkenes

The first example of this type of complex, [Cp*(CO)(NO)Re-C(OSiMe$_3$)=P$^t$Bu], was published by Weber in 1985 (**Scheme 1.75**).[229] The Re-C=P fragment was confirmed by the characteristic four bond P-C coupling between phosphorus and the SiMe$_3$ group ($^4J_{P\text{-}C}$ = 8.4 Hz). The phosphaalkene initially forms the *E*-isomer ($\delta_P$ = 240.1) which slowly rearranges to the *Z*-isomer ($\delta_P$ = 272.8). The configuration of the P=C bond was determined spectroscopically by $^{13}C\{^1H\}$ NMR data and the *Z*-isomer was additionally confirmed by X-ray data.[229]

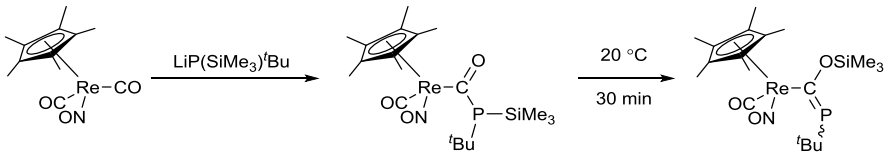


**Scheme 1.75**: First example of *C*-metallaphosphaalkene.[229]

*C*-lithiophosphaalkenes can be made from the lithium/halogen exchange of *C*-halogenated phosphaalkenes using alkyllithium reagents. An example of this is shown in **Scheme 1.76a** where $^{n}$BuLi is added at low temperatures in THF to form (*E*)- and (*Z*)-phosphaethenyllithiums in a 1:5 ratio, as determined by $^{31}P\{^{1}H\}$ NMR spectroscopic data ($\delta_P$ = (*E*); 369.7, (*Z*); 254.6).[230] Lithium/hydrogen exchange can also be used to generate the *C*-lithiophosphaalkene shown in **Scheme 1.76b** which was identified by quenching with methyl iodide, as the lithiophosphaalkene decomposes at ambient temperature to the Mes*C≡P.[231] The *Z*-isomer of the *C*-lithiophosphaalkene shown in **Scheme 1.76c** has been shown to further undergo transmetallation reactions with various metal derivatives, or the addition of half an equivalent of these metal halides to afford a bis(phosphaalkenyl) metal complex.[232]

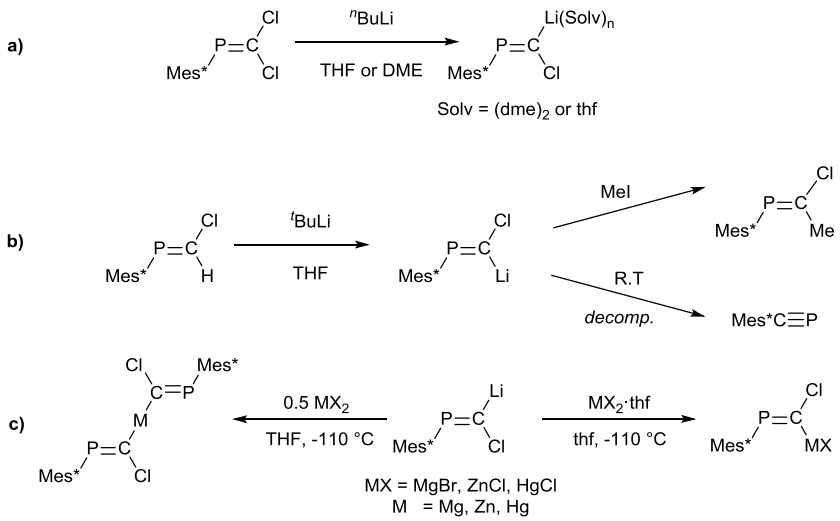


**Scheme 1.76**: Lithiation of phosphaalkenes, featuring **a)** lithium/halogen exchange, **b)** lithium/hydrogen exchange to form the *E*-isomer and **c)** further reactivity of the *Z*-isomer.[230,231,233]

Grignard reagents are often used in organic synthesis, and phosphavinyl-Grignard reagents (*C*-magnesiophosphaalkenes) are commonly formed through the addition of a Grignard to a

phosphaalkyne. **Scheme 1.77** shows the addition of magnesium reagents "RMgX" across the triple bond of $^{t}$BuC≡P to form a variety of reagents.[234]

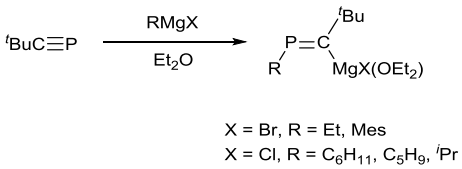


**Scheme 1.77**: Addition of Grignard reagents to phosphaalkynes.[234]

Magnesiophosphaalkenes are also reagents for various transmetallation processes. For example, the addition of bromocatecholborane to [CyP=C($^{t}$Bu)MgCl] affords the borylated phosphaalkene shown in **Scheme 1.78**.[235]

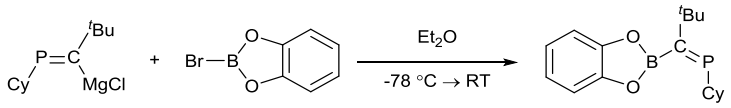


**Scheme 1.78**: Formation of a borylated phosphaalkene.[235]

Other examples of further reactivity of magnesiophosphaalkenes include the reaction of three equivalents with group 13 halides to afford diphospha-metallobicyclo[1.1.1]pentane derivatives (**Scheme 1.79**).[236]

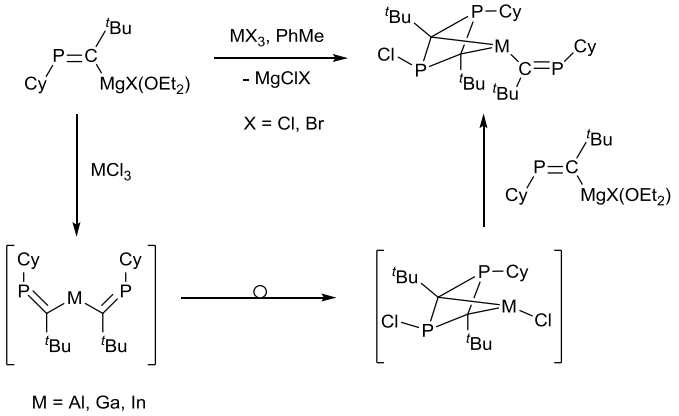


**Scheme 1.79**: Formation of diphospha-metallobicyclo[1.1.1]pentane derivatives.[236]

#### 1.2.2.4.2 *P*-Metallaphosphaalkenes

These can be made from one of three general methods. The first is to generate the P=C fragment from a metal-phosphorus complex. This is exemplified (**Scheme 1.80a**) by the addition of $CS_2$ to $[Cp^*(CO)_2Fe\text{-}P(SiMe_3)_2]$ to generate $[Cp^*(CO)_2Fe\text{-}P{=}C(SiMe_3)_2]$, although the ferraphosphaalkene degrades, but was trapped by the addition of $[(COT)Cr(CO)_5]$ which adds $[Cr(CO)_5]$ to the lone pair of phosphorus.[237] Another method which gives amino substituents on the carbon involves the addition of trimethylsilyl(aminomethylene)phosphanes $[Me_3SiP{=}C(NR_2)R']$ to $[Cp^*Fe(CO)_2Cl]$ to reveal $[Cp^*(CO)_2FeP{=}C(NR_2)R']$ (**Scheme 1.80b**).[238]

The phosphaalkyne complex $[Pt(dppe)(\eta^2\text{-}^t BuC{\equiv}P)]$ has been shown by Nixon and co-workers to undergo hydrozirconation with $[ZrHCl(\eta^5\text{-}C_5H_5)_2]$ to furnish the $\eta^2$ ligated metallaphosphaaalkene complex $[Pt(dppe)\{\eta^2\text{-}^t BuCH{=}PZrCl(\eta^5\text{-}C_5H_5)_2\}]$ (**Scheme 1.80c**). The last, and frequently used method for the synthesis of *P*-metallophosphaalkenes features the 1,2 addition of a transition metal hydride across P≡C bond, this is best demonstrated by Hill *et al*. in the high yielding formation of the ruthenaphosphaalkene system $[RuCl(CO)(PPh_3)_2(P{=}CH^tBu)]$ *via* the hydroruthenation of $^t$BuC≡P shown in **Scheme 1.80d**.[239]

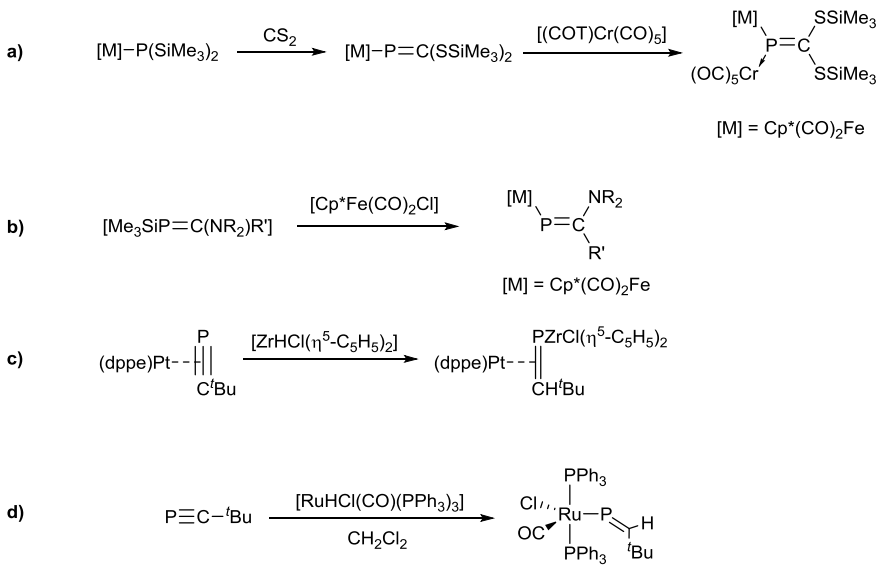


**Scheme 1.80**: Synthesis of metallaphosphaalkenes, either by building up the P=C bond from precursors (**a**), using preformed P=C bonds (**b**) or reducing the bond order from 3 to 2 (**c** and **d**).

### 1.2.3 Concluding Remarks

The area of low-coordinate phosphorus chemistry has rapidly expanded since the breaking of the 'double-bond rule' with the formation of the first phosphaalkyne HC≡P. Since this discovery, key contributions from Kroto and Nixon led the way for the synthesis of other multiply bonded phosphorus-carbon compounds. However, it was only with Becker's synthesis of the first stable phosphaalkyne $^{t}$BuC≡P that organometallic chemistry of low coordinate phosphorus began to be explored and all possible phosphaalkyne and phosphaalkene bonding modes have been exemplified in the literature. Investigations into these systems remain limited, but there are some emerging works with more exotic phosphaalkynes (MeC≡P, $R_3$SiC≡P). Herein (**Chapter 4**), synthesis of some novel silyl-based phosphaalkynes and their hydroruthenation products are described, alongside investigations of their chemistry.

# 2. Synthesis and structure of phosphine-boranes.

## 2.1 Introduction

Frustrated Lewis Pair is the term for a combination of Lewis acids (electron pair acceptors with low lying LUMOs) and Lewis bases (electron pair donors) which are sterically precluded from forming Lewis acid/base adducts. These 'encounter complexes' retain unquenched reactivity which has been shown to activate small molecules.

One of the more common types of FLP are intramolecular ones, and within this category, many are phosphine-borane based. There are two published methods for the preparation of compounds of the type $R_2BC(R)=C(Ph)PPh_2$. The first examples were published by Binger and Koster in 1974, who combined $Na[R_3BC{\equiv}CMe]$ with $ClPR'_2$ to generate a variety of 1-boryl-2-phosphinoethenes.[97] In 1988 Baleuva and Erastov published a new method for the synthesis of these borylphosphinoethene compounds (**Scheme 2.1**). Their method was based upon lithiating phenylacetylene before sequentially adding tributylborane and chlorodiphenylphosphine to afford $Bu_2BC(Bu)=C(Ph)PPh_2$ (**1**). Allowing the product to crystallise from the reaction mixture yielded white crystals, which were then washed with cold pentane, resulting in a 21% yield. They confirmed the structure of the 1-boryl-2-phosphinoethene, on the basis of the single $^{31}P\{^1H\}$ NMR resonance at 10.0 ppm, and X-ray diffraction data, though the latter appear to be unpublished.[240] In 1993 Balueva *et al.* prepared $Ph_2BC(Ph)=C(Ph)PPh_2$ (**2**) using an equivalent methodology to that of **1**, where the purification step was modified due to the insolubility of the phenyl analogue in $Et_2O$. The product was instead separated from LiCl through recrystallisation from DMF:MeCN (DMF = dimethylformamide).[241]

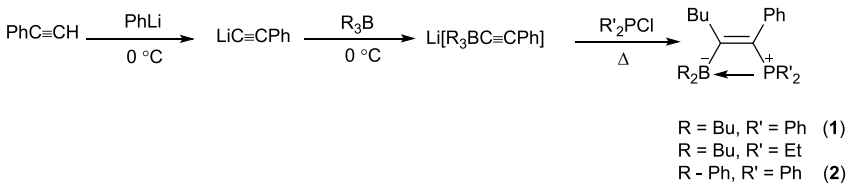


**Scheme 2.1**: Published synthesis of borylphosphinoethenes.[240–242]

The synthesis of "$Ph_2BC(Ph)=C(Ph)PPh_2$" was also published by Gröbe and co-workers in 2006, they used the sodium salt $Na[BPh_4]$ under UV illumination to form a diphenylboron anion. This

anion is isoelectronic to carbenes and therefore adds to the triple bond of phenylacetylene, forming a boracyclopropene species. The addition of $Ph_2PCl$ ring-opens the boracyclopropene to yield $Ph_2P(Ph)C{=}C(Ph)BPh_2$ (**Scheme 2.2**), which exhibits a $^{31}P\{^1H\}$ NMR signal at -15.6 ppm.[100] However, this conflicts with the data published by Balueva, who reported the same molecule had the phosphorus resonance at 6.9 ppm.[241]

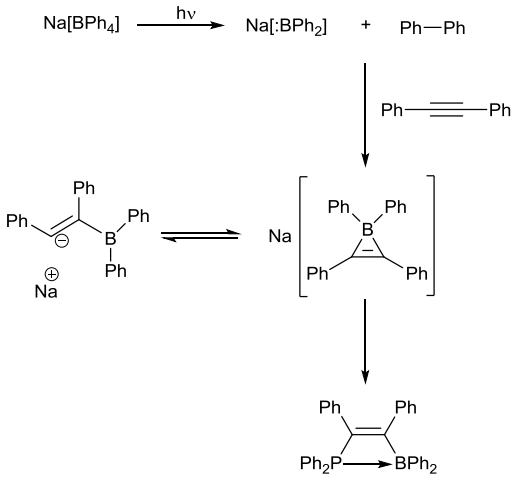


**Scheme 2.2**: Gröbe's published synthesis of $Ph_2BC(Ph){=}C(Ph)PPh_2$ (**2**).[241]

Balueva *et al*. investigated the reactivity of $Bu_2BC(Bu){=}C(Ph)PPh_2$ with various aldehydes including PhCHO, $^{i}$PrCHO, MeCHO, chloral ($Cl_3CC(O)H$), and *p*-chlorobenzaldehyde. It was found that the aldehydes added across the P-B coordinative bond, to form 2,3,3-tributyl-1,6,6-triphenyl-3,4,6-borata-oxaphosphoniacyclohexanes, which were stable when under inert atmosphere, but dissociated to $Bu_2BC(Bu){=}C(Ph)PPh_2$ and aldehydes in dilute solution.[240]

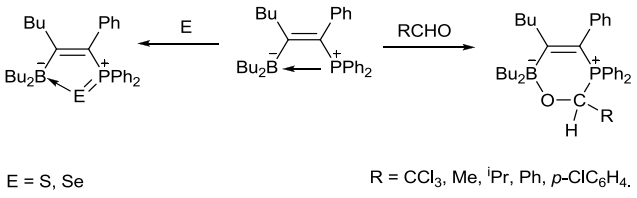


**Scheme 2.3**: Addition reactions of electrophiles and aldehydes.[240,243]

Substituting the phenyl groups on the phosphorus atom for alkyl groups altered the reactivity of the compound. Whereas **1** did not react with $R_2C{=}N$ and $R_2C{=}S$ moieties, changing to a $Et_2P$

fragment, resulted in the ambiphilic compound $Bu_2B(Bu)C=C(Ph)PEt_2$, an oil distillable under high vacuum. It also reacted at ambient temperature with $CS_2$ over one day, to form a 6-membered ring, confirmed through X-ray diffraction. Substituting the phenyl groups on the phosphorus atom for alkyl chains leads to increased basicity and thus increases reactivity. The strength of the P-B bond does not change, and therefore the phosphorus has a higher charge density. The $Et_2P$ analogue was also found to react with chloral to form a 6-membered ring, a cyclic betaine, in the same manner as **1**, indicated by a slight shift to lower frequency of its associated $^{31}P\{^1H\}$ NMR signal ($\delta_P = 13$).[242]

Herein, attempts to make **1** and similar systems will be explored, using a number of synthetic routes. The solid state data has also been complemented by DFT studies.

## 2.2. Preparation of compounds $R_2BC(R)=C(Ph)PPh_2$

While **1** is a known compound,[240] it had not been fully characterised before this work. Additionally the aryl analogue of **1**, $Ph_2BC(Ph)=C(Ph)PPh_2$ (**2**), has been reported in two separate articles but contain contradictory spectroscopic data.[100,241] In view of this, the synthesis of these and $Et_2BC(Et)=C(Ph)PPh_2$ (**3**) were investigated. In addition, the synthesis has been modified, to reduce the formation of the side product $Ph_2PC{\equiv}CPh$ (**4**) from 20% to 3%.

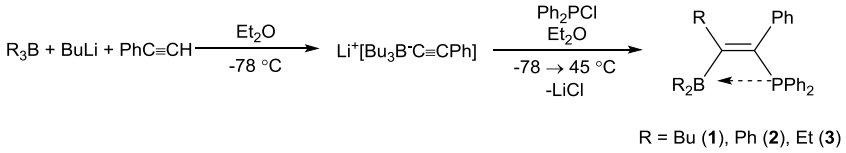


**Scheme 2.4**: Synthesis of **1**-**3**.

As previously described in the literature, the compounds **1**-**3** are built up from phenylacetylene in a three step, one-pot reaction, whereby $BR_3$ and then $Ph_2PCl$ were added to a solution of lithiated phenylacetylene at -78 °C. It is this cold addition which reduces the formation of the side product ($Ph_2PC{\equiv}CPh$) compared with literature methods, which operate at 0 °C.[242] After these additions, the solution was heated until reflux under argon, before the cooled suspension was filtered to ensure removal of LiCl before a concentrated solution of **1** was left to crystallise at room temperature. In contrast, **2** was isolated by extracting the resulting precipitate with $CH_2Cl_2$. Where R = Et, it was found that the reflux step resulted in the formation of $PhC{\equiv}CPPh_2$; consequently, the reaction was instead stirred for four hours at ambient temperature.

Compounds **1**-**3** are air sensitive, but are found to be stable under inert conditions for extended periods (> 2 years). The formation of a single product in each case was indicated by a single $^{31}P\{^1H\}$ NMR resonance in $CDCl_3$ solution($\delta_p$ = 10.0 **1**; 7.4 **2**; 9.8; **3**), and a single $^{11}B\{^1H\}$ NMR resonance ($\delta_B$ = 13.5 **1**; 4.1 **2**; 13.2; **3**). In the case of **1** the phosphorus resonance is identical to that reported by Balueva *et al.*[240] They suggest the positive chemical shift indicates the presence of a coordinative bond between the phosphorus and boron atoms, which is based upon broad agreement with $^{11}B\{^1H\}$ spectra data from Binger *et al.* on similar systems (See **Table 2.1** for data).[97] The $^{11}B\{^1H\}$ NMR spectroscopic data indicates the boron atom is in a 4-coordinate environment, suggesting that the phosphorus lone pair is donating into the vacant boron *p*-orbital. This geometry is confirmed through X-ray diffraction studies (*vide infra*).

In the case of **2,** the phosphorus is in good agreement with Balueva *et al.* who observed a single boron resonance at 6.9 ppm, in $C_6D_6$. However, the same compound is also reported by Gröbe *et al.*, who observed this resonance at -15.6 ppm and attribute this unusually low signal to the intramolecular P→B interaction.*

It has been hypothesised that the discrepancies in $^{31}P\{^1H\}$ NMR resonance are due to a difference in the isomeric form. When the borane and phosphine units are *cis* to each other, the phosphorus coordinates to the boron, however if the phosphine and borane were *trans*, the phosphorus would no longer be coordinating to boron and therefore the resonance in the $^{31}P\{^1H\}$ NMR data would occur at a lower frequency. This change in isomerisation would therefore result in a 3-coordinate boron atom which would be reflected in the $^{11}B\{^1H\}$ NMR data. However, Gröbe *et al.* did not report $^{11}B\{^1H\}$ NMR spectroscopic data for the compound, so it is not possible to conclude which isomer they actually prepared. This proposed difference in isomerisation could be attributed to the use of UV illumination in the preparation method of Gröbe *et al.* While Balueva *et al.* did not report any $^{11}B\{^1H\}$ NMR either, the analogous compound **1** has a resonance at 13.5 ppm, which is within the region expected for 4-coordinate boron, this is further evidence for the presence of the coordinative bond between the phosphorus and boron atoms.

The key spectroscopic data for **1**-**3** are reported in **Table 2.1**, along with limited data available from similar compounds in the literature, which all indicate the presence of 4-coordinate boron, consistent with the a P-B bond. The data from the similar compounds presented by Erker *et al.* show that the substituent on the C=C backbone has minimal effect of the

*The shift was corrected from the $P(OMe)_3$ standard used by Gröbe *et al*.

electronics of boron. While it is known that modifying the phosphine group will change the electronic effects, this change could be countered by changing the groups on the C=C backbone as shown by the identical $^{31}P\{^{1}H\}$ NMR signal at 15.2 ppm for both $(C_6F_5)_2BC(C_6F_5)=C(Pr)PPh_2$ and $(C_6F_5)_2BC(C_6F_5)=C(Ph)PMes_2$. Though this is contradicted by the data for $Et_2BC(Et)=C(Me)PPh_2$, reported by Binger and Köster, who described the $^{11}B$ shift as a range (0→-10 ppm), while the preparation of $Et_2BC(Et)=C(Ph)PPh_2$ (**3**) has an $^{11}B\{^{1}H\}$ NMR spectroscopic shift of 13.2 ppm. Though data were reported in different solvents, this shift would seem excessive for a solvent shift.

**Table 2.1**: Data given for **1**-**3**, **5**, **6** and similar compounds from the literature. $^{11}B\{^{1}H\}$ signals referenced to $Et_2O{\cdot}BF_3$ $^{31}P\{^{1}H\}$ signals referenced to 85% $H_3PO_4$

| | | $^{31}P\{^{1}H\}$ (ppm) | $^{11}B\{^{1}H\}$ (ppm) |
|---|---|---|---|
| **1** | $Bu_2BC(Bu)=C(Ph)PPh_2$ [a] | 10.0 | 13.5 |
| **2** | $Ph_2BC(Ph)=C(Ph)PPh_2$ [a] | 7.4 | 4.1 |
| **3** | $Et_2BC(Et)=C(Ph)PPh_2$ [a] | 9.8 | 13.2 |
| **5** | $Bu_2BC(Bu)=C(Ph)P^{i}Pr_2$ [a] | 30.2 | 8.8 |
| **6** | $Et_2BC(Et)=C(Ph)\ P^{i}Pr_2$ [a] | 30.7 | 9.4 |
| | $Me_2BC(Me)=C(Me)PPh_2$ [97] | - | -22 |
| | $Et_2BC(Et)=C(Me)PPh_2$ [97] | - | 0 → -10 |
| | $Et_2BC(Et)=C(Me)PCy_2$ [97] | - | -9.6 |
| | $Et_2BC(Et)=C(Me)PEt_2$ [97] | - | -9 |
| | $Bu_2BC(Bu)=C(Ph)PPh_2$ [240] | 10 | - |
| | $Ph_2BC(Ph)=C(Ph)PPh_2$ [241] | 6.9 | - |
| | $Bu_2BC(Bu)=C(Ph)PEt_2$ [242] | 13 | - |
| | $Ph_2BC(Ph)=C(Ph)PPh_2$ [100] | -15 † | - |
| | $(C_6F_5)_2BC(C_6F_5)=C(Ph)PPh_2$ [244] | 13.8 | -6 |
| | $(C_6F_5)_2BC(C_6F_5)=C(Pr)PPh_2$ [244] | 15.2 | -6 |
| | $(C_6F_5)_2BC(C_6F_5)=C(Ph)PMes_2$ [244] | 15.2 | 1 |

[a] Data collected from this work. † $^{31}P\{^{1}H\}$ signal referenced to $P(OMe)_3$ $\delta$= 125 ppm ± 0.5

Further analysis into the effects of the nature of the phosphorus and boron groups on the phosphorus and boron resonances might lead to understanding the nature of the P-B interaction. Unfortunately, the limited $^{31}P\{^{1}H\}$ and $^{11}B\{^{1}H\}$ NMR spectroscopic resonances

available in the literature do not provide enough data to compare a single variable. The structural analysis of compounds **1**-**3** is found in **Section 2.2:1**.

### 2.2.1 Ancillary reactions to the synthesis of 1-3

Modifying the synthesis of **1**, to perform reagent additions at −78 ˚C was found to vastly reduce the amount of side product phenylethynyldiphenylphosphine ($Ph_2PC{\equiv}CPh$, $\delta_P$ = −33.4, **4**) which Balueva *et al.* observed in an 8:2 mix of **1** and **4**.[240] By varying the temperature of addition of $Bu_3B$ and $Ph_2PCl$, the ratio of **1** to **4** was reduced to 100:3.

The presence of trace phenylethynyldiphenylphosphine was confirmed by preparing an authentic sample by the lithiation of phenylacetylene and the subsequent addition of $Ph_2PCl$, which was stirred for two hours at −78 °C, to yield $Ph_2PC{\equiv}CPh$ (**Scheme 2.4**). The $^{31}P\{^1H\}$ NMR spectra of the crude product contained a resonance at −33.4 ppm.

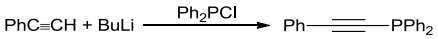


**Scheme 2.5**: Synthesis of phenylethynyldiphenylphosphine (**4**).

By changing variables in the formation of **3**, it was noted that reducing the reaction time had little effect of the purity in $^{31}P\{^1H\}$ NMR spectra, but did impact the $^{11}B\{^1H\}$ NMR spectra. After a shorter reaction time of 20 minutes the $^{11}B\{^1H\}$ NMR data show the presence of two main impurities $\delta_B$ = 86 and −18 ppm. These impurities are likely to be intermediates since they are not present when the reaction time is increased. The nature of these intermediates remain unidentified although one could be $Li[Et_3BC{\equiv}CPh]$, which is thought to be the first step in the synthesis (**Scheme 2.4**).[240]

The formation of $PhC{\equiv}CPPh_2$ (**4**) would seem to be evidence of a thermal rearrangement with the subsequent elimination of $BEt_3$, (**Scheme 2.6**) given a higher percentage being found in reactions which were heated to reflux, compared to left stirring at ambient temperature or cooled to −78 ˚C.

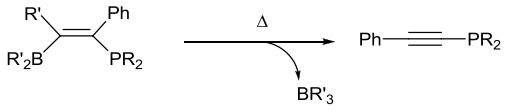


**Scheme 2.6**: Suggested thermal rearrangement. Where R = Ph, $^{31}P\{^{1}H\}$ NMR $\delta$ = −33 ppm, where R = $^{i}$Pr, $^{31}P\{^{1}H\}$ NMR $\delta_P$ = −10 ppm.[245]

Where the alternative phosphines $^{i}Pr_2PCl$ and $^{t}Bu_2PCl$ were used, the analogous $R_2PC{\equiv}CPh$ compounds were found to occur. Following the same modified method as **1-3**, reactions with lithiated phenylacetylene, $^{i}Pr_2PCl$ and $R_3B$ (R = $^{n}$Bu (**5**), Et (**6**)) each yielded a yellow, viscous oil. Attempts to crystallise the products were unsuccessful, as were attempts to allow their precipitation from solution. The major product observed in the NMR spectra of the crude oil (R = $^{i}$Pr) were attributed to be the desired product; the $^{31}P\{^{1}H\}$ NMR spectra revealed a main signal at 30.2, and an additional signal at −11.56 ppm which corresponds to $^{i}Pr_2PC{\equiv}CPh$,[245] (**5**) and a subsequent lack of phosphine starting material, ($^{i}Pr_2PCl$, $\delta_P$ = 133.9). The similar ligand $Bu_2BC(Bu)=C(Ph)PEt_2$ ($\delta_P$ = 13) is a distillable liquid (147−150 ˚C, 0.001 mm).[242] However, attempts to distil the oil ($1.73x10^{-1}$ mbar, 51 ˚C) revealed a small amount of colourless liquid with a number of products in both the $^{31}P\{^{1}H\}$ and $^{11}B\{^{1}H\}$ NMR spectra, crucially none of these were the dominant signals from the crude mixture. No further fraction distilled, so the bulk viscous oil was re-analysed by NMR to show a single phosphorus and boron signal ($\delta_P$ = 30.2, $\delta_B$ = 8.9) $^{1}$H NMR spectroscopy revealed a range of resonances in the aromatic region between 7.13 and 7.31 ppm. However, when cooled the oil appeared cloudy, indicating the continued presence of an impurity, such as LiCl, which redissolves upon heating the oil. When R = Et, attempts to distil the viscous oil under partial vacuum were unsuccessful, and the boiling point of the oil was determined to be greater than 200 ˚C at $3x10^{-2}$ mbar. Sublimation of the crude mixture resulted in the condensation of a cloudy, viscous, white/yellow oil which solidified on the cold finger, while a translucent yellow oil remained. NMR analysis of the remaining oil revealed a much cleaner (96% purity by integration of $^{31}P\{^{1}H\}$ NMR spectra) sample with a single phosphorus and boron signal ($\delta_P$ = 30.7, $\delta_B$ = 9.4).

The synthesis of the phosphine-borane $Bu_2B(Bu)C=C(Ph)P^{t}Bu_2$**,** using $^{t}Bu_2PCl$ was first attempted in diethyl ether (as for the analogous compounds **1**-**3**, **Scheme 2.4**). However, the borane failed to react as was indicated by the NMR spectra which predominately showed starting materials ($\delta_B$ = 86.5; $Bu_3B$ and $\delta_P$ = 146.8; $ClPPh_2$). Substituting diethyl ether for the more coordinating solvent THF, or the higher boiling toluene, led to the formation of an oily

residue, the colour of which was solvent dependent (green in THF, orange in toluene). Upon standing for 14 hours, small, colourless, X-ray quality crystals formed, however, these were found to be crystals of the free phosphinoalkyne ($^{t}Bu_2PC{\equiv}CPh$), **7** rather than that of the desired phosphine-borane (**Figure 2.1**).

During the attempted synthesis of $Bu_2B(Bu)C{=}C(Ph)P^{t}Bu_2$, an aliquot of the reaction mixture taken prior to the addition of phosphine suggested the mixture initially forms the borate anion $Li^{+}[R_3B^{-}C{\equiv}CPh]$ (**Scheme 2.4**) as shown by the 4-coordinate species apparent in the $^{11}B\{^{1}H\}$ NMR spectra ($\delta_B$ = 19.2). This borane must add as intended, before it is eliminated in favour of the phosphine to form the linear alkyne as shown in **Scheme 2.7**.

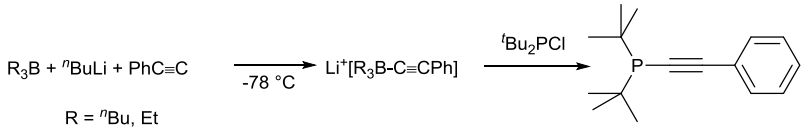


**Scheme 2.7**: Apparent formation of alkyne **7**.

The compound $^{t}Bu_2PC{\equiv}CPh$ (**7**) was first prepared by Empsall *et al.* by refluxing lithiated phenylacetylene, adding it to a cooled ethereal solution of $^{t}Bu_2PCl$ and bringing to reflux again for 20 hours before an aqueous work-up. The distilled product, upon cooling, formed white prisms with a $^{31}P\{^{1}H\}$ NMR resonance at 12.6 ppm.[246] It has since been synthesised using copper or nickel catalysts in diethylamine with long reaction times and high temperatures.[245,247]

Attempts to directly synthesise and isolate **7** directly, using less forcing conditions were successful (**Scheme 2.8**). First, $^{t}Bu_2PCl$ in diethyl ether was added to lithiated phenylacetylene in diethyl ether at −78 °C and allowed to warm to 17 ˚C over six hours. An anaerobic work up and a pentane extraction, was found to be more successful than the organic work up procedure suggested by Wang,[248] and Kondoh for $PhC{\equiv}CPPh_2$.[249] This air and moisture free synthesis is most successful for analogous compounds $R_2PC{\equiv}CPh$ where R = Ph, (yield 82%, $\delta_P$ = −33.0; **4**) $^{t}Bu$ (yield 60%, $\delta_P$ = 11.5; **7**) and $^{i}Pr$ (yield 94%, $\delta_P$ = −11.6; **8**) and for $Ph_2PC{\equiv}CSiMe_3$[250] (yield 76%, $\delta_P$ = −32.8; **9**).

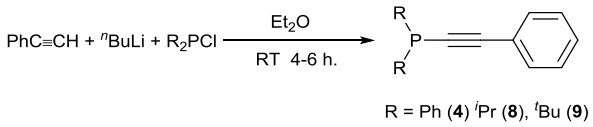


R = Ph (**4**) $^{i}$Pr (**8**), $^{t}$Bu (**9**)

**Scheme 2.8**: Synthesis of alkynes **4**, **7**, **8**.

The structure of **7** is unknown in the CCDC database (CCDC = Cambridge Crystallographic Data Centre), though it has been crystallised upon coordination to a variety of metal centres, typically resulting in deviation of the alkynyl bond from linearity. The data (**Table 2.2**) are largely unremarkable, the bond length 1.1722(10) Å (C16-C7) is indicative of a C≡C bond, the C-C-C backbone is linear (178.19(3)˚) while the C16-P1 distance (1.7909(10) Å) is similar to that in $Mes_2PC{\equiv}C$-*p*-tol (1.766 Å).[251] The (Mes)C-P bond length is stastically similar on each side and comparable with other phosphines, the geometry around phosphorus is distorted trigonal pyramidal.

**Table 2.2**: Selected data of **7** (with estimated standard deviations in parentheses).

| Bond | Distance (Å) | Bond | Angle (°) |
|---|---|---|---|
| **C16-C7** | 1.1722(10) | **C16-P1-C13** | 98.18(5) |
| **C7-C1** | 1.4524(10) | **C16-P1-C11** | 99.91(4) |
| **P1-C16** | 1.7909(10) | **C16-C7-C1** | 178.19(3) |
| **P1-C13** | 1.8992(10) | **C11-P1-C13** | 112.91(3) |
| **P1-C11** | 1.8922(11) | | |

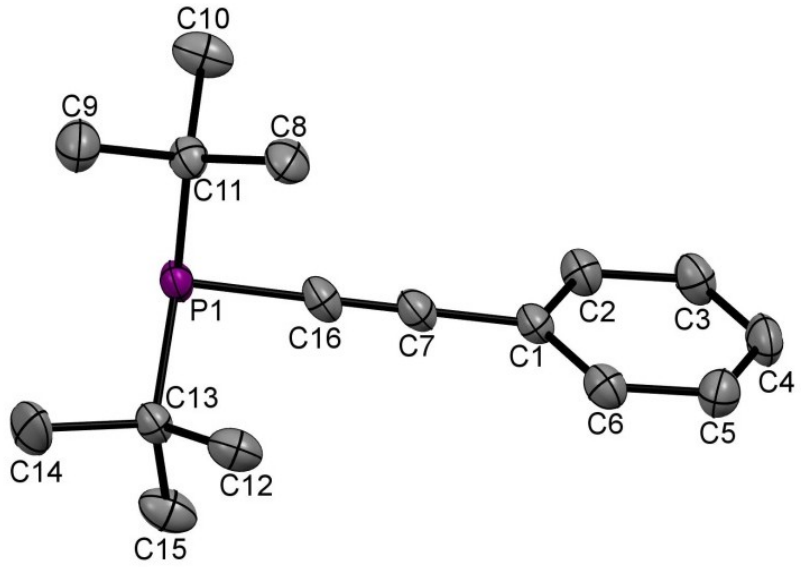


**Figure 2.1**: Crystal structure of **7**, hydrogen atoms omitted for clarity, 50% thermal ellipsoids.

### 2.2.2 Structural data of $Ph_2PC(Ph)=C(R)BR_2$ (1-3)

Crystallographic data confirm the presence of the *Z*-isomers of $Ph_2PC(Ph)=C(R)BR_2$ where R = Bu, Et, Ph (**Figure 2.4**). Single crystals of X-ray quality of **1** and **2** were obtained from ethereal (**1**) or $CH_2Cl_2$ (**2**) solutions stored at -80 ˚C over 48 hours. In the case of **3**, storage of the crude oil at ambient temperature over several weeks resulted in spontaneous crystallisation upon standing. Structural data for **3** are of low quality, but do confirm comparable connectivity to **1** and **2**.

While Balueva has previously claimed X-ray data for **1** showed a phosphorus-boron bond length of (2.104 Å), which the author argues to be determined by the intracyclic angles of the double bond,[243] no further details were provided, nor are data present in CCDC. These are therefore the first crystallographic studies of $R_2PC(R)=C(R')BR'_2$ (**Table 2.3**, where **Figure 2.2** shows the numbering scheme for atoms in **1**-**3**).

**Table 2.3**: Key data for compounds **1**-**3.**

| | **1** | **2** | **3*** |
|---|---|---|---|
| **P1-B1** | 2.107(2) | 2.002(2) | 2.077(5) |
| **P1-C1** | 1.799(2) | 1.799(2) | 1.797(4) |
| **C1-C2** | 1.361(3) | 1.363(3) | 1.385(6) |
| **C2-B1** | 1.630(3) | 1.659(3) | 1.634(8) |
| **P1-B1-C2** | 77.82(12) | 80.31(12) | 78.5(3) |
| **P1-C1-C2** | 96.51(14) | 96.53(15) | 95.6(3) |
| **P1-C1-C10** | 131.61(15) | 130.44(16) | 131.9(3) |
| **C1-P1-B1** | 76.59(10) | 78.25(9) | 77.7(2) |
| **C1-C2-B1** | 108.50(17) | 104.90(17) | 107.5(4) |
| **B1-C2-C60** | 124.91(18) | 128.74(18) | 127.8(5) |

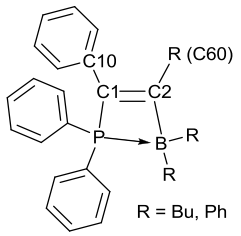


**Figure 2.2**: Schematic representation of the solid state structure of $R_2BC(R)=C(Ph)PPh_2$ (**1**).

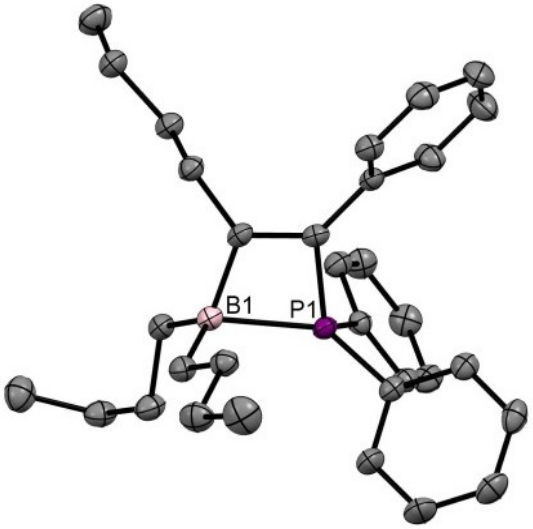


**Figure 2.4**: Solid state structures of **1**, 50% thermal ellipsoids. H-atoms omitted for clarity.

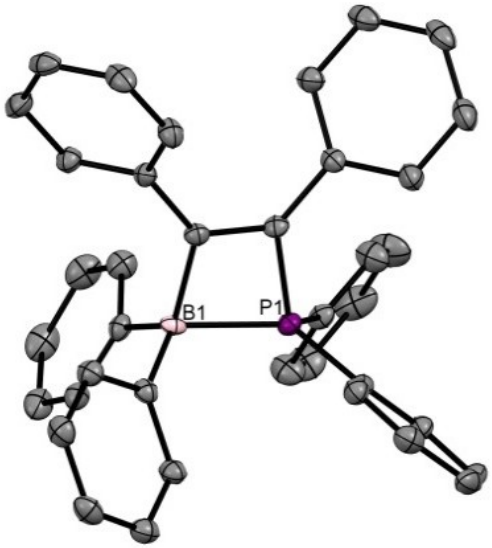


**Figure 2.3:** Solid state structures of **2**, 50% thermal ellipsoids. H-atoms omitted for clarity.

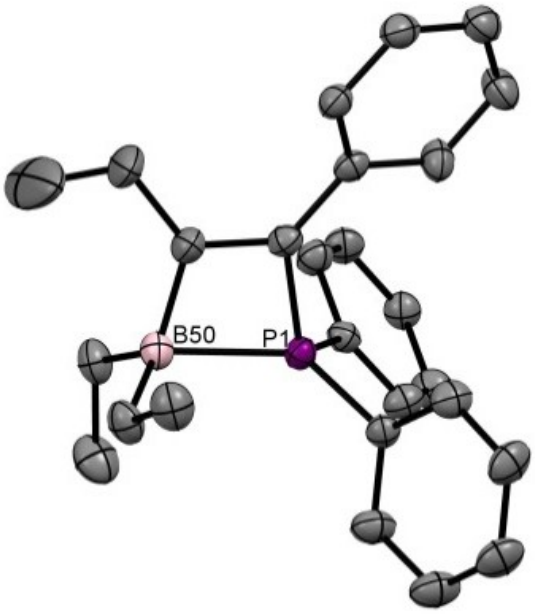


**Figure 2.5:** Solid state structure of **3**, 50% thermal ellipsoids. H-atoms omitted for clarity.

From crystallographic data, it is apparent that, in the solid state, **1** exists as a 1-borata-4-phosphoniacyclobut-2-ene with a P-B bond distance of 2.107(2) Å, which is in agreement with that claimed by Balueva. This closed, cyclic structure is supported by the $^{11}B\{^{1}H\}$ NMR spectroscopic data, which shows a 4-cordinate boron atom. The intracyclic angles are detailed in **Table 2.3** along with the key bond lengths and angles.

Analysis of the bond lengths in **Table 2.3** reveals statistically comparable P1-C1 lengths for both **1** and **2** and almost identical angles around the C1 and P1 atoms, which is not unusual given the identical composition of that half of the molecule. However, the C1-C2-B1 and B1-C2-C60 angles are significantly higher in **2** which is attributed to the increased steric bulk of the phenyl groups compared to that of the *n*-butyl groups. This is because the P1-B1 interaction is shorter in **2**, than **1** (and **3**). Incidentally, the length of the P-B interaction in **2**, (2.002(2) Å) is only marginally smaller than a similar geometric cycle (**Figure 2.6**), reported by Stephan in 1997 which features the smallest P-B bond length reported in the literature.[252] The P-B bond lengths for similar adducts of the form $Ph_2RP\rightarrow B(C_6F_5)_2R$, tend to lie between 2.03-2.18 Å.[253]

The difference in P-B bond length is attributed to the increased acidity due to the phenyl group being a weaker electron donor than *n*-alkyl groups, the less electron donating the substituent, the lower the relative electron density on boron. The more electropositive the boron, the more strongly it will accept electrons from phosphorus, resulting in a shorter P-B bond. This

implies that the electronics of the system are, to a degree, more important than the steric bulk in the determination of their structure.

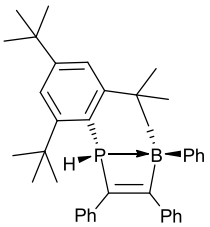


**Figure 2.6**: Smallest P-B interaction from a similar geometry.[252]

### 2.2.3 Computational Studies

Computational studies of **1**-**3** were undertaken to supplement the experimental data. Optimised structures indicate that the bond lengths and angles calculated geometries (6-311+G**) are comparable to experimental data (presented in **Table 2.4**) for **1**, **2** and **3**. It is known that $Me_2BC(Me)=C(Me)PMe_2$ (**10**) has been shown to coordinate to $[Rh(CO)_2Cl]_2$ therefore its structure was also calculated in order to demonstrate the geometry properties which might allow coordination.

It can be seen in **Table 2.4**, that the bond lengths and angles of **1**-**3** and **10** are all similar. The computational data presented, indicate that the structure of **10** is similar to **2** in terms of the angles around the P-C=C-B ring, and both have a similar P-B bond length, and the C=C bond remains the same length regardless of the borane (Me *vs*. Et, Bu, Ph) or phosphine groups (Me *vs*. Ph).

**Table 2.4:** Table of bond lengths (Å) and angles (°) from DFT calculations (B3LYP, 6-311+G**) and from experimental data.

**Structural Data**

| | DFT | | | | Experimental | | * |
|---|---|---|---|---|---|---|---|
| | **10** | **3** | **1** | **2** | **1** | **2** | **3** |
| **P-B** | 2.14 | 2.21 | 2.21 | 2.15 | 2.107(3) | 1.992(4) | 2.077(5) |
| **C=C** | 1.35 | 1.36 | 1.36 | 1.36 | 1.358(3) | 1.367(5) | 1.385(6) |
| **P-C** | 1.80 | 1.81 | 1.81 | 1.81 | 1.796(2) | 1.797(3) | 1.797(4) |
| **B-C** | 1.63 | 1.63 | 1.63 | 1.64 | 1.626(4) | 1.660(5) | 1.634(8) |
| **$C_{20}$-$B_1$-$P_1$** | 77.5 | 76.91 | 76.9 | 78.0 | 77.81(12) | 80.65(3) | 78.5(3) |
| **$C_1$-$P_1$-$B_1$** | 75.9 | 74.2 | 74.2 | 75.4 | 76.58(10) | 78.42(15) | 77.7(2) |
| **$C_1$-$C_{20}$-$B_1$** | 108.8 | 109.6 | 109.7 | 108.2 | 108.53(18) | 104.5(3) | 107.5(4) |
| **$C_{20}$-$C_1$-$P_1$** | 97.8 | 99.2 | 99.1 | 98.4 | 96.50(15) | 96.5(2) | 95.6(3) |

* data for **3** is shown for geometric comparison only, the structure has significant disorder of the two molecules in the asymmetric unit.

NMR spectroscopic data were also calculated and compared to those obtained experimentally. It was found that using the functional PBE[254] allowed slightly more accurate spectroscopic calculations, although it must be noted that for computational efficiency these were conducted in the gas phase, without a solvent model. The computational data for **10** do not closely correlate with the experimental data in the same way as **1-3** do. This may be a sign that there is an inconsistency with either the model or the literature data, unfortunately this cannot be independently verified.

**Table 2.5**: Table of key spectroscopic data (calculated and experimental)

| | | Experimental | B3LYP | PBE |
|---|---|---|---|---|
| $^{31}$P | **10** | -9* | -10.157 | -20.149 |
| | **3** | 9.84 | 15.9759 | 6.25567 |
| | **1** | 10 | 18.5934 | 9.18105 |
| | **2** | 7.48 | 9.45021 | 1.10256 |
| $^{11}$B | **10** | -1.2* | 5.6019 | 2.8867 |
| | **3** | 13.22 | 20.2417 | 18.4 |
| | **1** | 13.9 | 19.0291 | 16.9716 |
| | **2** | 4.08 | 7.93522 | 5.15383 |

*Experimental data for **10** is from literature.[100]

### 2.2.3.1 Atoms in Molecules

Atoms in Molecules is a powerful computational approach, developed by Bader[255] which reveals the electron density shown by a gradient map of the electron density, this shows how the electronic charge is distributed through the molecule, taking into account the attractive field exerted by the nuclei. The critical points (CP) are points where the gradient vanishes, these points can be characterised as a stationary point, a bond CP, a ring CP or a cage CP. Various parameters can be calculated at these bond critical points, and the density of all electrons (ρ(r)) is an indicator of how strong the bond is, the bigger the value, the stronger the bond. However, this number is only comparative for very similar systems (**Figure 2.7, Table 2.6**).

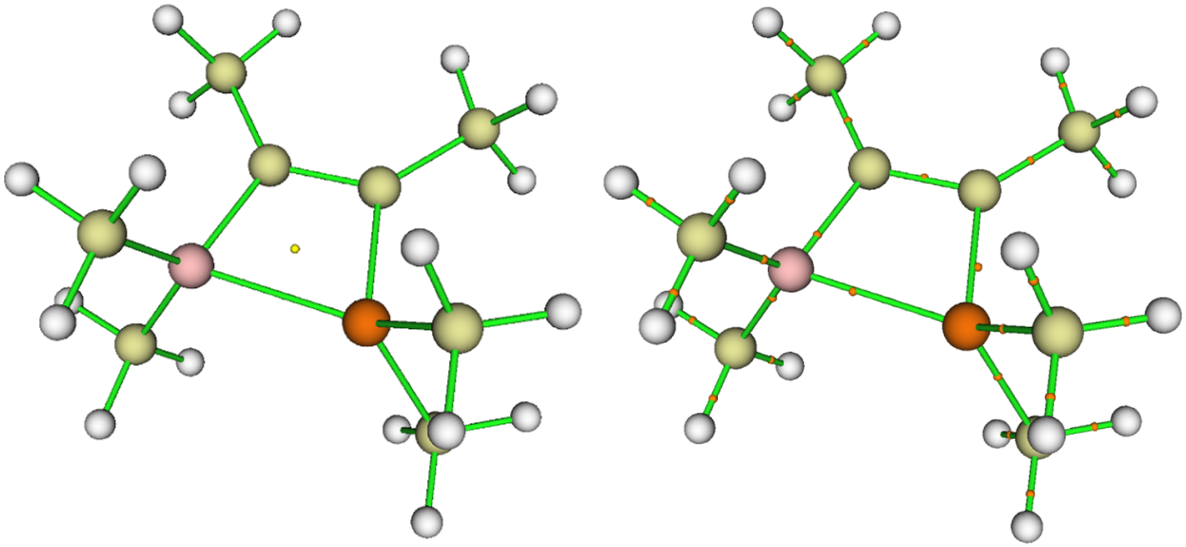

**Figure 2.7:** AIM schematic of **10** showing critical points (*orange = bond CP, yellow = ring CP*).

**Table 2.6:** Atoms in Molecules – data for **1-3, 10**, ordered in decreasing bulk of the R group.

| | **10** | **3** | **1** | **2** |
|---|---|---|---|---|
| **ρ(r)** | 0.079 | 0.068 | 0.068 | 0.079 |
| **$\nabla^2$ (r)** | -0.063 | -0.027 | -0.027 | -0.067 |
| **G(r)** | 0.028 | 0.024 | 0.024 | 0.025 |
| **V(r)** | -0.071 | -0.055 | -0.055 | -0.065 |

**ρ(r)** = density of all electrons - indicator of how strong bond is

**$\nabla^2$(r)** = Laplacian of electron density (*2nd gradient of electron density*)

**G(r)** = Lagrangian energy – gradient kinetic energy

**V(r)** = Potential energy density

Comparing the phosphine-boranes (**Figure 2.8**) suggests that the P-B bond of **10** and **2** are the strongest, compared to **1** and **3**. Combining the NMR and X-ray data with the DFT calculations indicates the P-B bond strength for the phosphine borane is **10** > **2** > **3** > **1**. The ligand **10** has the strongest bond, determined by it having the lowest frequency phosphorus NMR resonance, the shortest P-B length by DFT calculations, and the highest electron density (ρ(r)) determined by AIM calculations. In contrast, **1** has the weakest P-B bond, although the

difference in strength between **1** and **2** is negligible. The $^{31}P\{^{1}H\}$ NMR resonance for **1** being the higher frequency, it also has the longest P-B bond in both X-ray diffraction studies and DFT calculations. AIM calculations suggest this to be a stronger bond than the P-B bond in **3**, though the difference is minimal.

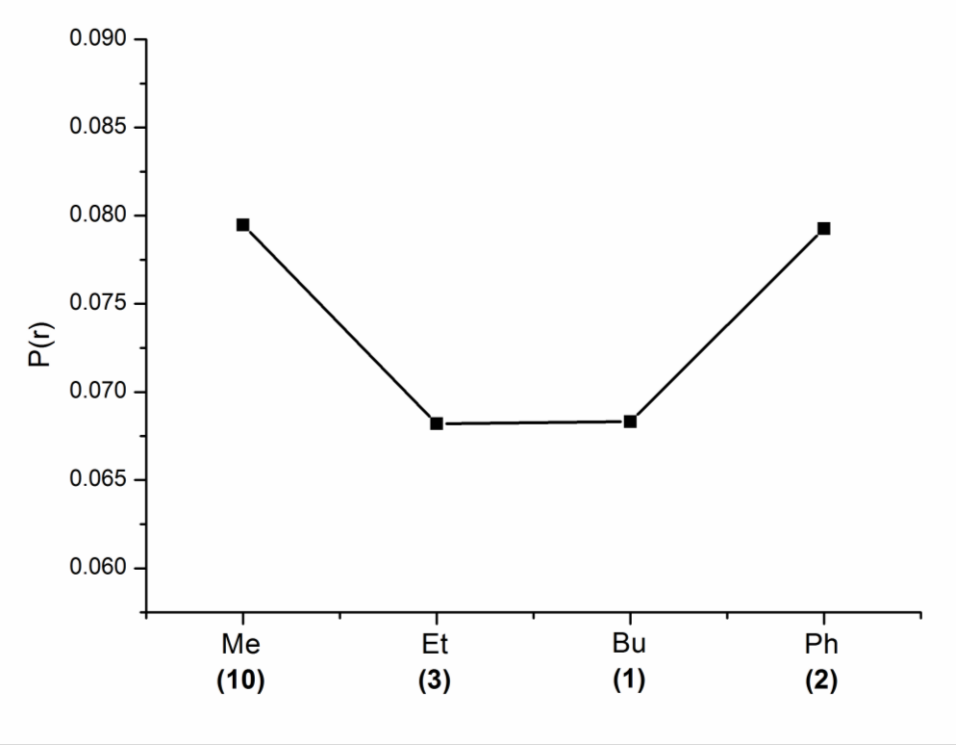


**Figure 2.8**: Electron density (ρ(r)) at the critical point along the P-B bond of **1**-**3** and **10**. Me, Et, Bu and Ph refer to substituents on boron atom ($R_2B(R)C=C(R')PR'_2$ R' = R = Me (**10**), R' = Ph, R = Et (**3**), Bu (**1**), Ph (**2**)).

### 2.2.3.2 Natural Bond Orbital Analysis

Intuitively, the molecule with the weakest P-B bond should therefore be the one that is most easy to break the P-B interaction and to replace it with a phosphorus-metal interaction (see **Section 3.2**). However, the calculated molecular orbitals of **1** show a general lack of involvement of the P-B bond on the frontier molecular orbitals. Indeed the molecular orbitals are complex and show hyper-conjugation, but generally show that the HOMO involves some contribution of the P-B bond, and the HOMO-1 contains the σ-phosphorus-boron interaction and the alkenic π-bond. The LUMO and LUMO+1 are mostly centred on the phosphorus aryl units and contain little contribution from boron (**Figure 2.9**). Similar areas of electron density are seen in **2**-**3** and **10**.

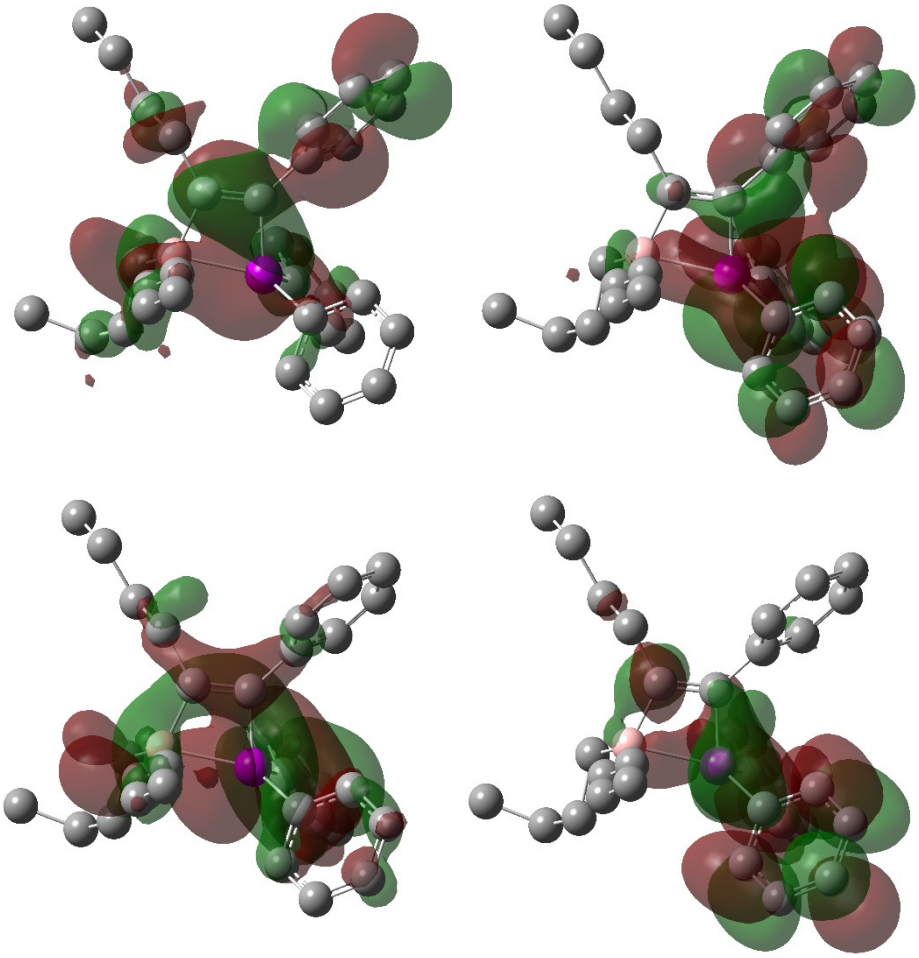

**Figure 2.9**: Molecular orbitals of **1**, HOMO (*top left*), LUMO (*top right*), HOMO-1 (*bottom left*), LUMO+1 (*bottom right*).

Natural Bond Orbital analysis was used to visualise an approximation for the atomic orbitals on the phosphine-borane systems. It indicates the aromatic systems feature heavily in the frontier orbitals. The P-B bonding orbitals are found in HOMO-10 for **1** and **3**, with the corresponding antibonding orbitals at LUMO+10 (**Figure 2.10**). Whereas in the **10** system, there are no aromatic phenyl rings, and the HOMO and LUMO are centred on the C=C bridge, the HOMO-1 and the LUMO+1 are on the P-B bond (**Figure 2.11**).

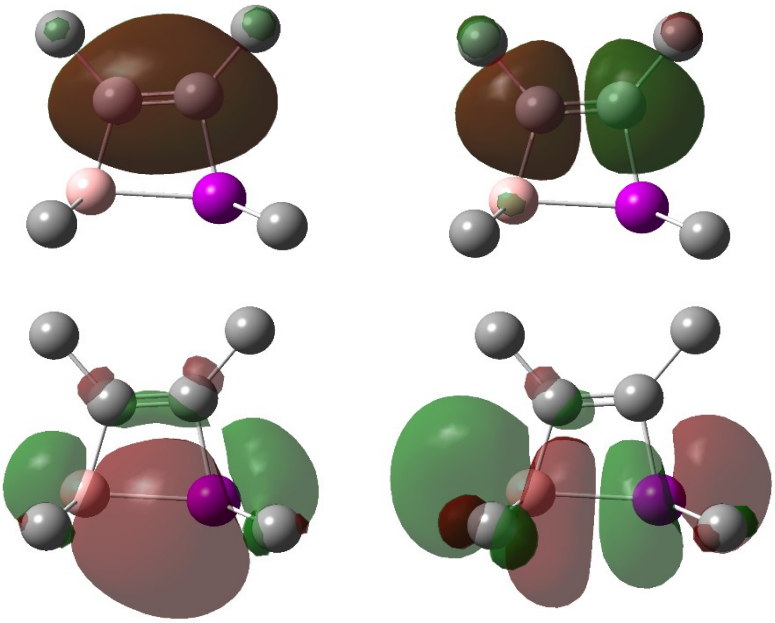

**Figure 2.10**: NBO orbitals for **1**, HOMO (*top left*), LUMO (*top right*), HOMO-10 (*bottom left*) LUMO+10 (*bottom right*).

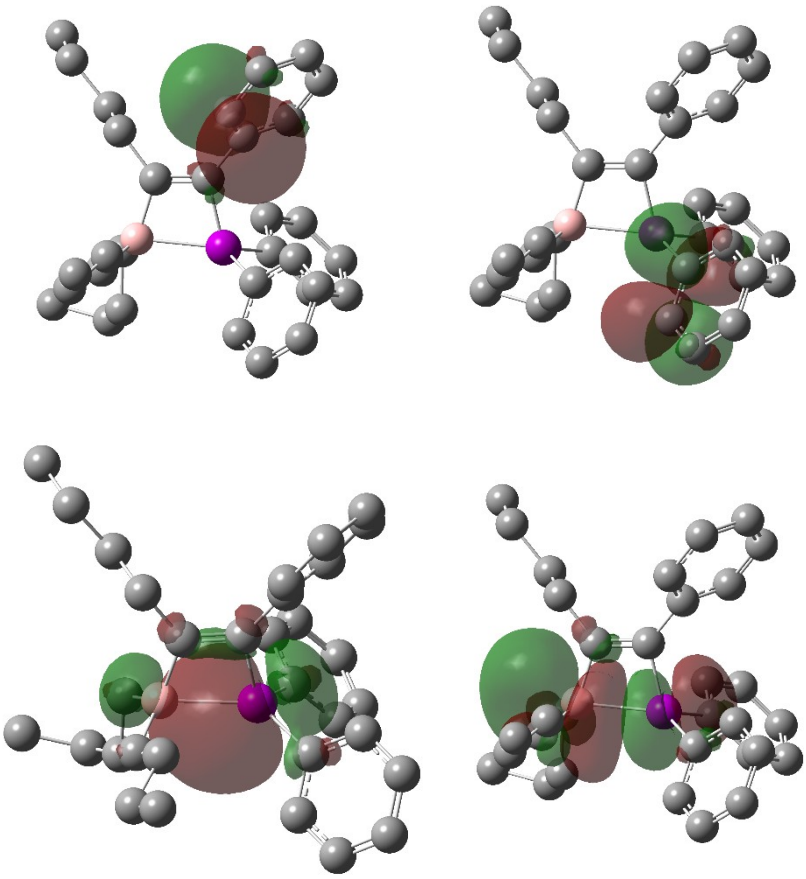

**Figure 2.11**: NBO analysis for **10**. HOMO (*top left*), LUMO (*top right*), HOMO-1 (*bottom left*), LUMO+1 (*bottom right*).

NBO data also can be used to provide the breakdown of the *s*- and *p*- character of various bonds, and also describes the hybridisation of the bond shown in **Table 2.7**. This shows that **10** and **2** have a marginally higher contribution from boron, and more *s*- character in the bond than **3** and **1**. The P-B bond in **10** is also more closely described as $sp^2$ hybridised orbital, this may account for the stronger bond in **10**.

**Table 2.7**: NBO analysis of **1-3, 10**.

| | **Contribution (%)** | | **Breakdown of P contributions (%)** | | | **Breakdown of B contributions (%)** | | | sp hybrid |
|---|---|---|---|---|---|---|---|---|---|
| | **P** | **B** | *s* | *p* | *d* | *s* | *p* | *d* | |
| **10** | 70.86 | 29.14 | 32.99 | 66.79 | 0.22 | 12.38 | 87.43 | 0.20 | $sp^{2.02}d^{0.01}$ |
| **2** | 69.54 | 30.46 | 30.35 | 69.50 | 0.15 | 12.27 | 87.59 | 0.15 | $sp^{2.29}$ |
| **3** | 73.64 | 26.36 | 31.13 | 68.77 | 0.1 | 10.76 | 89.09 | 0.15 | $sp^{2.21}$ |
| **1** | 73.66 | 26.34 | 31.03 | 68.86 | 0.1 | 10.67 | 89.19 | 0.14 | $sp^{2.22}$ |

### 2.2.4 Attempts to expand the range of phosphine-boranes

Alternative methods for the synthesis of similar compounds to **1-3** were briefly explored in order to have differing groups on the C=C backbone. The synthesis of $Bu_2BC(Bu)=C(SiMe_3)PPh_2$ (**11**) was attempted using the same reaction conditions as for **1**, *i.e*. the addition of $Bu_3B$ and $Ph_2PCl$ to a lithiated alkyne (in this case $LiC{\equiv}CSiMe_3$) before being heated to reflux in $Et_2O$. Attempts to distil the product failed despite heating to >200 °C at $3.0x10^{-2}$ mbar. However, subsequent NMR spectroscopy of the bulk mixture revealed fewer signals in both the $^{31}P\{^1H\}$ and $^{11}B\{^1H\}$ NMR spectra compared to the initial crude NMR spectra, suggesting an insufficiency of the initial reflux conditions. Sublimation did not remove the impurities and preliminary thin layer chromatography failed to elucidate a solvent system which could separate the products. The 2D silicon-proton correlation NMR experiments indicated three separate silicon environments, The main $^{31}P\{^1H\}$ and $^{11}B\{^1H\}$ NMR resonances ($\delta_P$ = 12.1, $\delta_B$= 11.9 ppm) are similar to other borylphosphinoethenes derived from the same phosphine

starting material, or borane (as shown in **Table 2.1**), suggesting that the desired product is one component of the otherwise intractable mixture.

### 2.2.5 Attempted synthesis *via* carboboration.

Many papers have been published containing molecules of phosphine-boranes, where the boron component is fluorinated.[256–260] Similar systems to **1**-**3**, for example $(C_6F_5)_2BC(C_6F_5)=C(R)PR'_2$, have been synthesised by Jiang *et al.* who described the synthesis as being a straightforward addition of $B(C_6F_5)_3$ to the phosphinoacetylene in toluene, followed by heating to 70 °C for six hours (**Scheme 2.9**). The resulting orange solid was washed in pentane and dried under vacuum to reveal a high yielding yellow solid (77% yield).[244]

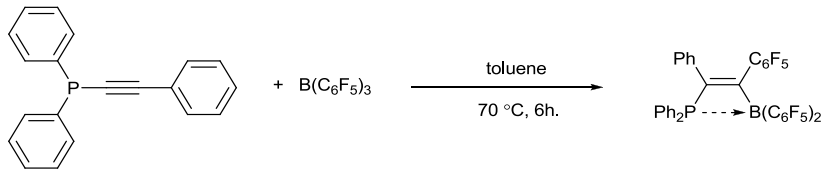


**Scheme 2.9**: Literature precedent for formation of $Ph_2P(Ph)C=C(C_6F_5)B(C_6F_5)_2$.[244]

By analogy to this procedure, stirring a toluene solution of **4** with $B(C_6F_5)_3$, led to a yellow solid with consistent spectroscopic data for $Ph_2P(Ph)C=C(C_6F_5)B(C_6F_5)_2$ (**12**) ($\delta_P$ = 13.6, $\delta_B$ = -6.3 ppm) in admixture with other impurities. A similar result was achieved with, $^tBu_2PC{\equiv}CPh$ (**7**) gave similar spectroscopic data (**13**; $\delta_P$ = 13.9, $\delta_B$ = −3.6 ppm). In contrast, analogous reactions with $^iPr_2PC{\equiv}CPh$ (**8**) or $Ph_2PC{\equiv}CSiMe_3$ (**9**) and $B(C_6F_5)_3$ led to mixtures of products; while the $^{11}B\{^1H\}$ NMR data ($\delta_B$ = −3.7 and −3.0, respectively) could suggest phosphine-boranes of the form $R_2P(R')C=C(C_6F_5)B(C_6F_5)_2$, there were multiple phosphorus containing species present, none of which seem consistent with the targeted phosphine-boranes.

An alternate methodology was thus attempted instead, using the same procedure as for the formation of $R_2C(R)=C(Ph)PPh_2$ (R = Bu (**1**), Et (**2**), Ph (**3**)). This synthesis was also unsuccessful as shown by the lack of consistent NMR data. If successful though, the one-pot reaction would not depend upon the formation of $R_2PC{\equiv}CPh$, therefore the reaction could occur at a lower temperature or shortened reaction times and could be further used to synthesise a wider range of compounds.

### 2.3.6 Attempted Hydroborations

In a typical hydroboration reaction, the hydride transfers from boron to the more substituted carbon, in an anti-Markovnikov fashion, with concomitant formation of a carbon to boron bond. This means that the hydrogen adds to the most sterically congested side of the alkyne.

The use of large/bulky secondary boranes provides the necessary steric screening against any further additions, in addition to the steric hindrance being vital to any application of these alkenes in FLP chemistry. It is, however, documented that the hydroboration of internal alkynes often results in a mixture of products unless the alkyne is symmetrically substituted. Hydroboration of $R_2PC{\equiv}CR'$ would allow the formation of phosphine-boranes with an ethene-bridge between the phosphorus and boron units, similar to **1**-**3**.

#### 2.3.6.1 Attempted hydroboration of 4, 7-8 with 9-BBN

$Ph_2PC{\equiv}CPh$ (**4**) and 9-BBN were dissolved in toluene and left to stir at ambient temperature for four days, after which the colourless solution was dried to an oily, white solid which was then washed with pentane (**Scheme 2.10**). NMR spectroscopic data of the washings show only starting materials ($\delta_P$ = −33.4, $\delta_B$ = 58.4) whilst crystals grown were found to be of the adduct $Ph_2P$(H-BBN)C≡CPh (**4-BBN**)(**Figure 2.12**).

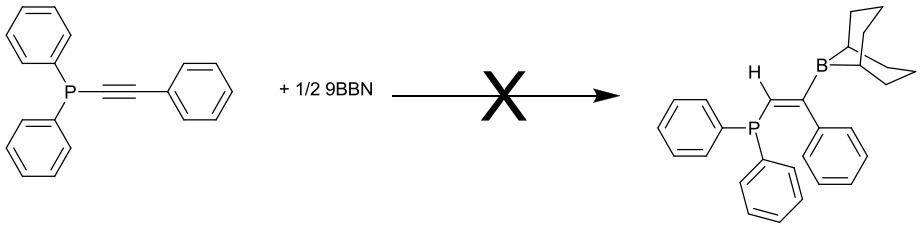


**Scheme 2.10**: Attempted hydroboration of $Ph_2PC{\equiv}CPh$ (**4**) with 9-BBN.

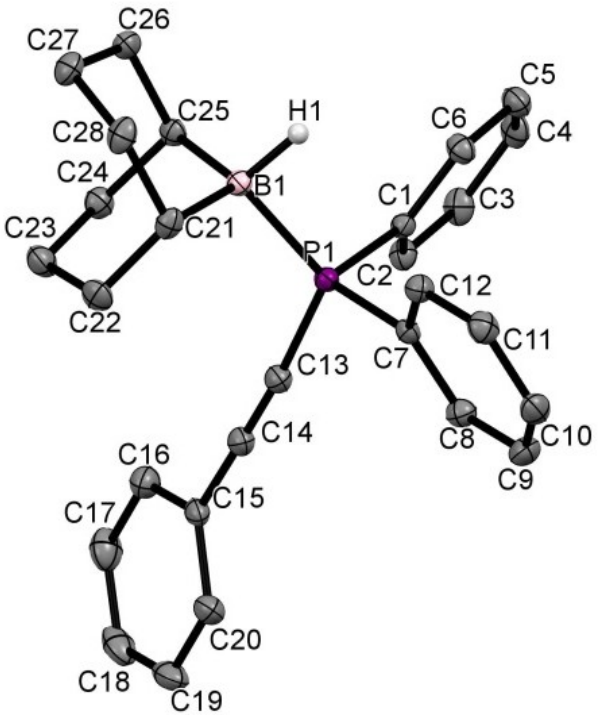


**Figure 2.12**: Structure of **4-BBN**, with the exception of B-H, hydrogen atoms removed for clarity, ellipsoids at 30%.

**Figure 2.12** shows that the geometry around phosphorus is pyramidal. **Table 2.8** shows key data for the structure of **4-BBN**, it shows that the C≡C bond length is marginally longer than that of $^{t}Bu_2PC{\equiv}CPh$ (**7**), and the C-C-C angle is almost linear, with similar $R_2$-P distances to **7**. No crystallographic data of **4** exist other than as coordination complexes, so the effect of the 9-BBN adduct on the solid state structure of **4** is unknown. However, crystallographically characterised coordination complexes of **4** [*cis*-$PtCl_2$(**4**)$_2$], [Cp*$RhCl_2$(**4**)] and [*trans*-$PdI_2$(**4**)$_2$] adopt a similar geometry to **4-BBN**. Indeed the P-aryl (1.813−1.846 Å), P-C (1.754−1.759 Å), and C≡C (1.194−1.204 Å) bond distances of the complexes all encompass the values for **4-BBN**. The P-B bond is obviously much smaller than the range of P-metal distance described for metal complexes of **4** (2.235−2.327 vs 1.9737(18) Å) and the presence of the metal distorts the linearity of the alkynic bond (167.92−175.19 °) compared to **4-BBN** (176.09(18) °).[253]

**Table 2.8**: Key bond lengths and selected angles of **4-BBN** (with estimated standard deviations in parentheses)**.**

| Bond | Length (Å) | Bond | Angle (°) |
|---|---|---|---|
| **C13-C14** | 1.202(2) | **C13-P1-C1** | 103.28(7) |
| **C14-C15** | 1.439(2) | **C13-P1-C7** | 103.97(7) |
| **P1-C13** | 1.7546(16) | **C13-C14-C15** | 176.09(18) |
| **P1-B1** | 1.9737(18) | **C13-P1-B1** | 119.21(7) |
| **P1-C7** | 1.8221(15) | **C1-P1-C7** | 105.14(7) |
| **P1-C7** | 1.8158(15) | | |

It is possible that the adduct, (**4-BBN**) (**Scheme 2.11**) is not very stable in solution as NMR spectra of the crystals reveal mostly starting material (**4**) and low levels of the adduct ($\delta_P$ = −7.4 $\delta_B$ = −13.3). The broadness of the phosphorus signal of this second species (half-height width: 85 Hz) suggests it is in proximity to boron, and the boron chemical shift suggests that it is four-coordinate, this correlates with the structure and indicates the B-H unit is intact. It is suggested that the B-H proton would lie in the range 1.6 - 2.4 ppm, and thus overlap with the protons associated with 9-BBN, (as Luck proposes is the case with similar adduct, $MePh_2P{\cdot}BH(C_8H_{14})$[261]) though, as this is the minor product in the NMR sample, separate $^{13}C\{^1H\}$ and $^1H$ data for the adduct have not yet been obtained.

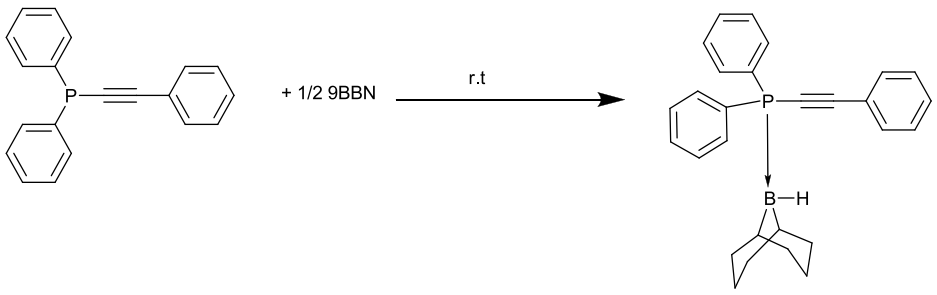


**Scheme 2.11**: Formation of $PPh_2PC{\equiv}CPh$ - borane adduct (**4-BBN**).

Stirring **7** and half an equivalent of 9-BBN at room temperature in toluene for three days led to crystallisation of colourless rods, the unit cell of which revealed it was the starting material (**7**).

When half an equivalent of 9-BBN and **8** were dissolved in toluene and left to stir at ambient temperature for four days, $^{31}P\{^{1}H\}$ NMR spectra revealed mostly unreacted **8**. Also present in the solution was a species with a broad $^{31}P\{^{1}H\}$ NMR signal at 6.3 ppm. The width of the signal (half-height width: 100 Hz) could indicate a phosphorus/boron interaction, but it is not possible to prove this without more complex NMR experiments than are readily available (such as P/B 2D correlation spectroscopy or phosphorus-decoupled boron spectra). The $^{11}B\{^{1}H\}$ NMR spectra show the presence of 9-BBN and also an additional signal at −15.8 ppm. It is not possible to determine if this signal corresponds to the $^{31}P\{^{1}H\}$ NMR resonance at 6.3 ppm, and attempts to grow crystals from the solution were unsuccessful.

Heating **4** or **7** and 9-BBN to reflux in toluene or THF for 3-18 hours resulted in recovered starting materials, 9-BBN and **4** or **7**.

After heating **4** for three hours with 9-BBN in toluene (55 °C), in addition to unreacted starting materials, $^{31}P\{^{1}H\}$ and $^{11}B\{^{1}H\}$ NMR spectra suggest the formation of the adduct ($\delta_P$ = −6.9, $\delta_B$ = −13.2), with the lack of a hydroboration product being confirmed by the absence of a corresponding alkenic proton. Attempts to use two equivalents of 9-BBN to drive the reaction towards the hydroboration product were unsuccessful, and spectroscopic data showed mostly **4** and 9-BBN. When the same mixture was heated to reflux in toluene (four hours) before the straw coloured solution was dried to a yellow oil, the $^{31}P\{^{1}H\}$ NMR data showed an intractable mixture of products ($\delta_P$ = 5.7, −11.8 and −15.4). The $^{11}B\{^{1}H\}$ NMR data indicate the presence of a 3-coordinate species at 78.0 ppm, which would be consistent with the possible hydroboration product. In the crude mixture a doublet can be seen in the proton NMR spectrum at 7.74 ppm ($J$ = 8 Hz), which could indicate the formation of an alkene, which is expected for hydroboration, however, this was a minor product in the mixture.

Under the same reaction conditions, **7** failed to react. However, when refluxing in THF, the colourless solution again turned yellow, and was subsequently dried to afford a yellow oil. Other than the 9-BBN starting material at 58.6 ppm, $^{11}B\{^{1}H\}$ NMR data revealed only 4-coordinate species (some of which may be a result of thf-borane adducts), which is not consistent with an expected hydroboration product.

The $^{31}P\{^{1}H\}$ NMR spectra indicated that the major species was **7**, in addition to a small broad signal observed at 59.4 ppm. This may be consistent with the formation of an adduct; however, the difference in chemical shift compared to **7** is perhaps more consistent with that observed upon conversion of **4** to **1**, than upon formation of the **4-BBN** adduct. This might suggest the formation of the *Z*-alkene hydroboration product which has formed a closed P-B

system, similar to that of **1**-**3**. This phosphorus-boron interaction would account for the 4-coordinate resonance in the $^{11}B\{^1H\}$ NMR spectra, however, given the inability to observe the alkenic proton, due its likely overlap with the resonances of 9-BBN, this remains speculative.

#### 2.3.6.2 Using Catecholborane

The ambient temperature addition of HBcat (HBcat = Catecholborane) to **4** did not result in adduct formation as demonstrated with 9-BBN. Spectroscopic data indicated only **4** ($\delta_P$ = −33.4) and HBcat ($\delta_B$ = 23.1). Alkynes **4** and **8** were also heated to reflux with HBcat, a doublet in the $^1H$ NMR spectrum at 6.1 ppm ($J$ = 6 Hz) was observed after refluxing **4** with HBcat in toluene for 18 hours, this could indicate successful hydroboration, however, the $^{31}P\{^1H\}$ NMR spectrum reveals mostly unreacted **4** with a minor product at 8.1 ppm, while $^{11}B\{^1H\}$ NMR data show only HBcat ($\delta_B$ = 23.1). Similarly, while spectroscopic data after heating a mixture of **8** and HBcat in toluene to reflux, exhibited multiple small signals in $^{31}P\{^1H\}$ NMR spectrum, the major component was unreacted **8**. The $^{11}B\{^1H\}$ NMR spectrum indicated the presence of HBcat and some unknown compounds ($\delta_B$ = 23.1 14.5, 7.7 and −44.0 (d, $J$ = 63 Hz)) which have not yet been identified. The doublet in the proton decoupled boron spectrum is likely to come from interaction with phosphorus, however, the nature of this interaction remains unknown.

Apart from crystallographic data for the formation of **4-BBN**, no other discernible products were found from the attempted hydroboration of these unsymmetrical alkynes with 9-BBN or HBcat. This may imply the combination of 9-BBN and $(^tBu)_2PC{\equiv}CPh$ or $^iPr_2PC{\equiv}CPh$ are too bulky, either for hydroboration, or adduct formation.

#### 2.3.6.3 Attempted hydroalumination

The hydroalumination of **4** with H-Al($^i$Bu)$_2$ was attempted in the same manner as for hydroboration attempts, by heating to reflux in a toluene solution. $^{31}P\{^1H\}$ NMR spectroscopic data of the isolated yellow solid revealed the presence of greater than 15 resonances between −35 and 25 ppm. Unfortunately, over time the $CDCl_3$ solution assumed a red colouration as the products degraded into further unidentified species.

## 2.4 Other alkynes

Previous results (**Scheme 2.12**) within the group have yielded a series of alkynes bearing main group termini; $^{i}Pr_3SiC{\equiv}CCH_2Cl$ (**13**), $^{n}Pr_3SiC{\equiv}CCH_2Cl$ (**14**), $^{n}Bu_3SiC{\equiv}CCH_2Cl$ (**15**), $Me_2PhSiC{\equiv}CCH_2Cl$ (**16**) and $Me_2PhSiC{\equiv}CCH_2PPh_2$ (**17**).[262,263] Attempts have been made to hydroborate these alkyne fragments in order to prepare a novel range of boranes.

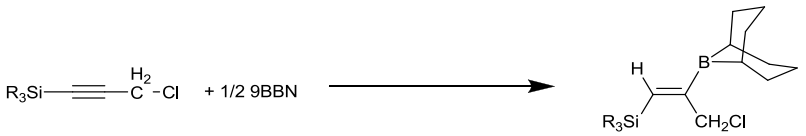


**Scheme 2.12**: Expected hydroboration reaction upon the addition of 9-BBN to **13** - **17**.

### 2.4.1 With 9-BBN and HBcat

A toluene solution of **13** and one equivalent HBcat was heated to reflux for 18 hours. Spectroscopic analysis revealed no reaction had occurred. Equimolar amounts of **14** and **15** and either HBcat or 9-BBN were dissolved in toluene and heated to reflux for between 8-18 hours, after which point the solution was dried and extracted with pentane.

In the reaction of **14** with one equivalent of 9-BBN, the proton NMR resonances of the resulting oils were all broadened and had shifted with respect to the starting material, this might suggest that the alkyne itself has degraded. The $^{11}B\{^{1}H\}$ NMR spectra revealed the presence of multiple products in the case with 9-BBN, and in the case of HBcat, only revealed the presence of HBcat.

When two equivalents of 9-BBN in toluene were heated to reflux with **14** for two days, $^{11}B\{^{1}H\}$ NMR data revealed a signal at 58.3 ppm, which is an impurity from the 9-BBN starting material, and two very broad signals at 77.0 and 86.3 ppm as shown in **Figure 2.13**.

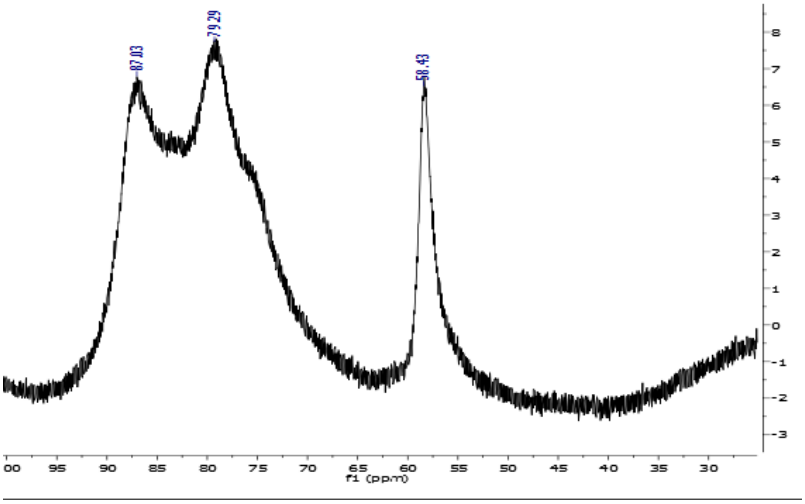


**Figure 2.13**: NMR spectrum showing boron signals from the reaction of **14** with two equivalents of 9-BBN.

The $^{1}$H NMR spectrum show additional signals between 5.0 and 5.8 ppm. The $CH_2$ signal from the alkyne at 3.55 ppm, now appears as a doublet at 3.67 ppm ($J$ = 7 Hz). This would seem consistent with successful hydroboration, exhibiting coupling to the *trans*-alkenic proton. In this case, the triplet at 5.93 ppm ($J$ = 7 Hz) would be the corresponding proton coupling to the $CH_2Cl$ group. However, the integration of these signals is 1:1.5, which is inconclusive though this could be the result of broadening/shimming effects. Many other species are also apparent.

Crude spectroscopic data show no reaction in the case of **15** with 9-BBN**,** as the $^{11}B\{^{1}H\}$ NMR spectrum only indicated the presence of 9-BBN, and $^{1}$H NMR data show very little change from the alkyne starting material other than the broad multiplets associated with 9-BBN protons. The $CH_2Cl$ signal of the starting material remained, with no evidence for coupling between this and any other alkenic protons, as would be expected if hydroboration had occurred. In contrast, the $CH_2Cl$ proton signal had been replaced by a number of doublets and multiplets in a similar region, it cannot be concluded if this is a trace of the hydroboration product or not, and there were a number of less intense triplets in the aromatic region with similar coupling values.

Heating a mixture of 9-BBN and **16** to reflux in toluene for 18 hours led to the formation of a mixture of products. Complete consumption of **16** was apparent from the loss of characteristic resonances associated with the $CH_2Cl$ moiety. The $^{1}$H NMR spectrum contains a triplet at 6.65 ppm (=CHR) which couples (7.2 Hz) to a corresponding doublet at 4.06 ppm ($CH_2Cl$), both of these integrate consistently against a signal at 0.48 ppm ($SiMe_2$). Based upon integrations of

signals around the $CH_2Cl$ resonance of **16**, 50% of the mixture is consistent with this *E*-alkene, hydroboration product (**Scheme 2.13**). The remaining components in this mixture were unassignable, and did not correspond to those of **16**. Due to the hydroboration product being the largest signal in the $^{1}H$ NMR spectrum, it is likely that the strongest signal in the $^{11}B\{^{1}H\}$ NMR spectrum ($\delta_B$ = 83.6) corresponds to the same compound. In addition $^{11}B$ NMR data show residual 9-BBN, a minor signal at 17.0 ppm, which lies in the 4-coordinate region, and broadened signal at 70.1 ppm in the 3-coordinate region.

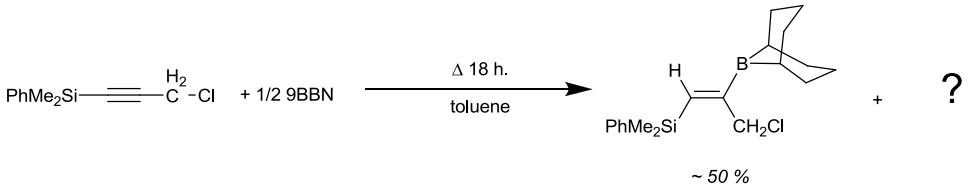


**Scheme 2.13**: Formation of hydroboration product of **16** with 9-BBN.

The proportion of product was not able to be increased by alternative reaction conditions such as heating to refluxing for 18 hours in THF or heating a toluene solution to 55-60 °C (as suggested by Schmidbaur[91] to minimise side reactions). Attempts to isolate this hydroboration product by extraction (pentane, hexane or diethyl ether), or sublimation were unsuccessful.

Previous work within the group afforded $Me_2PhSiC{\equiv}CCH_2PPh_2$ (**17**), a phosphine derivative of **16**. This was prepared through the addition of $Li[PPh_2]$ to $Me_2PhSiC{\equiv}CCH_2Cl$ (**16**).[193] Attempts to hydroborate **17** with 9-BBN led to upwards of 20 phosphorus environments, ranging from -40 to 120 ppm. Boron NMR data showed a single resonance at 58 ppm, which corresponds to 9-BBN. This suggests that the hydroboration by does not occur in any detectable quantities under any of the conditions utilised.

## 2.5 Synthesis of alkane-bridged phosphine borane ligands.

### 2.5.1 Synthesis of $Ph_2PCH_2CH_2BBN$ (18), $Ph_2CH_2CH_2CH_2BBN$ (19) and $Fu_2PCH_2CH_2BBN$ (21)

The compounds $Ph_2PCH_2CH_2BBN$ (**18**)[264] and $Ph_2PCH_2CH_2CH_2BBN$ (**19**),[91] have been made through the hydroboration of vinylic phosphines $Ph_2PCH{=}CH_2$ and $Ph_2PCH_2CH{=}CH_2$ respectively

following literature methods. Previous work within the group has established a method for the synthesis for the new phosphine-borane ligand, $Fu_2PCH_2CH_2BBN$ (**20**) (Fu = $C_4H_4O$), which has shown promise towards coordinating to a number of metal complexes.[265]

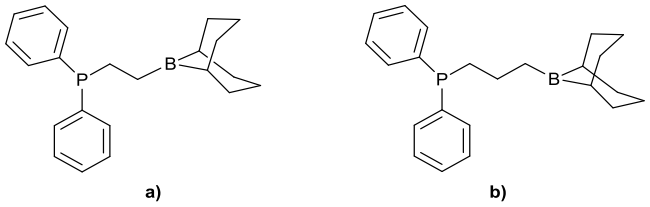


**Figure 2.14: a)** $Ph_2PCH_2CH_2BBN$ (**18**)[264] and **b)** $Ph_2PCH_2CH_2CH_2BBN$ (**19**).[91]

Following on from this precedent, the work has been extended. First, the vinylic compound $Fu_2PCH{=}CH_2$ (**20**) was made from the addition of $Fu_2PCl$ to $H_2C{=}CHMgBr$, which was then heated (60 ˚C) in toluene with 9-BBN, to form the phosphine-borane, $Fu_2PCH_2CH_2BBN$ (**21**) (**Scheme 2.14**). The spectroscopic data ($\delta_B$ = 87.2) fits with similar borane containing systems, **18** ($\delta_B$ = 87.9),[264] $(C_8H_{14})BCH_2CH_2CH_3$ ($\delta_B$ = 88.6)[266] and $Ph_2PCH_2CH_2BCy_2$ ($\delta_B$ = 81.8)[264] (**Table 2.9**) which also suggest the phosphine-borane exists in its open configuration, with no discernible phosphorus-boron interaction.

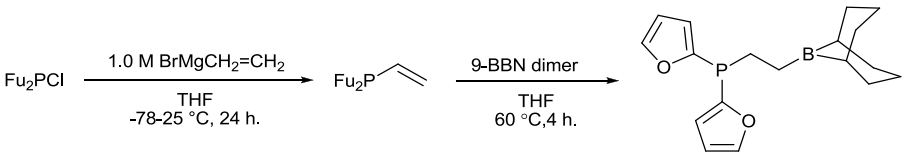


**Scheme 2.14**: Synthesis of $Fu_2PCH_2CH_2BBN$ (**21**).

**Table 2.9**: Spectroscopic data of **18**, **19**, **21** and others of the type - $R_2PCH_2CH_2BR'_2$.

| | $^{31}P$ | $^{11}B$ |
|---|---|---|
| **$Ph_2PCH_2CH_2BBN$ (18)** | -10.0 | 86.7 |
| **$Ph_2PCH_2CH_2CH_2BBN$ (19)** | 9.8 | 0.8 |
| **$Fu_2PCH_2CH_2BBN$ (21)** | -56.0 | 87.2 |
| **$Mes_2PCH_2CH_2B(C_6F_5)_2$** [93] | 20.6 | 8.5 |
| **$Ph_2PCH_2CH_2B(Cy)_2$** [90] | 8.5 | 83.0 |
| **$(C_6F_5)_2PCH_2CH_2B(C_6F_5)_2$** [267] | -39.8 | 73.0 |
| **$Mes_2PCH_2CH_2B(C_6F_5)(C{=}C^nPr)$** [94] | -15.9 | 0.5 |
| **$Mes_2PCH_2CH_2B(C_6F_5)(CH_2CH_2Ph)$** [94] | -15.9 | 1.6 |
| **$(C_2H_3)(^iPr_3C_6H_2)PCH_2CH_2B(C_6F_5)_2$** [268] | 7.1 | 0.7 |

Structural data were not forthcoming with $Fu_2PCH_2CH_2BBN$ (**21**). However, once coordinated to a metal centre by the stirring of **21** with $[Rh(CO)_2Cl]_2$ in $CH_2Cl_2$ for 18 hours, single crystals were obtained from the slow evaporation of pentane to reveal the structure of the coordination complex $[RhCl(CO)(Fu_2PCH_2CH_2BBN)_2]$ (**22**) (**Section 3.3**).

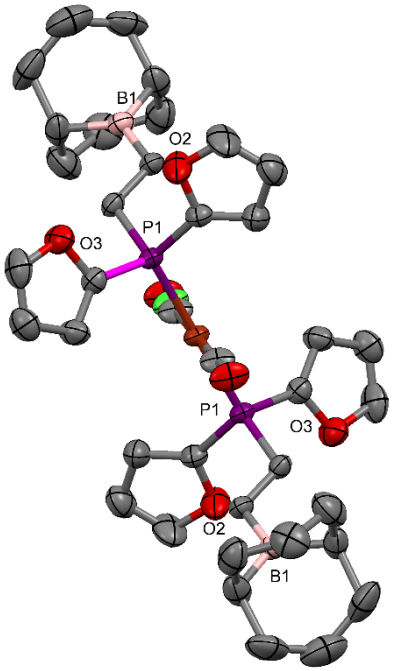


**Figure 2.15**: Ortep plot of **22** showing the ligand **21** (thermal ellipsoids plotted at 30% level and hydrogens atoms have been removed for clarity). Note the CO and Cl ligands are refined across two sites 50:50. This disorder between the Cl and CO ligands has been noted in similar structures.[100]

### 2.5.2 Synthesis of $^{t}$Bu(Ph)PCH=CH$_2$

Attempts were made to synthesise the analogous phosphine-borane $^{t}$Bu(Ph)PCH$_2$CH$_2$BBN, from the vinyl phosphine $^{t}$Bu(Ph)PCH=CH$_2$,[265] in the same manner as Fu$_2$PCH=CH$_2$ (**20**). The $^{31}$P{$^{1}$H} NMR spectra revealed a total of four distinct phosphorus containing species, including $^{t}$Bu(Ph)PCH=CH$_2$ ($\delta_P$ = 146.6). The mixture formed crystals of [$^{t}$Bu(Ph)P]$_2$ (**23**) upon standing; though X-ray diffraction data demonstrated connectivity (**Figure 2.16**), these were not of publication quality. The dimer, **23** observed in the $^{31}$P{$^{1}$H} NMR spectrum at −4.0 ppm,[269] has been documented to form as a side product from the addition of $^{n}$BuLi to $^{t}$Bu(Ph)PCl in THF.[270]

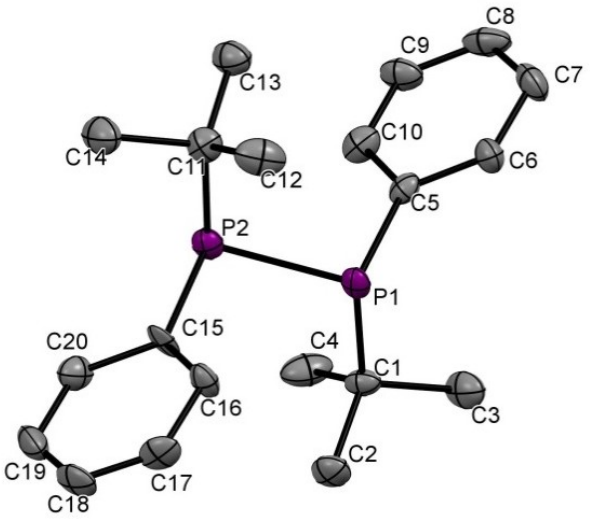


**Figure 2.16**: Molecular geometry obtained of [$^{t}$Bu(Ph)P]$_2$ (**23**).

$^{i}$Pr$_2$PCH=CH$_2$ and $^{t}$Bu$_2$PCH=CH$_2$ have been previously synthesised using [PdCl$_2$(MeCN)$_2$] or CuCl respectively as catalysts.[271] Attempts herein to synthesis these using the more direct method as used to prepare Fu$_2$PCH=CH$_2$ (**20**) were unsuccessful, as $^{31}$P{$^{1}$H} NMR spectra indicate mostly unreacted R$_2$PCl, while $^{1}$H NMR data do not reveal any vinylic protons.

### 2.5.3 Attempted hydroboration reactions

Thangavelu *et al.* uses Cp$_2$Ti(HBcat)$_2$ as a catalyst in the hydroboration of Ph$_2$PCH=CH$_2$ with HBcat,[272] but no reports document the direct hydroboration, therefore attempts were made to synthesise Ph$_2$PCH$_2$CH$_2$BCat (**24**) and Fu$_2$PCH$_2$CH$_2$BCat (**25**), without the use of a transition metal catalyst (**Scheme 2.15**). However, the addition of borane did not occur in either case,

spectroscopic data of the resulting white solids showed starting materials ($\delta_P$ = −10.7; $Ph_2PCH=CH_2$, −57.1; **20**) and ($\delta_B$ = 28.4, HBcat) and $^1$H NMR data confirmed the continued presence of the vinylic species.

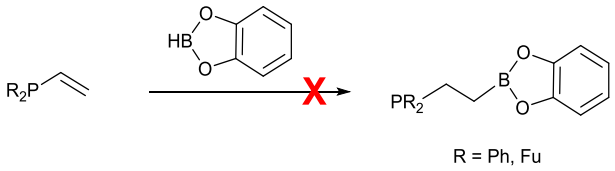


**Scheme 2.15**: Attempted hydroboration of $R_2PCH=CH$ with HBcat.

## 2.6 Summary of the preparation of saturated and unsaturated phosphine-boranes.

The synthesis of unsaturated phosphine-borane systems $Bu_2BC(Bu)=C(Ph)PPh_2$ (**1**) and $Bu_2BC(Bu)=C(Ph)PPh_2$ (**2**) have been improved and the compounds fully characterised for the first time, alongside the analogue $Et_2BC(Et)=C(Ph)PPh_2$ (**3**). The solid state structures of compounds **1**-**3** have been determined, and used as a basis for DFT studies of these and related compounds. In addition, the relative strengths of the P-B bonds in **1**-**3** and $Me_2BC(Me)=C(Me)PMe_2$ (**10**) have been compared using the computational tool 'Atoms In Molecules' alongside crystallographic and spectroscopic data of **1**-**3**, indicating that **10** has the strongest P-B bond. The same methodology was not successful using alternate phosphines ($^iPr_2PCl$ or $^tBu_2PCl$) or with a modified backbone (using $Me_3SiC{\equiv}CH$ instead of $PhC{\equiv}CH$).

The attempted hydroboration of phosphine-alkynes $R_2PC{\equiv}CPh$ (**4**, **7**-**9**) with 9-BBN or HBcat led to the isolation of crystals of a $Ph_2PC{\equiv}CPh$/BBN adduct (**4-BBN**), with no evidence for the hydroboration of the C≡C bond in **7**-**9**. The hydroboration of alkynes featuring main group termini (**13**-**17**) using HBcat and 9-BBN were also ultimately unsuccessful.

The literature hydroborations of $Ph_2PCH=CH_2$ and $Ph_2PCH_2CH=CH_2$ to afford $Ph_2PCHCH_2BBN$ (**18**) and $Ph_2PCH_2CH_2CH_2BBN$ (**19**) were repeated, alongside the formation of $Fu_2PCH_2CH_2BBN$ (**20**) following on from previous work within the group. Spectroscopic data of these saturated phosphine-boranes show they exist in an open configuration, with no discernible phosphorus-boron interaction. No structural data for the ligand $Fu_2PCH_2CH_2BBN$ exists, however, after coordination to a rhodium complex, crystals of have been obtained of the $RhCl(CO)(Fu_2PCH_2CH_2BBN)_2$ (**22**) confirming its structure.

Formation of the analogous phosphine-borane $^{t}$Bu(Ph)PCH$_2$CH$_2$BBN was unsuccessful, and a sample of the vinyl phosphine precursor $^{t}$Bu(Ph)PCH=CH$_2$ crystallised out as [$^{t}$Bu(Ph)P]$_2$ (**23**). A similar, catalyst-free synthesis to Fu$_2$PCH=CH$_2$ was not found to afford the vinyl systems $^{i}$Pr$_2$PCH=CH$_2$ and $^{t}$Bu$_2$PCH=CH$_2$. The catalyst free hydroboration of Ph$_2$PCH=CH$_2$ or Fu$_2$PCH=CH$_2$ with HBcat was also unsuccessful, with spectroscopic data showing the continued presence of vinylic starting materials.

# 3. Exploring the reactivity and coordination chemistry of phosphine-boranes

Transition-metal based FLPs have found applications in a number of organic reactions and transformations.[10] Both metal-based (whereby the metal acts as a Lewis acid)[68,273] and metal-free FLP systems have also found use in the activation of small molecules, notably $H_2$, $H_2O$ and $CO_2$. These reactivities were comprehensively reviewed by Stephan and Erker in 2010.[18] More recent reviews by Hounjet and Stephan[274] and Paradies[275] have focused on the search for transition-metal free catalysts for reducing a variety of unsaturated hydrocarbons including alkenes, alkynes and aromatic systems. The coordination chemistry of unsaturated phosphine-boranes **1**-**3**, and saturated boranes **18, 19 21** (**Scheme 3.1**) has therefore been explored to gauge their potential to act as components in transition metal-basic FLPs.

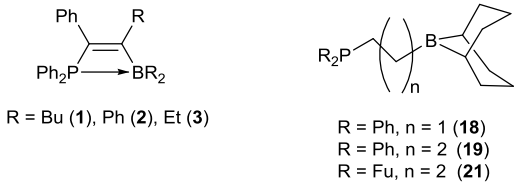


**Scheme 3.1:** Unsaturated systems (**1**-**3**) and saturated systems (**18**, **19**, **21**).

## 3.1 Investigation of the reactivity of $Bu_2BC(Bu)=C(Ph)PPh_2$ (1) towards other molecules

Baleuva *et al.* suggested that the phosphorus atom in $Ph_2PC(Ph)=C(Bu)BBu_2$ (**1**) will be much more reactive than that in $Ph_2PC(Ph)=C(Ph)BPh_2$ (**2**), based on the reactivity of **1** with $CS_2$ and that of **2** with sulphide.[241] It is suggested that this is due to the strengthening of the intramolecular donor-acceptor interactions as indicated by the shorter P-B bond in **2**. Balueva *et al.* also note that while **2** is air stable in the solid state, it oxidises slowly in dilute solution in the presence of air. Compound **2** was also found to react with oxygen with the resulting oxide having a $^{31}P\{^1H\}$ NMR resonance at 62.85 ppm (*cf.* 7.4 ppm for **2**). These reactions show that despite the strong bond, the P-B interaction can be interrupted for **2**, and by extrapolation, for **1** and **3**. Investigations were undertaken to explore ways to disrupt the interaction and encourage coordination to metal centres.

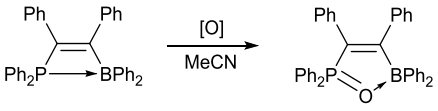


**Scheme 3.2:** Oxidation of solutions of **2** occur in dilute solutions, crystallised from MeCN.[241]

### 3.1.1 Reactions with 1 and CO

An NMR scale reaction of **1** with one atmosphere of CO was attempted, monitored by $^{31}P\{^{1}H\}$ NMR spectroscopy. No reaction was observed over four weeks at ambient temperature, or with heating (50 °C), spectroscopic data showing only the retention of signals associated with **1**. Similarly, prolonged bubbling of CO gas through a solution of **1** or **2** in $CD_2Cl_2$ did not result in any reaction.

### 3.1.2 Reactions with 9-BBN

As previously discussed (**Section 1.1.7.2**), the known FLP, $Mes_2PCH_2CH_2B(C_6F_5)_2$ undergoes a 'H for $C_6F_5$' exchange at boron upon the addition of 9-BBN,[94] thus, a comparable reaction of **1** with 9-BBN was attempted. An alternative possibility would be the hydroboration of the unsaturated backbone of **1** in a manner comparable to that described by as Tilley *et al.* who demonstrated the *trans*-hydroboration product shown in **Section 1.1.7.2**, **Scheme 1.31**, when $H_2C{=}CHPPh_2$ and 9-BBN were refluxed in toluene for three hours.[90] However, due to the increased steric bulk around the C=C backbone, a *trans*-product might be unfavoured.

The 9-BBN dimer was heated at reflux with two equivalents of **1** in toluene, over a period of four days, after which the solution was removed under reduced pressure to afford a white, sticky solid. The $^{11}B\{^{1}H\}$ NMR spectrum indicated two signals, one of which corresponded to **1** ($\delta_B$ = 13.2), while the other was assigned to the 9-BBN starting material ($\delta_B$ = 58.2). The $^{31}P\{^{1}H\}$ NMR spectrum indicated the presence of **1** ($\delta_P$= 10.0), along with three other minor signals, none of which suggest successful hydroboration due to the lack of a corresponding $^{11}B\{^{1}H\}$ signal.

## 3.2 Exploration of the coordination of $R_2BC(R)=C(Ph)PPh_2$

Following from Gröbe's report of the coordination of $Me_2PC(Me)=C(Me)BMe_2$ (**10**) to $[Rh(CO)_2Cl]_2$ (**Figure 3.1**) by stirring in toluene for three hours (**Section 1.1.8.3**),[100] similar

conditions were used to attempt coordination of **1**, **2** and $Ph_2PC(Ph)=C(Ph)BPh_2$ (**3**) to a number of metal complexes *viz.* $[RhL_2Cl]_2$, $L_2$ =$(CO)_2$, $\eta^4$-$C_8H_{12}$; $ML_2Cl_2$, M = Pt, Pd, $L_2$ = $(NCPh)_2$, $\eta^4$-$C_8H_{12}$ and $[Pd(PPh)_4]$. These reactions were monitored by the $^{31}P\{^1H\}$ NMR spectra of aliquots taken at regular intervals. Spectroscopic data of these reactions confirmed either unchanged **1**-**3**, or revealed the degradation of the starting materials to intractable species.

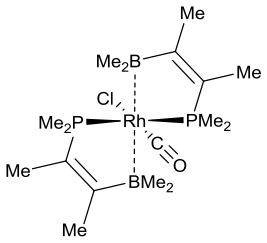


**Figure 3.1:** Gröbe's complex, from the coordination of (**10**) to $[Rh(CO)_2Cl]_2$.[100]

### 3.2.1 Attempted Coordination to $PtCl_2$ and $PdCl_2$

Two equivalents of **1** were stirred with $[PtCl_2]_n$ or $[PdCl_2]_n$ in $CH_2Cl_2$ for an extended time (several weeks), both reactions showed a large number of phosphorus-containing species, which could not be separated, alongside some remaining starting material in both mixtures. The $^{31}P\{^1H\}$ NMR spectra for the $PtCl_2$ mixture did not show any signals with resolvable platinum-satellites, and the only signal resolved in the $^{11}B\{^1H\}$ NMR spectrum was that of the starting material ($\delta_B$ = 13.8). Heating the reaction in order to break up the polymeric nature of $[PtCl_2]_n$ and $[PdCl_2]_n$ and increase reactivity proved ineffective.

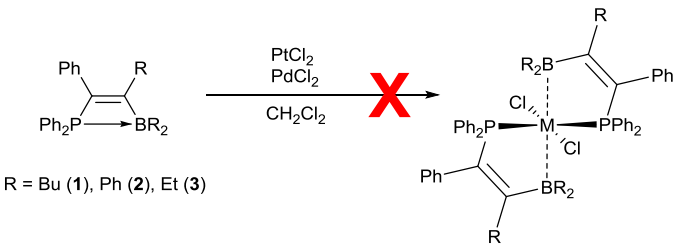


**Scheme 3.3**: Attempted coordination of **1**-**3** to $[PtCl_2]$ or $[PdCl_2]$.

### 3.2.2 Attempted Coordination with Pd complexes

As the polymeric dihalides proved ineffective substrates, discrete complexes were also employed. The palladium complexes $[Pd(PhCN)_2Cl_2]$, $[Pd(C_8H_{12})Cl_2]$ and $[Pd(OAc)_2]$ were each stirred for 24 hours in $CH_2Cl_2$ with two equivalents of **1** and reaction mixtures were monitored by $^{31}P\{^1H\}$NMR spectroscopy.

It was found that stirring $[Pd(PhCN)_2Cl_2]$ for a longer period of time caused little change in spectroscopic data. Reaction mixtures were monitored by $^{31}P\{^1H\}$ NMR spectroscopy over a 24 hour period, by the end of which the starting material (**1**) had been appreciably consumed, with several new species apparent ($\delta_P$ = 48.2 - 12.7). The reaction mixtures were subsequently left for 30 days and it was found that the proportion of **1** had reduced to 2% and the number of additional signals had increased. However, despite consumption of starting material, no new resonances were apparent in $^{11}B\{^1H\}$ NMR spectra.

The identification of the products from the reaction of **1** with palladium complexes $[Pd(PhCN)_2Cl_2]$ and $[Pd(C_8H_{12})Cl_2]$ was not possible, however, $^{31}P\{^1H\}$ NMR data of both palladium mixtures each contain the same signal, a singlet peak ($\delta_P$ = 47.4), and two over-lapping singlets ($\delta_P$ = 46.3 and 46.2) with equal integration. In contrast, $[Pd(OAc)_2]$ and two equivalents of **1** in $CH_2Cl_2$ did not afford the signal ($\delta_P$ = 47.4) despite the apparently complete consumptions of **1**. Attempts to separate the resulting mixture of products proved unsuccessful.

Stirring both $[Pd(PPh_3)_4]$ and **1** in $CH_2Cl_2$ for seven days at ambient temperature, or heating to reflux in $CH_2Cl_2$ for 18 hours, resulted in unchanged **1** and free $PPh_3$, as indicated by $^{31}P\{^1H\}$ and $^{11}B\{^1H\}$ spectroscopic data.

### 3.2.3 Attempted Coordination to modified metal salts

#### 3.2.3.1 Attempted Coordination to $[Pd(PhCN)_2Cl_2]$

To attempt to improve the reactivity of $[Pd(PhCN)_2Cl_2]$ with **1**, the two reagents were stirred overnight in the presence of $AgBF_4$ in the hope that the vacant coordination site would lead to the coordination of **1**.[276] After filtering and the removal of solvent, $^{11}B\{^1H\}$ NMR spectra of the resulting orange solid showed the presence of the $[BF_4]^-$ counter ion ($\delta_B$ = −0.79) and an additional broad signal at 16.7 ppm. The $^{31}P\{^1H\}$ NMR data suggest many phosphorus

containing species exhibiting resonances between 5 and 45 ppm, and no evidence of unreacted **1**. The $^{1}H$ NMR spectra were extremely broad, due to the ionic strength of the samples, and the mixture proved intractable.

### 3.2.3.2 Attempted Coordination to $[PtCl_2(PPh_3)_2]$

All coordination reactions of **1** or **2** to $[PtCl_2(PPh_3)_2]$ were attempted in the presence of $AgBF_4$, either in one pot, or by pre-stirring of $[PtCl_2(PPh_3)_2]$ with $AgBF_4$ for one hour prior to the addition of **1**. The reaction of $[PtCl_2(PPh_3)_2]$ with **1** and **2** was also undertaken both with and without separation from AgCl before addition to **1** or **2**.

In all variations, only the $BF_4^-$ counter-ion was observed in the $^{11}B\{^1H\}$ NMR spectra, ($\delta_B$ = 0.64 ppm), and in each case $^{31}P\{^1H\}$ NMR data revealed the presence of $[PtCl_2(PPh_3)_2]$ ($\delta_P$ = 14.3 ppm, $^{1}J_{P\text{-}Pt}$ = 3679 Hz), and $[Pt_2(\mu\text{-}Cl)_2(PPh_3)_4][BF_4]_2$ ($\delta_P$ = 14.6 ppm, $^{1}J_{P\text{-}Pt}$ = 3855 Hz), a known dimerization product of $[PtCl_2(PPh_3)_2]$ in the presence of $AgBF_4$.[277]

Where all three reagents were combined in one pot, $^{31}P\{^1H\}$ NMR data additionally showed numerous signals in the range 10−25 ppm, with a trace of **1** left in the reaction mixture ($\delta_P$ = 10.0) but no free $PPh_3$, implying no displacement of the phosphine ligands had occurred. The addition of **1** or **2** after the platinum complex had been treated with $AgBF_4$, led to broad doublets in the $^{31}P\{^1H\}$ NMR spectra ($\delta_P$ = 18.9, 22.2), prior to the addition of phosphine-borane, spectroscopic data showed predominately $[Pt_2(\mu\text{-}Cl)_2(PPh_3)_4][BF_4]_2$. Upon reaction with **1**, observed $^{31}P\{^1H\}$ NMR signals include a singlet at 7.23 ppm and also two broad doublets at $\delta_P$ = 8.0 and 12.0 ppm ($J$ = 19.1 Hz). While the ethereal washings contained an additional two broad $^{31}P\{^1H\}$ NMR resonances, ($\delta_P$ = 25 (s) and 22 (br) from **1**; $\delta_P$ = 24 and 30 from **2**), though these are devoid of platinum satellites.

### 3.2.3.3 Attempted Coordination to $[Rh(C_8H_{12})Cl]_2$

$[Rh(C_8H_{12})Cl]_2$ was treated with two equivalents of $AgBF_4$ in $CH_2Cl_2$ for one hour, before the addition of two equivalents of **1** and stirring for 2.5 hours. After filtering the mixture, $^{31}P\{^1H\}$ NMR spectroscopy revealed the presence of three separate doublets showing coupling to rhodium ($\delta_P$ = 56.5 $^{1}J_{Rh\text{-}P}$ = 170 Hz, 49.7 $^{1}J_{Rh\text{-}P}$ = 130 Hz, 42.7 $^{1}J_{Rh\text{-}P}$ = 160 Hz). Attempts to

separate the reaction mixture were unsuccessful and fractional crystallisation from $CH_2Cl_2$, with or without hexane, only resulted in crystals of $[Rh(C_8H_{12})Cl]_2$.

The reaction of four equivalents of **1** with the $[Rh(C_8H_{12})Cl]_2$ / $AgBF_4$ mixture afforded a red solid, the $^{31}P\{^1H\}$ NMR spectrum of which showed the presence of unreacted **1**, and two mutually coupling doublet signals ($\delta_P$ = 22.1 and 18.9, $J$ = 37.5 Hz), neither of which showed any coordination to rhodium. The $^{11}B\{^1H\}$ NMR spectra contained a sharp $BF_4$ resonance, the broad signal for **1** being lost to the background at this concentration.

Where **2** was used instead, $^{31}P\{^1H\}$ NMR spectroscopy indicated unreacted phosphine-borane and other minor phosphorus signals, inconsistent with rhodium containing species. When the reaction time was increased to one week, $^{31}P\{^1H\}$ NMR spectroscopy of the orange solution indicated the presence of **2** and a new species ($\delta_P$ = 46.8, $J_{P\text{-}Rh}$ = 137.6 Hz). This might indicate some coordination to the rhodium centre as the rhodium phosphorus coupling is consistent with previously reported $^1J_{P\text{-}Rh}$ coupling values, however, the product was not able to be isolated or definitively identified.[100]

**3.2.4 Using basic solvents to disrupt the P-B interaction.**

The limited engagement in coordination is most likely due to the strength of the phosphorus-boron interaction. Disrupting this interaction should, therefore increase the reactivity of the phosphine-boranes. The best way to achieve this was considered to be the reversible coordination of a small molecule to the empty $p_z$ orbital on the boron atom, the freeing of the phosphorus lone pair might then allow coordination to a metal centre.

The addition of THF, however, did not disrupt this interaction and spectroscopic data remained unchanged, confirming the continued presence of the P-B bond. Pyridine was also added to solutions of both **1** and **2,** and left to stir. After solvent removal under partial vacuum, the spectroscopic data indicated only retention of the phosphorus-boron bond. The *in situ* formation of the pyridine adduct of **1** is seen by $^{31}P\{^1H\}$ NMR spectra when **1** is dissolved in pyridine (with $CDCl_3$), this shows there is a mixture of products, including starting material and the pyridine adduct. This is suggested by a broad signal at -0.8 ppm, which is consistent with a change in equilibrium between the coordinated and uncoordinated products as shown in **Scheme 3.4**. However, the boron signal was too weak to be apparent in the spectrum and the proton NMR spectra were overwhelmed by the vast amount of pyridine. Using the same process in the case of **2** led to three resonances in the phosphorus NMR spectrum. The major product was starting material ($\delta_P$ = 7.4) and two additional signals, an unknown resonance at

29.2 ppm, and a broad signal at -4.4 ppm, the latter signal might relate to the **2-$NC_5H_5$** adduct as the resonance has shifted to lower frequency in the same manner as the **1-$NC_5H_5$** adduct. Proton NMR signals were all lost under the pyridine solvent resonances. This is consistent with Balueva's report that pyridine coordinates to the $BBu_2$ unit of **1** in solution (**Scheme 3.4**), but is in equilibrium and can be removed under vacuum.[243]

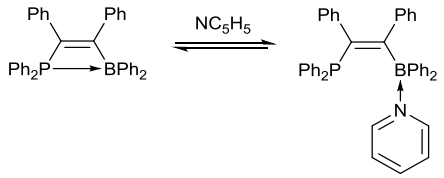


**Scheme 3.4**: The B-P bond in **1** is cleaved by pyridine to form **1-$NC_5H_5$**.

Having established the capacity for pyridine to disrupt the phosphorus-boron bond in **1** reversibly, solutions of **1** (10-30 mg) in excess pyridine were added to various metal complexes ([$PtCl_2$], [$PtCl_2(PPh_3)_2$], [$Pt(PPh_3)_4$], [$PtCl_2(PhCN)_2$], [$PdCl_2(PhCN)_2$], [$Pt(C_8H_{12})Cl_2$], [$Pd(OAc)_2$], [$Pd(Cl)(C_{12}H_{12}N)$] and [$Rh(C_8H_{12})Cl]_2$ and monitored over a period of several days. The resulting $^{31}P\{^1H\}$ NMR spectra indicated no coupling to rhodium or platinum or an appreciable shift in the phosphorus resonances, and hence no reaction would seem to have occurred.

In a similar manner, $[Rh(CO)_2Cl]_2$[278] was added to **1-$NC_5H_5$** in pyridine. Using $^{31}P\{^1H\}$ NMR spectroscopy to monitor the reaction, showed the presence of multiple rhodium-bound phosphines, as indicated by a series of doublets ($\delta_P$ = 42.9 and 52.3, $^1J_{P\text{-}Rh}$ = 140 Hz) in addition to the pyridine adduct, **1-$NC_5H_5$**. The $^{11}B\{^1H\}$ NMR contained two signals in the 4-coordinate region of the spectrum ($\delta_B$ = 4.1 and 0.6), which is most likely due to retention of the pyridine. After warming the NMR tube under partial vacuum, pyridine was removed to afford a sticky yellow solid. The $^{11}B\{^1H\}$ NMR spectrum exhibited a resonance for unreacted **1** and an additional signal at 66.0 ppm corresponding to a new species. The $^{31}P\{^1H\}$ NMR spectrum was sharpened after the removal of pyridine, while the signal at 42.9 ppm was lost, perhaps suggesting the corresponding rhodium complex contained coordinated pyridine. The $^{31}P\{^1H\}$ NMR spectrum also indicated the presence of **1** ($\delta_P$ = 10.0) and several signals exhibiting rhodium-phosphorus coupling, including the predominant species at $\delta_P$ = 52.6 ($^1J_{P\text{-}Rh}$ = 146 Hz), and several minor signals [$\delta_P$ = 55.2 $^1J_{P\text{-}Rh}$ = 163 Hz), 31.1 ($^1J_{P\text{-}Rh}$ = 124 Hz), and 49.3 ($^1J_{P\text{-}Rh}$ = 170 Hz)].

It is reasoned that the aforementioned boron signal ($\delta_B$ = 66.0), relates to the more intense phosphorus signal at 52.6 ppm and that those for the minor species are too weak to resolve. Due to the complexity of the mixture, proton NMR proved uninformative. However, it does reveal a broad signal at 9.11 ppm, which does not correspond to free pyridine and is consistent with the presence of a pyridine adduct, (*cf.* 9.28 ppm).[279] Assignment of this signal to a specific species has not been possible.

Attempts to shift the equilibrium by addition of more pyridine to NMR samples of **1** in the presence of $[Rh(CO)_2Cl]_2$ proved ineffective, while spectroscopic data for the comparable reaction with **2** revealed only starting material present.

## 3.3 Coordination chemistry of saturated phosphine-boranes

Four equivalents of $Ph_2PCH_2CH_2BBN$ (**18**), or $Fu_2PCH_2CH(BBN)$ (**21**) with the rhodium chlorocarbonyl dimer $[Rh(CO)_2Cl]_2$, were stirred in $C_6D_6$ overnight resulting in the formation of $[(CO)RhCl(R_2PCH_2CH_2BBN)_2]$ (R= Ph (**24**), Fu (**22**)).

Compounds **24** and **22** were both isolated and found to contain a single phosphorus environment (**24**; $\delta_P$ = 29.0, d, $^1J_{P\text{-}Rh}$ = 127 Hz, **22**; $\delta_P$ = −5.6, d, $^1J_{P\text{-}Rh}$ = 129 Hz). The $^{13}C\{^1H\}$ NMR spectra of **24** and **22** show a doublet of virtual triplets, where the doublet results from coupling to rhodium and the triplet results from second order effects. This virtual coupling suggests that the carbon atom couples to two mutually *trans*-phosphorus atoms, which are chemically equivalent, but magnetically inequivalent, and therefore appear as one signal in the phosphorus spectrum.[280] The phosphorus-rhodium coupling magnitudes of both **24** and **22** fit into the range noted by van Gaal and van den Bekerom, ($^1J_{P\text{-}Rh}$ = 104−153 Hz) for similar complexes with two *trans*-$PR_3$ (R=alkyl or aryl) groups.[281]

The reaction of $[Rh(CO)_2Cl]_2$ with $Ph_2PCH_2CH_2CH_2BBN$ (**19**) formed a mixture of products, the predominant complex (**25**; $\delta_P$ = 24.8, $^1J_{P\text{-}Rh}$ = 124 Hz, $\delta_B$ = 6.2 ppm) had spectroscopic data consistent with **24** and **22**, but could not be isolated in purity. The $^{11}B\{^1H\}$ NMR resonance lies within the three-coordinate region, and it would thus seem that the added flexibility from the longer backbone of **19** does not increase the favourability of an interaction between the boron and the metal centre.

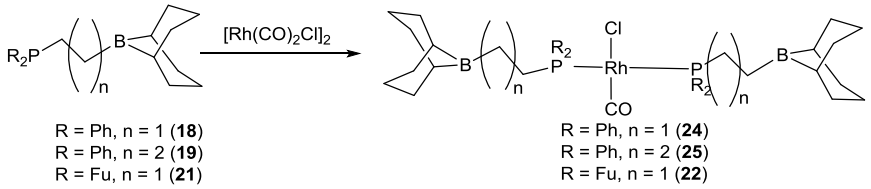


**Scheme 3.5:** Synthesis of $[(CO)RhCl(R_2P(CH_2)_nCH_2BBN)_2]$ (**22**, **24**, **25**).

Infrared data for **22** ($\upsilon_{CO}$ = 1994 $cm^{-1}$) and **24** ($\upsilon_{CO}$ = 1966 $cm^{-1}$) indicate appreciable shift of the carbonyl stretches in comparison to the parent dimer ($[Rh(CO)_2Cl]_2$ $\upsilon_{CO}$ = 2107, 2092, 2036, 2001 $cm^{-1}$).[282] The data for **22** and **24** fit into the range of similar complexes [Rh(CO)Cl(phosphine)$_2$] ($\upsilon_{CO}$ = 1939-2024 $cm^{-1}$) (**Table 3.1**). While the absorbance frequency of **22** is significantly higher than that of **24**, this is likely due to the relative basicity of the furyl *vs*. phenyl. **Figure 3.2** represents the only similar reported 4-coordinate 'Rh(CO)Cl(L)$_2$' complex with furyl-based phosphine ligands with a stretch of 1985 $cm^{-1}$ which is comparable to that of **22**.

**Table 3.1**: Table showing IR stretches of $Rh(CO)ClL_2$ complexes.[283–287]

| L | $\upsilon_{CO}$ ($cm^{-1}$) | |
|---|---|---|
| $PCy_3$ | 1939 | 285 |
| $PBu_3$ | 1953 | 284 |
| $PMe_3$ | 1957 | 285 |
| $P(NMe_2)_3$ | 1959 | 285 |
| $PPh_3$ | 1960 | 284 |
| $P^iPr_3$ | 1962 | 285 |
| P(*o*-tolyl)$_3$ | 1965 | 284 |
| **24** | 1966 | - |
| P(*p*-tolyl)$_3$ | 1970 | 284 |
| $P(Ph_2Et)$ | 1973 | 287 |
| TPF | 1985 | 288 |
| **22** | 1994 | - |
| $P(C_6F_5)_3$ | 2003 | 285 |
| $P(NC_4H_4)_3$ | 2024 | 286 |

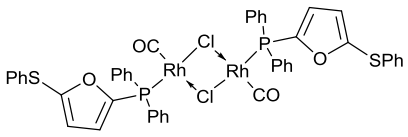

**Figure 3.2**: The only other known furyl phosphine-based rhodium chlorocarbonyl complex. ($\upsilon_{CO}$ = 1985 $cm^{-1}$).[287]

The structure of **22** was confirmed by the growth of X-ray quality single crystals by the slow evaporation of a $CH_2Cl_2$ solution (**Figure 3.3**). Disorder in the crystallographic data are explained by the molecule having a pseudo-inversion centre, with the carbonyl and chlorine refined across two sites with 50% occupancy. The phosphine ligands are mutually *trans*, and the geometry of the donor atoms (P1, Cl, P2, C1) is rigorously square-planar, with interligand angles about rhodium in the range 89.4-90.1°. Selected bond lengths and angles are listed in

**Table 3.2**. Comparison to the similar compound *trans*-$[Rh(CO)Cl(PPh_2Et)_2]$[286] shows comparable inter-substituent angles about phosphorus and Rh-P distances. In **22**, however, the Rh-Cl bond length is slightly longer (2.479(1) *vs.* 2.375(5) Å) and the Rh-C1 distance slightly shorter (1.744(16) *vs.* 1.827(8) Å). The pendant borane units in **22** are directed away from the rest of the molecule, and exhibit 3-coordinate boron, as reflected in the $^{11}B\{^1H\}$ NMR signals (**24** $\delta_B$ = 84.5, **22** $\delta_B$ = 85.9, **25** $\delta_B$ = 86.2).

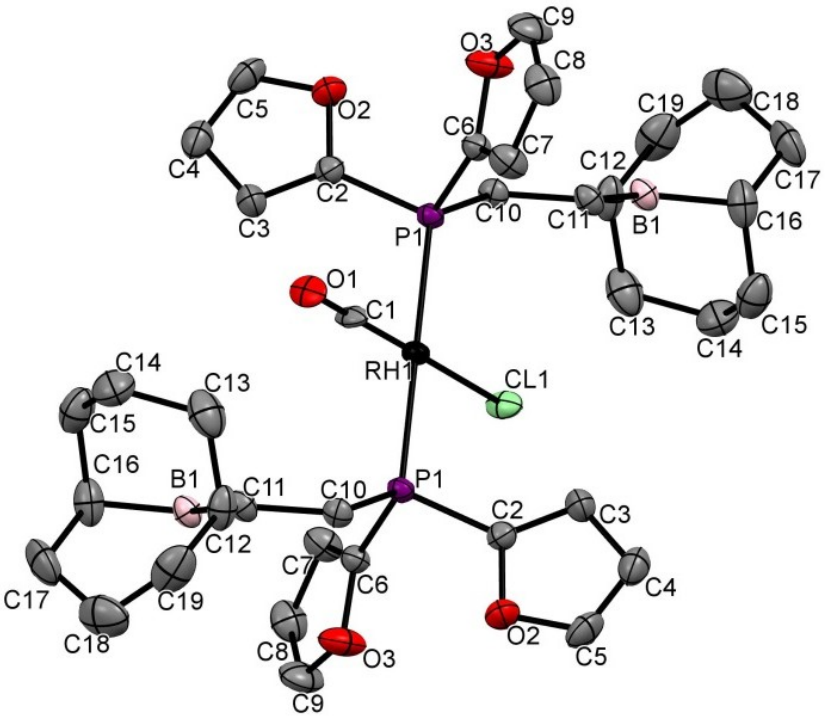


**Figure 3.3**: Ortep plot of **22** (thermal ellipsoids plotted at 50% level and hydrogens atoms have been removed for clarity). Note the CO and Cl ligands are refined across two sites 50:50. This disorder between the Cl and CO ligands has been noted in similar structures.[100]

**Table 3.2**: Selected geometric data for **22**, with estimated standard deviations in parentheses.

| Bond | Length (Å) | Bond | Angle (°) |
|---|---|---|---|
| **Rh1-P1** | 2.3111(9) | **C1-Rh1-CL1** | 178.4(5) |
| **Rh1-C1** | 1.744(16) | **P1-Rh1-P1** | 180.00(5) |
| **Rh1-CL1** | 2.375(5) | **P1-Rh1-CL1** | 89.89(8), 91.11(8) |
| **C10-C11** | 1.518(6) | **P1-Rh1-C1** | 90.1(4), 89.9(4) |
| **C11-B1** | 1.572(6) | **C2-P1-C6** | 106.5(2) |
| **C2-P1** | 1.806(5) | **P1-C10-C11** | 115.1(3) |
| **C6-P1** | 1.796(5) | **C10-C11-B1** | 116.3(4) |
| **P1-C10** | 1.838(4) | | |
| **C1-O1** | 1.160(15) | | |

Two equivalents of **21** have previously been shown to coordinate to both [$PdCl_2$] and [$PtCl_2$] at ambient temperature, with spectroscopic data revealing the formation of *cis*-[$PtCl_2(Fu_2PCH_2CH_2BBN)$] (**26**) and a 3:1 ratio of *cis*/*trans*-[$PdCl_2(Fu_2PCH_2CH_2BBN)$] (**27**) respectively.[265]

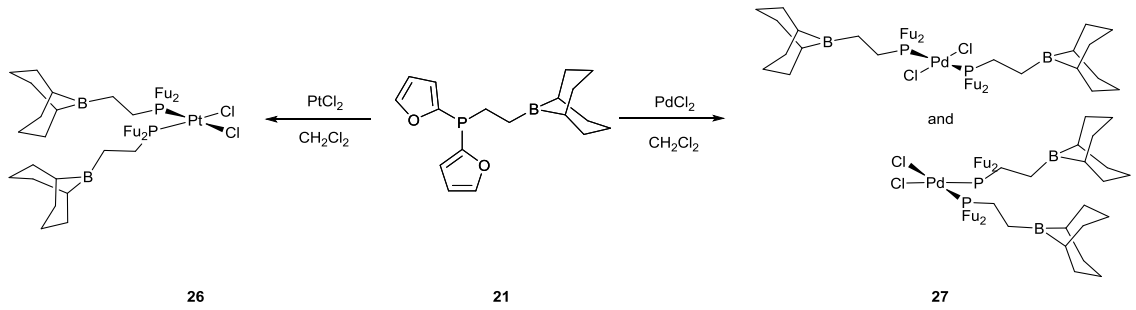


**Scheme 3.6**: Coordination of **21** to [$PdCl_2$] and [$PtCl_2$].

In the case of the platinum analogue, the *cis* configuration was determined by the magnitude of platinum-phosphorus coupling ($^1J_{Pt\text{-}P}$ = 3690 Hz) which is consistent with those typically observed of *cis*-diphosphine platinum complexes in the literature. In the case of the palladium complexes, the *cis* and *trans* isomers of [$PdCl_2(Fu_2PCH_2CH_2BBN)_2$] were able to be assigned due

to comparison to the spectroscopic data of **22** (*cis*-**27** $\delta_P$ = 0.9, $\delta_B$ = 86.8; *trans*-**27** $\delta_P$ = −11.4, $\delta_B$ = 86.8).

Both isomers have identical resonances in the $^{13}C\{^1H\}$ NMR spectra for both the 9-BBN and $CH_2CH_2$ bridge of the ligand, the only differences are seen in the 2-furanyl units. In the *cis*-configuration, the C2 carbon of the furyl units couple to both chemically equivalent, but magnetically inequivalent phosphorus atoms, the presence of the oxygen allows a through-space coupling pathway which is more efficient than the *cis*- through metal pathway, resulting in coupling between the two ligands. This results in these signals appearing as doublet of doublets, in contrast to the *trans*-isomer, where virtual triplets are observed. The latter results from the known second order effect in *trans*-bis(phosphine) complexes.[280]

The $^{11}B\{^1H\}$ NMR spectra of the platinum and palladium complexes are both indicative of three-coordinate boron, thus implying no interaction to the metal centre in either case.[265,288] Attempts to form one isomer preferentially by heating the reaction mixture were unsuccessful. When heated to 40 °C for four hours, the ratio of *cis*:*trans* isomers was 4:1, refluxing the suspension in toluene led to the isolation of a colourless oil with a single $^{11}B\{^1H\}$ NMR resonance at 31.5 ppm and upwards of 15 resonances in the $^{31}P\{^1H\}$ NMR spectrum. A yellow solid was extracted from the remaining palladium salt mixture using $CH_2Cl_2$, though was not identified.

The simple coordination to $[PdCl_2]$ was attempted using the related ligands, **18** and **19**. However, the expected compounds did not form or could not be isolated from an intractable mixture of products. In the case of stirring **18** with $[PtCl_2]$, a mixture of two species was apparent, though neither could be identified from spectroscopic data. Both of these exhibit a shift to higher frequency in the phosphorus spectra, and coupling to platinum, ($\delta_P$ = 10.5, $^1J_{P\text{-}Pt}$ = 3690 Hz (major) $\delta_P$ = 9.5, $^1J_{P\text{-}Pt}$ = 3660 Hz, (minor)) and are thus both essentially consistent with the formation of $[PtCl_2(P(Ph_2)CH_2CH_2BBN)_2]$. There were two signals in the $^{11}B\{^1H\}$ NMR spectra, the minor signal at ($\delta_B$ = 86.4) seems more consistent with that reported for $[PtCl_2(Fu_2PCH_2CH_2BBN)_2]$ ($\delta_B$ = 86.3). The major signal ($\delta_B$ = 57.7) is more consistent with 9-BBN starting material, suggesting decomposition of the ligand.

Ligand **19** had previously been found to cleave the dimer $[Rh(C_8H_{12})Cl]_2$ to form $[(C_8H_{12})RhCl(L)]$ (L = $Ph_2PCH_2CH_2CH_2BBN$) (**28**). The synthesis of **28** was repeated to obtain $^{13}C\{^1H]$ spectroscopic data. With ligands **18** and **21**, similar behaviour was noted, but afforded crude mixtures containing $[(C_8H_{12})RhCl(Ph_2PCH_2CH_2BBN)]$ (**29**) and $[(C_8H_{12})RhCl(Fu_2PCH_2CH_2BBN)]$ (**30**). It was

shown that the simple stoichiometric addition of a solution of the phosphine to a solution of the metal complex in an NMR scale reaction, resulted in formation of [($C_8H_{12}$)RhCl(L)] (L = **18**, **21**). The yields of **29**-**30** were found to be improved by dramatically shortening the reaction time, from stirring for 18−90 hours to just 10 minutes, yielding **29** and **30** in spectroscopic and analytical purity. Orange solids, **29** and **30** were obtained in high yield and shown to contain single phosphorus environments by $^{31}P\{^1H\}$ NMR spectroscopic data at 28.9 ($^1J_{P\text{-}Rh}$ = 147 Hz) and 2.81 (d, $^1J_{P\text{-}Rh}$ = 154.8 Hz) ppm, respectively. Whereas **19** itself has a $^{11}B\{^1H\}$ resonance in the 4-coordinate region (0.8 ppm), when coordinated to rhodium in the complex, [($C_8H_{12}$)RhCl($Ph_2PCH_2CH_2CH_2BBN$)] (**28**), the $^{11}B\{^1H\}$ NMR spectrum ($\delta_B$ = 87.3) is consistent with 3-coordinate boron. Complexes **29** and **30** exhibit resonances consistent with three-coordinate pendant borane units ($\delta_B$ = 86.4 and 78.8, respectively), which therefore show no interaction with the rhodium metal centre.

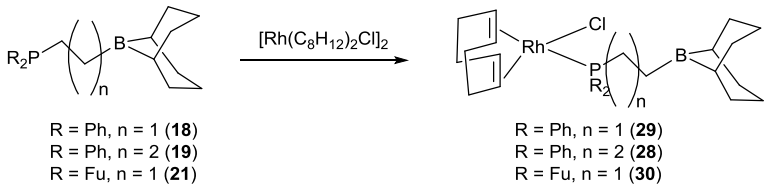


**Scheme 3.7**: Synthesis of **28**-**30**.

Ligands **18** and **21** were also found to cleave $[Cp^*IrCl]_2$;[265,288,289] the formation of [$Cp^*IrCl_2(Fu_2PCH_2CH_2BBN)$] (**31**) with **21** was repeated in order to obtain more complete data. However, shortening the reaction time from 90 hours to 18 hours at ambient temperature, did not afford the complexes in higher purity than had previously been obtained.[265] Neither did heating the reaction mixture to reflux in $CH_2Cl_2$ for 6 hours.

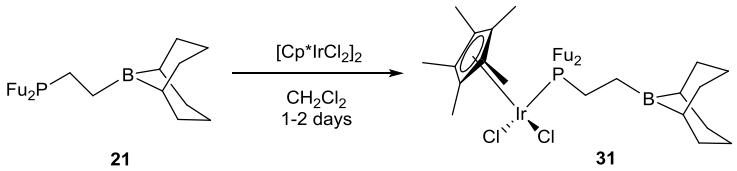


**Scheme 3.8:** Synthesis of [$Cp^*IrCl_2(Fu_2PCH_2CH_2BBN)$] (**31**).

Attempts were also made to coordinate **21** to [$Ir(PPh_3)_2Cl(CO)$] by stirring both compounds in a $CH_2Cl_2$ solution over several days. $^{31}P\{^1H\}$ NMR spectral data revealed multiple products had

been formed. None of these signals corresponded to **21** ($\delta_P$ = −57.0), however, $^{11}B\{^1H\}$ NMR did suggest the presence of a similar system to **21** ($\delta_B$ = 85.9 *vs*. 87.2 (**21**)).

### 3.3.1 Attempted gas reactivity studies

Prior work had indicated that $[PtCl_2(Fu_2PCH_2CH_2BBN)_2]$ (**26**), $[(C_8H_{12})RhCl(Fu_2PCH_2CH_2BBN)]$ (**30**), $[Cp^*IrCl_2(Fu_2PCH_2CH_2BBN)]$ (**31**) do not react with $H_2$.[265] However, co-workers had determined the addition of an atmosphere of $H_2$ to the *cis*/*trans*-$[PdCl_2(Fu_2PCH_2CH_2BBN)_2]$ (**27**) mixture results in a white precipitate that is soluble in acetone-$d_6$.[265] Spectroscopic data revealed the retention of *cis*-$[PdCl_2(Fu_2PCH_2CH_2BBN)_2]$ (*cis*-**27**) and what was speculated to be the result of $H_2$ activation of *trans*-**27** ($\delta_B$ = 20.3, $\delta_P$ = -21.7 $\delta_H$ = −0.47) (**Figure 3.4a**). The boron resonance is intermediate between a 3 and 4 coordinate centre, suggesting an increase of electron density at boron, and the proton spectrum is consistent with $BH^-$. However, no Pt-H resonance was detected and repeating the reaction under the same conditions or varying temperatures were unsuccessful.

None of the complexes from this work reacted with CO, however, *cis*-$[PtCl_2(Fu_2PCH_2CH_2BBN)_2]$ (**26**) in the presence of syngas ($CO/H_2$) had previously shown signs of formyl formation. After addition of the syngas to **26**, the $^{31}P\{^1H\}$ NMR spectroscopic data showed two chemically inequivalent phosphorus environments ($\delta_P$ = −13.9 $^2J_{P\text{-}P}$ = 15 Hz, 18.5 $^2J_{P\text{-}P}$ = 15 Hz). This combined with the signal in the proton spectra at 8.82 ppm and an IR absorption stretch at 1693 $cm^{-1}$ was deemed consistent with a formyl C-H bond, and the tentatively assigned complex shown in **Figure 3.4b**.[265]

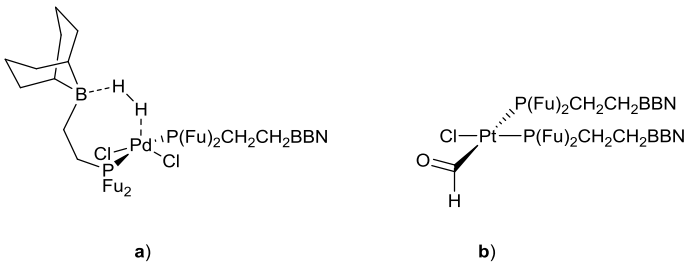


**a**) **b**)

**Figure 3.4**: Proposed structure of $H_2$ addition product of $PdCl_2(Fu_2PCH_2CH_2BBN)_2$ **a)**, and $CO/H_2$ addition product of $PtCl_2(Fu_2PCH_2CH_2BBN)_2$ **b)**.[265]

The addition of syngas was repeated to get more definitive results, but the same reactivity was not observed. Approximately one atmosphere of $H_2$ and CO were added within minutes of

each other, and after allowing the complex to react with $H_2$ for one week before the addition of CO. The proposed reactivity of the platinum complex was further investigated. A precise amount of gas was measured using a Töepler line, for the addition of 0.84 bar of CO, $CO_2$ or $H_2$/CO to a Youngs NMR tube. However, no reaction was observed. The similar system, $[PtCl_2(Ph_2PCH_2CH_2BBN)_2]$ (**32**) was also investigated and was reacted with 0.84 bar $H_2$, $CO_2$, CO and 0.42 bar of both $H_2$ and CO. An excess of $CO_2$ was also bubbled through a solution of **32**, however, spectroscopic data only indicated the presence of $[PtCl_2(Ph_2PCH_2CH_2BBN)_2]$ (**32**).

## 3.4 Summary of the coordination chemistry of saturated and unsaturated phosphine-boranes

The interruption of the phosphorus-boron bond in unsaturated phosphine-borane systems 1-borata-4-phosphoniacyclobut-2-enes $R_2BC(R)=C(Ph)PPh_2$ (**1**-**3**) has been investigated using tetrahydrofuran and pyridine, however, the strength of the phosphorus-boron bond preclude coordination to a Lewis basic metal.

More success has been found in the coordination of saturated ambiphilic phosphine-boranes $R_2P(CH_2)_nBBN$ (R = Ph, n = 2; **18**, n = 3; **19**, R = Fu, n = 2; **21**) to Lewis basic metals. The synthesis was improved to allow the acquisition of bulk purity data for $[(C_8H_{12})RhCl(Ph_2PCH_2CH_2BBN)]$ (**29**) and $[(C_8H_{12})RhCl(Fu_2PCH_2CH_2BBN)]$ (**30**). New rhodium complexes of $[(CO)RhCl(R_2P(CH_2)_nCH_2BBN)_2]$ (R = Ph, n = 2; **24**, n = 3; **25**, R = Fu, n = 2; **22**) have been synthesised and the only solid state data for rhodium complex **22**, featuring the novel ligand $Fu_2PCH_2CH_2BBN$ (**21**) has been obtained. Unfortunately, in each case the borane was pendant, and thus there was no desired metal-boron interaction to further explore.

# 4. Synthesis and reactivity of ruthenaphosphaalkenyls

## 4.1 Summary of known complexes from the hydrometallation of $^{t}$BuC≡P

While hydroruthenation of C≡C bonds has been well established since the 1960's, there has been limited expansion of this chemistry to P≡C analogues due to the limited availability of stable phosphaalkynes. The first example of phosphaalkyne hydroruthenation was reported by Hill and Jones in 1996, the reaction of $^{t}$BuC≡P (**33**) with [RuHCl(CO)($PPh_3$)$_3$] (**58**) affording the *P*-metallaphosphaalkenyl [RuCl(CO)($PPh_3$)$_2$(P=CH$^{t}$Bu)] (**34**); subsequently, the thiocarbonyl analogue and AdC≡P congeners were similarly obtained.[239,290] Jones later reported the hydroruthenation of the diphosphaalkyne P≡CC($C_6H_4$)$_3$CC≡P to form the bis-ruthenium phosphaalkenyl complex, [{($PPh_3$)$_2$(CO)ClRu}$_2${μ-P=C(H)C($C_6H_4$)$_3$CC(H)=P}] (**Scheme 4.1**).[150]

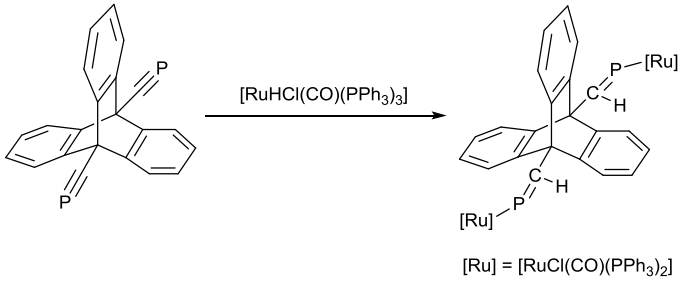


**Scheme 4.1**: Synthesis of the bis-ruthenium phosphaalkenyl complex, [{($PPh_3$)$_2$(CO)ClRu}$_2${μ-P=C(H)C($C_6H_4$)$_3$CC(H)= P}].[150]

Attempts to expand the chemistry to osmium based systems were unsuccessful, the osmium analogue [OsHCl(CO)($PPh_3$)$_3$], failing to react with $^{t}$BuC≡P. In contrast the addition of $^{t}$BuC≡P to the osmium complex [OsHCl(CO)($PPh_3$)$_2$(BTD)] (BTD = 2,1,3-benzothiadiazole) instead results in the incorporation of a second unit of $^{t}$BuC≡P to form the phosphaalkenyl-phosphaalkene complex [Os{κ$^{1}$*P*,κ$^{1}$*P′*-P=C$^{t}$BuP(=CH$^{t}$Bu)Cl(CO)($PPh_3$)$_2$] (**Scheme 4.2**).[291]

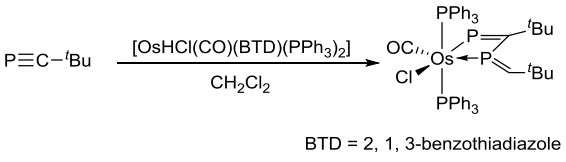


**Scheme 4.2**: Unexpected reactivity of $^{t}$BuC≡P with [OsHCl(CO)(BTD)($PPh_3$)$_2$].[291]

### 4.1.1 Reactivity of [RuCl(CO)(PPh$_3$)$_2$(P=CH$^t$Bu)]

Hill investigated the reactivity of ruthenaphosphaalkenyls (**Scheme 4.3**), and found that electrophiles add across the Ru-P bond to afford the $\eta^1$-phosphaalkene complexes [RuClX(CO)(PPh$_3$)$_2${P(ML)=CH$^t$Bu}]. The addition of HCl and MeI were shown to proceed in the same manner to generate [RuClX(CO)(PPh$_3$)$_2${PR=CH$^t$Bu}] (R = H, X = Cl (**35**) or R = Me, X = I). The $^{31}$P{$^1$H} NMR spectroscopic data of the resulting complexes shows the phosphaalkenic phosphorus undergoes a significant shift to lower frequency, the most dramatic of these shifts ($\delta_P$ = 450.4 to 187.9) is being demonstrated by [RuCl$_2$(CO)(PPh$_3$)$_2${PH=CH$^t$Bu}] (**35**). Hill concluded from this that the Ru-P linkage is now a dative bond from the lone pair on phosphorus, rather than a discrete phosphido-linkage.[239,290,292–296]

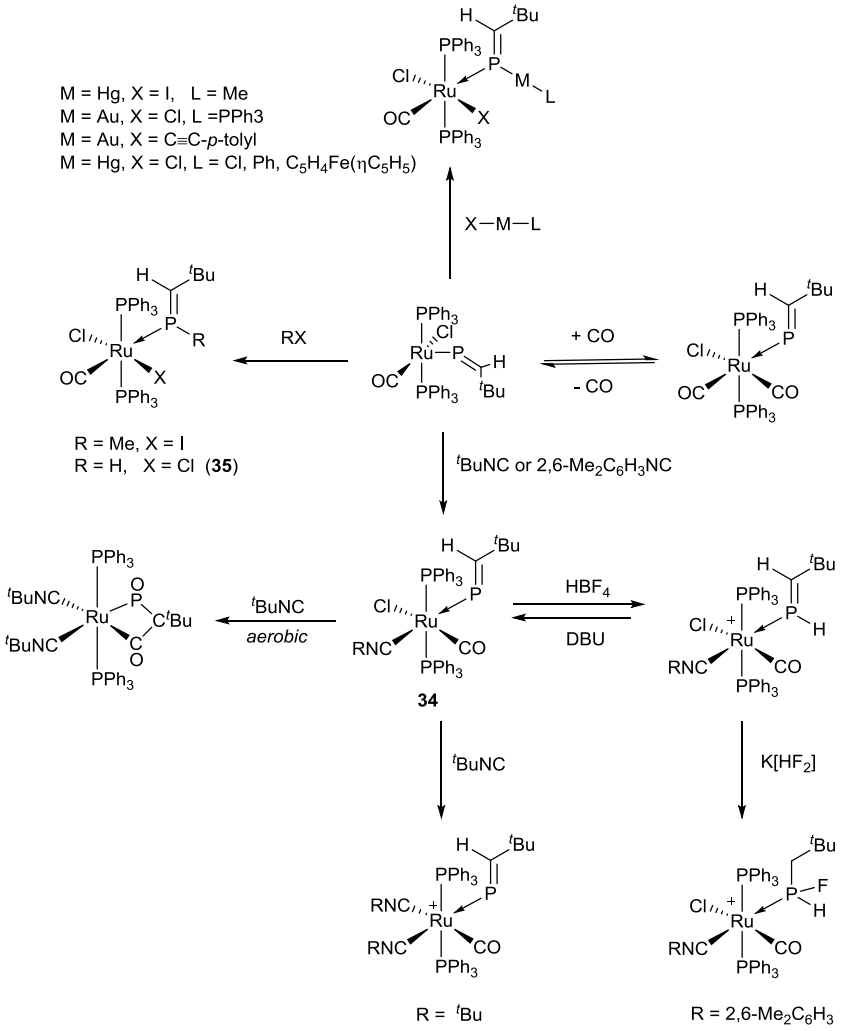


**Scheme 4.3**: Reactivity of [RuCl(CO)(PPh$_3$)$_2$(P=CH$^t$Bu)].[239,290,292–296]

The ruthenaphosphaalkenyl (**34**) has also been shown to readily form 6-coordinate species upon the addition of RN≡C or CO, the latter proving to be reversible under vacuum (**Scheme 4.3**). Upon the addition of a single equivalent of $^{t}$BuN≡C to **34**, the expected 6-coordinate complex forms, however, with an excess of $^{t}$BuN≡C the chloride salt [Ru(CO)($PPh_3$)$_2$($CN^{t}Bu$)$_2$(P=C$H^{t}$Bu)]Cl is formed. The complex [RuCl(CO)($PPh_3$)$_2$($CN^{t}Bu$)(P=C$H^{t}$Bu)] can also be treated aerobically with additional $^{t}$BuN≡C in dichloromethane and X-ray diffraction studies of the resulting crystals show the formation of a novel metallacyclic $\lambda^5$ *P*-phosphaalkenyl complex, [Ru{$\kappa^2$-P(=O)C$^{t}$BuC(=O)}($CN^{t}Bu$)$_2$($PPh_3$)$_2$]. The isonitrile complex [RuCl(CO)($PPh_3$)(CN-2,6-$Me_2C_6H_3$)(P=C$^{t}$Bu)] was also shown to protonate at phosphorus upon treatment of $HBF_4$ to form the cation [RuCl(CO)($PPh_3$)$_2$(CN-2,6-$Me_2C_6H_3$)(PH=C$^{t}$Bu)]$^{+}$. This was then reacted with K[$HF_2$] to saturate the P-C bond by the addition of HF to form a $H_2$C-PH(F) moiety.

### 4.1.2 Reactivity of [RuCl(CO)($PPh_3$)$_2${P=CH($SiMe_2$R)}]

The silyl phosphaalkynes $Me_3$SiC≡P (**36**) and $Me_2$PhSiC≡P (**37**) were synthesised recently[138,144] and have proven amenable to the hydroruthenation protocol, allowing the expansion of the range of ruthenaphosphophosphaalkenyl complexes to include [RuCl(CO)($PPh_3$)$_2${P=CH($SiMe_3$)}] (**38**) and [RuCl(CO)($PPh_3$)$_2${P=CH($SiMe_2$Ph)}] (**39**).[143,190,297,298] The reactivity of these complexes has been compared to that of [RuCl(CO)($PPh_3$)$_2$(P=C$H^{t}$Bu)] (**34**) through the addition of electrophiles (MeI, [AuCl($PPh_3$)] and [ClHg($PPh_3$)]) to **38** to form complexes of the type [RuClX(CO)($PPh_3$)$_2${PR=CH$SiMe_3$}] (X=Cl, I; E = Me, HgPh, Au$PPh_3$).[293,294]

When previous attempts were made to modify the ancillary ligands of **38** with KTp and KTp*, it was discovered that the trispyrazolylborate undergoes fragmentation to afford a complex mixture, the main product of which was partially characterised by a series of multiplets in the $^{31}P\{^{1}H\}$ NMR spectra. The large shift to lower frequency in the phosphorus NMR spectra of the product ($\Delta\delta_P$ ~ 110) shows the loss of the phosphalkenyl moiety, while $^{1}$H NMR spectroscopy demonstrated the retention of the C$HSiMe_3$ unit. X-ray diffraction studies indicated the complex contained a three-membered Ru-P-C ring with a bridging pyrazolyl group. This alongside spectroscopic evidence allowed the identification of the complexes [Ru(CO){$\kappa^3$-N,C,P-P(Pz)CH($SiMe_3$)}($PPh_3$)$_2$] (**40**) and [Ru(CO){$\kappa^3$-N,C,P-P(Pz*)CH($SiMe_3$)}($PPh_3$)$_2$] (**41**) (**Figure 4.1**). The nature of the metallacyclic unit (Ru–P–C) could be described either as a ruthenaphosphirane, where the pyrazolyl ligand forms a bridge over the Ru–P bond, or as a

pyrazolyl-tethered $\eta^2$-phosphaalkene complex. As the data were ambiguous towards the nature of the Ru-P-C linkage, further investigation was deemed appropriate.

The structures of [Ru(CO){$\kappa^3$-N,C,P-P(Pz)CH($SiMe_3$)}($PPh_3$)$_2$] (**40**) and [Ru(CO){$\kappa^3$-N,C,P-P(Pz*)CH($SiMe_3$)}($PPh_3$)$_2$] (**41**) were first thought to be that of a phosphosphirane-type complex, due to the pyramidalisation at the carbon centre, with the P-C bond (1.782 Å) lengthened compared to reported phosphaalkenyls (1.655(3)-1.665(2) Å),[298] and the acute angles around carbon supporting a geometry between $sp^2$ and $sp^3$. However, the P-C bond length is also shorter than a typical single bond (P($sp^3$)-C($sp^3$) = 1.85 Å)[117] and the spectroscopic data, such as carbon resonances ($\delta_C$ = 39−45), proton resonances ($\delta_H$ = 1.6−1.7) and carbon-proton coupling ($^1J_{C\text{-}H}$ = 123-136 Hz *vs*. $CH_4$, $^1J_{C\text{-}H}$ = 125 Hz, $C_2H_2$ $^1J_{C\text{-}H}$ = 156 Hz)[299] suggest an $sp^2$-like carbon centre. While these conflicting data do not confirm the nature of the Ru-P-C linkage, the IR data ($\nu_{CO}$ = 1905-1915 $cm^{-1}$) are consistent with reduction of the metal, from Ru(II)[300] for **34**, **38**, **39**, **59**-**61** ($\nu_{CO}$ = 1925-1940 $cm^{-1}$) to a ruthenium (0) center, more consistent with an $\eta^2$-ruthenaphosphaalkene.

The reaction of lithiated pyrazolates (Lipz') with **38** was found to be a route for direct synthesis of **40** and **41**, and this method was employed for the installation of 'Pz' and 'Pz*' to **34**, **38** and **39**.[297,298] Building on this work, herein are described further investigations of the chemistry of phosphaalkenyls, and the influence of ancillary substituents upon their chemistry.

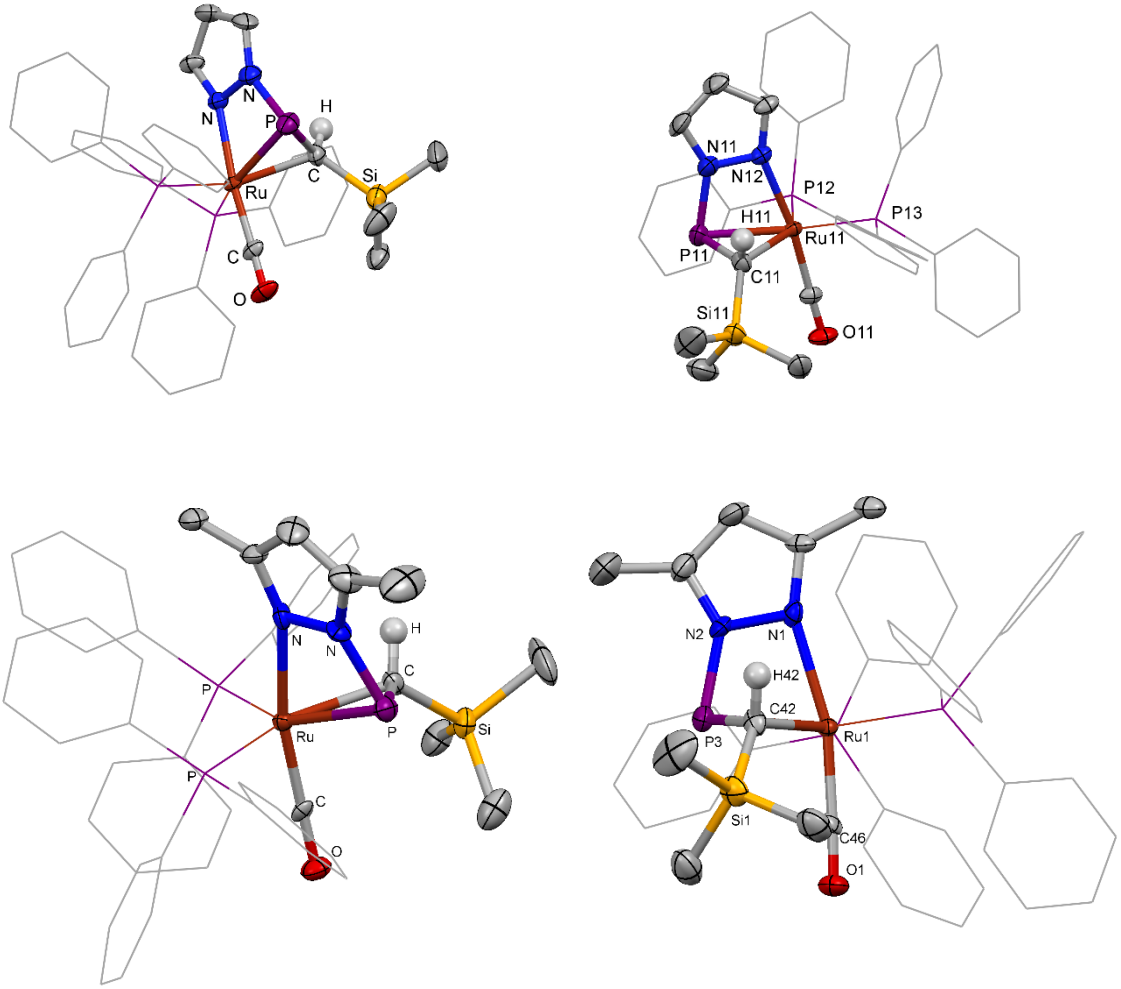


**Figure 4.1**: Structural data for [Ru(CO){κ$^3$-N,C,P-P(Pz)CH(SiMe$_3$)}(PPh$_3$)$_2$] (**40**)[190,297] (*top*) and [Ru(CO){κ$^3$-N,C,P-P(Pz*)CH(SiMe$_3$)}(PPh$_3$)$_2$]* (**41**)[143] (*bottom*).

## 4.2 Synthesis of novel silyl-phosphaalkynes

It has been well established that phosphaalkynes can be synthesised from the double dehydrohalogenation of $RCH_2PCl_2$. To expand the range of known phosphaalkynes, attempts have been made to produce a new range of dichlorophosphines of the type $RMe_2SiCH_2PCl_2$ (**Scheme 4.4**).

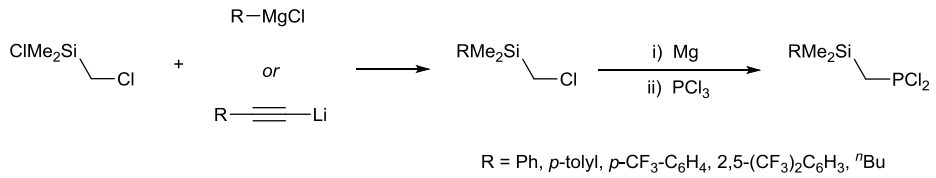


**Scheme 4.4**: Synthesis of $RMe_2SiCH_2PCl_2$.

### 4.2.1 Synthesis of $RSiMe_2Cl$

#### 4.2.1.1 From Grignard reagents

Commencing from the precursor $ClMe_2SiCH_2Cl$, various substituents have been installed on the silyl group by metathesis with Grignard reagents to afford systems of the type $RMe_2SiCH_2Cl$ (R = $^{i}$Pr (**42**), *p*-tolyl (**43**), $C_6F_5$ (**44**), *p*-$CF_3$-$C_6H_4$ (**45**), and 2,5-$(CF_3)_2C_6H_3$) (**46**).

In the case of $^{i}$PrMgBr, magnesium salts precipitated immediately upon addition of the Grignard reagent to the silane. After stirring at ambient temperature for 18 hours, the solvent was removed from the product by distillation, to afford a colourless liquid. The major product could not be isolated in purity, but was unequivocally identified from spectroscopic data as $^{i}PrMe_2SiCH_2Cl$ (**42**).

A similar procedure allowed the synthesis of $RMe_2SiCH_2Cl$, (R = *p*-tolyl **43**,[301] $C_6F_5$ **44**, *p*-$CF_3$-$C_6H_4$ **45**,[302] 2,5-$CF_3$-$C_6H_3SiMe_2CH_2Cl$ **46**[303]) some of which have limited precedent data reported in the literature. In contrast, the reaction between MesMgCl and $ClMe_2SiCH_2Cl$ proved to be unsuccessful, presumably attributable to the bulk of the mesityl group preventing access of the Grignard to the silyl-chloride.

The summary of the key spectroscopic data of **42**-**49** is shown in **Table 4.1** and shows that the '$CH_2Cl$' proton resonances lie within the range for similar systems in the literature ($\delta_H$ = $EtMe_2SiCH_2Cl$, 2.75; $^{n}PrMe_2SiCH_2Cl$, 2.76; $PhMe_2SiCH_2Cl$, 2.95).[304,305]

**Table 4.1**: Summary of key spectroscopic data for **R**$SiMe_2CH_2Cl$ (ppm).

| R = | | $^1$H ($SiMe_2$) | $^1$H ($CH_2Cl$) | $^{29}$Si |
|---|---|---|---|---|
| **$^i$Pr** | **42** | 0.24 | 2.78 | - |
| ***p*-tolyl** | **43** | 0.41 | 2.37 | -4.1 |
| **$C_6F_5$** | **44** | 0.54 (*t*, 1.5 Hz) | 3.09 (*t*, 1.0 Hz) | -2.0 |
| ***p*-$CF_3$-$C_6H_4$** | **45** | 0.45 | 2.96 | -2.5 |
| **2,5-$CF_3$-$C_6H_3$** | **46** | 0.50 | 2.98 | -1.4 |
| **PhC≡C** | **47** | 0.37 | 2.94 | -17.3 |
| **$Me_3SiC{\equiv}C$** | **48** | 0.17 | 2.61 | -19.6 |
| **$^n$Bu** | **49** | 0.10 | 2.78 | 3.9 |

#### 4.2.1.2 From lithium reagents

In addition to using Grignard reagents to create a library of silanes for conversion to phosphaalkynes, the use of organolithium to modify the chloride precursor was also attempted. The preparation of the silane PhC≡CSi($Me_2$)$CH_2Cl$ (**47**) is well established,[306] although the method was modified to include an anaerobic/anhydrous work-up. Neat chloro(chloromethyl)dimethylsilane was added to lithiated phenylacetylene and stirred at −78 °C for one hour. After allowing the reaction to warm to ambient temperature, the solution was filtered away from the white solid and the solvent removed under partial vacuum, the product was then distilled to produce a colourless liquid. Similarly LiC≡$CSiMe_3$ and $^n$BuLi were employed to form $Me_3SiC{\equiv}CSi(Me_2)CH_2Cl$ (**48**) and the known compound $^n$$BuMe_2SiCH_2Cl$[307] (**49**), respectively (identified from key spectroscopic data shown in **Table 4.1**) in high yield.

### 4.2.2 Synthesis of dichlorophosphines.

Attempts to convert the silanes, $RMe_2SiCH_2Cl$, to the dichlorophosphines, $RMe_2SiCH_2PCl_2$, met with limited success. Using a similar procedure to that reported for $Me_3SiCH_2PCl_2$ (**50**) and $PhMe_2SiCH_2PCl_2$ (**51**),[138] the installation of a '$PCl_2$' unit was achieved for *p*-tolyl$Me_2SiCH_2Cl$ (**43**), *p*-$CF_3$-$C_6H_4SiMe_2CH_2Cl$ (**45**) and $^n$$BuMe_2SiCH_2Cl$ (**49**) by the formation of the respective Grignard reagent, $RMe_2SiCH_2MgCl$ (R = *p*-tolyl, *p*-$CF_3$-$C_6H_4$, $^n$Bu), and quenching with $PCl_3$. The resulting product was extracted in diethyl ether to separate it from the $MgX_2$ by-product; subsequent removal of the solvent, and distillation under reduced pressure afforded *p*-tolyl$Me_2SiCH_2PCl_2$

(**52**), *p*-$CF_3$-$C_6H_4SiMe_2CH_2PCl_2$ (**53**) and $^{n}BuMe_2SiCH_2PCl_2$ (**54**). The formation of these novel phosphines was confirmed by $^{31}P\{^1H\}$ and $^1H$ NMR spectroscopy, (**Table 4.2**). Samples of **52** and **54**, although spectroscopically pure, defied microanalysis, though bulk purity was confirmed for **53**.

**Table 4.2**: $^{31}P$ and $^1H$ data for dichlorophosphines (ppm).

| Compound | | $^{31}P\{^1H\}$ | $^1H$ ($CH_2PCl_2$) (d, $^1J_{P-H}$, Hz) |
|---|---|---|---|
| **$Me_3SiCH_2PCl_2$*** | **50** | 205.4 * | 2.04 (15.8) |
| **$PhMe_2SiCH_2PCl_2$*** | **51** | 203.4 * | 2.26 (15.8) |
| ***p*-tolyl$Me_2SiCH_2PCl_2$** | **52** | 203.3 | 2.24 (15.2) |
| **$^{n}BuMe_2SiCH_2PCl_2$** | **53** | 205.6 | 2.03 (15.4) |
| ***p*-$CF_3$-$C_6H_4SiMe_2CH_2PCl_2$** | **54** | 200.8 | 2.24 (15.6) |

*from published data [138]

Following the same procedure with the other silanes $RMe_2SiCH_2Cl$ (R = $^{i}Pr$ (**42**), $C_6F_5$ (**44**), 2,5-$(CF_3)_2$-$C_6H_3$ (**46**), PhC≡C (**47**) and $Me_3SiC$≡C (**48**)) did not lead to the same reactivity, suggesting difficulty in forming the Grignard reagents $RMe_2SiCH_2MgCl$, despite repeated attempts involving thermal and chemical initiators. Several initiators ($I_2$, 1,2-dibromoethane, $HgCl_2$) were employed with the reaction mixtures (in tetrahydrofuran or diethyl ether) brought to reflux for several hours. However, after the addition of $PCl_3$, $^{31}P\{^1H\}$ NMR spectra showed just residual $PCl_3$, with no evidence of any "$CH_2P$" unit in the proton spectra.

In view of these difficulties, other alkali metal reagents were considered. To this end, solutions of **47** or **48** were refluxed with approximately 2.2 equivalents of either Li, Na or K. Potassium was found to cause decomposition of the chlorosilane causing a red-brown suspension to form, and the heating of an ethereal solution of **48** with sodium led to the formation of a purple suspension. After these mixtures were filtered and added to cold $PCl_3$, and then left to stir for 18 hours, $^{31}P\{^1H\}$ NMR data revealed only the presence of unreacted $PCl_3$. While it had previously been shown that a hot hydrocarbon suspension of lithium with $Me_3SiCH_2Cl$[308] or $PhMe_2SiCH_2Cl$ results in lithiation, no lithium was consumed when added to **47** under comparable conditions.

Seeking to enhance the reactivity of the substrates, conversion of $RMe_2SiCl$ to the respective iodides was attempted by the addition of $Me_3Si$-I to NMR solutions of **47** and **44** in $CDCl_3$ or $C_6D_6$. The substitution of 'Cl' for 'I' should result in a significant change in the $^1H$ NMR resonance of the $CH_2X$ unit, as exemplified for $Me_3SiCH_2X$ ($\delta_H$ = 2.75; 'Cl',[309] 1.93; 'I').[310]

However, $Me_3Si$-I did not facilitate the conversion to the iodide as determined by NMR spectroscopy, which exhibited no change in chemical shift of the $CH_2$ resonance, implying only retention of the chloride.

### 4.2.3 Synthesis of phosphaalkynes

Phosphaalkynes were made *via* the double dehydrohalogenation of $RMe_2SiCH_2PCl_2$ (R = Me (**50**), Ph (**51**), *p*-tol (**52**), *p*-$CF_3$-$C_6H_4$ (**53**), $^n$Bu (**54**)) to form $RMe_2SiC{\equiv}P$ (R = Me (**36**), Ph (**37**), *p*-tolyl (**55**), *p*-$CF_3$-$C_6H_4$ (**56**), $^n$Bu (**57**)). This reaction is effected by addition of two equivalents of AgOTf and DABCO in toluene or diethyl ether and the products obtained in solution; isolation from solution cannot be effected, due to their instability and propensity to form azeotropic mixtures with most common solvents. The phosphalkynes were thus identified on the basis of $^{31}P\{^1H\}$ NMR spectroscopic resonances (**Table 4.3**) and their subsequent reactivity. Each phosphaalkyne solution was calibrated for concentration by integration of the respective $^{31}P\{^1H\}$ NMR resonances against that of fully relaxed $PPh_3$ (d1 = 40).[†144,297,298]

**Table 4.3**: Spectroscopic data for phosphaalkynes **36**, **37**, **55**-**57**.

| R = | | $^{31}P\{^1H\}$ NMR (ppm) |
|---|---|---|
| **Me** | **36** | 98.8 |
| **Ph** | **37** | 104.1 |
| ***p*-tolyl** | **55** | 103.3 |
| ***p*-$CF_3$-$C_6H_4$** | **56** | 106.7 |
| **$^n$Bu** | **57** | 101.2 |

The chemical shifts of phosphaalkynes of the type $RMe_2SiC{\equiv}P$ are all very similar to each other, suggesting the nature of the R group has little effect on the nature of the phosphorus centre. However, the chemical shifts of these silyl-based phosphaalkynes are vastly different when compared to the more frequently used phosphaalkyne $^t$BuC≡P ($\delta_P$ = −67.6), and the lesser used AdC≡P ($\delta_P$ = −69.5).[311]

[†] as T1 for $PPh_3$ ~ 30s, to allow full relaxation would require d1 = 150s, however, for the concentrations involved 40s has been determined as the limit of statistical significance.

### 4.2.4 Synthesis of ruthenaphosphaalkenyl complexes

The addition of a slight molar excess (1.1 − 1.4 equiv) of the phosphaalkyne solutions to a stirred suspension of [RuHCl(CO)($PPh_3$)$_3$] (**58**) in $CH_2Cl_2$ results in the facile formation of [RuCl(CO)($PPh_3$)$_2$(P=CHSi$Me_2$R)] (R = Me (**38**), Ph (**39**), *p*-tol (**59**), *p*-$CF_3$-$C_6H_4$ (**60**), $^n$Bu (**61**)) as shown in **Scheme 4.5**. The reaction was typically left to stir for 1-2 hours, but is largely complete within 15 minutes at ambient temperature. After the removal of solvent and excess phosphaalkyne under reduced pressure, the resulting orange solid was agitated vigorously with hexanes, before being isolated by filtration and dried *in vacuo* to afford an orange/yellow solid in high yield.

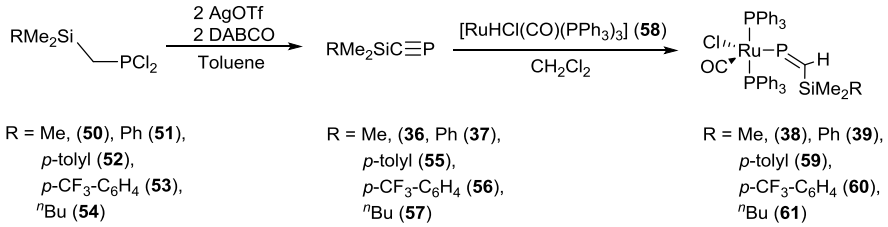


**Scheme 4.5**: Synthesis of ruthenaphosphaalkenyls **38**, **39**, **59**-**61**.

## 4.3 Characterisation and structural features of phosphaalkenyl complexes.

### 4.3.1 Spectroscopic data of ruthenaphosphaalkenyl complexes

The ruthenaphosphaalkenyl complexes (**38**, **39**, **59**-**61**), similar to Hill's [RuCl(CO)($PPh_3$)$_2$(P=CH$^t$Bu)] (**34**),[239] are readily characterised by NMR spectroscopic data as shown in **Table 4.4**. The most distinctive of these data is the heavily de-shielded P=C phosphorus centre which displays coupling to two retained $PPh_3$ units. The absence of a hydride resonance is consistent with insertion of a phosphaalkyne into the Ru-H linkage of [RuHCl(CO)($PPh_3$)$_3$] (**58**). The vinylic proton was identified through its correlation ($^{31}$P-$^1$H HMBC) to the phosphaalkenic phosphorus centre, and the carbon and silicon nuclei of the phosphaalkenic group. The $^{13}$C{$^1$H} spectroscopic data confirm the presence of the carbonyl ligand, which is also demonstrated by infrared spectroscopic data ($\nu_{CO}$ = 1920−1939 cm$^{-1}$) which are consistent with a Ru(II) centre, the force constants lying between 14.9-15.2 k/Ncm$^{-1}$ as is typical for Ru(II) metal centres in both monocarbonyl[312] and dicarbonyl[313] complexes.

It is noteworthy that the P=C resonances are appreciably more deshielded when compared to that of **34** ($\delta_P$ = 450.4).[239] Though one might consider this to imply distinct differences in the

structure or chemical nature of the product, it is found to arise purely from the differences of $^{t}$Bu and $SiR_3$ groups, as the parent phosphaalkenes (RC≡P) follow the same spectroscopic trend, ($\delta_P$ = −67 **33**, *cf.* 98-106 $SiMe_2R$ (**38**, **39, 59**-**61**).[144,298] Moreover, Density Functional Theory was employed to prove this substituent effect using NMR calculations from optimised structures of **34** and **38** showed the same de-shielding of **38** compared to **34** (see **Section 4.3.3**).

**Table 4.4**: Spectroscopic data of phosphaalkenyls **34**, **38**, **39**, **59**-**61**.

| | **34**[239] | **38** | **39** | **59** | **60** | **61** |
|---|---|---|---|---|---|---|
| **[RuC(P=CH(R))(CO)(PPh$_3$)$_2$]** | 450.4 | 548.5 | 553.8 | 552.6 | 559.7 | 545.3 |
| **[RuCl(P=CH(R))(CO)(PPh$_3$)$_2$]** | 33.9 | 34.6 | 33.7 | 33.7 | 33.8 | 33.8 |
| **[RuCl(P=CH(R))(CO)(PPh$_3$)$_2$]** | 7.12 | 7.28 | 7.40 | 7.41 | 7.33 | 7.32 |
| **[RuCl(P=CH(R))(CO)(PPh$_3$)$_2$]** | 184.9 | 168.0 | 163.7 | 165.2 | 162.9 | 165.9 |
| **[RuCl(P=CH(R))(CO)(PPh$_3$)$_2$]** | 202.4 | 203.0 | 201.9 | 202.5 | 202.5 | 202.1 |
| **$^{29}$Si NMR** | - | -9.4 | -14.3 | -14.4 | -14.0 | -7.3 |
| **$\nu_{CO}$** | 1929 | 1920 | 1938 | 1936 | 1939 | 1930 |

**34** [RuCl(CO)(P=C$^{t}$Bu)($PPh_3$)$_3$] – resonances were taken from published data.[290]

### 4.3.2 X-ray structural data

The successful growth of single crystals of ruthenaphosphaalkenyls suitable for X-ray diffraction has been achieved from saturated $Et_2O$ (**38**), $CH_2Cl_2$/hexane (**39**) or by the slow evaporation of $CH_2Cl_2$ solution (**59**) respectively. Molecular geometries are illustrated in **Figure 4.2**, with selected bond distances and angles summarised in **Table 4.5**.

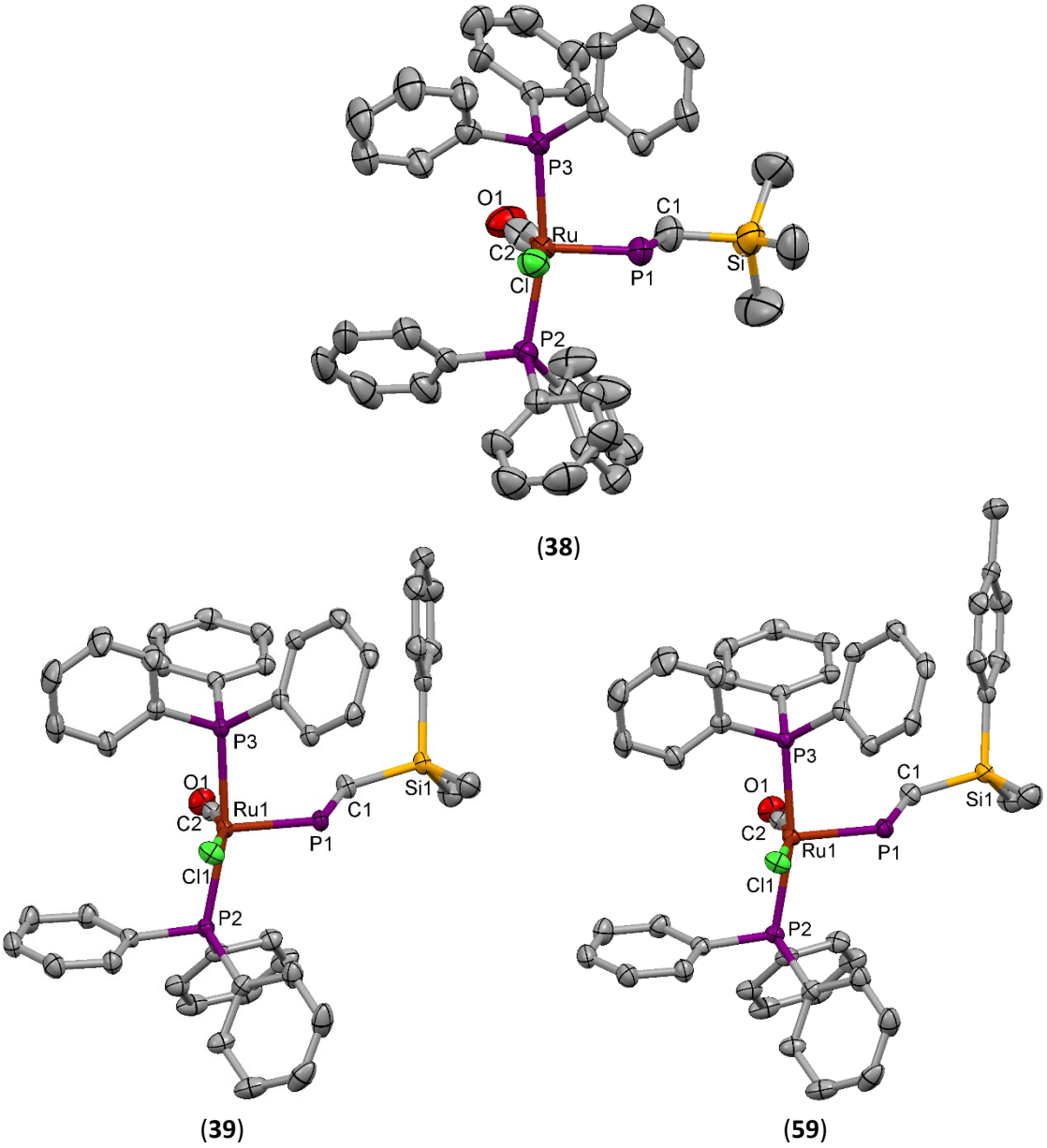


**Figure 4.2**: Molecular structures of $[RuCl(CO)(PPh_3)_2(P{=}CHSiMe_2R)]$ (R = Me; **38** in $Et_2O$ solvate, Ph; **39**, *p*-tolyl; **59**) with thermal ellipsoids at the 50% probability level and H atoms omitted for clarity.

**Table 4.5**: Selected bond lengths (Å) and angles (°) from crystallographic data of **38**, **39** and **59**.

| | **38** | **39** | **59** |
|---|---|---|---|
| **Ru-P(C)** | 2.226(2) | 2.2468(5) | 2.2504(8) |
| **Ru-CO** | 1.735(9) | 1.835(2) | 1.824(3) |
| **Ru-Cl** | 2.411(2) | 2.4006(5) | 2.4014(7) |
| **P=C** | 1.660(11) | 1.665(2) | 1.655(3) |
| **C≡O** | 1.183(12) | 1.143(3) | 1.163(4) |
| **C-Si** | 1.836(10) | 1.8576(19) | 1.854(3) |
| **Ru-P=C** | 124.4(4) | 121.49(7) | 121.31(11) |
| **P-Ru-P** | 167.18(7) | 166.615(16) | 166.84(3) |
| **Cl-Ru-CO** | 159.0(3) | 162.68(6) | 163.57(10) |
| **P-C-Si** | 122.5(7) | 124.88(12) | 125.64(17) |

The data for [RuCl(P=CHR)(CO)($PPh_3$)$_2$] (**38**, **39** and **59**) prove the *cis*-addition of the ruthenium-hydride bond across the 'P≡C' bond and reveal geometries consistent with a discrete 1-electron phosphaalkenyl moiety, as indicated by the bent nature of the Ru-P=C fragment (∠ Ru-P-C 121.31(11)−124.4(4) °, ∠ P-C-Si 122.5(7)−125.64(17) °). The Ru-P distances (2.226(2) - 2.2504(8) Å) are short compared to reported $\eta^1$−phosphaalkene complexes [Ru{$\eta^1$−P(E)=CH$^t$Bu}$Cl_2$(CO)($PPh_3$)$_2$] (E = Au($PPh_3$),[293] HgFc)[296] and [Ru{$\eta^1$−P(HgPh)=CHSi$Me_3$}-$Cl_2$(CO)($PPh_3$)$_2$[297] (2.256(2) − 2.296(2) Å), and Hill's 18-electron phosphaalkenyl complex [Ru{P=CH$^t$Bu}($O_2$CH)(CO)($PPh_3$)$_2$] (2.295(2) Å).[290] They are also shorter than those reported for a Ru=P bond for the complex [Ru{$\kappa^4$−Si($C_6H_4PPh_2$)$_3$}($PR_2$)] (R = Ph, $^i$Pr) (2.2592(4)−2.2700(3) Å),[314] while the Ru-$PPh_3$ bond distances are similar to Ru←$PPh_3$ distances reported for other square-based pyramidal Ru(II) complexes (2.16−2.47 Å).[253]

The P=C bond lengths (1.655(3)-1.665(2) Å) are, however, consistent with precedent data for other $\eta^1$ phosphaalkene complexes (1.640(4)-1.679(4) Å), including those mentioned in **Section 4.1.2**.[218,293,297,315] The geometries are otherwise unremarkable, with *cis*-inter-ligand angles in the range (∠Cl-Ru-CO = 162.68(6) − 163.57(10) ˚; ∠$P_{PPh3}$-Ru-$P_{PPh3}$ = 166.62(2) − 167.18(7) ˚) consistent with typical Ru(II) square based pyramidal complexes.

### 4.3.3 DFT studies

The ground state geometries of the phosphaalkenyls (**34**, **38**, **39**, **59**-**61**) were optimised using DFT methods, at the B3LYP level of theory with the LANL2DZ basis set for ruthenium, and all other atoms at 6-31G** (**Figure 4.3**). The starting points for these calculations in each case were the solid state structures **38**, **39**, **59** while for **60** and **61** the models were derived from **38** and **59**, respectively. The calculated geometries (**Table 4.6**) are in close agreement with the solid state structures (**38**, **39** and **59**).

**Table 4.6**: Bond lengths (Å) and bond angles (˚) from DFT calculations of **34**, **60** and **61** for $[RuCl(P=C(H)ER(CO)(PPh_3)_2]$.

| | **34 (E = C)** | **60 (E = Si)** | **61 (E = Si)** |
|---|---|---|---|
| **Ru-P(C)** | 2.31799 | 2.29156 | 2.29917 |
| **Ru-CO** | 1.84550 | 1.85390 | 1.84866 |
| **Ru-Cl** | 2.47521 | 2.47794 | 2.47744 |
| **P=C** | 1.68008 | 1.67776 | 1.67461 |
| **C≡O** | 1.16594 | 1.16267 | 1.16492 |
| **C-E** | 1.52381 | 1.87478 | 1.88130 |
| **Ru-P=C** | 118.048 | 120.44971 | 120.51637 |
| **P-Ru-P** | 170.038 | 167.47234 | 169.20877 |
| **Cl-Ru-CO** | 160.415 | 163.44828 | 161.92236 |
| **P-C-E** | 126.539 | 123.11604 | 123.30285 |

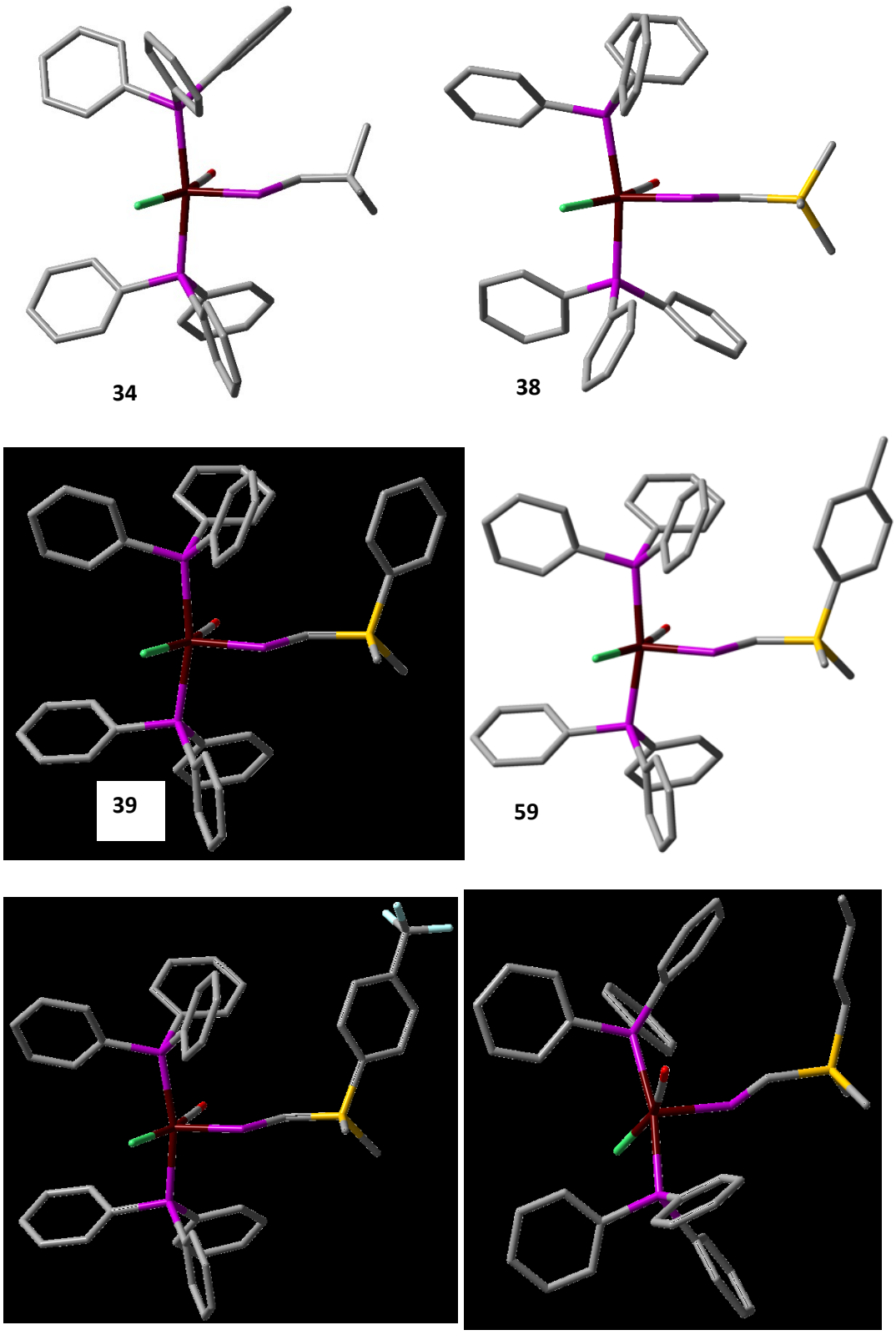


**Figure 4.3**: DFT optimised structures for **34**, **38**, **39**, **59**-**61**.

As the spectroscopic data for **34** differ from those of the silyl systems (**38**, **39**, **59**-**61**) it does not discount the possibility of different coordination modes. Hill concluded that **34** must contain a phosphaalkenyl unit, behaving as a one-electron ligand. However, a phosphavinylidne structure might explain the differences in the phosphorus spectra, as unsaturation at the metal centre has been established for early transition metals to result in the additional donation of the phosphorus lone pair to the metal centre as a three electron phosphavinylidene.[316–318] Therefore the structure of **34** was also optimised starting from a phosphavinylidine structure. This geometry relaxed to the bent geometry shown in **Figure 4.4**, suggesting the 'P=CH$^{t}$Bu' phosphaalkyenyl unit is more stable as a one-electron ligand.

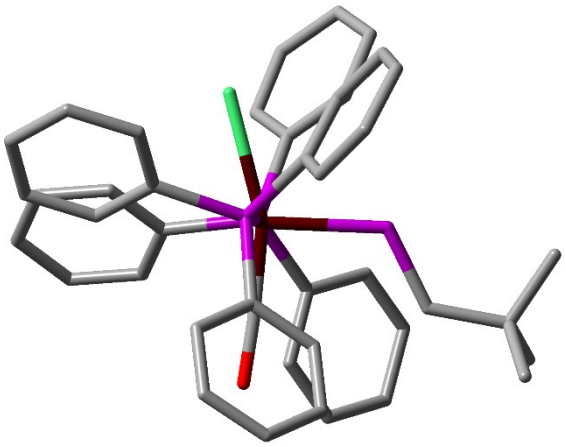

**Figure 4.4**: The optimised geometry of **34** (*below*) using B3LYP/6-31G**, Lanl2dz (Ru).

The $^{31}P\{^{1}H\}$ NMR and IR spectra were also calculated from the optimised geometries, using both the B3LYP and PBE functionals. The CO stretches in all cases showed broad agreement with experimental data. In respect of the NMR data, consistent trends were observed in all cases, while the PBE[319] functional offered more accurate values for the $^{31}P\{^{1}H\}$ data, which showed close correlation to the observed trends in chemical shift shown in **Table 4.47**.

**Table 4.7**: Comparison of $^{31}$P NMR data (P=C).

| Compound | ν(CO) | | $\delta_{P(P=C)}$ | | |
|---|---|---|---|---|---|
| | **Calc‡** | **Exp.** | **B3LYP** | **PBE** | **Exp.** |
| **34** | 1933.4 | 1929* | 482.0 | 455.4 | 450.4 |
| **38** | 1938.5 | 1920* | 584.4 | 537.2 | 548.5 |
| **39** | 1952.3 | 1938 | 606.8 | 558.0 | 553.8 |
| **59** | 1951.8 | 1939 | 604.7 | 557.9 | 552.6 |
| **60** | 1953.7 | 1939 | 619.8 | 567.4 | 559.7 |
| **61** | 1939.4 | 1930 | 588.3 | 540.6 | 545.3 |

* data provided by colleagues in the group. ‡ Frequency scaling factor of 0.961 applied.[320]

Both the $^{t}$Bu and the silyl-based systems show a significant energy difference between the HOMO and LUMO orbitals ($\Delta$E ~ 3.76-3.87 eV). The HOMO and LUMO of **38**, **39**, **59**-**61** are similar in distribution, with the HOMO of **38** centred around the metal and the phosphorus lone pair, while the HOMO-1 involves metal centre and the P=C bond (**Figure 4.5**). Conversely, in **34**, HOMO and HOMO-1 are reversed (**Figure 4.6**). The LUMO's for **38**, **39**, **59**-**61** are predominately metal based and are potentially accessible to nucleophiles through the Cl-Ru-CO plane. In each case, the LUMO+1's are only marginally higher in energy than the LUMOs (*ca.* 0.6eV) and contain P=C antibonding components (**Figure 4.5**), in contrast, the same components are found in the LUMO+2 for **34** (**Figure 4.6**) and the energy gap is similar at 0.8 eV. Combined with NBO data for **38**[190] that indicate a significant $\delta^{+}$ character for the phosphaalkenic phosphorus, these might seem consistent with intrinsic ambiphilicity of this centre, accounting for both the addition of electrophiles, and the nucleophilic addition of pyrazolates (*vide infra*).[190,297,298]

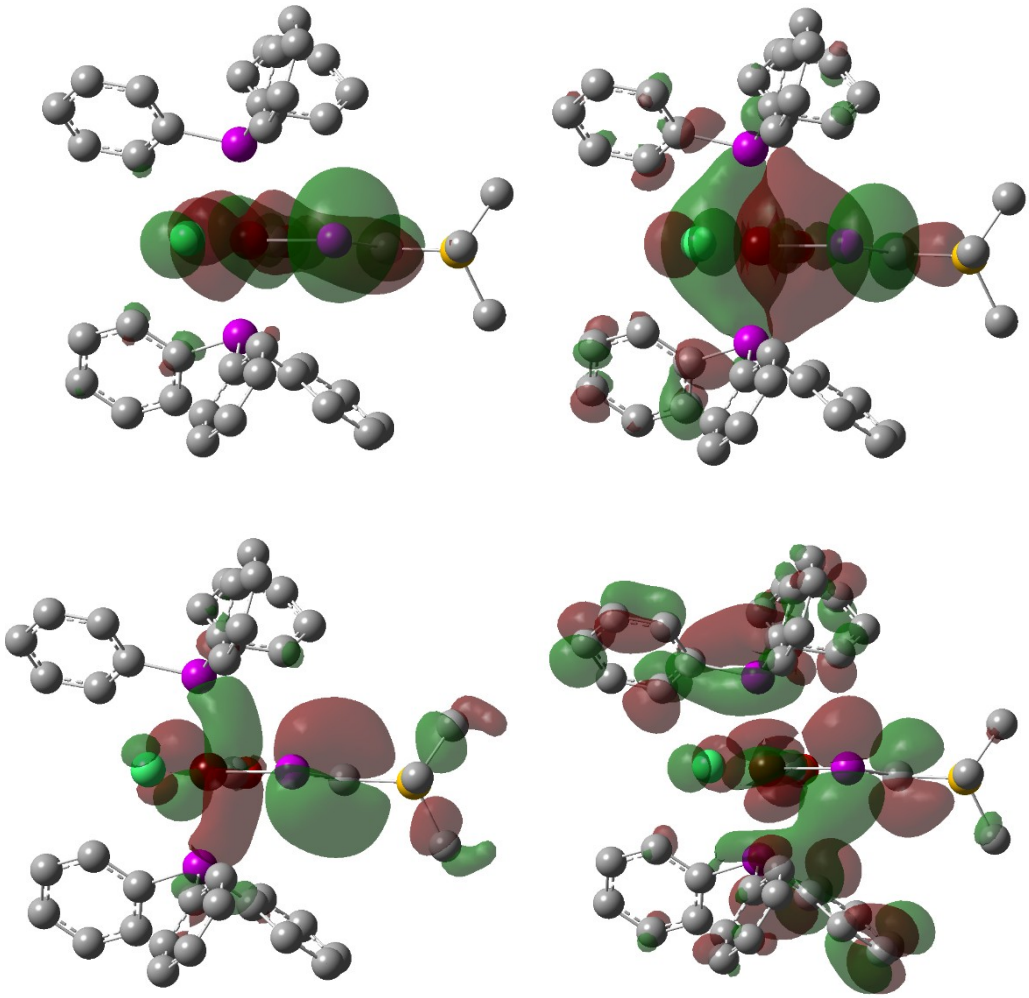

**Figure 4.5**: Calculated frontier molecular orbitals for **38**. HOMO (*top left*) LUMO (t*op right*) HOMO-1 (*bottom left*) and LUMO+1 (*bottom right*).

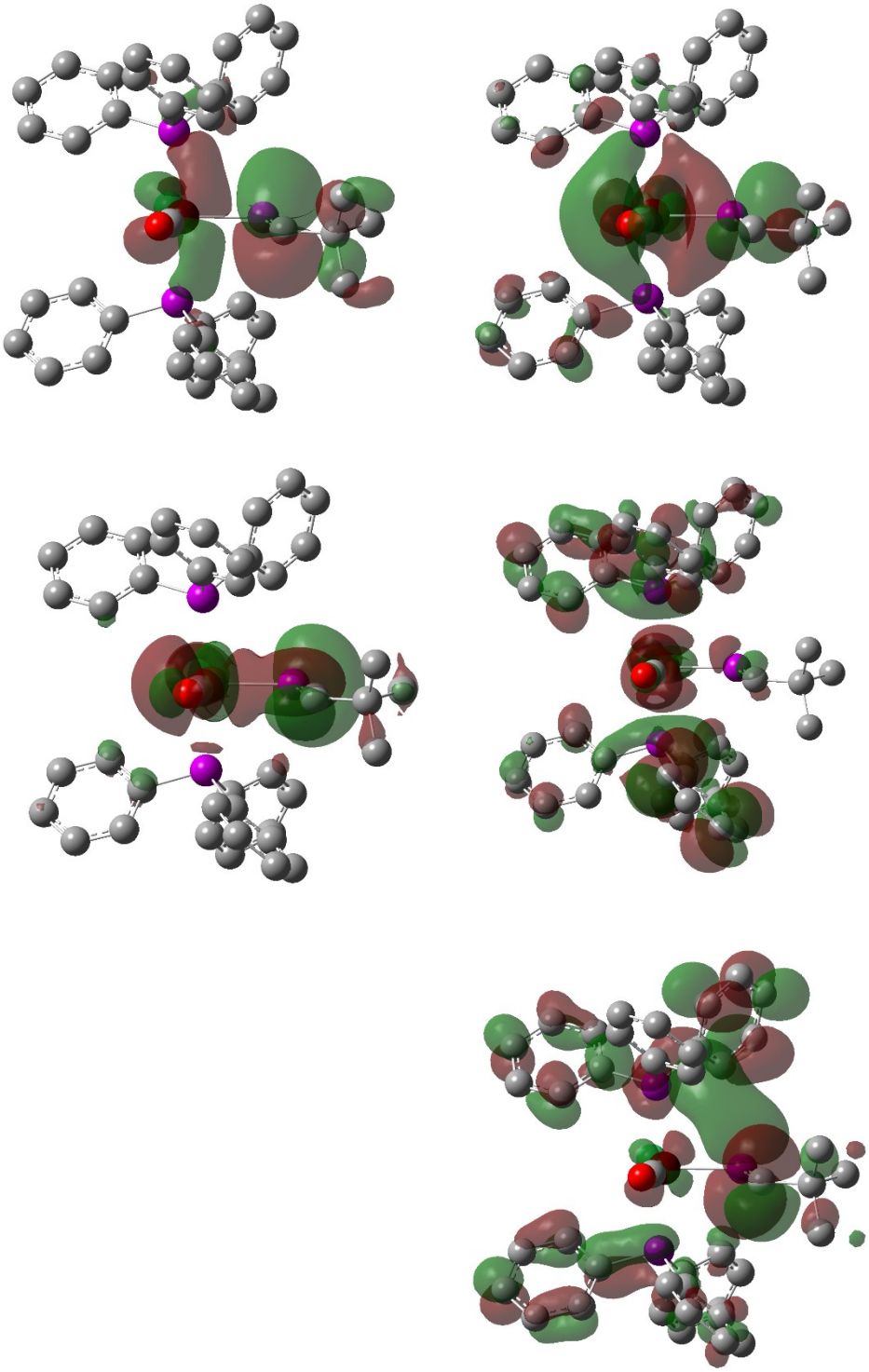

**Figure 4.6**: Calculated frontier molecular orbitals of **34**. HOMO (*top left*) LUMO (*top right*) HOMO-1 (*middle left*) LUMO+1 (*middle right*) and LUMO+2 (*bottom right*).

## 4.4 Expanding the range of bridging pyrazolyl η²–phosphaalkene compounds

### 4.4.1 The addition of LiPz* to ruthenaphosphaalkenyls (59-61)

LiPz* was added to **59**-**61** in tetrahydrofuran and left to stir for 1-2 hours before the solvent was removed and the product extracted with $CH_2Cl_2$ to effect removal of LiCl and afford a yellow solid. These complexes all showed the indicative spectroscopic features to support the formation of [Ru(CO){κ³-N,C,P-P(Pz*)CH(SiMe$_2$R)}(PPh$_3$)$_2$], where R = *p*-tolyl; **64,** *p*-$CF_3$-$C_6H_4$; **65**, $^n$Bu; **66** (**Table 4.8**). The $^{31}P\{^1H\}$ NMR spectra of each compound consist of three multiplet resonances ($\delta_P$ = 32.1−34.3 (d, $^2J_{P\text{-}P}$ *ca.* 50 Hz), 38.6−39.3 (dd, $^2J_{P\text{-}P}$ *ca.* 50, 17 Hz) and 46.5−46.7 (d, $^2J_{P\text{-}P}$ *ca.* 17 Hz), while proton NMR spectra confirmed the presence of the $SiMe_2$ units. The resonance for the previously alkenic carbon centre was assigned based on 2D spectra ($\delta_P$ = 41.8; **64**, 39.8; **65**, 39.4; **66**). The retention of the carbonyl group was proven by $^{13}C$ NMR ($\delta_C$ ~ 209) and IR ($\nu_{CO}$ ~ 1913 cm$^{-1}$) spectroscopic data, the latter being consistent with a Ru(0) species.[297,298]

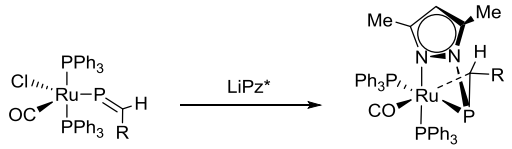


R = $^t$Bu (**34**), SiMe$_3$ (**38**), SiMe$_2$Ph (**39**), SiMe$_2$tolyl (**59**), SiMe$_2$*p*-$CF_3$-$C_6H_4$ (**60**), SiMe$_2$$^n$Bu (**61**),

R = $^t$Bu (**62**), SiMe$_3$ (**41**), SiMe$_2$Ph (**63**), SiMe$_2$tolyl (**64**), SiMe$_2$*p*-$CF_3$-$C_6H_4$ (**65**), SiMe$_2$$^n$Bu (**66**),

**Scheme 4.6**: Reactivity of **34**, **38**, **39**, **59**-**61** with LiPz*.

**Table 4.8**: Spectroscopic data for **64**-**66** and comparisons to published data (**41, 62, 63**).

| | $\delta_P$ | | $\delta_H$ | | $\delta_C$ | |
|---|---|---|---|---|---|---|
| | **P=C** | **PPh$_3$** | **P=CH** | **$^1J_{C\text{-}H}$** | **P=CH** | **ν(CO)** |
| **62 *** | 14.7 | 45.5, 41.4 | 2.90 | 137 | 79.8 | 1927 |
| **41 *** | 32.9 | 46.6, 39.2 | 1.62 | 123 | 44.9 | 1906 |
| **63 *** | 32.3 | 47.0, 38.4 | 1.77 | 128 | 41.8 | 1919 |
| **64** | 32.6 | 46.7, 39.1 | 1.75 | 135 | 41.8 | - |
| **65** | 34.3 | 46.5, 39.3 | 1.73 | 135 | 39.4 | 1913 |
| **66** | 32.1 | 46.6, 38.6 | 1.66 | 136 | 39.8 | 1913 |

* data collected by colleagues.[297,298]

Crystals of **65** grew from a concentrated $CDCl_3$ solution at ambient temperature. The solid state structure (**Figure 4.7**) matches that of **41** and the bond lengths and angles around the core "Ru-P(Pz*)CHSiMe$_2$*p*-CF$_3$-C$_6$H$_4$" unit are similar to those for [Ru(CO){κ$^3$-N,C,P-P(Pz*)CH(SiMe$_3$)}(PPh$_3$)$_2$] (**41**) and [Ru(CO){κ$^3$-N,C,P-P(Pz)CH(SiMe$_3$)}(PPh$_3$)$_2$] (**40**).[143,297]

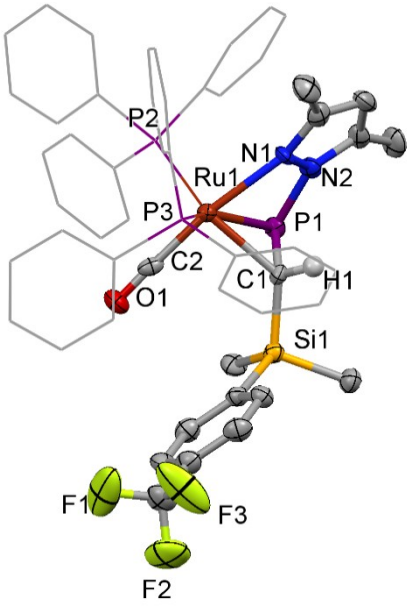


**Figure 4.7**: Solid state structure of **65** in crystals of the $CDCl_3$ solvate, with thermal ellipsoids at the 50% probability level and hydrogens (except P-CH) omitted and $PPh_3$ groups reduced for clarity. Note: there is rotational disorder in the $CF_3$ moiety. Selected bond lengths (Å) and angles (˚). Ru1-P1 2.3808(12), P-C 1.782(4), Ru1-C1 2.211(4), Ru1-N1 2.230(4), P1-N2 1.779(4); P1-C1-Si1 113.4(2), P1-C1-H1 112.04(15), Si1-C1-H1 112.04(15).

### 4.4.2 Asymmetric bridging pyrazolyl η$^2$ –phosphaalkene complexes

The reactivities of [RuCl(CO)(PPh$_3$)$_2$(P=CHSiMe$_2$R)] (R = *p*-tolyl; **59**, *p*-CF$_3$-C$_6$H$_4$; **60** and $^n$Bu; **61**) were further investigated with the asymmetric pyrazolates, LiPz$^{CF3}$ and LiPz$^{Me,CF3}$, in order to explore the effects that varying substitution patterns of the pyrazole ring might have on formation of bridging pyrazolyl η$^2$–phosphaalkene compounds (**Scheme 4.7**). This is an extension of the work by Trathen, who investigated the reactivity of **34**, **38**, **39** with LiPz$^{CF3}$, LiPz$^{Me,CF3}$ and LiPz$^{tBu}$ and showed them to react in an analogous manner to LiPz*.[190]

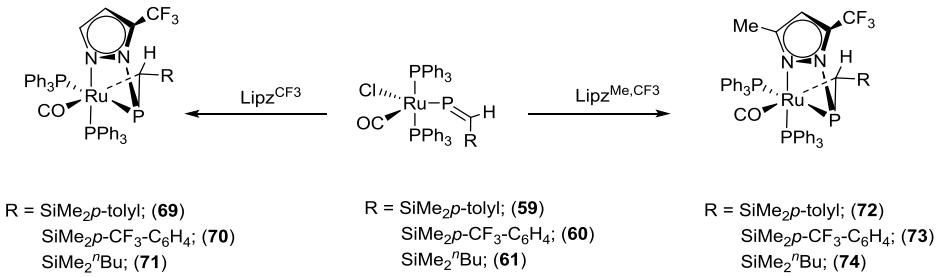


R = $SiMe_2$*p*-tolyl; (**69**)
$SiMe_2$*p*-$CF_3$-$C_6H_4$; (**70**)
$SiMe_2{}^n$Bu; (**71**)

R = $SiMe_2$*p*-tolyl; (**59**)
$SiMe_2$*p*-$CF_3$-$C_6H_4$; (**60**)
$SiMe_2{}^n$Bu; (**61**)

R = $SiMe_2$*p*-tolyl; (**72**)
$SiMe_2$*p*-$CF_3$-$C_6H_4$; (**73**)
$SiMe_2{}^n$Bu; (**74**)

**Scheme 4.7**: Synthesis of $Pz^{CF3}$ based complexes **68**-**70** and $Pz^{Me,CF3}$ based complexes **71**-**73**.

Solutions of $LiPz^{R,CF3}$ (R = H, Me) were added to stirring solutions of **59**-**61** in tetrahydrofuran to afford $[Ru(CO)\{\kappa^3\text{-N,C,P-P}(Pz^{CF3})CH(SiMe_2R)\}(PPh_3)_2]$ (R = *p*-tolyl; **68**, *p*-$CF_3$-$C_6H_4$; **69**, $^n$Bu; **70**) and $[Ru(CO)\{\kappa^3\text{-N,C,P-P}(Pz^{MeCF3})CH(SiMe_2R)\}(PPh_3)_2]$ (R = *p*-tolyl; **71**, *p*-$CF_3$-$C_6H_4$; **72**, $^n$Bu; **73**). Spectroscopic data for **68**-**73** (shown in **Table 4.9**) confirm the presence of an $\eta^2$-phosphaalkene fragment with a bridging pyrazolyl moiety.

**Table 4.9**: Spectroscopic data for **68**-**73**.

| **Starting material** | $Pz^{R',CF3}$ | | $\delta_P$ | | $\delta_C$ | $\delta_H$ | | | |
|---|---|---|---|---|---|---|---|---|---|
| | **R'** | | **P=C** | **$PPh_3$** | **P=C** | **P=CH** | **$^1J_{C\text{-}H}$** | **$Pz^{CF3}$** | **$\nu_{CO}$** |
| **59** | H | **68** | 75.0 | 47.9, 41.3 | 45.6 | 1.90 | 134.1 | -60.0 | |
| | Me | **71** | 62.6 | 47.2, 38.4 | 42.1 | 1.97 | 137.4 | -59.9 | 1918 |
| **60** | H | **69** | 73.8 | 47.8, 40.9 | 43.8 | 1.82 | 137.7 | -60.13 | 1913 |
| | Me | **72** | 62.0 | 47.1, 37.8 | 40.7 | 1.85 | 135.2 | -59.9 | 1917 |
| **61** | H | **70** | 77.1 | 47.8, 41.5 | 42.8 | 1.77 | 134.6 | -60.15 | |
| | Me | **73** | 65.0 | 47.0, 38.5 | 43.4 | 1.68 | 133.5 | -60.1 | 1920 |

The reactions of asymmetric pyrazolates with **61** proved more complex than those with **59** and **60**. The addition of $LiPz^{Me,CF3}$ to **61** resulted in the formation of **73** and an additional product. While the $^{31}P\{^1H\}$NMR spectra did not indicate the presence of multiple products (due to the apparent coincidence of their $^{31}P\{^1H\}$ resonances), the $^{13}C\{^1H\}$ NMR data showed two separate $CF_3$ groups. The integrals of these resonances match the integrals of two resonances found in the $^{19}F$ NMR spectra - neither of which correspond to $LiPz^{Me,CF3}$ ($\delta_P$ = −62.07). The doublet at −59.9 ppm (*J* = 19.5 Hz) is likely, in part, to be caused by through space coupling between phosphorus and the nearby $CF_3$ group (**73-P-N-$CCF_3$**) (as seen in the $^{19}F$ NMR spectra of **71** and **73**), while the singlet at −60.5 ppm is thought to correspond to the alternate orientation with

the $CF_3$ group directed into proximity with the ruthenium centre, and the methyl group proximal to the phosphaalkene (**73-Ru-N-CCF$_3$**).

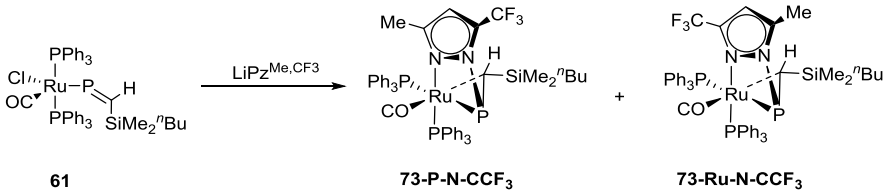


**Figure 4.8**: Both isomers of **73** from the addition of $Pz^{MeCF3}$ to **61**.

Similarly, spectroscopic data for the product obtained upon reaction of $LiPz^{CF3}$ with **61** would again seem to imply the presence of two isomers ($\delta_F$ = −60.0, (**70-P-N-CCF$_3$**) and −60.5 (**70-Ru-N-CCF$_3$**). However, it is not as clear cut in this case as the two separate $CF_3$ groups cannot be resolved in the $^{13}C\{^1H\}$ NMR spectrum.

The reactivity of $LiPz^{Ph}$ with ruthenaphosphaalkenyls **38**, **39** and **60** all proceed in the same manner as other pyrazoles, as illustrated by the key spectroscopic data of ([Ru(CO){κ$^3$-N,C,P-P($Pz^{Ph}$)CH($SiMe_2$R)}($PPh_3$)$_2$] (R = Me; (**74**), Ph; (**75**), *p*-tolyl; (**76**), *p*-$CF_3$-$C_6H_4$; (**77**), $^n$Bu; (**78**)), displayed in **Table 4.10**. However, with the addition of $LiPz^{Ph}$ to **59** and **61**, additional species are again observed.

**Table 4.10**: Spectral data for **74**-**78**.

| Starting material | Compound number | $\delta_P$ | | $\delta_H$ | $\delta_C$ | | |
|---|---|---|---|---|---|---|---|
| | | P=C | $PPh_3$ | P=C<u>H</u> | $^1J_{C-H}$ | P=<u>C</u>H | ν(CO) |
| **38** | **74** | 64.4 | 47.4, 41.8 | 1.74 | 135.9 | 47.5 | 1908 |
| **39** | **75** | 61.1 | 47.9, 41.6 | 1.86 | 134.5 | 41.6 | 1912 |
| **59** | **76** | 61.6 | 47.2, 38.4 | 1.97 | 131.6 | 42.1 | 1910 |
| **60** | **77** | 60.6 | 47.7, 41.3 | 1.86 | 134.0 | 45.3 | 1912 |
| **61** | **78** | 64.5 | 47.6, 41.8 | 1.76 | 134.5 | 45.9 | 1913 |

With **61**, the reaction affords approximately half of the expected η$^2$–phosphaalkene complex (**78**) along with an unknown species which could not be separated or isolated. The new species has distinctive $^{31}P\{^1H\}$ NMR resonances, a triplet at 219 ppm, and an associated doublet at 18.5

ppm ($J$ = 35.2 Hz) in a 1:2 ratio, consistent with two $PPh_3$ groups and a phosphaalkene-type phosphorus, which lies at a significantly lower frequency than the parent phosphaalkenyl (**61**; $\delta_P$ = 545.3). However, the rest of the configuration around the metal centre is unknown. A comparable species was also noted in the reaction of **59** with $LiPz^{Ph}$ ($\delta_P$ = 293 (t, $J$ = 34 Hz) 18.0 (d, $J$ = 34 Hz)), albeit, in much smaller quantities (~10% by phosphorus NMR integrals) with the major product the $\eta^2$-phosphaalkenyl (**76**). Significantly, similar spectroscopic signatures have been reported by co-workers upon reaction of the phosphaalkenyls with organolithium or Grignard reagents (*vide infra*). The identification of these species might lead to a greater understanding of the mechanistic features of these pyrazolate reactions.

### 4.4.3 Mechanistic studies on formation of bridging pyrazolyl $\eta^2$–phosphaalkenic compounds

The choice of asymmetric pyrazoles resulted in variable steric and electronic properties. The fluoromethyl group in '$Pz^{CF3}$' (**Figure 4.9a**) provides steric bulk on one side while rendering the proximal nitrogen less nucleophilic, while '$Pz^{Me,CF3}$' (**Figure 4.9b**) more closely resembles the bulk of Pz*, but again with one nitrogen less nucleophilic than the other. The pyrazolyl moiety '$Pz^{tBu}$' (**Figure 4.9c**) adds significantly more bulk which may sterically shield the nitrogen atom, though does not diminish its nucleophilicity, while the steric influence of '$Pz^{Ph}$' (**Figure 4.9d)** remains unclear, as this depends on if the orientation of the aromatic ring is planar or orthogonal to the pyrazolyl ring.

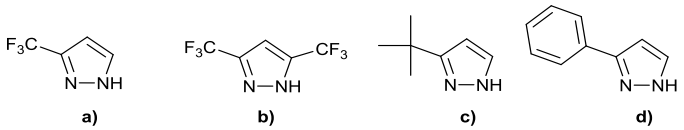


**Figure 4.9**: Structures of asymmetrical pyrazoles a) 3-(Trifluoromethyl)pyrazole, b) 3,5-Bis(trifluoromethyl)pyrazole c) 3-*tert*-Butyl-1H-pyrazole d) 3-Phenyl-1H-pyrazole.

Previous studies completed by Trathen *et al.*, indicated pyrazolyl $\eta^2$–phosphaalkene compounds based on asymmetric pyrazolates exist as a single isomer, spectroscopic data suggesting the bulkier groups are directed away from the ruthenium centre. In order to confirm this notion, single crystals suitable for x-ray diffraction of [Ru(CO){$\kappa^3$-N,C,P-$P(Pz^{tBu})CH(SiMe_3)$}$(PPh_3)_2$] (**67**) have been grown from the slow evaporation of $CDCl_3$ from a saturated solution of **67**.

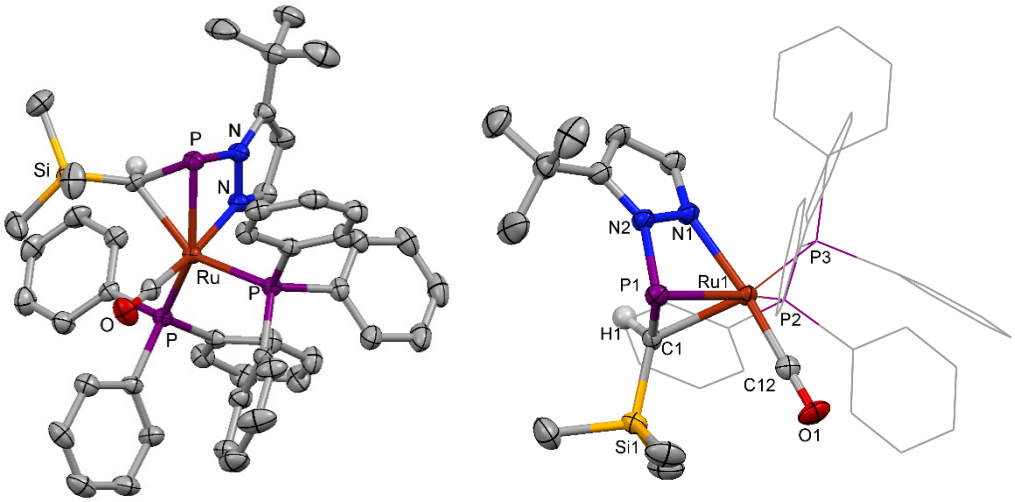


**Figure 4.10**: Molecular structure of **67** with thermal ellipsoids at the 50% probability level and hydrogens omitted for clarity (except P-CH) (*left*) with $PPh_3$ groups reduced for clarity, (*right*) with heteroatoms labelled. Selected bond lengths (Å) and angles (˚). Ru1-P1 2.3624(6), P-C 1.779(3), Ru1-C1 2.217(2), Ru1-N1 2.167(2), P1-N2 1.813(2); P1-C1-Si1 116.77(14).

The structural data for **67** confirm that the $^{t}$Bu fragment is directed away from the bulk at the ruthenium centre. The geometry is otherwise unremarkable, the Ru-P1 bond (2.362(6), the P-C bond (1.779(3) Å) and the Ru1-N1 and P1-N2 bonds (2.167(2), 1.813(2) Å, respectively) are comparable to those found for the key "N-Ru-P-N" unit for [Ru(CO){$\kappa^3$-N,C,P-P(Pz*)CH($SiMe_3$)}($PPh_3$)$_2$] (**41**), [Ru(CO){$\kappa^3$-N,C,P-P(Pz)CH($SiMe_3$)}($PPh_3$)$_2$] (**40**) and [Ru(CO){$\kappa^3$-N,C,P-P(Pz*)CH($SiMe_2$*p*-$CF_3$-$C_6H_4$)}($PPh_3$)$_2$] (**65**).[143,297]

It has been speculated that the first step is likely to consist of an initial nucleophilic attack either at ruthenium, or on phosphorus. Nucleophilic attack at ruthenium is supported by the accessible plane and the large contribution of the metal centre to the LUMO, while NBO analysis of the precursor **38**, suggests an appreciable δ+ character on phosphorus (0.55 - 0.76),[298] and the previously established reactivity with electrophiles at phosphorus for the ruthenaphosphaalkenyls to give rise to $\eta^1$-phosphaalkene complexes.[290,297]

The observed steric discrimination would seem consistent with the initial site of pyrazolate attack being at ruthenium. Indeed, this is consistent with the spectroscopic data of the unknown species formed alongside **78** ($\delta_P$ = 291.0 (t, $^2J_{P\text{-}P}$ = 35.2 Hz), 18.5 (d, $^2J_{P\text{-}P}$ = 35.2 Hz)) suggesting the addition of LiPz' across the Ru-P bond of **61** in the same manner previously observed of other electrophilic species, with lithium as the electrophilic fragment (see **Section**

**4.1.1).** Additionally, almost identical resonances are seen in spectroscopic data from the addition of the bulkier pyrazolate, $LiPz^{(CF3)2}$ to **61** to form unknown species (**79**) ($\delta_P$ = 291.0 (t, $J_{P-P}$ = 35.2 Hz), 18.5 (d, $J_{P-P}$ = 35.2 Hz). The higher frequency resonance is consistent with a phosphaalkene ligand, coordinating to a metal in an $\eta^1$ fashion through the phosphorus lone pair. Similar spectroscopic data were reported by Trathen, from the product of reacting **38** with a range of lithium salts ($LiN(SiMe_3)_2$, $LiN^iPr_2$, $LiPz^{(CF3)2}$, $LiPz^{(tBu)2}$ and LiMe),[190] suggesting that similar species are obtained. The IR spectrum of **79** ($\nu_{CO}$ = 1939 $cm^{-1}$) more closely resembles IR spectra of **38**, **39**, **59**-**61** ($\nu_{CO}$ = 1920−1939 $cm^{-1}$) suggesting a Ru(II) centre.

Assuming ruthenium to be the initial site of pyrazolate addition, the formation of isomeric mixtures of **70** and **73** suggest this step to be reversible. It is expected that when the $CF_3$ unit is closest to phosphorus, it is less nucleophilic and therefore the final addition step - nucleophilic attack at phosphorus - would be slow compared to the dissociation from the metal. However, when the $CF_3$ side of the pyrzolate adds to the metal, in the less favourable initial step, the opposite group (Me or H), closer to phosphorus is more nucleophilic and the second addition step occurs more readily and once the Ru-N-N-P unit is closed, dissociation is prevented. The formation of the statistical mixture of **70-P-N-CCF$_3$** and **70-Ru-N-CCF$_3$,** therefore indicates the requirement of a subtle balance between the relative rates of the individual steps, thus definitive proof will require detailed kinetic investigations.

It was speculated by Trathen that the NMR resonances obtained from the reaction of **38** with a range of lithium salts[190] might be related to the complex shown in **Figure 4.11A**. The $Li^+$ cation interacts with the P=C phosphorus centre - accounting for the shift in frequency in the $^{31}P\{^1H\}$ spectra - while the nucleophilic fragment may be interacting with lithium or behaving as a counter-ion.[190]

The reaction of $LiPz^{(CF3)2}$ with **61** forms unknown complex **79**, this is thought to represent the first step in the mechanism for the addition of LiPz' to ruthenaphosphaalkenyls. **Figure 4.11B** suggests one possible structure for **79**, where after the formation of the Ru-N bond, the lithium is associated with both the pyrazolate and the phosphorus atom. Another possible structure is shown in **Figure 4.11C**, here, lithium is partially associated with the phosphorus atom. The $^6Li$ and $^7Li$ NMR spectra of **79** do not indicate any evolved Li-$^{31}P$ coupling, however, as these spectra are broad, this does not necessarily preclude the formation of a P-Li bond. Elemental analysis data are not consistent with either structure, but this might also be explained by NMR-silent impurities and, therefore, the exact structure of the complex and kinetics of the mechanism of formation remains unknown.

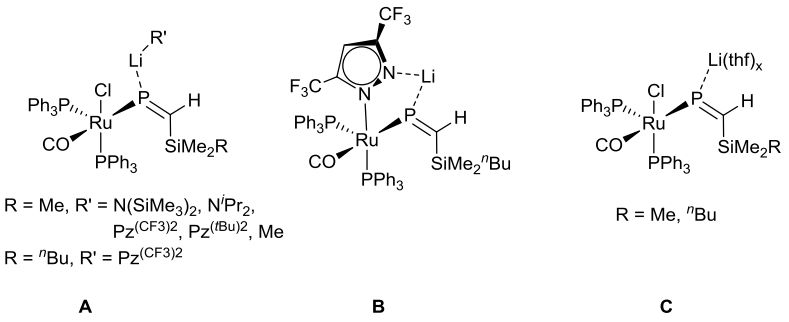


**Figure 4.11**: **A** - Structure proposed by Trathen.[190] **B** and **C** - Proposed structures of lithium salts added to **38** and **61** (**79**, R'=R'' = $CF_3$, R = $^n$Bu).

### 4.4.3.1 The addition of $PR_3$ to $[RuCl(CO)(PPh_3)_2\{P=CH(SiMe_3)\}]$ (38)

The insertion of phenylacetylene into a ruthenium (II) complex with two differing phosphine ligands ($PPh_3$ and $PMe_3$) is shown in **Scheme 4.8a**, while **Scheme 4.8b** shows the addition of $PMe_3$ to a solution of $[RuHCl(CO)(PPh_3)_3]$ (**58**) and the insertion of alkynyls into the Ru-H bond. These examples of the use of alternate phosphine ligands could introduce ligands with a different donor strength and therefore would result in a change in the sterics and electron density on the metal centre and changing the reactivity of the complex. For example, replacing the triphenylphosphine groups in **38** and similar systems (**39**, **59**-**61**) would reduce the bulk around the ruthenium centre which may affect the reactivity of the ruthenaphosphaalkenyls. Replacing a single triphenylphosphine unit with a trimethylphosphine group might also aid mechanistic studies of the bridging pyrazolyl complexes due to the $PMe_3$ phosphorus being in a distinct environment, thus introducing an additional $^{31}P\{^1H\}$NMR resonance.

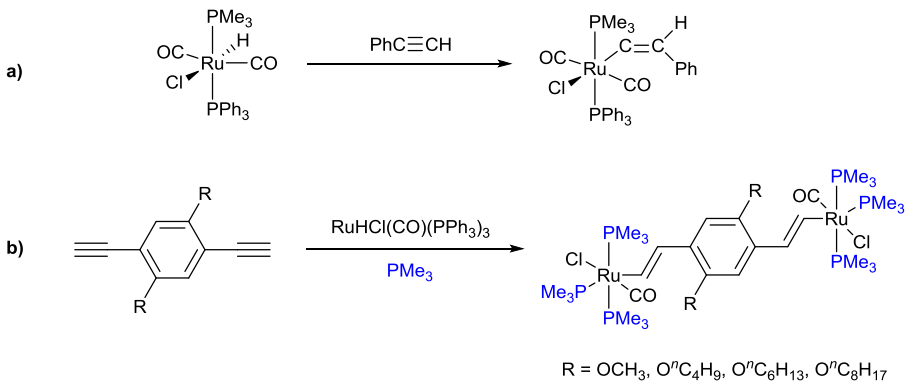


**Scheme 4.8**: The formation of a *hexa*-coordinate ruthenalkenyl complex with a $PMe_3$ group (**a**)[321] and the formation of bimetallic ruthenalkenyl complexes with $PMe_3$ groups (**b**).[322]

The stirring of $[RuHCl(CO)(PPh_3)_3]$ with an excess of $PMe_3$ for a number of hours results in the formation of the previously unknown complex $[RuHCl(CO)(PMe_3)(PPh_3)_2]$, obtained as a white solid (**80**). The structure of **80** is indicated by spectroscopic data, which confirm the retention of the hydride ($\delta_H$ = −5.9), and the presence of two different phosphine ligands ($\delta_P$ = −23.6, 41.0) in a two to one ratio, respectively. Increasing the amount of $PMe_3$ in the solution did not drive the replacement of the other triphenylphosphine ligands. While leaving a solution of **58** and $PMe_3$ to stir for an additional 30 days resulted in the partial decomposition of the complex, with no evidence of formation for $[RuHCl(CO)(PPh_3)(PMe_3)_2]$ or $[RuHCl(CO)(PMe_3)_3]$.

Colourless single crystals of **80** were obtained from *n*-hexane solution, confirming the molecular connectivity and showing the ligands around ruthenium to include a chloride and a carbonyl group (**Figure 4.12**). The structural data also shows that the substituted phosphine is *trans* to the hydride and the two remaining triphenylphosphine units are pseudo-axial.

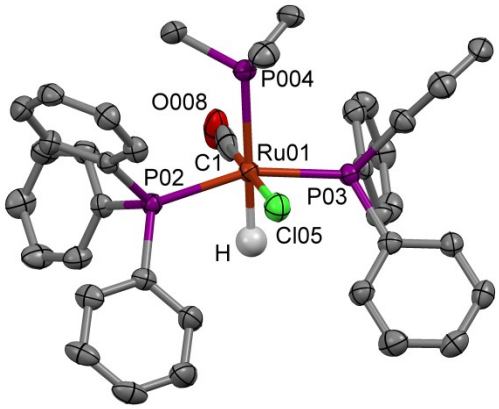


**Figure 4.12**: Crystal structure of $[RuHCl(CO)(PPh_3)_2(PMe_3)]$ (**80**), with thermal ellipsoids at the 50% probability level and hydrogen atoms omitted for clarity (except Ru-H). Selected bond lengths (Å) and angles (˚). Ru-$P_{PMe3}$ 2.4338(11), Ru-$P_{PPh3}$ 2.3641(10) / 2.3553(10), Ru-$C_{CO}$ 1.928(8), Ru-Cl 2.4819(12), $P_{PPh3}$-Ru-$P_{PPh3}$ 159.91(4), $P_{PMe3}$-Ru-$P_{PPh3}$ = 100.80(4) / 98.92(4).

Unfortunately the addition of $Me_3SiC{\equiv}P$ (**36**) to **80** does not result in the formation of a new ruthenaphosphaalkenyl. An excess of **36** was added to a stirred suspension of **80** in dichloromethane and led to the formation of a yellow solid after 1.5 hours, however, spectroscopic analysis revealed only unreacted **80**. The post-insertion substitution of $PPh_3$ for $PMe_3$ was also attempted for **38**, through the addition of $PMe_3$ to a stirring solution of **38** in toluene. The $^{31}P\{^1H\}$ NMR spectrum of the resulting mixture indicated the formation of **80**, and

a number of unknown impurities, including a small amount of two additional species, each with a doublet and a triplet exhibiting mutual coupling ($\delta_P$ = 290 (t, *J* = 35 Hz), 18.5 (d, *J* = 35 Hz) and $\delta_P$ = 112.2 (t, *J* = 31 Hz), −8.0 (d, *J* = 31 Hz)). The additional species are present in trace amounts, however, 2D $^{31}P$-$^{1}H$ NMR spectroscopy shows that the signals at lower frequency are consistent with $PMe_3$ ligands. The two triplet resonances each show a large shift to lower frequency when compared to the starting material (**38**), this is inconsistent with the formation of [Ru(CO)Cl(P=CHSiMe$_3$)(PPh$_3$)(PMe$_3$)] or [Ru(CO)Cl(P=CHSiMe$_3$)(PMe$_3$)$_2$] and thus their identity remains unknown. The phosphorus signals of the additional species are similar to those for unidentified $\eta^1$-phosphaalkenes seen in **79**, and from the reaction of **59** or **61** with LiPz$^{Ph}$ as discussed in **Section 4.4.2**, similar species would seem likely, however, given the trace levels obtained, these cannot be reasonably formulated. However, after stirring the mixture of $PMe_3$ and **38** in $CH_2Cl_2$ for 18 hours, $^{31}P\{^1H\}$ NMR data showed a new product in addition to starting material ($\delta_P$ = 290.3, (t) and 18.4 (d)) showing mutual coupling, consistent with an $\eta^1$ phosphaalkene complex. This new compound cannot be the addition of $PMe_3$ to the phosphaalkenic centre as this would result in additional coupling in the $^{31}P\{^1H\}$ NMR spectrum and its identity remains unknown.

The addition of $PPh_3$ to a solution of **38** did not result in the coordination of $PPh_3$ to the ruthenium center as indicated by the $^{31}P\{^1H\}$ NMR spectra which provided no indication of the retention of P=CHSiMe$_3$ moiety, and instead showed numerous signals, all at lower frequency, none of which were consistent with the formation of [RuCl(CO)(P=CHSiMe$_3$)(PPh$_3$)$_3$].

## 4.5 Comparing the reactivity of vinyl complexes to phosphaalkenyl complexes

### 4.5.1 Known reactivity of vinyl complexes

The carbo-centric analogue to the phosphaalkyne hydrometallation reactions were published in 1986 by Torres *et al.* featuring insertion reactions of [RuHCl(CO)(PPh$_3$)$_3$] (**58**) with non-activated acetylenes (pent-1-ene, phenylacetalyne, diphenylacetylene), resulting in *penta*-coordinate complexes [RuCl(CO)(RC=CHR)(PPh$_3$)$_2$] as supported by spectroscopic data and elemental analysis. The known reactivity of these systems is described in **Scheme 4.9**, and was explored in order to expand the reactivity of the ruthenaphosphaalkenyl systems.

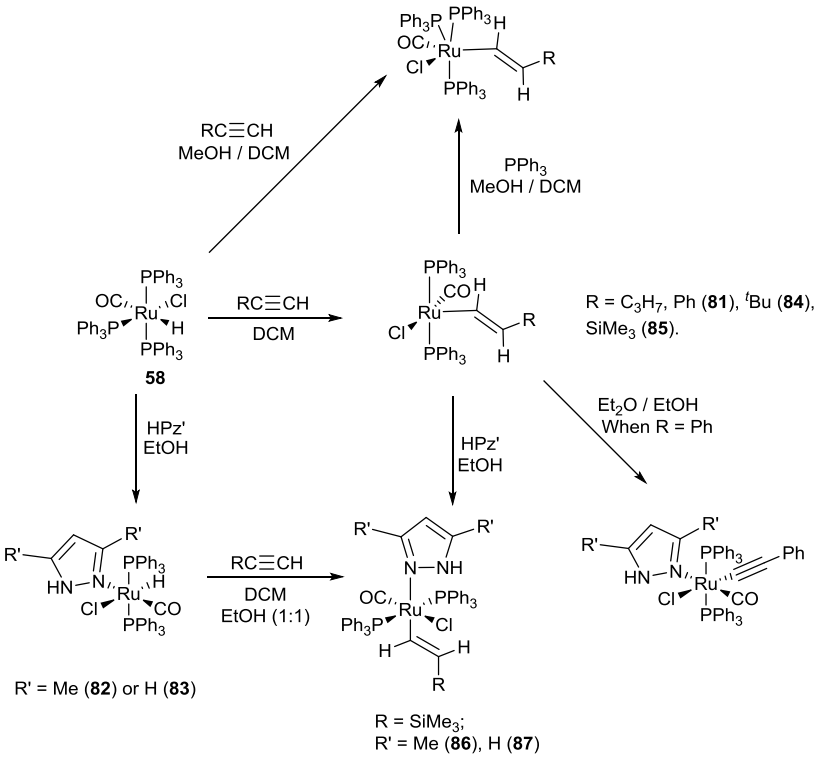


**Scheme 4.9**: Reactivity of ruthenium vinyl systems.[323–325]

### 4.5.2 Synthesis of comparative ruthenium vinyls

The carbocentric equivalents to **34** and **38** are synthesised using the commercially available alkynes PhC≡CH, $^{t}$BuC≡CH and $Me_3SiC$≡CH. Complexes of the form [Ru(HC=CHR)Cl(CO)($PPh_3$)$_2$] (R = Ph; **81**, $^{t}$Bu; **84** and $SiMe_3$; **85**)[323,324] were made in order to compare their reactivity to the phosphorus analogues (**Scheme 4.10**). The reactivity of **81** is well established and was made as a test system, while **84** and **85** are direct analogues of **34** and **38**, respectively.

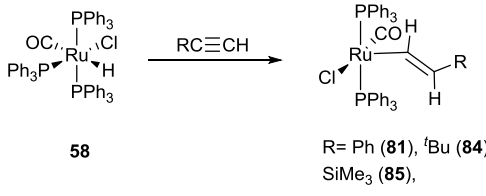


**Scheme 4.10**: Synthesis of *penta*-coordinate ruthenium vinyls **81**, **84**, **85**.[323,324]

There are no structural data in the CCDC for these ruthenium vinyls to compare to the structural data obtained of the ruthenaphosphaalkynls. Attempts to crystallise the ruthenium vinyls led to suitable crystals of only **85**, however, the structure is disordered in the equatorial plane, and CO and Cl are refined across two sites with 50% occupancy.

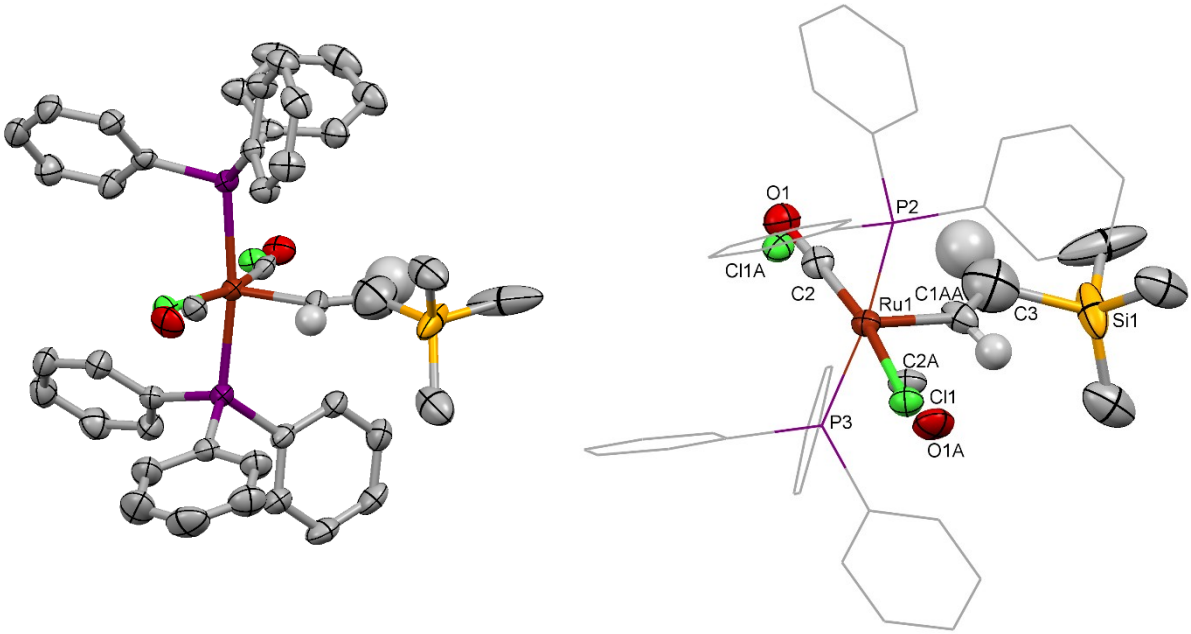


**Figure 4.13**: Crystal structure of **85**, with thermal ellipsoids at the 50% probability level and hydrogen atoms omitted for clarity (except HC=CH) (*left*) with $PPh_3$ groups reduced for clarity, (right) with heteroatoms labelled. Note: the disorder around the equatorial plane (OC-Ru-Cl axis).

While the bond lengths and angles around the equatorial plane must be treated with caution, they do show a close similarity to those in [RuCl(CO)(P=CSiMe$_3$)(PPh$_3$)$_2$] (**38**). Comparison of the bond lengths and angles from the solid state structures of **38** and **85** are shown in **Table 4.11**, the structures are broadly similar in geometry around the ruthenium centres, and the presence of phosphorus rather than a carbon atom is noted by the 20˚ difference in the Ru-P=C/Ru-C=C angle between the "C=CHSiMe$_3$" and "P=CHSiMe$_3$" units. This, alongside the presence of the lone pair on phosphorus, accounts for some differences in reactivity, *vide infra*.

**Table 4.11**: Comparative X-ray data of **38** and **85**.

| | **38** | | **85** |
|---|---|---|---|
| **Ru-$P_{alkenic}$** | 2.226(2) | **Ru-$C_{alkenic}$** | 2.009(5) |
| **Ru-$C_{(CO)}$** | 1.735(9) | **Ru$C_{(CO)}$** | 1.782(10) |
| **Ru-Cl** | 2.411(2) | **Ru-Cl** | 2.436(3) |
| **P=C** | 1.660(11) | **C=C** | 1.242(9) |
| **C≡O** | 1.183(12) | **C≡O** | 1.170(13) |
| **C-Si** | 1.836(10) | **C-Si** | 1.964(10) |
| **Ru-P=C** | 124.4(4) | **Ru-C=C** | 143.3(6) |
| **P-Ru-P** | 167.18(7) | **P-Ru-P** | 170.81(4) |
| **Cl-Ru-CO** | 159.0(3) | **Cl-Ru-CO** | 166.0(3) |
| **P=C-Si** | 122.5(7) | **C=C-Si** | 118.7(7) |

The addition of HPz* or HPz to a solution of **85** affords the complexes [Ru(CO)Cl(HC=CSi$Me_3$)($PPh_3$)$_2$(HPz*)] (**86**), and [Ru(CO)Cl(HC=CSi$Me_3$)($PPh_3$)$_2$(HPz)] (**87**) respectively. The same products can also be synthesised from the addition of HPz* or HPz to **58** to form [Ru(CO)HCl(HPz*)($PPh_3$)$_2$] (**82**) or [Ru(CO)HCl(HPz)($PPh_3$)$_2$] (**83**), before the addition of $Me_3$SiC≡CH (**Scheme 4.9**).[325] However, the addition of $Me_3$SiC≡P (**36**) to **82** or **83** does not react in a comparable reaction to afford the phospha-analogues, [Ru(CO)Cl(P=CSi$Me_3$)($PPh_3$)$_2$(HPz')] (**Scheme 4.11**). Instead, a retention of **82**, (where Pz' = Pz*) or **83** (where Pz' = Pz) is observed alongside the formation of some [RuCl(CO)(P=CHSi$Me_3$)($PPh_3$)$_2$] (**38**), indicated by key $^1$H and $^{31}$P{$^1$H} NMR spectroscopic data ($\delta_H$ = −0.04 ($SiMe_3$), 7.28 (P=CH). $\delta_P$ = 545 (P=C), 34 ($PPh_3$)). Spectroscopic data from the addition of HPz* and $Me_3$SiC≡P (**36**) to a solution of [RuHCl(CO)($PPh_3$)$_3$] (**58**) in $CH_2Cl_2$, suggest the formation of **34** and [Ru(CO)ClH($PPh_3$)$_2$(HPz*)] (**82**) (**Scheme 4.12**).

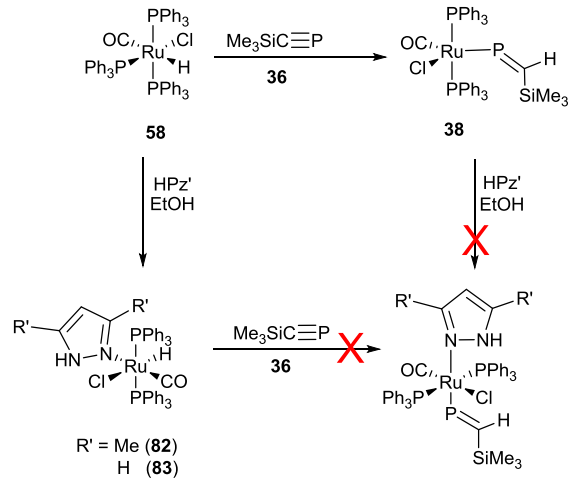


**Scheme 4.11**: Attempted synthesis of [Ru(CO)Cl(P=CSiMe$_3$)(PPh$_3$)$_2$(HPz')].

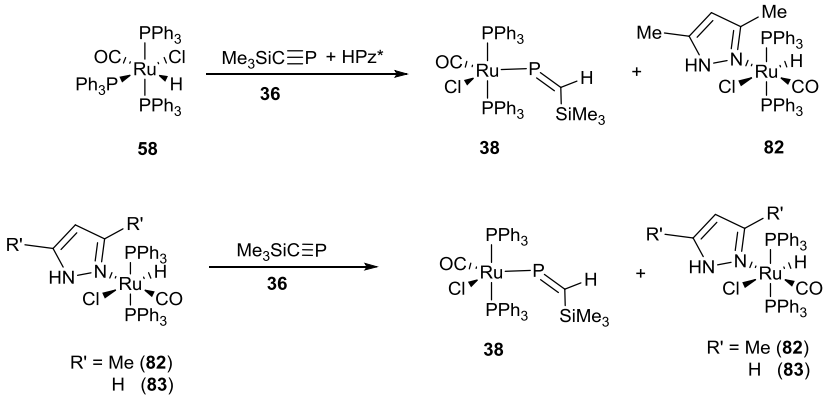


**Scheme 4.12**: Reactivity of [RuHCl(CO)(PPh$_3$)$_3$] (**58)** and [Ru(CO)ClH(HPz')(PPh$_3$)$_2$] (Pz' = Pz* **82**, Pz **83**) with Me$_3$SiC≡P (**36**).

## 4.6 Addition of other 2-electron donors to ruthenaphosphaalkenyl systems

The vacant coordination site in the 5-coordinate ruthenaphosphaalkenyls offers scope for the addition of various donors such as CO, and RN≡C (R = $^t$Bu,[295] C$_6$H$_3$Me$_2$)[326] and electrophiles including H$_2$, MeI and HCl which are demonstrated for **34** in **Scheme 4.3**, (**Section 4.1.2**). The addition of a bridging unit to form a bimetallic complex is an attractive target, as they will allow conjugation through the two ruthenium and the phosphaalkenic systems.

### 4.6.1 Bimetallic systems

The five-coordinate ruthenium vinyl-complexes has been shown to form bimetallic species through the double hydroruthenation of a dialkyne such as HC≡C-R-C≡CH, shown in **Scheme 4.13**,[327,328] or through the addition of 4,4'−dipyridyl, or 1,4-disocyanide to ruthenium vinyl systems as shown in **Figure 4.14**.[327]

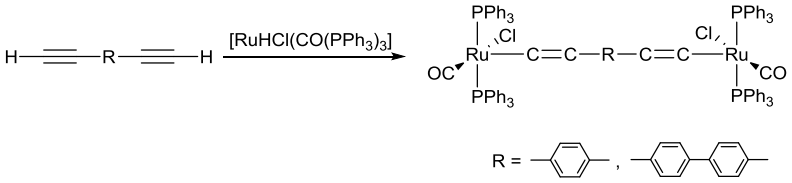


**Scheme 4.13**: Synthesis of bimetallic ruthenium vinyl complexes.[327,328]

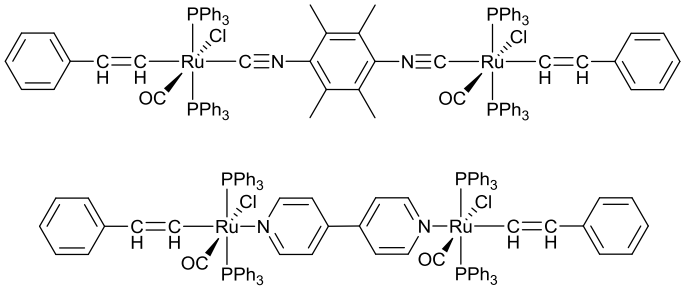


**Figure 4.14**: Known bimetallic ruthenium complexes, with bridging 4,4'−dipyridyl and 2,3,5,6-tetramethylphenyl diisocyanide.[327]

Due to the lack of suitable bis-phosphaalkynes, the synthesis of bimetallic systems derived from the ruthenaphosphaalkenic systems **38**, **39** and **59** were attempted using molecules that might bridge two ruthenium centres. The addition of a suspension of ½ equivalent of bipyridine in $CH_2Cl_2$ to a $CH_2Cl_2$ solution of **38**, resulted in a slight discolouration of the orange solution. After stirring for two hours, the products were precipitated by the addition of diethyl ether, before the isolated precipitate was washed with hexanes. The $^{31}P\{^1H\}$ NMR data indicate the presence of starting material **38** ($\delta_P$ = 544.5 (t), 34.1 (d)), along with a similar, though distinct, complex ($\delta_P$ = 554.5 (t), 33.9 (d)), alongside another minor species and a significant amount of $PPh_3$. This unknown phosphaalkenic complex might be consistent with a bimetallic

complex, however, it could not be isolated, nor its proportion increased within the mixture. The attempt to use a single equivalent of bipyridine was unsuccessful, and does not result in addition to the ruthenium centre either.

### 4.6.2 The attempted addition of pyridine, isocyanides and nitriles

The addition of pyridine to **85** was attempted as a test system and results in a shift in the $^{31}P\{^{1}H\}$ NMR resonance associated with the $PPh_3$, from 30.7 ppm in **85**, to 26.0 ppm. Proton NMR spectroscopic data are inconclusive, due to an excess of pyridine and it is not possible to conclude if the addition of **85** was successful, or if the alkenyl unit remained intact. The addition of pyridine to **38** resulted in decomposition of the phosphaalkenyl unit, as indicated by spectroscopic data.

While the addition of $^{t}$BuN≡C to **34** results in $\eta^1$-coordination to the ruthenium centre, stirring $^{t}$BuN≡C with **38** does not result in the analogous coordination. The resulting $^{31}P\{^{1}H\}$ NMR data showed some **38** remained, but the predominant complex exhibited no coupling ($\delta_P$ = 41.6) and appears to be a result of the decomposition of the phosphaalkenyl unit.

After the addition of acetonitrile to **38**, $^{31}P\{^{1}H\}$ NMR data showed initially a mixture of **38** and a new complex, ($\delta_P$ = 137.4, (t, *J* = 27 Hz), 24.4 (overlapping dd)). Refluxing the solution in toluene resulted in the conversion of all remaining **38** to this new complex, and to a number of side products. However, the major product could not be separated and the spectroscopic data do not allow the species to be identified, although the triplet resonance in the phosphorus NMR spectrum is at too low a frequency to be consistent with $[RuCl(CO)(PPh_3)_2(N{\equiv}CMe)(P{=}C(H)SiMe_3)]$.

### 4.6.3 Reactivity of ruthenium complexes with CO

The reaction of $[RuHCl(CO)(PPh_3)_3]$ (**58**) with carbon monoxide is known to result in the removal of $PPh_3$ and the addition of CO to produce $[RuHCl(CO)_2(PPh_3)_2]$[329] (in $CD_2Cl_2$; $\delta_P$ = 45.2).[330] Therefore the addition of CO to **38** might result in either the replacement of $PPh_3$ with CO, or the addition of CO to the ruthenium atom to afford a *hexa*-coordinate ruthenium phosphaalkenyl complex, as shown by the addition of CO to **34** to form $[RuCl(CO)(P{=}CH^{t}Bu)(PPh_3)_2]$ (**Scheme 4.3, Section 4.1.2**).[239] Bubbling CO through a $CD_2Cl_2$ solution of **38** in a Youngs NMR tube resulted in decolourisation of the solution. Phosphorus NMR spectra indicated predominately a single phosphorus signal ($\delta_P$ = 39.4), while $^{1}$H NMR spectroscopy showed the presence of a hydride ($\delta_H$ = −4.49), with coupling to two phosphorus atoms (J = 19 Hz), this might be explained by an impurity found in the synthesis of **58**. Over

four days, a minor species became apparent in the $^{31}P\{^{1}H\}$ NMR spectra ($\delta_P$ = 112.1 (t, *J* = 24 Hz), 25.4 (d, *J* = 24 Hz), 23.7 (d, *J* = 24 Hz)). This new species is unlikely to be $[RuCl(CO)_2(P{=}CHSiMe_3)(PPh_3)_2]$, as this would mean a much more dramatic shift to lower frequency for the phosphaalkenic phosphorus ($\delta_P$ = 450.4 **34** *vs*. 365.5 ppm after addition of CO) than Hill reported.[239]

With **39** or **59** instead, the addition of CO resulted in three major signals in the $^{31}P\{^{1}H\}$ NMR spectra, these were all singlets ($\delta_P$ = 39.4, 27.1, 17.2), the signal at 39.4 ppm is the same as for **38**, and proton NMR spectroscopic data showed the same hydride ($\delta_H$ = −4.49). The similarities between these systems suggest that the singlet resonances are a result of decomposition of the phosphaalkenic unit.

The methodology was tested with the addition of CO to **85**, while the resulting proton NMR spectrum matches that reported for $[Ru(CH{=}CH(SiMe_3))Cl(CO)_2(PPh_3)_2]$,[331] the resulting $^{31}P\{^{1}H\}$ NMR signal was found to shift to lower frequency compared to the starting material ($\delta_P$ = 21.9, *cf*. 30.7; **85**), although Roper and co-workers did not report any phosphorus data themselves.[331]

The similar systems $[RuCl(CO)(RC{=}CHR')(PPh_3)_2]$ (R = R' = Me, Ph or R = Ph, R' = Me), exhibit different reactivity with CO gas (**Scheme 4.14**). In these systems, the adidtion of CO leads to a the insertion or migration of CO between the ruthenium and alkenic moiety and this $\eta^2$-acyl complex reacts further in MeOH to form a $\eta^2$-alkenecarboxylate ligand, confirmed by diffraction studies reported by Torres *et al.*[332] This reactivity was rationalised as consisting of a nucleophilic attack of the methanol on the acylic carbon.[332] It is possible that similar reactivity occurs with **38** and CO, as it might explain the dramatic shift to lower frequency in the observed $^{31}P\{^{1}H\}$ NMR spectrum, although the data is inconclusive. No reaction occurs upon the attempted carbonylation of **41** or $[Ru(CO)\{\kappa^3\text{-}N,C,P\text{-}P(Pz^*)CH(SiMe_2Ph)\}(PPh_3)_2]$, and $^{31}P\{^{1}H\}$ NMR data just indicate starting material.

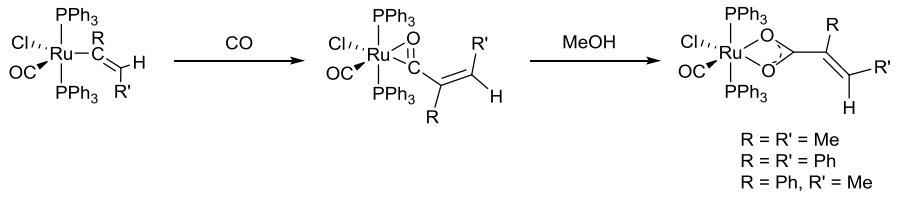


**Scheme 4.14**: Alternate reactivity of $[RuCl(CO)(RC{=}CHR')(PPh_3)_2]$ with CO.[332]

### 4.6.4 Attempted cycloaddition reactions with 38

Cycloadditions of phosphaalkenes are widely established (See **Section 1.2.3.3.2**). Therefore a variety of reagents were added to **38** in order to test the reactivity of the phosphaalkenyl moiety. The addition of refluxing cyclohexene to **38**, did not result in any reaction with the phosphaalkenyl unit, neither did the addition of cyclopentadiene to **38** and **41**.

Toluene solutions of complexes **38** and **41** were heated to 60 ˚C, separately with both furan and maleic anhydride in order to test if the P=C unit would be reactive. Spectroscopic data of the crude solutions indicated no reaction occurred with either mixture of **38**, or of **41** with furan, and the partial degradation of **41** with maleic anhydride.

### 4.6.5 Addition of boranes to 38

The addition of boranes to ruthenaphosphaalkenyls could result in the hydroboration of the C=P bond. When **38** was combined with half an equivalent of 9-BBN dimer in either refluxing $CH_2Cl_2$ for three hours, or at ambient temperature and stirred for three days, no phosphaalkenyl resonance was detectable in the $^{31}P\{^1H\}$ NMR spectrum. However, boron NMR data revealed only unreacted 9-BBN and traces of 9-BBN-OH. When the same reaction was completed in toluene and heated to reflux for three hours, the $^{31}P\{^1H\}$ NMR spectrum showed some remaining **38** and an additional triplet signal was observed at 113.4 ppm, however, no other phosphorus signal was noted with corresponding coupling values and integration within the spectral window ($\delta_P$ = −40−600 ppm).

When HBcat and **38** were heated to reflux in toluene, the phosphaalkenyl complex decomposed and only $PPh_3$ was detected in the $^{31}P\{^1H\}$ NMR data. In contrast stirring in toluene at ambient temperature for three days, there were multiple products indicated by the $^{31}P\{^1H\}$ NMR data. The first of these consists of a triplet ($\delta_P$ = 244.8), showing coupling to a doublet ($\delta_P$ = 16.0) with integration of 2, the other signal in the $^{31}P\{^1H\}$ NMR consists of two complex multiplets at 228.7 and 32.5 ppm, of equal integration. However, $^{11}B\{^1H\}$ and $^{11}B$ NMR spectra show only the presence of HBcat, with no further coupling to indicate interaction with phosphorus. The identities of these products remain unknown.

Triethylborane was also added to **38** and **39**. In the case of **38**, phosphorus NMR spectra showed residual **38** and a similar complex to that observed from HBcat addition, *i.e.* a triplet at 290.1 ppm, with an associated coupling to a doublet at 18.5 ppm, and a boron NMR resonance at 55.4 ppm, again, the identity of the product remains unclear. The phosphorus signals are

similar to those for the unidentified $\eta^1$-phosphaalkenes seen in **79**, and from the reaction of **59** or **61** with $LiPz^{Ph}$ as discussed in **Section 4.4.2** in addition to the combination of $Me_3SiC{\equiv}P$ (**36**) and $[RuHCl(CO)(PPh_3)_2(PMe_3)]$ (**80**) (**Section 4.4.3.1**), perhaps suggesting a similar species. The borane $BH_3$·thf did not react with **38** under similar conditions.

## 4.7 Addition of acids to ruthenaphosphaalkenyls

### 4.7.1 Formation of novel alkylchlorohydrophosphane complexes

It has been shown that MeI adds comparably across the Ru-P bond of either **34** or **38**,[143,290] and the hydrochlorination of **34** has been briefly reported to form $[Ru(\eta^1\text{-}PH{=}CH^tBu)Cl_2(CO)(PPh_3)_2]$.[294] The addition of HCl to **38**, **39**, **59**-**61** was therefore anticipated to result in analogous complexes.

Following the literature precedent, one equivalent of HCl (1 M in diethyl ether) was added to a stirring solution of phosphaalkenyl **38** in $CH_2Cl_2$. Immediately the orange/red solution formed a very pale yellow solution. The solution is typically stirred for 30 minutes, however, the same product can be isolated immediately after the addition of the acid. After removal of the solvents, spectroscopic data of the resulting solid indicated retention of **38** in a 1:1 mixture with a new ruthenium complex (**88**). Using two or more equivalents of HCl results in the exclusive formation of **88**, while sub-stoichiometric amounts result in statistical mixtures with **38**.

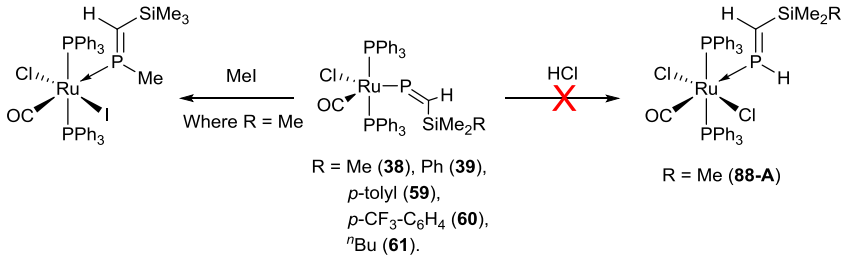


**Scheme 4.15**: Expected reactivity of **38**, **39**, **59**-**61** with HCl.

Using an excess of HCl led to the complete conversion of **39**, **59**-**61** to analogous ruthenium complexes **89**-**92**. The resulting $^{31}P\{^1H\}$ spectroscopic data are distinctive and based upon an ABB' spin system, from the phosphaacarbon and the now inequivalent $PPh_3$ moieties (**Figure 4.15**). All phosphorus signals are noticeably shielded compared to the parent

ruthenaphosphaalkenyls ($\delta_P$ = 545.3 − 559.7). The phosphacarbon unit specifically experiences a significant shift to lower frequency ($\Delta\delta_P$ ~ −460), which is also far greater than typically observed for other electrophilic addition products ($\Delta\delta_P$ ~ −122 − 126)[143] and is more consistent with a saturated phosphane unit. The presence of a P-H unit was confirmed in each case by $^{31}P$-$^{1}H$ coupling in the $^{31}P$ and $^{1}H$ NMR spectra (**Figure 4.15**). Heteronuclear correlation experiments confirmed the retention of the silyl groups and demonstrated the *α*-carbon had become saturated "$CH_2SiMe_2R$" the $CH_2$ protons of which show $^{2}J_{P\text{-}H}$ coupling to phosphorus.

**Table 4.12**: NMR Spectroscopic data for compounds **88**-**92**.

| | **88** | **89** | **90** | **91** | **92** |
|---|---|---|---|---|---|
| **$P_{(P\text{-}C)}$** | 84.2 | 81.5 | 82.5 | 83.3 | 79.86 |
| **$P_{(PPh3)}$** | 26.5 (27, 343 Hz) | 27.0 (27, 344 Hz) | 26.9 (28, 342 Hz) | 26.8 (28, 343 Hz) | 27.3 (28, 342 Hz) |
| **$P_{(PPh3)}$** | 22.7 (24, 343 Hz) | 22.6 (23, 344 Hz) | 22.8 (244, 343 Hz) | 22.7 (23, 343 Hz) | 22.6 (23, 343 Hz) |
| **P<u>H</u>** | 5.27 (11, 425 Hz) | 5.28 (11, 428 Hz) | 5.30 (11, 426 Hz) | 5.24 (10, 426 Hz) | 5.21 (11, 428 Hz) |
| **P<u>CH</u>$_2$** | 1.40 (15 Hz) | 1.70 (15 Hz) | 1.70 (15 Hz) | 1.42 (15 Hz) | 1.74 (15 Hz) |
| **$^{29}$Si** | 3.07 | -2.7 | -2.8 | 4.1 | -1.9 |
| **P<u>C</u>H$_2$** | 16.9 (21 Hz) | 16.8 (21 Hz) | 17.0 (21 Hz) | 16.3 (21 Hz) | 16.5 (21 Hz) |
| ***$\nu_{(CO)}$*** | 1970 | 1968 | 1969 | 1970 | 1968 |

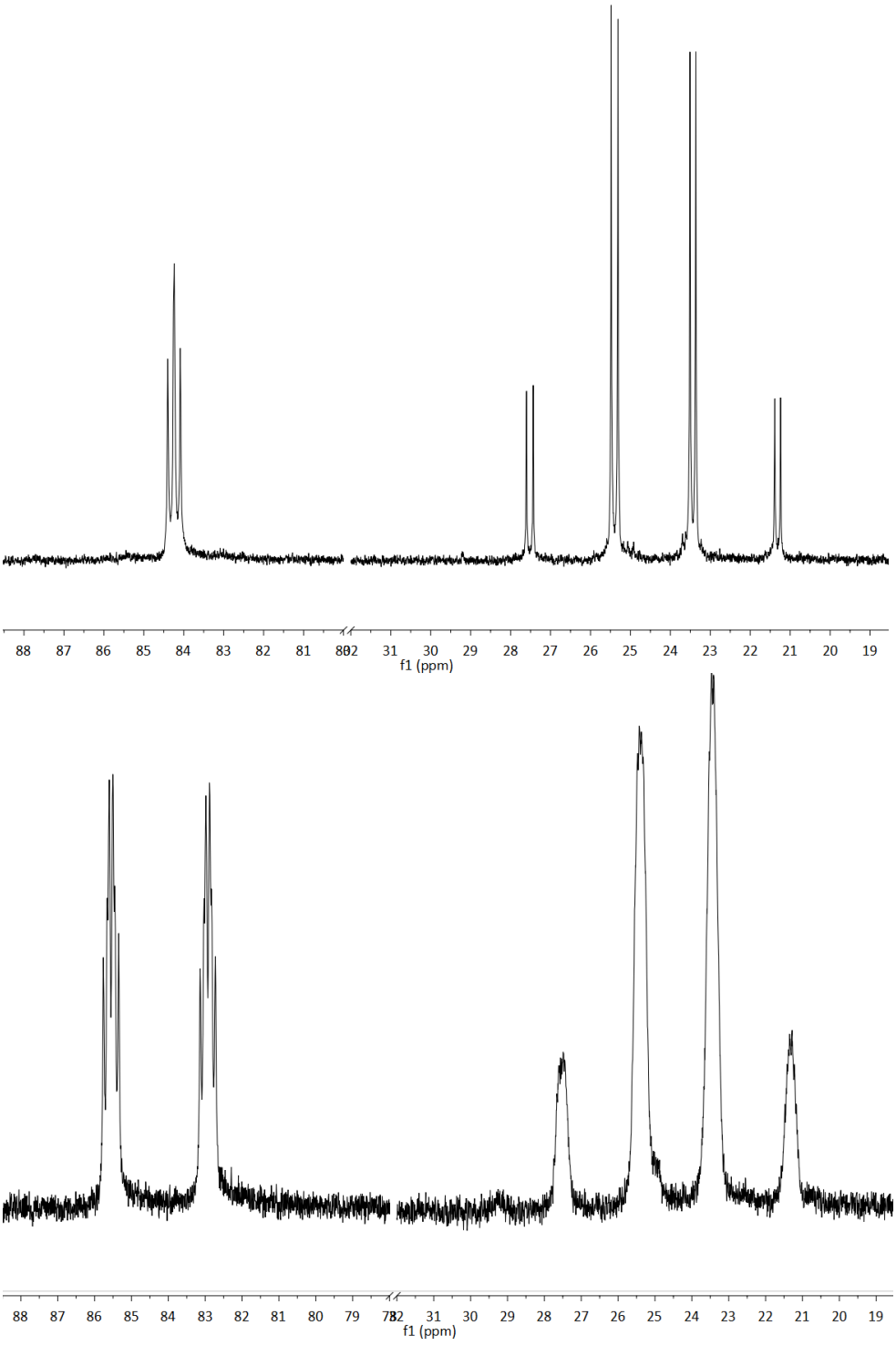


**Figure 4.15**: $^{31}$P NMR spectra of **88**, decoupled spectra (*above*), proton-coupled spectra (*below*).

Infrared data in each case confirm the retention of the ruthenium(II) centre ($\nu_{CO}$ ~ 1970 $cm^{-1}$), supporting the addition of a chloride ligand to the metal. The spectroscopic data are consistent with the addition of two equivalents of HCl leading to the formation of $[Ru(P(H)ClCH_2SiMe_2R)Cl_2(CO)(PPh_3)_2]$ (R = Me (**88**), Ph (**89**), *p*-tolyl (**90**), *p*-$CF_3$-$C_6F_4$ (**91**), $^n$Bu (**92**). Elemental analysis confirms the bulk composition in each case, and the structure was ultimately confirmed by a single crystal X-ray diffraction study of **88** (**Figure 4.16**).

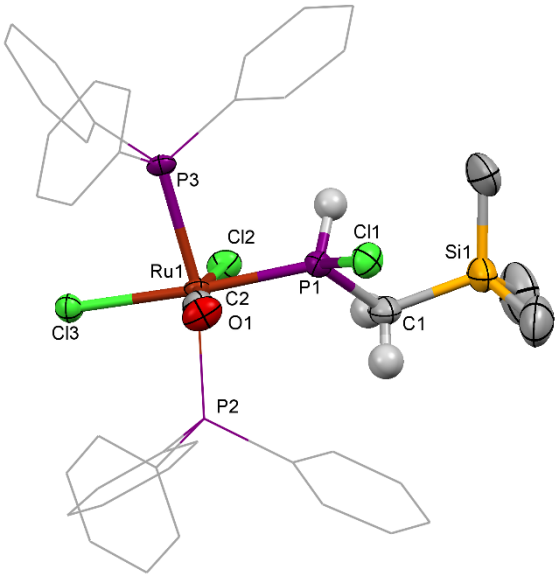


**Figure 4.16**: Molecular structure of $[Ru(P(H)ClCH_2SiMe_3)Cl_2(CO)(PPh_3)_2]$ (**88**), with thermal ellipsoids at the 50% probability level and hydrogen atoms omitted for clarity (except on P-C unit).

The structures of **88**-**92** were found to include a fully saturated P-C unit, caused by the addition of two equivalents of HCl, one across the ruthenium-phosphorus bond as expected, and the second addition across the phosphorus-carbon bond. Solid state data of $[Ru(P(H)ClCH_2SiMe_3)Cl_2(CO)(PPh_3)_2]$ (**88**) show a distorted octahedral geometry around ruthenium and non-linear *trans*-Cl-Ru-CO (168.0(3) °) and $Ph_3P$-Ru-$PPh_3$ (166.50(7) °) angles (**Table 4.13**), these are attributed to the steric bulk of the phosphaacarbon unit. The phosphaacarbon moiety is significantly displaced from the equatorial plane (ϕ = 56.3(4) °), which contrasts the situation for the phosphaacarbon moiety in the superficially similar fragment "$P(H)FCH_2$" from $[Ru(P(H)FCH_2{}^tBu)Cl(CNXyl)(CO)(PPh_3)_2]$ (**93**) (xyl = 2,6 dimethylphenyl) (**Figure 4.17**) which lies along the plane.[292]

**Table 4.13**: X-ray data of [Ru(P(H)ClCH$_2$SiMe$_3$)Cl$_2$(CO)(PPh$_3$)$_2$] (**88**)

| Bond | (Å) | Angle | (˚) |
|---|---|---|---|
| **Ru-P$_{(P-C)}$** | 2.281(2) | **Ph$_3$P-Ru-PPh$_3$** | 166.50(7) |
| **Ru-P$_{(PPh3)}$** | 2.402(2)<br>2.419(2) | **OC-Ru-P(P-C)** | 100.7(3)<br>88.9(3) |
| **P-C** | 1.790(11) | **OC-Ru-Cl** | 168.0(3) |
| **P-Cl** | 2.059(3) | **Cl-Ru-Cl** | 91.33(6) |
| **C-Si** | 1.914(10) | **Ru-P-Cl** | 115.67(10) |
| **Ru-CO** | 1.850(9) | **Ru-P-C** | 125.2(3) |
| **Ru-Cl** | 2.469(2)<br>2.447(2) | **P-C-Si** | 118.0(6) |

The phosphaacarbon fragments themselves, however, are similar, both exhibiting short Ru-P (2.281(2) Å **88**; 2.352(2) Å **93**) and P-C (1.790(11) Å **88**; 1.794(6) Å **93**) bonds. The saturation of the P-C linkage has also resulted in the widening of associated bond angles (Ru-P-C (125.2(3) **88**; 120.1(2) Å **93**) Å) and P-C-Si or P-C-C components (118.0(6) Å **88**; 121.1(5) Å **93**).

Hill and co-workers describe the P(H)FCH$_2$ phosphorus atom in **93** to have a chiral tetrahedral structure, with the Ru-P distance (2.352(2) Å) suggesting an increased π-acidity of the P-C unit, relative to the triphenylphosphine moieties, despite it being coordinated *trans* to a π-acidic ligand.[292] In the same manner, the increased π-acidity in the 'P(H)ClCH$_2$' systems account for the reduced electron density at the metal, implied by the observed increase in $\nu_{CO}$ values ($\nu_{CO}$ = 1968 - 1970 cm$^{-1}$) in comparison to the parent ruthenaphosphaalkenyls **38**, **39**, **59**-**61** ($\nu_{CO}$ = 1920-1939 cm$^{-1}$).

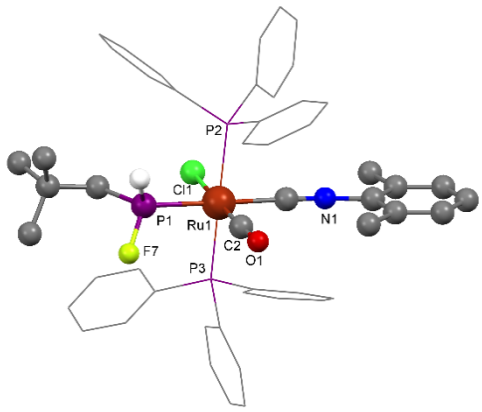


**Figure 4.17**: Hill's structure of [RuCl(P(H)FCH$_2$$^t$Bu)(CNXyl)(CO)(PPh$_3$)$_2$].[292]

The conformational arrangement of the phosphaacarbon moiety with respect to the plane is also apparently retained in solution, indicated by the magnetic inequivalence of the $PPh_3$ ligands in **88**-**92**. This inequivalence might have been explained by the chirality of the PHClR' unit - the equivalent NMR spectra of **93** do not show this second order effect, which could be explained by a more rapid rotation of the 'PHFCH$_2$$^t$Bu' fragment. However, $^{31}$P-$^1$H HMBC spectra of **88**-**93** show a spin-spin interaction between the 'PH' and one of the $PPh_3$ phosphorus atoms, and a much lower magnitude interaction with the other $PPh_3$ ligand, indicating some geometric constraint. This coupling likely results from a $^3J_{P\text{-}P}$ bond mediated coupling, the disparity being consistent with a Karplus-like torsion dependence (P-H *vs*. Ru-P vectors). Defined by Karplus originally for vicinal H,H couplings,[333] variants of the Karplus equation and curves have been defined for a range of heteronuclear X,H couplings, including P-Ru-S-H where $\phi$ = 180˚ represents a maximum, and $\phi$ = 90˚ a minimum in coupling magnitude.[334] Considering the structural data for **88** ($\phi$ = −31.5, 152.1), a comparable situation is likely, which alongside the fact that the coupling was able to evolve on the NMR timescale, implies a significantly restricted rotation around the 'Ru-PHClR' moiety. This is consistent with a more tightly bound phosphaacarbon fragment when compared to 'PFCH$_2$$^t$Bu'.

These results contrast the situation reported for the addition of HCl to **34** which results in the single addition of HCl over the Ru-P bond to form **35** ($\delta_P$ = 187.9).[294] This was thus reinvestigated in light of the results from the addition of HCl to the silyl-based phosphaalkenyls. It was found that the addition of a single equivalent of HCl to **34** does indeed afford **35**, however, an excess or two equivalents results in the double addition product [Ru(P(H)ClCH$_2$$^t$Bu)Cl$_2$(CO)(PPh$_3$)$_2$] (**94**) the spectroscopic data of which ($\delta_P$ = 84.1 ($^1J_{P\text{-}H}$ = 430 Hz), 26.3 (dd, $J_{P\text{-}P}$ = 29, 344 Hz), 22.3 (dd, $J_{P\text{-}P}$ = 25, 344 Hz) are similar to those observed for **38**, **39**, **59**-**61** (**Scheme 4.16**).

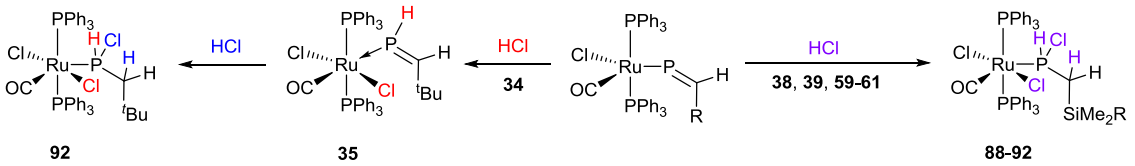


**Scheme 4.17**: Reactivity of ruthenaphosphaalkenyls **34**, **38**, **39**, **59**-**61** with HCl.

The formation of **88**-**92** could be considered broadly similar to the formation of **93** from the saturated ruthenium system, [Ru(P=CH$^t$Bu)Cl(CO)(CNXyl)(PPh$_3$)$_2$] by sequential addition of $HBF_4$ and K[$HF_2$] (**Scheme 4.3**). The addition of excess HCl to the *penta*-coordinate system **34** is

unique in that it first seems to form the mono-addition product, which is detectable by NMR spectroscopy, before additional equivalents of HCl drive the formation of the saturated P-C bond. However, in the case of the silyl systems (**88**-**92**) the mono-addition product is never observed, instead the reaction appears to follow a 'cascading' pathway to form the double-addition product only.

DFT calculations have been used to compare the relative energies associated with the optimised geometries of the mono-addition products of **38** and **34** and the double addition product **88** and **94** (**Figure 4.18** and **Figure 4.19**).

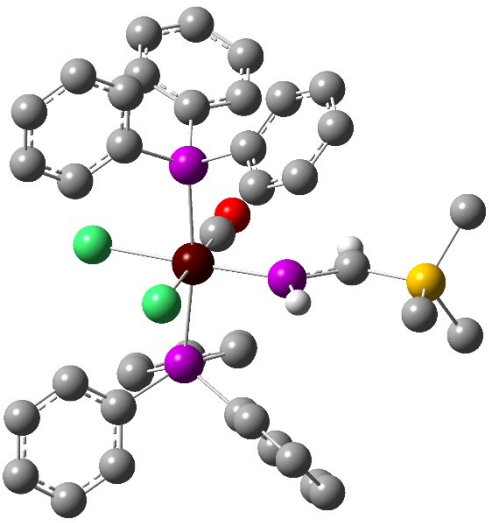

**88-A**

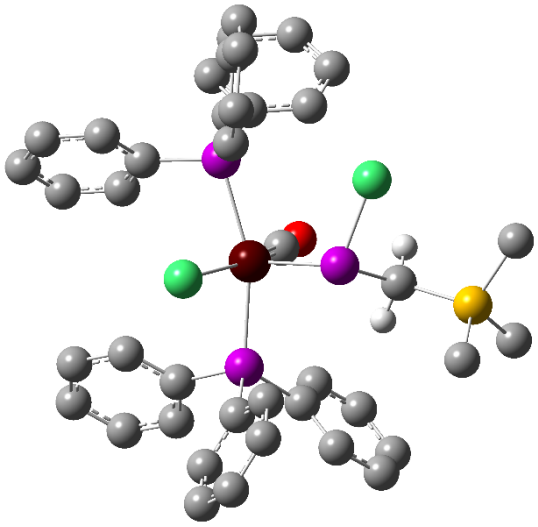

**88-B**

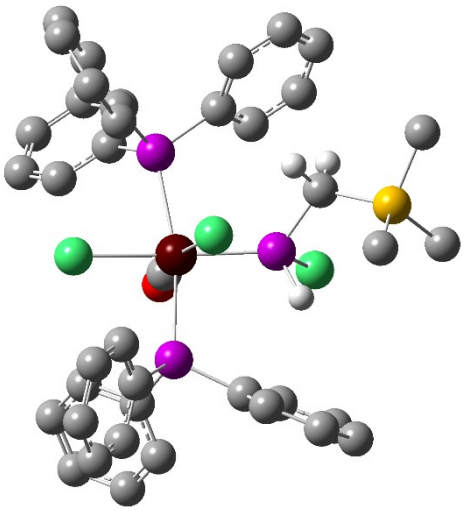

**88**

**Figure 4.18**: DFT geometries representing the addition of HCl over the Ru-P (**88-A**) and the P-C bond (**88-B**) of **38** and the double addition product **88**.

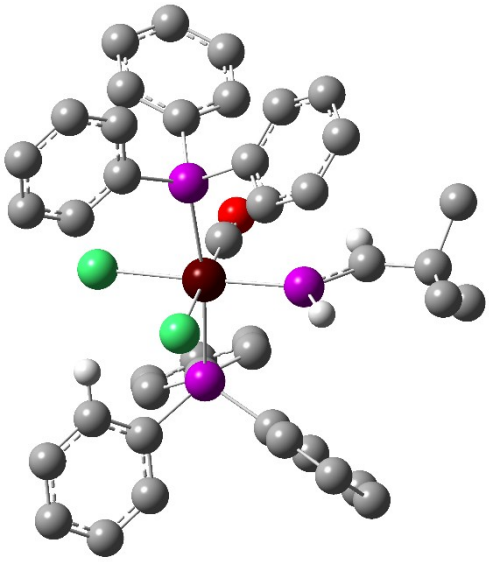

**35**

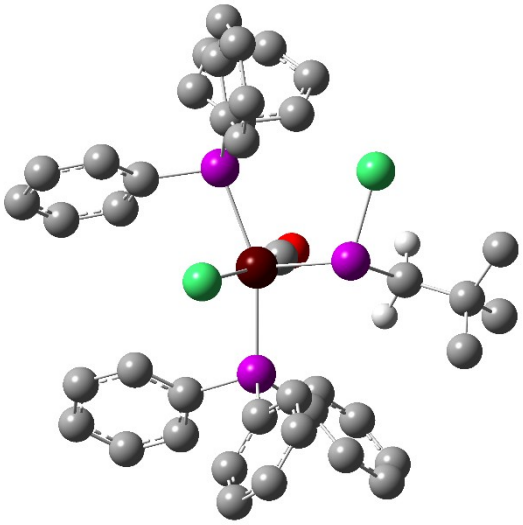

**94-B**

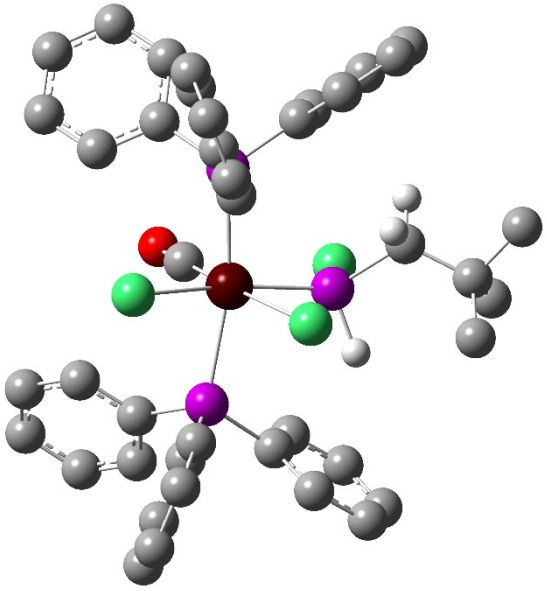

**94**

**Figure 4.19**: DFT geometries representing the addition of HCl over the Ru-P (**35**) and the P-C bond (**94-B**) of **34** and the double addition product **94**.

**Table 4.14**: Energies of sequential HCl additions starting from **38** or **34**.
(Energies calculated relative to **88** and **94**, respectively)

| Complex | Energy (kcal/mol) | | Complex | Energy (kcal/mol) | |
|---|---|---|---|---|---|
| | B3LYP | MP2 | | B3LYP | MP2 |
| **38** | -2793113.125 | -2787031.446 | **34** | -2635340.12 | -2629506.356 |
| **88-A** | -2793127.928 | -2787033.926 | **35** | -2635355.120 | -2629508.520 |
| **88-B** | -2793138.345 | -2787041.327 | **94-B** | -2635365.973 | -2629516.889 |
| **88** | -2793528.496 | -2787053.060 | **94** | -2635386.989 | -2629529.901 |

Optimised at B3LYP - 6-31G**/Lanl2dz, with additional single point energy calculations run at MP2.

The calculated energies for the HCl-addition products of **34** and **38** are displayed in **Table 4.14** in kcal/mol. For these data to be comparative, each calculation must have the same number of atoms, hence the calculated values for the parent phosphaalkenyls (**34** and **38**) have been combined with the value for two molecules of HCl, and the energies of mono-addition products (**88-A**, **88-B**, **35** and **94B**) have been combined with the calculated energy of one molecule of HCl under the same computational theory levels.

The energies suggest that the first addition of HCl (either over the P-C or the Ru-P bond) is relatively facile. Complexes **88-A** and **35** represent the addition of the Ru-P bond, and are lower in energy than the parent phosphaaalkenyls **34** and **38** ($\Delta_{kcal/mol(MP2)}$ ~ −2.48 **3**→**88-A**; −2.16 **34**→**35**). An initial addition of HCl across the P-C bond (as in **88-B**, **94-B**) is also lower in energy than the parent phosphaalkenyls ($\Delta_{kcal/mol(MP2)}$ ~ −9.88 **38**→**88-B**; −10.53 **34**→**94-B**).

The first addition occurring over the Ru-P bond, as other electrophiles, is also more stable than the parent phosphaalkenyls **34** and **38**. However, the fact that the silyl systems spontaneously add the second equivalent of HCl, may imply a more favourable kinetic pathway, given that the thermodynamics of the products are comparable to the $^{t}$Bu system complex, **34**.[294]

After the second addition, the resulting complexes (**88** and **94**) are more stable than their precursors ($\Delta_{kcal/mol(MP2)}$ ~ −21.61 **38**→**88**; −23.54 **34**→**94**). However, the calculations do not reveal why the second addition is more facile in the case of the silyl system, relative to the $^{t}$Bu system, and more detailed calculations are required. In addition the difference between the calculated energies from both models (B3LYP and MP2) demonstrate the importance of the basis set in these calculations, and suggest the need for further, more detailed investigation before any conclusions can be drawn.

## 4.8 Summary of synthesis and reactivity of metallaphosphaalkenyl

A wide range of silanes of the type $RMe_2SiCH_2Cl$ (**42**-**49**) have been synthesised, and the addition of a $PCl_2$ unit to form $RMe_2SiCH_2PCl_2$ (**50**-**54**) was met with success in some cases. A series of new phosphaalkynes of the type $P{\equiv}CSiMe_2R$ (**55**-**57**) were furnished from the double dehydrohalogenation of **52**-**54**. These were inserted into the Ru-H bond of $[RuHCl(CO)(PPh_3)_3]$ (**58**) to afford novel ruthenaphosphaalkenyl complexes **59**-**61**. The first examples of solid state data have been obtained for the ruthenaphosphaalkenyl complexes **38**, **39** and **59**, alongside DFT studies of **59**-**61**. The computational data show the HOMO in each case is associated with the ruthenium centre and phosphorus lone pair, while the LUMOs are predominately metal-based and accessible to nucleophiles. This combined with NBO data indicates a partial $\delta^+$ character for the phosphaalkenic phosphorus - this can be used to explain the ambiphilic reactivity observed for the complexes.

The reactivity of these ruthenaphosphaalkenyl complexes with electrophiles is well established in the literature, the addition of nucleophiles has been expanded with the reaction of **59**-**61** with LiPz*, $LiPz^{CF3}$ and $LiPz^{Me,CF3}$ to form $[Ru(CO)\{\kappa^3\text{-}N,C,P\text{-}P(Pz')CHSiMe_2R\}(PPh_3)_2]$ (**62**-**66**, **68**-**73**). In the case of $LiPz^{Ph}$, however, additional reactivity was observed providing preliminary indicators in respect of the mechanism of the formation of these bridging pyrazolyl $\eta^2$–phosphaalkenic complexes.

Finally, the addition of various electrophiles (N-based donors, phosphines, boranes and CO) to **38** was investigated, alongside the reactivity of the P=C unit in cycloaddition reactions. The addition of HCl to **38**, **39**, **59**-**61** to form **88**-**92** was found to be much different than expected. The presence of the silicon in these systems in comparison to **35**/**94** was found to change the reactivity from a simple addition across the Ru-P bond, to the saturation of the P-C bond with two equivalents of HCl. DFT studies were used to investigate the reasons behind the difference in reactivity, however, no conclusions can be drawn from the available data.

# 5. Experimental

## 5.1 General Experimental Methods

Unless otherwise stated, all manipulations were conducted under an atmosphere of dry argon using Schlenk line techniques, or under an atmosphere of dry dinitrogen in an MBraun glove box (< 1 ppm $H_2O$ and < 10 ppm $O_2$). Argon and dinitrogen gases were supplied by BOC Gases UK. Glassware was stored at 140 °C and repeatedly evacuated and purged with argon prior to use. Celite® 545 filter aid was stored at 200 °C, and filter cannulas equipped with Whatman® 25 mm glass microfibre filters were also stored at 140 °C prior to use. Solvents were dried for a minimum of 72 hours before use by refluxing over the appropriate drying agents; *i.e.* sodium-potassium alloy (pentane, hexane, diethyl ether), potassium (THF, toluene) or CaH (DCM). Dried solvents were stored over potassium mirrors except in the case of THF, $Et_2O$ and DCM which were stored over 4 Å molecular sieves. All were degassed prior to use. Deuterated solvents were obtained from GOSS Scientific Ltd and were degassed by freeze-pump-thaw and dried over potassium ($d_6$-benzene, $d_8$-toluene), or calcium hydride ($d_2$-dichloromethane, $d_1$-chloroform). The solvents were vacuum transferred into ampoules and stored under nitrogen. All NMR analyses were undertaken using a Varian VNMRS 500 or VNMRS 400 Spectrometer at the following frequencies; $^{13}$C NMR (125.72 or 100.46 MHz), $^{1}$H NMR (499.91 or 399.50 MHz), $^{11}$B (128.17 MHz), $^{19}$F NMR (375.86 MHz), $^{29}$Si NMR (79.37 MHz), $^{31}$P (161.73 MHz) and $^{6}$Li NMR (58.79 MHz). Carbon-13, boron-11 and phosphorus-31 spectra were run proton decoupled unless otherwise stated and chemical shifts are reported in parts per million (δ). Spectra were obtained from samples at 303 K unless otherwise stated. Proton and carbon shifts were internally referenced to residual solvent resonances set using external $SiMe_4$. Phosphorus shifts were externally referenced to 85% $H_3PO_4$, boron spectra were externally referenced to $BF_3{\cdot}Et_2O$, lithium shifts were externally referenced to LiCl and fluorine spectra were externally referenced to $CFCl_3$.

Mass spectra were recorded by Dr. A. Abdul-Sada using a VG Autospec Fisons instrument (electron ionisation at 70 eV) or a KratosMS25 mass spectrometer. Single crystal X-ray diffraction experiments were performed using an Agilent Excalibur with CCD plate detector using Cu-Kα (λ = 1.514184 Å) or Mo- Kα (λ = 0.71 Å), and solved using SHELXS,[335] SHELXL[335] or SHELXT[335] running under Olex2.[336] Elemental Analyses were obtained by Mr S. Boyer, London Metropolitan Analytical Service.

The alkynes $^{i}Pr_3SiC{\equiv}CCH_2Cl$ (**13**) and $^{n}Bu_3SiC{\equiv}CCH_2Cl$ (**15**) was kindly donated by Amy Saunders,[193] and the sample of $[Ru(CO)\{\kappa^3\text{-N,C,P-P}(Pz^{tBu})CH(SiMe_3)\}(PPh_3)_2]$ (**67**) which was crystallised, was prepared by Nicola Trathen.[190]

The following chemicals were purchased from Sigma–Aldrich, Fisher Scientific or Fluorochem Chemicals: $^{n}$BuLi (in hexanes 2.5 M), $RuCl_3{\cdot}H_2O$, $PPh_3$, HPz, HPz*, $HPz^{(CF3)}$, $HPz^{(Me,CF3)}$, $HPz^{(CF3)2}$, $HPz^{Ph}$ AgOTf, $Ph_2PCH_2CH{=}CH_2$, $Ph_2PCH{=}CH_2$, $Fu_2PCl$, $BrMgCH{=}CH_2$ (in thf, 1 M), $Bu_3B$, $Ph_3B$, $Et_3B$, $^{i}Pr_2PCl$, $^{t}Bu_2PCl$, $(C_6F_5)_3B$, propargyl chloride, $^{n}Pr_3SiCl$, $Me_2PhSiCl$, $HPPh_2$, $[Rh(CO)_2Cl]_2$, $^{t}$Bu(Ph)PCl, $C_6F_5Br$, *p*-$CF_3$-$C_6H_4Br$, 2,5-$CF_3$-$C_6H_3Br$, $Me_3SiCH_2Cl$, $PMe_3$ and HCl (in diethyl ether, 1 M) were used as supplied. DABCO and 9-BBN were purified by sublimation before use. $Ph_2PCl$, $^{i}Pr_2PCl$, PhC≡CH, HC≡CSiMe$_3$, HC≡C$^{t}$Bu, $ClMe_2SiCH_2Cl$ and $PCl_3$ were distilled before use.

The Grignard reagents $^{i}$PrMgBr, *p*-tolylMgBr and MesMgBr (all in thf) were available in the lab, and titrated before use. The compounds; $[PtCl_2]$, $[PdCl_2]$, $[Rh(C_8H_{12})Cl]_2$[337] and $[Cp^*IrCl_2]_2$[338] were available in the lab. The following compounds were synthesised following literature procedures: $[RuHCl(CO)(PPh_3)_3]$,[339,340] $[Rh(CO)(Cl)]_2$,[278] $Me_3SiCH_2PCl_2$,[138] $PhMe_2SiCH_2PCl_2$.[138] Magnesium was activated by heating magnesium turnings under vacuum, and stirring under argon for 24−36 hours.

#### 5.1.1 Computational Details

All DFT calculations were performed using Gaussian 09W,[341] and visualised using GaussView 5.0. Geometry optimisation and frequency calculations were performed in the absence of any solvent, and using the B3LYP hybrid functional, with the LANL2DZ effective core potential basis set for ruthenium, while all other atoms used the basis set 6-311G** or 6-31G**, for chapters 2 and 4, respectively. Energy minima were confirmed by the absence of any imaginary frequencies, and frequencies adjusted using standard scaling factors.[320] NBO calculations were performed at the same level of theory as the optimised structures.[342] NMR shielding tensors were calculated at the same level of theory as the optimised structures and were performed with the B3LYP and the PBE functional using the GIAO method, and compared against those similarly calculated for the respective reference standards to derive chemical shifts. Bader's Atoms in Molecules[255,343] method was used to determine critical points using Multiwfn[344] which reads as input, the '.wfn' file generated by Gaussian 09.

**5.1.2 Selection of model and basis set**

Density Functional Theory (DFT) is a powerful approach to compute the electronic structure of molecules. It can be used to predict a range of properties including, molecular geometries, molecular energies, electron density and IR/NMR spectral data. DFT calculations are dependent on both the method and the basis set used, with intrinsic assumptions present in each case. These options are balanced against the increased accuracy of the calculations and the additional computational cost.

The basis sets in Gaussian calculations are a way of describing the shape of the atomic orbitals. The more Gaussian functions representing each electronic orbital in the system increases accuracy, but also increases the calculation time. Some basis sets can just be added to specific atoms, such as LANL2DZ which is often only added to the metal atom in a system, it contains an 'effective core potential' which freezes the movement of core electrons for all atoms larger than Ne, therefore allowing good accuracy with low computational cost. Sometimes Gaussian functions can be complemented by the addition of diffuse functions (+) and polarisation functions (*) which allow the electron more freedom compared to the otherwise spherical confines of the electronic orbital, this is of particular importance when considering strongly electronegative atoms or where lone pairs are present. The less restrictions placed on the electrons, the more accurate the result, but this also has to be balanced with the size of the molecule, as molecules with more atoms, or heavier atoms also have more electrons, this can significantly increase computational cost.

Various methods are available, many of which are suited to particular types of calculation, for example, B3LYP is a hybrid functional which combines the exact Hartree Fock (HF) exchange for non-interacting electrons with the correlation effects from DFT exchange functionals. This extra layer of complexity improves the results obtained from the calculation, while only marginally increasing computational cost, compared to DFT, leading to B3LYP being the most widely used functional, representing 80% of density functionals used in the literature up to 2007.[345]

PBE is another hybrid functional which uses a different mixture of DFT and exchange energies to B3LYP, and has been found to be useful for the calculating of $^{31}$P NMR shielding tensors.[319] MP2 (the second order energy correction for Møller–Plesset theory) is an *ab initio* method, making the method more computationally expensive than modern DFT methods.

However, MP2 is commonly used for more accurate calculation of energies, where DFT can be deficient, though in many cases it suffices provided that absolute energies are not required.

In the cases discussed herein; the functional and basis sets used represent the balance between accuracy and computational cost to provide a comparison between similar systems and a starting point for further investigation. The methods and basis set most commonly used (B3LYP and LANL2DZ/6-31G**) has been previously found to be a well balanced selection for the systems of the type being studied. For NMR calculations, the PBE method was used specifically to enable more accurate calculations of the $^{31}$P shielding tensors.

The addition of polarisation and diffuse functions into the basis sets will affect the calculated energies of molecules, especially those featuring a lone pair, such as on phosphorus. Therefore single point energy calculations on already optimised geometries with a more *ab initio* approach, allowed the calculation of more accurate energies to allow comparison between compounds.

## 5.2 Experimental details for Chapter 2

### 5.2.1 Synthesis of phosphine-boranes (1-3)

**Synthesis of $Bu_2BC(Bu)=C(Ph)PPh_2$ (1)**

$^{n}$BuLi ($7.2x10^{-3}$ mol, 2.5 M in hexanes) was added dropwise to a cold (−78 °C) solution of phenylacetylene (0.73 g, $7.19x10^{-3}$ mol) in $Et_2O$ (6 $cm^3$). The resulting colourless mixture was allowed to stir for 1 h. at −78 °C before an ethereal solution of tributylborane ($7.2x10^{-3}$ $cm^3$, 1 M solution in $Et_2O$) was added dropwise. The stirring reaction mixture was allowed to warm slowly to ambient temperature over 1.5 h. before the dropwise addition of chlorodiphenylphosphine (1.58 g, $7.2x10^{-3}$ mol) as a solution in $Et_2O$ (1.5 $cm^3$), the resulting suspension was heated to reflux for 3 h. After the reaction was complete the reaction mixture was left to cool, then the filterate filtered from LiCl and concentrated under reduced pressure. Storage at −80 °C in $Et_2O$ for 48 h. resulted in precipitation of a white solid, which was isolated by filtration and washed with cold pentane (−78 °C) before drying *in vacuo* to afford a pale yellow micro-crystalline powder. Yield: 1.02 g, 30.2 %.

$^1$H NMR ($CDCl_3$): $\delta_H$ 0.73 (t, $J$ = 6.65 Hz, 6 H, $B(CH_2)_3C\mathbf{H}_3$), 0.82 (m, 4 H, $BC\mathbf{H}_2$), 0.89 (t, $J$ = 7.71 Hz), 3 H, $(CH_2)_3C\mathbf{H}_3$), 1.16 (br., 6 H, $C\mathbf{H}_2$), 1.33 (m, 2 H, $(CH_2)_2C\mathbf{H}_2CH_3$), 1.52 (m, 4 H, $B(CH_2)_2C\mathbf{H}_2$), 2.5 (m, 2 H, $CC\mathbf{H}_2$), 7.13-7.26 (m, 5 H, Ar-C**H**), 7.34-7.49 (m, 10 H, PAr-C**H**) ppm. $^{13}C\{^1H\}$ NMR ($CDCl_3$): $\delta_C$ 14.1 (s, $\mathbf{C}H_3$), 14.2 (s, $B(CH_2)_3\mathbf{C}H_3$), 23.5 (br., $(CH_2)_2\mathbf{C}H_2$), 26.6 (s, $B(CH_2)\mathbf{C}H_2$), 30.4 (d, $J_{C\text{-}P}$ = 10.6 Hz, $(CH_2)CH_2$), 30.7 (d, $J_{C\text{-}P}$ = 2.1 Hz, $B(CH_2)_2\mathbf{C}H_2$), 34.3 (d, $J_{C\text{-}P}$ = 46.7 Hz, $C{=}C(\mathbf{C}H_2)$), 126.5 (s, $=\mathbf{C}(BR_2)$), 126.8 (s, Ar), 128.4 (s. Ar), 128.6 (d, $J_{C\text{-}P}$ = 3.4 Hz, PPh), 128.6 (d, $J_{C\text{-}P}$ = 8.5 Hz, PPh), 130.1 (d, $J_{C\text{-}P}$ = 2.2 Hz, PPh), 131.6 (d, $J_{P\text{-}C}$ = 17.4 Hz, *i*-C**H**), 132.9 (d, $J_{C\text{-}P}$ = 11.0 Hz, PPh-**C**H), 136.9 (d, $J_{C\text{-}P}$ = 1.89 Hz, Ar), 195.2 (d, $J_{C\text{-}P}$ = 83.0 Hz, PC=) ppm. $^{31}P\{^1H\}$ NMR ($CDCl_3$): $\delta_P$ 10.0 (s, $\mathbf{P}Ph_2$) ppm. $^{11}B\{^1H\}$ NMR ($CDCl_3$): $\delta_B$ 13.9 (s, $\mathbf{B}Bu_2$). M/z: 468 $[M]^+$. Calcd for $C_{32}H_{42}BP$ (468.47): C 82.04, H 9.04. Anal Found: C 81.95, H 9.17.

Crystal data for **1**: $C_{32}H_{42}BP$, $M_w$=468.44, Monoclinic, $P2_1/c$ (no. 14), a = 9.1875(7), b = 29.734(2), c = 10.5528(9) Å, α = 90, β = 94.933(2), γ = 90°. V= 2872.2(4) $A^3$, Z = 4, Dc = 1.083 $Mg/m^3$, μ(Mo-Ka) = 0.113 $mm^{-1}$, T = 173(2) K, 6120 independent reflections. Full-matrix *F2* refinement *R*1 = 0.0588, w*R*2 = 0.1605 on 4371 independent absorption corrected reflections [I2σ(I); 2θmax = 55°], 307 parameters. A colourless square crystal with dimensions 0.8 x 0.6 x 0.2 mm was used.

**Synthesis of $Ph_2BC(Ph)=C(Ph)PPh_2$ (2)**

$^{n}$BuLi ($5.0x10^{-3}$ mol, 2.5 M in hexanes) was added dropwise at −78 °C to a cold solution of phenylacetylene (0.6 g, $5.0x10^{-3}$ mol) in $Et_2O$ (2 $cm^3$). The resulting colourless mixture was left to stir for 1 h. at −78 °C before the addition of an ethereal solution of triphenylborane (1.22 g, $5.03x10^{-3}$ mol) in $Et_2O$ (15 $cm^3$) was added dropwise at −78 °C. Upon addition the solution initially turned yellow, which faded over time with mixing. After the stirring reaction mixture was allowed to warm to ambient temperature over 1.5 h., a solution of chlorodiphenylphosphine (0.82 g, $4.6x10^{-3}$ mol) in $Et_2O$ (2 $cm^3$) was added dropwise, and the resulting suspension was heated to reflux (54 °C) for 3 h. After the reaction was complete, the solution was partially reduced under vacuum, and the solution (5 $cm^3$) filtered off. The remaining solid consisting of LiCl and the product were dissolved in dichloromethane and the solution was left at −80 °C in diethyl ether for 48 h. before the white solid was removed, and the remaining yellow solution dried *in vacuo* to yield a white powder. Yield 0.80 g, 30.3%.

$^{1}$H NMR ($CD_2Cl_2$): $\delta_H$ 7.12 (m, 6 H, Ar-**H**), 7.16-7.28 (m, 16 H, Ar-**H**), 7.33-7.39 (m, 6 H, Ar-**H**), 7.42 (t, $^{2}J_{H-H}$ = 6.76 Hz, 2 H, Ar-**H**).$^{13}$C{$^{1}$H} NMR ($CD_2Cl_2$): $\delta_C$ 126.0 (d, $J_{C-P}$ = 4.0 Hz, PAr), 127.5 (d, $J_{C-P}$ = 2.74 Hz, PAr), 128.0 (s, =C($BR_2$)), 128.1 (s, Ar), 128.3 (s, Ar), 128.5 (s, Ar), 128.5 (s, Ar), 128.6 (d, $J_{C-P}$ = 4.1 Hz, PAr), 128.9 (d, $J_{C-P}$ = 10.0 Hz, PAr), 129.1 (s, Ar), 131.2 (d, $J_{C-P}$ = 3.5 Hz, PAr), 132.6 (s, Ar), 133.0 (s, Ar), 133.5 (d, $J_{C-P}$ = 9.4 Hz, PAr-**C**), 136.2 (d, $J_{C-P}$ = 9.3 Hz, PAr), 136.8 (br. d, $J_{C-P}$ = 2.6 Hz, PAr), 140.0 (d, $J_{C-P}$ = 1.2 Hz, PAr), 140.5 (s), 140.9 (s), 181.3 (br. m, P**C**=) ppm. $^{31}$P{$^{1}$H} NMR ($CD_2Cl_2$): $\delta_P$ 7.5 (s, **P**$Ph_2$) ppm. $^{11}$B{$^{1}$H} NMR ($CD_2Cl_2$): $\delta_B$ 4.1 (s, **B**$Ph_2$) ppm. m/z = 528 [M+].

Crystal data for **2**: $C_{38}H_{30}BP$, $M_w$=528.40, triclinic, P-1 (no. 2), a = 10.3576(3), b = 11.1069(5), c=14.6458(3) Å, α = 107.201(2), β = 90.840(2), γ = 112.862(4)°. V= 1466.92(10) $A^3$, Z = 2 Mg/m^3. *m*(Mo-Ka) = 1.196 $mm^{-1}$, T = 173(2) K, 5495 independent reflections. Full-matrix *F2* refinement *R*1 = 0.0624, w*R*2 = 0.2135 on 4984 independent absorption corrected reflections [I2σ(I); 2θmax = 140.4°], 361 parameters. A colourless crystal with dimensions 0.22 x 0.2 x 0.16 mm was used.

**Synthesis of $Et_2BC(Et)=C(Ph)PPh_2$ (3)**

$^{n}$BuLi ($7.25x10^{-3}$ mol, 2.5 M in hexanes) was added dropwise to a cold (−78 °C) solution of phenylacetylene (0.73 g, $7.19x10^{-3}$ mol) in diethyl ether (5 $cm^3$). The colourless mixture was left to stir for 1 h. at −78 °C before an ethereal solution of triethyl borane ($7.2x10^{-3}$ mol, 2M solution in $Et_2O$) was added dropwise. The reaction mixture was maintained at this cold

temperature while stirring for 1.5 h., before a solution of chlorodiphenylphosphine (1.58 g, 7.2x10$^{-3}$ mol) in diethyl ether (2 cm$^3$) was added dropwise. The resulting mixture was allowed to attain ambient temperature and then stirred for 4 h. After the reaction was complete, the solution was filtered from LiCl and the filtrate taken to dryness under reduced pressure to afford an yellow oil, which crystallises upon standing. Yield, 1.78 g, 64%.

$^1$H NMR ($CDCl_3$): $\delta_H$ 0.79 (m, 6 H, $BCH_2C\mathbf{H}_3$), 0.86 (m, 4 H, $BC\mathbf{H}_2$), 1.11 (t, $^3J_{H-H}$ = 7.66 Hz, 3 H, $CCH_2C\mathbf{H}_3$), 2.55 (qd, $^3J_{H-H}$ = 7.65 Hz, $^4J_{H-P}$ = 2.96 Hz, 2 H C=C-C$\mathbf{H_2}$), 7.13 (m, 1 H, CAr-C**H**), 7.19 (m, 1 H, CAr-C**H**), 7.23 (m, 2 H, PAr-C**H** ), 7.36 (m, 2 H, PAr-C**H**), 7.41 (m, 2 H, PAr-C**H**), 7.42 (m, 2 H, PAr-C**H**) ppm. $^{13}$C{$^1$H} NMR ($CDCl_3$): $\delta_C$ 11.5 (d, $^4J_{C-P}$ = 11.5 Hz, $BCH_2\mathbf{C}H_3$), 13.2 (d, $^3J_{C-P}$ = 2.9 Hz, $CH_2CH_3$), 13.7 (br., B**C**H$_2$), 27.2 ($^3J_{C-P}$ = 51.0 Hz, C=C**C**H$_2$), 126.4 (s, =C(B)), 128.2 (*s,* Ar), 128.3, (d, $J_{P-C}$ = 4.1 Hz, Ar), 128.5 (d, $^3J_{C-P}$ = 8.7 Hz, PAr), 130.0 (d, $^4J_{C-P}$ = 2.2 Hz, PAr), 131.3 (d, $^1J_{C-P}$ = 17.2 Hz, *P*Ar), 132.9 (d, $J_{C-P}$ = 10.9 Hz, PAr) 136.7 (br. Ar), 196.5 (PC=C) ppm. $^{31}$P{$^1$H} NMR ($CDCl_3$): $\delta_P$ 9.84 (**P**Ph$_2$) ppm. $^{11}$B{$^1$H} NMR ($CDCl_3$): $\delta_B$ 13.22 (**B**Et$_2$) ppm. Calcd for $C_{26}H_{30}BP$ (384.31): C 81.26, H 7.87. Anal Found: C 81.16, H 7.78.

Crystal data for **3**: $C_{26}H_{30}BP$, $M_w$=384.33, Monoclinic, $P2_1/c$ (no. 14), a = 29.5171(11), b = 8.9505(4), c=17.1873(7) Å, α = 90, β = 91.625(4), γ = 90°. V= 4538.9(3) A$^3$, Z = 8, Dc = 1.125 Mg/m$^3$, μ(Cu-Ka) = 1.107 mm$^{-1}$, T = 173(2) K, 8363 independent reflections. Full-matrix *F2* refinement *R*1 = 0.1404, w*R*2 = 0.4164 on 7081 independent absorption corrected reflections [I2σ(I); 2θmax = 55°], 510 parameters. A colourless square crystal with dimensions 0.4 x 0.4 x 0.2 mm was used.

### 5.2.2 Synthesis of unsaturated phosphine-boranes

#### Synthesis of $Ph_2PC{\equiv}CPh$ (4)

$^n$BuLi (7.7 cm$^3$, 2.5 M in hexanes) was added to a solution of phenylacetylene (2.0 cm$^3$, 1.82 x10$^{-2}$ mol) in diethyl ether (10 cm$^3$) at −78 °C and stirred for 1 h., before a solution of $Ph_2PCl$ (3.3 cm$^3$, 1.78 x10$^{-2}$ mol) in $Et_2O$ (2.5 cm$^3$) was added at −78 °C and the mixture left to stir while warming to −20 °C over 2 h. The solution was then filtered, dried under partial vacuum and extracted with pentane. The pentane solution was dried under partial vacuum to yield a white solid. Yield: 4.46 g, 82%.

$^1$H NMR ($CDCl_3$): $\delta_H$ 6.62-6.68 (m, 3H, *meta*-C**H** + *para*-C**H**), 7.67-7.77 (m, 2 H, *para*-PC**H**), 6.82 (tofd, $^3J_{C-H}$ = 7.55, $^3J_{C-H}$ = 1.45 Hz, 4H, *ortho*-PC**H**), 7.08 (dofd, $^3J_{C-H}$ = 8.09 Hz, $^5J_{P-H}$ = 1.52 Hz, 2H,

*ortho*-C**H**), 7.49 (tofd, $^{3}J_{C\text{-}H}$ = 8.40, $^{4}J_{P\text{-}H}$ = 1.52 Hz, 4H, *meta*-PC**H**). $^{13}C\{^{1}H\}$ NMR ($CDCl_3$): $\delta_C$ 86.9 (d, $^{1}J_{C\text{-}P}$ = 9.1 Hz, P**C**≡C ), 108.5 (d, $^{2}J_{C\text{-}P}$ = 4.0 Hz, PC**≡C** ), 123.3 (d, $^{3}J_{C\text{-}P}$ = 0.8 Hz, PC≡C**C**H), 129.1 (d, $^{4}J_{C\text{-}P}$ = 30.0 Hz, *para*-P**C**H), 129.0 (s, *ortho*-P**C**H), 129.6 (*meta*-**C**H + *para* **C**H), 132.5 (d, $^{4}J_{C\text{-}P}$ = 1.7 Hz, *ortho*-**C**H), 133.1 (d, $^{3}J_{C\text{-}P}$ = 20.8 Hz, *meta*-P**C**H), 137.1 (d, $^{4}J_{C\text{-}P}$ = 7.1 Hz, *ipso*-**C**P). $^{31}P\{^{1}H\}$ NMR ($CDCl_3$): $\delta_P$ -33.01 (s).

**Synthesis of $Bu_2BC(Bu)=C(Ph)P^{i}Pr_2$ (5)**

Synthesised in a similar manner to **1** using $^{i}Pr_2PCl$ instead of $Ph_2PCl$. After the removal of LiCl, the filtrate was dried to a pale yellow viscous oil. Some impurities were removed by sublimation under partial vacuum at 60-70 °C, remaining impurities could not be removed.

$^{1}H$ NMR ($CDCl_3$): $\delta_H$ 0.76 (m, 4H, BC**H**$_2$), 0.84 (t, 3H, $^{2}J_{H\text{-}H}$ = 7.17 Hz, C**H**$_3$), 0.92 (t, 6H, $^{2}J_{H\text{-}H}$ = 6.91 Hz, $CH_3$), 1.20 (m, 12H, $^{i}$Pr-C**H**$_3$ + 4H, (C**H**$_2$)$_2$), 1.36 (m, 8H, BC(C**H**$_2$)$_2$C$H_3$), 2.32 (m, 2H, BC=CC**H**$_2$ + 2H, $^{i}$Pr-**H**) 7.16 (m, 2H, *m*-**H**, 1 H, *p*-**H**), 7.30 (m, 2H, *m*-**H**). $^{31}P\{^{1}H\}$ ($CDCl_3$): $\delta_P$ 30.2. $^{11}B\{^{1}H\}$ ($CDCl_3$): $\delta_B$ 8.8.

**Synthesis of $Et_2BC(Et)=C(Ph)P^{i}Pr_2$ (6)**

Synthesised in a similar manner to **5**, after the reaction was complete, the solution was filtered from LiCl and dried to a pale yellow viscous oil. Impurities were then removed by sublimation under partial vacuum at 60-70 °C.

$^{1}H$ NMR ($CDCl_3$): $\delta_H$ 0.79 (m, 4 H, BC**H**$_2$), 0.94 (t, $^{2}J_{H\text{-}H}$ = 7.52 Hz, 6 H, $BCH_2C$**H**$_3$), 1.00 (t, $^{2}J_{H\text{-}H}$ = 7.13 Hz, 3 H $CCH_2C$**H**$_3$), 1.21 (dt, $^{2}J_{H\text{-}H}$ = 13.26 Hz, $^{3}J_{H\text{-}P}$ = 7.38 Hz, 12 H CC**H**$_3$), 2.34 (m, 2H, BCC**H**$_2$ + 2H, C**H**$CH_3$), 7.17 (m, 2H, *o*-C**H** + 1H *p*-C**H**) 7.29 (t $^{2}J_{H\text{-}H}$ 7.77 Hz, *m*-C**H**). $^{13}C$ NMR ($CDCl_3$): $\delta_C$ 12.03 (d, *J* = 12.4 Hz, $BCH_2$**C**$H_{3)}$, 13.39 (d, *J* = 2.68 Hz, B**C**$H_2CH_3$) 14.03 (br) 19.02 (d, 3.39 $^{i}$Pr), 19.88 (d, $^{i}$Pr), 24.42 (d, *J* = 3.51 Hz, ), 26.76 (d, $^{1}J_{C\text{-}P}$ = 46.28 Hz, **C**H of $^{i}$Pr), 126.20 (s, 194.9 (br, C=**C**-B). $^{31}P\{^{1}H\}$ NMR ($CDCl_3$): $\delta_P$ 30.68 (s, **P**$^{i}Pr_2$). $^{11}B\{^{1}H\}$ NMR ($CDCl_3$): $\delta_B$ 9.43 (s, **B**$Et_2$).

**Synthesis of $^{t}Bu_2PC≡CPh$ (7)**

$^{n}$BuLi (3.00 $cm^3$, 2.5 M in hexanes) was added to a solution of phenylacetylene (0.79 $cm^3$, $7.19x10^{-3}$ mol) in $Et_2O$ (4 $cm^3$) at −78 °C and stirred for 1.5 h., before a solution of ($^{t}Bu)_2PCl$ (1.3 g, $7.19x10^{-3}$ mol) in $Et_2O$ (3 $cm^3$) was added at −78 °C and the mixture was left to warm to 17 °C and stir over a period of 6 h. The solution was then filtered away from LiCl, and dried under partial vacuum before being extracted with pentane. The filtered pentane solution was dried under partial vacuum to yield a yellow-white solid. Yield: 1.05 g, 60.0%.

$^{1}$H NMR ($CDCl_3$): $\delta_H$ 1.31 (d, $^{2}J_{P\text{-}H}$ = 11.94 Hz, 18 H C**H**$_3$), 7.31 (m, 3H, Ar-C**H**), 7.46 (m, 2H Ar-C**H**). $^{13}$C NMR ($CDCl_3$): $\delta_C$ 29.89 (d, $^{2}J_{C\text{-}P}$ =14.5 Hz, C(**C**H$_3$)$_3$), 33.00 (d, $^{1}J_{C\text{-}P}$ = 17.01 Hz, **C**(CH$_3$)$_3$), 88.41 (d, $^{1}J_{C\text{-}P}$ = 21.78 Hz, P-**C**≡C), 106.00 (d, $^{2}J_{C\text{-}P}$ =3.12Hz C≡**C**-C), 123.82 (d, $^{3}J_{P\text{-}C}$ 1.37 Hz, *ipso*-**C**H), 128.32 (s, p-**C**H), 128.34 m-**C**H), 131.58 (s, *o*-**C**H). $^{31}$P{$^{1}$H} NMR ($CDCl_3$): $\delta_P$ 11.52 (s).

Crystal data for **7**: $C_{21.33}H_{30.67}P_{1.33}$, $M_w$=328.45 Monoclinic, $P2_1/c$ (no. 14), a = 11.2104(9), b = 5.8588(5), c = 23.379(2) Å, α = 90, β = 98.358(8), γ = 90°. V= 1519.2(2) A$^3$, Z = 3 $D_c$ = 1.0769 Mg/m^3. *m*(Cu-Ka) = 1.5418 mm$^{-1}$, T = 173(2) K, 2731 independent reflections. Full-matrix $F^2$ refinement $R1$ = 0.0877, w$R2$ = 0.3514 on 2731 independent absorption corrected reflections F(000) = 538.4.

**Synthesis of $^{i}$Pr$_2$PC≡CPh (8)**

$^{n}$BuLi (3.65 cm$^3$, 2.5 M in hexanes) was added to a solution of phenylacetylene (1.0 cm$^3$, 9.13x10$^{-3}$ mol) in $Et_2O$ (5 cm$^3$) at −78 °C and stirred for 2 h., before a solution of $^{i}Pr_2PCl$ (1.32 cm$^3$, 9.13x10$^{-3}$ mol) in $Et_2O$ (2 cm$^3$) was added at −78 °C and the mixture left to stir for 3 h. The solution was then filtered, dried under partial vacuum and extracted with pentane. The filtered pentane solution was dried *in vacuo* to yield a yellow oil. Yield: 1.88 g, 94%.

$^{1}$H NMR ($CDCl_3$): $\delta_H$ 1.14 (d, $^{3}J_{C\text{-}P}$ = 6.91 Hz, 3H, C**H**$_3$), 1.18 (d, $^{3}J_{C\text{-}P}$ = 6.9 Hz, 3H, C**H**$_3$), 1.23 (d, $^{3}J_{C\text{-}P}$ = 6.87 Hz, 3H, C**H**$_3$), 1.26 (d, $^{3}J_{C\text{-}P}$ = 6.93 Hz, 3H, C**H**$_3$), 1.97, (quin, $^{2}J_{C\text{-}P}$ = 7.25 Hz, 2H, C**H**), 7.30 (m, 3H, Ar-**H**), 7.45 (m, 2H, Ar-**H**). $^{31}$P{$^{1}$H} NMR ($CDCl_3$): $\delta_P$ -12.03.

**Synthesis of Ph$_2$PC≡CSiMe$_3$ (9)**

Trimethylsilylacetylene (1.0 cm$^3$, 7.02 mmol) was dissolved in diethyl ether (15 cm$^3$) at −78 ˚C before $^{n}$BuLi (3.3 cm$^3$, 2.5 M in hexanes) was added and the mixture stirred cold for 30 mins before the cold addition of neat $ClPPh_2$ (1.94 cm$^3$, 7.14 mmol). After leaving the mixture to stir for two hours, the cloudy mixture was concentrated under vacuum, and then filtered away from LiCl. The product was extracted with pentane and dried to form a pale straw-coloured oil. Yield: 1.54 g, 76%.

$^{1}$H NMR ($CDCl_3$): $\delta_H$ 0.21 (s, $SiMe_3$), 7.27 (m, 4H, CH), 7.33 (br, 2H, CH), 7.56 (m, 4H, CH). $^{31}$P{$^{1}$H} NMR ($CDCl_3$): $\delta_P$ -32.9.

**Attempted synthesis of Bu$_2$BC(Bu)=C(SiMe$_3$)PPh$_2$ (11)**

$^{n}$BuLi (3 cm$^3$, 2.5 M in hexanes) was added, with stirring, to a solution of $Me_3SiC{\equiv}CH$ (1.0 cm$^3$, 7.2x10$^{-3}$ mol) in $Et_2O$ (5 cm$^3$). The colourless solution was left to stir at −30 °C for 1 hour before

$Bu_3B$ (7.2 $cm^3$, in 1M $Et_2O$) was added slowly at −30 °C. The solution remained colourless as it was left to stir and warm to ambient temperature for 90 minutes. Upon initial dropwise addition of a solution of $Ph_2PCl$ (1.29 $cm^3$, 7.2x$10^{-3}$ mol) in diethyl ether (1 $cm^3$) the reaction mixture turned yellow but faded to an off-white suspension. The mixture was then heated to reflux for 3 hours before allowing to cool to ambient temperature. The solution was then dried *in vacuo* to remove all solvents before the product was extracted in diethyl ether and dried to a yellow turbid vicious oil.

$^{31}P\{^1H\}$ NMR ($CDCl_3$): $\delta_P$ 12.1 (s). $^{11}B\{^1H\}$ NMR ($CDCl_3$): δ 11.9 (s). $^{29}Si\{^1H\}$ NMR ($CDCl_3$): $\delta_{Si}$ -12.9. Proton spectra could not be assigned due to intractable mixture of products.

**Attempted synthesis of $(C_6F_5)_2B(C_6F_5)C=C(Ph)PPh_2$ (12)**

$B(C_6F_5)_3$ (0.020 g, 3.9 x$10^{-4}$ mol) and **4** (0.011 g, 3.9 x$10^{-4}$ mol) were suspended in a toluene solution (10 $cm^3$) to 70 ˚C for 5 h. The yellow solution was allowed to cool, before the toluene was removed under reduced pressure. The spectroscopic data of the resulting yellow solid revealed multiple products, some of the resonances were consistent with the formation of $Ph_2P(Ph)C=C(C_6F_5)B(C_6F_5)_2$ (**12**).[244]

$^{31}P\{^1H\}$ NMR ($CDCl_3$): $\delta_P$ 13.6. $^{11}B\{^1H\}$ NMR ($CDCl_3$): $\delta_B$ -6.3.

**Synthesis of $RSiC{\equiv}CCH_2Cl$ (R = $^nPr_3$; 14, $Me_2Ph$ 16)**

**$^nPr_3SiC{\equiv}CCH_2Cl$ (14)**

Propargyl chloride (4.03 g, 5.4x$10^{-2}$ mol) was dissolved in THF (10 $cm^3$) and cooled to -78 °C before the addition of $^n$BuLi (11.0 $cm^3$, 2.5 M in hexanes, 2.7x$10^{-2}$ mol) dropwise. After stirring for 30 min. $^nPr_3SiCl$ (5.2 g, 2.7x$10^{-2}$ mol) in THF (10 $cm^3$) was added slowly to the red/orange solution. After the mixture was stirred cold for 30 mins it was allowed to warm to ambient temperature and stirred under argon for 20 hours. The yellow/white cloudy mixture was then dried under partial vacuum and the product extracted with pentane and dried to reveal a yellow oil. The oil was then distilled (1.1x$10^{-1}$ mbar, 33 °C) to reveal the second fraction as a colourless oil. Yield: 6.2g, 98%. Product was identified by comparison to literature spectroscopic data.[193,263]

$^1H$ NMR ($CDCl_3$): $\delta_H$ 0.63 (m, 6H, SiC**H**$_2$), 0.98 (t, 9H, C**H**$_3$), 3.40 (m, 6H, C**H**$_2$), 4.34 (s, 2H, C**H**$_2$Cl).

**$Me_2PhSiC{\equiv}CCH_2Cl$ (16)**

Propargyl chloride (5.61 g, 7.5x$10^{-2}$ mol) was dissolved in THF (10 $cm^3$) and cooled to −78 °C before the addition of $^n$BuLi (15.1 $cm^3$, 2.5 M in hexanes, 3.8x$10^{-2}$ mol) dropwise. After stirring

for 30 min. $Me_2PhSiCl$ (6.43 g, $3.8x10^{-2}$ mol) in THF (10 $cm^3$) was added slowly to the red/orange solution. After the mixture was stirred cold for 30 mins. before being allowed to warm to ambient temperature and stirred under argon for 20 hours. The pink/orange mixture was then dried under partial vacuum and the product extracted with pentane and dried to reveal an orange oil. The oil was then distilled ($8.3x10^{-1}$ mbar, 86 °C) to reveal the second fraction as a colourless oil. Yield 4.99g, 65%. Product was identified by comparison to literature spectroscopic data.[193,263]

$^1$H NMR ($CDCl_3$): $\delta_H$ 0.44 (s, 6H, C**H**$_3$), 4.38 (s, 2H, C**H**$_2$Cl), 7.37-7.41 (m, 3H, C**H**), 7.60-7.64 (m, 2H, C**H**).

**Synthesis of $Me_2SiC{\equiv}CCH_2PPh_2$ (17)**

$^n$BuLi (1.0 $cm^3$, 2.5M, $2.5x10^{-3}$ mol) was added to a solution of $HPPh_2$ (0.423 g, $2.27x10^{-3}$) in $Et_2O$ (10 $cm^3$) at -78 °C and left to store for 30 min, before an ethereal solution of $Me_2PhSiC{\equiv}CCH_2Cl$ (0.472 g, $2.26x10^{-3}$ mol) was added to the bright yellow mixture. The mixture was left to stir for 30 min at -78 °C before being allowed to warm to ambient temperature overnight. The brown mixture was then dried and the product was extracted with pentane to afford a brown oil. Product was identified by comparison to literature spectroscopic data.[193,263] Yield: 0.51 g, 63%.

$^1$H NMR ($CDCl_3$): $\delta_H$ 0.28 (s, 6H, C**H**$_3$), 2.97 (s, 2H, C**H**$_2$P), 7.19-7.33 (m, 10H, C**H**), 7.44-7.47 (m, 5H, C**H**). $^{31}P\{^1H\}$ NMR ($CDCl_3$): $\delta_P$ -13.3.

### 5.2.3 Synthesis of saturated phosphine-boranes

**Synthesis of $Ph_2PCH_2CH_2BBN$ (18)**

A THF (10 $cm^3$) solution of $Ph_2PCH{=}CH_2$ (1.30 g, $6.1x10^{-3}$ mol) and 9-BBN (0.76 g, $3.1x10^{-3}$ mol) was heated to reflux for 14 hours before the solvent was removed under partial vacuum and washed with pentane to reveal a white solid, which was identified by comparison to literature data.[264] Yield: 71%, 1.50 g, $4.3x10^{-3}$ mol.

$^1$H NMR ($CDCl_3$): $\delta_H$ 1.23 (m, 2H, BBN-CH), 1.48 (m, 2H, $BCH_2$), 1.61-1.89 (m, 12H, BBN), 2.33 (t, $^2J_{H\text{-}P}$ = 7.5 H, 2H, $PCH_2$), 7.29-7.46 (m, 10H, Ph). $^{31}P\{^1H\}$ NMR ($CDCl_3$): $\delta_P$ -9.9.$^{11}B\{^1H\}$ NMR ($CDCl_3$): $\delta_B$ 86.6.

**Synthesis of $Ph_2PCH_2CH_2CH_2BBN$ (19)**

A solution of $Ph_2PCH_2CH{=}CH_2$ (0.5 g, $2.2x10^{-3}$ mol) in THF (15 $cm^3$) was added to a suspension of 9-BBN (0.28 g, $1.1x10^{-3}$ mol) in THF (5 $cm^3$) and heated to reflux. After 4 hours, the cooled solution was dried under partial vacuum and product extracted with pentane. This pentane solution was concentrated and cooled to −20 °C until a white solid, which precipitated and was subsequently isolated, was dried under partial vacuum and identified by comparison to literature data.[91] Yield: 0.51 g, 64 %.

$^1$H NMR ($CDCl_3$): $\delta_H$ 1.03, (m, 4H, $CH_2CH_2B$), 1.37-1.93, (m, 14H, BBN), 2.34, (dt, *J* = 9, 7.3 Hz , 2H, $PCH_2$) 7.38-7.59 (m, 10H, Ph). $^{31}P\{^1H\}$ NMR ($CDCl_3$): $\delta_P$ 9.8. $^{11}B\{^1H\}$ NMR ($CDCl_3$): $\delta_B$ 0.8.

**Synthesis of $Fu_2PCH{=}CH_2$ (20)**

A solution of *bis*-(2-furyl)phosphine chloride (2.82 g, $1.40x10^{-2}$ mol) dissolved in THF (10 $cm^3$), was cooled to −78 °C before a 1.0 M solution of vinyl magnesium bromide (15.0 $cm^3$, $1.5x10^{-2}$ mol) was added dropwise. The yellow mixture was left to slowly warm to 19 °C and stir under argon over a period of 20 h. The solution was then dried under reduced pressure to reveal a sticky orange oil. The product was extracted with hexane and dried under reduced pressure to reveal a pale yellow transparent oil and identified by comparison to data from colleagues.[265] Yield: 1.62 g, 60%.

$^1$H NMR ($CDCl_3$): $\delta_H$ 5.6 (dd, *J* = 18.0, 15.3 Hz, 1H, PCH=C**H**$_2${*cis*}), 5.86 (dd, *J* = 33.7, 11.8 Hz, 1H, PCH=C**H**$_2$), 6.41 (m, 2H, Fu-**H**$^3$), 6.64 (ddd, *J* = 18.4, 15.0, 11.6 Hz, 1H, PC**H**=$CH_2$), 6.75 (m, 2H, Fu-**H**$^4$), 7.64 (m, 2H, Fu-**H**$^5$). $^{31}P\{^1H\}$ NMR ($CDCl_3$): $\delta_P$ -57.1.

**Synthesis of $Fu_2PCH_2CH_2BBN$ (21)**

A toluene suspension of $Fu_2PCH{=}CH_2$ (1.34 g, $6.97x10^{-3}$ mol) and 9-BBN (0.90 g, $3.6x10^{-3}$ mol) was heated to 60 ˚C for 4.5 h, before the solvent was removed *in vacuo*. The resulting white solid was extracted in $CH_2Cl_2$ and washed with hexane and identified by comparison to data from colleagues.[265] Yield: 1.91 g, 87%.

$^1$H NMR ($CDCl_3$): $\delta_H$ 1.16-1.25 (m, 2H, 9-BBN-C**H**), 1.42 (dt, $^3J_{H\text{-}H}$ = 15.0, $^3J_{H\text{-}P}$ = 8.3 Hz, 2H, C**H**$_2$B), 1.61-1.99 (m, 12H, BBN-C**H**$_2$) 2.31 (t, $^2J_{H\text{-}P}$ = 8.0, 2H, C**H**$_2$P), 6.39 (m, 2H, Fu-**H**$^3$), 6.74 (m, 2H, Fu-**H**$^4$), 7.61 (m, 2H, Fu-**H**$^5$). $^{13}C\{^1H\}$ NMR ($CDCl_3$): $\delta_C$ 20.2 (d, $^1J_{C\text{-}P}$ = 1.6 Hz, **C**H$_2$P), 23.3 (s, 9-BBN-**C**), 23.5 (s, **C**H$_2$B), 24.7 (s, 9-BBN-**C**), 31.2 (s, 9-BBN-**C**), 33.4 (s, 9-BBN-**C**), 110.6 (d, $^2J_{C\text{-}P}$ = 6.5 Hz, Fu-**C**$^3$), 120.2 (d, $^3J_{C\text{-}P}$ = 23.9 Hz, Fu-**C**$^4$), 146.9 (s, Fu-**C**$^5$), 152.2 (d, $^1J_{C\text{-}P}$ = 18.3 Hz, Fu-**C**$^2$). $^{31}P\{^1H\}$ NMR ($CDCl_3$): $\delta_P$ −55.9.$^{11}B\{^1H\}$ NMR ($CDCl_3$): $\delta_B$ 87.2.

**Synthesis of [Rh(CO)Cl($Fu_2PCH_2CH_2BBN)_2$] (22)**

A solution of $Fu_2PCH_2CH_2BBN$ (0.026 g, $8.2x10^{-5}$ mol) in $CD_2Cl_2$ was added to a stirring yellow solution of $[Rh(CO)_2Cl]_2$ (0.007 g, $2.1x10^{-5}$ mol). After 20 hours the solvent was removed under reduced pressure to reveal a yellow/orange solid. $^1$H NMR ($CD_2Cl_2$): $\delta_H$ 1.21 (m, 2H, $CH_2B$), 1.78 (m, 14H, BBN-H), 2.79 (m, 2H C**H**$_2$P), 6.51 (m, 2H, Fu-H), 7.15 (d, ($^3J_{P-H}$=3.19 Hz) 2H, Fu-H), 7.74 (m, 2H, Fu-H). $^{13}$C NMR ($CD_2Cl_2$): $\delta_C$ 21.28 (t, $^1J_{C-P}$ = 17.3 Hz, **C**H$_2$P), 22.80 (br, **C**H$_2$B), 23.79 (s, BBN-**C**), 31.76 (br, BBN-**C**), 33.7 (s, BBN-**C**), 111.5 (t, $^1J_{C-P}$ = 3.7 Hz, Fu-**C**), 123.6 (t, $^1J_{C-P}$ = 9.9 Hz, Fu-**C**), 147.6 (dt, $J_{C--P}$ = 29.6, 1.6 Hz, **C**O), 148.3 (t, $^1J_{C-P}$ = 2.3 Hz, Fu-**C**). $^{31}$P{$^1$H} NMR ($CD_2Cl_2$): $\delta_P$ -5.59 (d, $^1J_{Rh-P}$ = 129 Hz.). $^{11}$B{$^1$H} NMR ($CD_2Cl_2$): $\delta_B$ 85.91. IR data: $\nu_{CO}$= 1994 $cm^{-1.}$ Anal. Found: C, 55.71; H, 5.82; Calcd for $C_{37}H_{48}B_2P_2ClO_5Rh$: C, 55.90; H, 6.08.

Crystal data for **22**: $C_{37}H_{48}O_5P_2B_2ClRh$, $M_w$=794.67, Monoclinic, $P2_1/n$ (no. 14), a = 11.2766(7), b = 11.8165(8), c = 14.3245(10) Å, α = 90, β = 98.265(6), γ = 90°. V= 1888.9(2) $A^3$, Z = 2 $D_c$ = 1.046 Mg/m^3. *m*(Cu-Ka) = 1.5418 $mm^{-1,}$ T = 173(2) K, 2667 independent reflections. Full-matrix $F^2$ refinement *R*1 = 0.0458, w*R*2 = 0.1322 on 2667 independent absorption corrected reflections F(000) = 824.

**Attempted synthesis of $^t$Bu(Ph)$PCH_2CH$**

A solution of $^t$Bu(Ph)PCl (1.0 $cm^3$, 5.2 mmol) in toluene (4 $cm^3$) was cooled to -78 ˚C before the addition of $BrMgCH=CH_2$ (4.8 $cm^3$, 1M in THF) solution was added dropwise. The yellow solution was left to stir and warm to ambient temperature over 16 hours before the solvent was removed and the product was extracted with hexanes to yield a colourless oil.[269] This formed a small amount of colourless rod crystals of 1,2-di(tert-butyl)-l,2- diphenyl-diphosphine (**23**).

$^1$H NMR ($CDCl_3$): $\delta_H$ 0.84 (t, 18 H, *J* = 6.7 Hz, $CH_3$) 1.22 (t, 2 H, *J* =7.3 Hz, CH), 7.2-7.9 (m, 10 H, CH) ppm. $^{31}$P{$^1$H} NMR ($CDCl_3$): $\delta_P$ −3.9 ppm.

## 5.3 Experimental details for Chapter 3

### 5.3.1 Coordination chemistry of saturated phosphine-boranes

**Synthesis of [Rh(CO)Cl($Ph_2PCH_2CH_2BBN)_2$] (24)**

A solution of $Ph_2PCH_2CH_2BBN$ (0.037 g, $1.11x10^{-4}$ mol) in $C_6D_6$ (0.5 $cm^3$) was added to a yellow solution of $[Rh(CO)_2Cl]_2$ (0.010 g, $2.57x10^{-5}$ mol) in $C_6D_6$ (0.5 $cm^3$) and the yellow orange solution was left to stir at ambient temperature under Ar for 20 hours. The solution was dried to an orange solid.

$^1$H NMR ($CD_2Cl_2$): $\delta_H$ 1.94 (m, $CH_2B$), 2.92 (m, $CH_2P$), 1.17 (m, 2H, BBN-CH), 1.66-1.82 (m, 12H, BBN-$CH_2$), 7.01-7.09 (m, 6H, m-CH, p-Ar), 7.87-7.91 (m, 4H, *o*-Ar). $^{13}C\{^1H\}$ NMR ($CD_2Cl_2$): $\delta_C$ 22.44 (t, 13.13 Hz, **C**$H_2P$), 23.13 (br, **C**$H_2B$), 23.29 (s, BBN-C), 30.93 (br, BBN-C), 33.22 (s, BBN-C), 128.08 (t $J_{C-P}$ = 5 Hz, *Ar*), 128.49 (d, $^1J_{C-P}$ =10 Hz *Ar*), 129.59 (s, Ar-C) 133.5 (t, $J_{C-P}$ = 6.0 Hz, Ar), 134.74 (tofd *J* = 20.64, 1.03 Hz, **C**O). $^{31}P\{^1H\}$ NMR ($CD_2Cl_2$): $\delta_P$ 29.0 (d, $^1J_{P-Rh}$ = 127.46 Hz). $^{11}B\{^1H\}$ NMR ($CD_2Cl_2$): $\delta_B$ 84.5. IR data: $\nu_{CO}$= 1966 $cm^{-1}$. Anal. Found: C, 64.62; H, 6.58; Calcd for $C_{45}H_{56}P_2B_2OClRh$: C, 64.71; H, 6.76.

**Synthesis of [Rh(CO)Cl($Ph_2PCH_2CH_2CH_2BBN)_2$] (25)**

A solution of $Ph_2PCH_2CH_2CH_2BBN$ (0.022 g, $6.0x10^{-5}$ mol) in $C_6D_6$ (0.5 $cm^3$) was added to a yellow solution of $[Rh(CO)_2Cl]_2$ (0.005 g, $1.5x10^{-5}$ mol) in $C_6D_6$ (0.5 $cm^3$) and the yellow-orange solution was left to stir at ambient temperature under Ar for 20 hours. The reaction mixture contains several species, but NMR spectroscopic data is consistent with the formation of $[Rh(CO)Cl(Ph_2PCH_2CH_2CH_2BBN)_2]$.

$^1$H NMR ($CDCl_3$) $\delta_H$ 7.45-7.52 (m, 2H, CH), 7.05-7.21 (m, 15H, CH), 7.94-8.00 (m, 3H, CH). $^{31}P\{^1H\}$ NMR ($CDCl_3$): $\delta_P$ 24.8 (d, $^1J_{P-Rh}$ = 125 Hz). $^{11}B\{^1H\}$ NMR ($CDCl_3$): $\delta_B$ 86.6.

**Synthesis of *cis*-[$PtCl_2$($Fu_2PCH_2CH_2BBN$)] (26)**

A solution of $Fu_2PCH_2CH_2BBN$ (0.28 g, $8.7x10^{-3}$ mol) in $CH_2Cl_2$ (5 $cm^3$) was added to a suspension of $PtCl_2$ (0.12 g, $4.51x10^{-3}$ mol) in $CH_2Cl_2$ (5 $cm^3$) and after stirring for four days, was filtered, washed with hexanes before solvent was removed under reduced pressure. The product was identified by comparison to data from colleagues.[265] Yield: 0.16 g, 40%.

$^{1}$H NMR ($CD_2Cl_2$): $\delta_H$ 1.02 (m, 2H, C**H$_2$**B), 1.39-1.72 (m, 28H, BBN), 2.73 (td, *J* = 12.3, 5.7 Hz, 4H, C**H$_2$**P), 6.38 (br, 4H, Fu-**H**), 6.87 (br, 4H, Fu-**H**), 7.51 (br, 4H, Fu-**H**). $^{31}$P{$^{1}$H} NMR ($CD_2Cl_2$): $\delta_P$ -17.9 (s, $^{1}J_{P\text{-}Pt}$ = 3695 Hz).$^{11}$B{$^{1}$H} NMR ($CD_2Cl_2$): $\delta_B$ 93.45.

**Synthesis of *cis*/*trans*-[PdCl$_2$(Fu$_2$PCH$_2$CH$_2$BBN)] (27)**

A solution of $Fu_2PCH_2CH_2BBN$ (0.18 g, 5.6x10$^{-3}$ mol) in dichloromethane (5 cm$^3$) was added to a suspension of [$PdCl_2$] (0.05 g, 2.8x10$^{-3}$ mol) in DCM (5 cm$^3$) and after stirring for 48 h, the suspension was filtered and dried *in vacuo* to reveal a yellow powdered solid. The product was identified by comparison to data from colleagues.[265]

$^{1}$H NMR ($CDCl_3$): $\delta_H$ 1.17 (br, BC**H$_2$**), 1.53-1.86 (m, BBN), 2.74 (b, PC**H$_2$**), 6.38 (Br, *cis*-Fu), 6.49 (br, *trans*-Fu), 6.92 (br, Fu), 7.50 (br, *cis*-Fu), 7.70 (br, *trans*-Fu).$^{31}$P{$^{1}$H} NMR ($CDCl_3$): $\delta_P$ 0.9 (*cis*), −11.4 (*trans*). $^{11}$B{$^{1}$H} NMR ($CDCl_3$): $\delta_B$ 85.7 ppm.

**Attempted synthesis of [(C$_8$H$_{12}$)RhCl(Ph$_2$PCH$_2$CH$_2$CH$_2$BBN] (28)**

[($C_8H_{12}$)RhCl]$_2$ (0.035 g, 7.1x10$^{-5}$ mol) and $Ph_2PCH_2CH_2CH_2BBN$ (0.049 g, 1.4x10$^{-4}$ mol) were dissolved in $CH_2Cl_2$ (5 cm$^3$). The yellow solution was then left to stir at room temperature under an atmosphere of argon for 5 h., before the solvent was removed under reduced pressure to give a dark orange solid, which was identified by comparison to data from colleagues.[265]

Proton spectra could not be assigned due to excess BBN and $C_8H_{12}$ protons from an intractable mixture of products. $^{31}$P{$^{1}$H} NMR ($CD_2Cl_2$): $\delta_P$ 25.8 (d,$^{1}J_{P,Rh}$ = 147 Hz). $^{11}$B{$^{1}$H} NMR ($CD_2Cl_2$): $\delta_B$ 58.2 (br.).

**Synthesis of [($\eta^4$-C$_8$H$_{12}$)RhCl(Ph$_2$CH$_2$CH$_2$BBN)] (29)**

[*Complex was made in order to obtain bulk purity data*] A solution of $Fu_2PCH_2CH_2BBN$ (0.0053 g, 1.6x10$^{-5}$ mol) in $CD_2Cl_2$ was added to [Rh($\eta^4$-$C_8H_{12}$)Cl]$_2$ (0.0039 g, 7.9x10$^{-6}$ mol). After 1 h. the solvent was removed under mild heating and reduced pressure to afford a yellow powder. Product was identified by comparison to data from colleagues.[265]

$^{1}$H NMR ($CD_2Cl_2$): $\delta_H$ 1.27 (m, 2H, BC**H$_2$**), 1.58-1.94 (m, 14H, 9-BBN-**H**), 1.97-2.41 (m, 8H, $C_8H_{12}$-C**H$_2$**), 2.62 (m, 2H, PC**H$_2$**), 3.09 (m, 2H, $C_8H_{12}$-C**H** *trans-Cl*), 5.38 (m, 2H, $C_8H_{12}$-C**H** *cis-Cl*), 7.39-7.68 (m, 10H, Ar-**H**). $^{13}$C{$^{1}$H} NMR ($CD_2Cl_2$): $\delta_c$ 22.9 (d, $^{1}J_{C\text{-}P}$ = 25 Hz, P**C**H$_2$), 24.1 (s, B**C**H$_2$), 29.3 (s, 9-BBN **C**$^{\gamma}$), 31.5 (s, 9-BBN **C**$^{\alpha}$), 33.8 (s, 9-BBN **C**$^{\beta}$) 70.8 (d, $^{2}J_{P\text{-}C}$ = 14 Hz, $C_8H_{12}$-**C**H *trans-Cl)*, 105.1 (m, $C_8H_{12}$-**C**H *cis-Cl*), 128. $^{7}$ (d, $^{3}J_{C\text{-}P}$ = 8 Hz, *m*-**Ar**), 130.5 (d, $^{3}J_{C\text{-}P}$ = 1 Hz,*p*-**Ar**), (missing *o*-**Ar**),

134.2 (d, $^{1}J_{C\text{-}P}$ = 10 Hz, *ipso*-**Ar**). $^{11}B\{^{1}H\}$ NMR ($CDCl_3$): $\delta_B$ 80.3 (s). $^{31}P\{^{1}H\}$ NMR ($CD_2Cl_2$): $\delta_P$ 28.8 (d, $^{1}J_{P\text{-}Rh}$ = 150 Hz). Elem. Anal.: Calcd for $C_{30}H_{40}BPClRh$: C, 62.02 %; H, 6.94 %. Found: C, 61.80 %; H, 6.77 %.

**Synthesis of [($\eta^4$-$C_8H_{12}$)RhCl($Fu_2PCH_2CH_2BBN$)] (30)**

[*Complex was made in order to obtain bulk purity data*] A solution of $Fu_2PCH_2CH_2BBN$ (0.0057 g, 1.8x10$^{-5}$ mol) in $CD_2Cl_2$ was added to $[Rh(\eta^4\text{-}C_8H_{12})Cl]_2$ (0.0045 g, 9.1x10$^{-6}$ mol). After 1 h., solvent was removed under mild heating and reduced pressure to reveal a yellow powder. Product was identified by comparison to data from colleagues.[265]

$^{1}H$ NMR ($CDCl_3$) $\delta_H$ 1.24 (m, 2H, C**H**$_2$B), 1.67-1.81 (m, 14H, 9-BBN-**H**), 1.95-2.44 (m, 8H, C**H**$_2$-$C_8H_{12}$), 2.60 (dt, *J* = 8.5, 7.7 Hz, 2H, C**H**$_2$P), 3.49 (m, 2H, C**H**- $C_8H_{12}$), 5.43 (br, 2H, C**H**- $C_8H_{12}$), 6.48 (m, 2H, Fu-**H**), 6.98 (m, 2H, Fu-**H**), 7.67 (s, 2H, Fu-**H**). $^{13}C\{^{1}H\}$ NMR ($CD_2Cl_2$): $\delta_C$ 21.2 (d, $^{1}J_{C\text{-}P}$ = 29 Hz, **C**H$_2$P), 22.2 (s, 9-BBN-**C**), 23.2 (s, **C**H$_2$B), 28.7 (s, $C_8H_{12}$-**C**H$_2$), 28.7 (s, 9-BBN-**C**), 30.8 (s, 9-BBN-**C**), 33.0 (s, 9-BBN-**C**), 33.2 (s, $C_8H_{12}$-**C**H$_2$), 70.5 (d, $^{1}J_{C\text{-}Rh}$ = 13 Hz, $C_8H_{12}$-**C**H), 105.6 (dd, $^{1}J_{C\text{-}Rh}$ = 12, $^{2}J_{C\text{-}P}$ = 7 Hz, $C_8H_{12}$-**C**H), 110.6 (d, $^{2}J_{C\text{-}P}$ = 6 Hz, Fu-**C**), 122.3 (d, $^{3}J_{C\text{-}P}$ = 16 Hz, Fu-**C**), 146.1 (d, $^{1}J_{C\text{-}P}$ = 54 Hz, Fu-**C**$_{)}$, 147.4 (d, $^{4}J_{C\text{-}P}$ = 4 Hz Fu-**C**). $^{31}P\{^{1}H\}$ NMR ($CD_2Cl_2$): $\delta_P$ 1.9 (d, $^{1}J_{P\text{-}Rh}$ = 157 Hz). $^{11}B\{^{1}H\}$ NMR ($CDCl_3$): $\delta_B$ 83.7 (br s). Elem. Anal.: Calcd for $C_{26}H_{36}O_2BPClRh$: C, 55.68 %; H, 6.47 %. Found: C, 55.52 %; H, 6.34 %.

**Synthesis of [Cp*$IrCl_2$($Fu_2PCH_2CH_2BBN$)] (31)**

[*Complex was synthesised in order to improve synthesis*] $[Cp^*IrCl_2]_2$ (0.020 g, 2.5x10$^{-5}$ mol) was dissolved in $CH_2Cl_2$ (1 cm$^3$), before adding to a solution of $Fu_2PCH_2CH_2BBN$ (0.016 g, 5.1x10$^{-5}$ mol) in $CH_2Cl_2$ (1cm$^3$). The orange solution was left to stir at ambient temperature for 67 hours before the solvent was removed under partial vacuum.[265,288]

$^{31}P\{^{1}H\}$ NMR ($CDCl_3$): $\delta_P$ -22.15. $^{11}B\{^{1}H\}$ NMR ($CDCl_3$): $\delta_B$ 86.5.

**Synthesis of [$PtCl_2$($Ph_2PCH_2CH_2BBN)_2$] (32)**

A solution of $Ph_2PCH_2CH_2BBN$ (0.201 g, 6.01x10$^{-4}$ mol) in $CH_2Cl_2$ (5 cm$^3$) was added to a suspension of $PtCl_2$ (0.080 g, 3.11x10$^{-4}$ mol) in $CH_2Cl_2$ (5 cm$^3$) and after stirring for four days, was filtered, washed with hexanes and dried *in vacuo*.

$^{1}H$ NMR ($CDCl_3$): $\delta_H$ 7.49 - 7.58 (m, 8H, CH), 7.35-7.41 (m, 5H, CH), 7.21-7.25 (m, 7H, CH), 1.48-1.82 (m, 14H, BBN). $^{31}P\{^{1}H\}$ NMR ($CDCl_3$): $\delta_P$ 10.1 (s, $^{1}J_{P\text{-}Pt}$ = 3646 Hz). $^{11}B\{^{1}H\}$ NMR ($CDCl_3$): $\delta_B$ 58.3.

## 5.4 Experimental details for Chapter 4

### 5.4.1 Synthesis of compounds $RMe_2SiCH_2Cl$ (42-49)

#### Synthesis of $^{i}PrMe_2SiCH_2Cl$ (42)

A solution of $^{i}$PrMgBr (68 $cm^3$, 1.15 M in THF) was added slowly to a cold (−5 ˚C) solution of $ClMe_2SiCH_2Cl$ (11.1 g, 0.077 mol) in diethyl ether (20 $cm^3$). After 30 min. the mixture was slowly allowed to warm to ambient temperature, and the resulting grey suspension was stirred for 18 hours before being heated to reflux for 2 h. After leaving to cool to ambient temperature, the paler mixture was filtered and the grey solids were washed with diethyl ether (2 x 20 $cm^3$) and tetrahydrofuran (20 $cm^3$). The solution and washings were combined, the solvent was removed and the product distilled to purity (−78 ˚C, 19 mbar). Yield: 2.8 g, 24%

$^1$H NMR ($CDCl_3$): $\delta_H$ 0.24 (*s*, 6H, Si(C**H**$_3$)$_2$), 1.17 (*d*, 6H, $^3J_{H\text{-}H}$ = 6.2 Hz, $CH_3$), 2.78 (*s*, 2H, C**H**$_2$Cl), 4.08 (*sept*, 1H, $^3J_{H\text{-}H}$ = 6.2 Hz, C**H**). $^{13}$C{$^1$H} NMR ($CDCl_3$): $\delta_C$ -2.8 (s, Si(**C**H$_3$)$_2$, 25.9 (s, **C**H$_3$), 30.2 (s, **C**H$_2$Cl), 65.1 (s, **C**H).

#### Synthesis of *p*-tolyl$Me_2SiCH_2Cl$ (43)

Following limited literature precedure,[301] a solution of *p*-tolylMgBr in tetrahydrofuran (57 $cm^3$, 1.33 M) was added slowly to a cooled (−10 °C) solution of chloromethylchlorodimethylsilane (10.0 $cm^3$, 0.076 mol) in diethyl ether (30 $cm^3$). After stirring cold for 45 min, the mixture was heated to reflux for 18 hours, before being left to stir and cool down for 48 h. The solvents were removed by distillation and the product was distilled under partial vacuum (2.3 mbar, 55 °C) yielding a colourless liquid (6.6 g, 43%).

$^1$H NMR ($CDCl_3$): $\delta_H$ 0.41 (s, 6H, Si(CH$_3$)$_2$), 2.37 (s, 3H, CH$_3$-Ar), 2.94 (s, 2H, CH$_2$Cl), 7.21 (d, *J* = 7.71 Hz, 2H, Ar-H), 7.45 (d, 2H, *J* = 7.71 Hz, Ar-H).$^{13}$C NMR ($CDCl_3$): $\delta_C$ 4.3 (s, $^1J_{C\text{-}Si}$ = 54.1 Hz, Si(CH$_3$)$_2$, 21.6 (s, Ar-CH$_3$), 30.7 (s, CH$_2$Cl), 128.98 (s, Ar-H), 133.9 (s, Ar-H). $^{29}$Si NMR ($CDCl_3$): $\delta_{Si}$ -4.1.

#### Synthesis of $(C_6F_5)Me_2SiCH_2Cl$ (44)

$C_6F_5$MgBr was made through the slow dropwise addition of $C_6F_5$Br in diethyl ether (50 $cm^3$) to a cold (−10 → 0 °C) ethereal slurry of excess, activated, magnesium, before allowing it to warm to ambient temperature. After 1-3 hours the brown solution was filtered from the remaining magnesium and titrated against dilute HCl (0.0829 M) with phenolphthalein to determine concentration.

A solution of $C_6F_5MgBr$ (0.31 M in diethyl ether, 0.042 mol) was added to a stirring solution of $ClMe_2SiCH_2Cl$ (5.5 $cm^3$, 0.042 mol) in diethyl ether (30 $cm^3$) at −5 °C, upon addition the solution was heated to reflux for 18 hours and allowed to cool. The brown solution was filtered from the precipitated brown solid. The washings of the brown solid was combined with the filtrate and the diethyl ether was removed through distillation. The resulting brown oil was distilled to purity ($3.1x10^{-2}$ mbar, 34 °C) to yield colourless oil. (8.2g, 0.03 mol, 71%).

$^1H$ NMR ($CDCl_3$): $\delta_H$ 3.09 (t, 2H, $^4J_{H-H}$ = 1.0 Hz, $CH_2Cl$), 0.54 (t, 6H, $J$ = 1.5 Hz, $SiMe_2$). $^{19}F$ NMR ($CDCl_3$): $\delta_F$ -126.75 (dd, 2F, $^3J_{F-F}$ = 10.5, 24.6 Hz), -150.18 (tt, 1F, $^1J_{F-F}$ = 3.7, 19.7 Hz, *p*-F), -160. 70 (m, 2F). $^{13}C\{^1H\}$ NMR ($CDCl_3$): $\delta_C$ -3.1 (t, $J_{C-F}$ = 2.9 Hz, $SiMe_2$), 29.6 (t, $J_{C-F}$ = 3.8 Hz, $CH_2Cl$), 107.9 (tm, $^2J_{C-F}$ = 32.6 Hz, *ipso*-CF), 137.43 (dm, $J_{C-F}$ = 254 Hz, *o*-CF), 142.6 (dm, $J_{C-F}$ = 254 Hz, *p*-CF), 149.3 (dm, $J_{C-F}$ = 243 Hz, *m*-CF). $^{29}Si$ NMR ($CDCl_3$): $\delta_{Si}$ -2.0. Elem. Anal.: Calcd for $C_9H_8F_5SiCl$: C, 39.37 %; H, 2.94 %. Found; C, 39.45 %; H, 3.02 %.

**Synthesis of (*p*-$CF_3$-$C_6H_4$)$Me_2SiCH_2Cl$ (45)**

*p*-$CF_3C_6H_4MgBr$ was made through the slow dropwise addition of *p*-$CF_3C_6H_4Br$ (20 g, 0.089 mol) in diethyl ether (50 $cm^3$) to an ethereal slurry of excess, activated, magnesium, reflux was maintained during second half of addition and the reaction was left to cool to ambient temperature. After 1.5 hours the brown solution was filtered from the remaining magnesium and into a cold (−10 °C) ethereal (20 $cm^3$) solution of $ClMe_2SiCH_2Cl$ (10.5 g, 0.073 mol) and left to warm for one hour, before heating to reflux for 18 hours. The solution was then filtered and washed with diethyl ether. The diethyl ether was distilled and the brown oil was distilled to purity (46 °C, $8.5x10^{-1}$ mbar). Yield: 8.7 g, 0.034 mol, 46.6%. Spectroscopic data was comparative to the limited data reported.[302]

$^1H$ NMR ($CDCl_3$): $\delta_H$ 0.45 (s, 6H, $SiMe_2$) 2.96 (s, 2H, $CH_2Cl$), 7.62 (d, 2H, $^3J_{H-H}$ = 8.22 Hz, CH), 7.68 (d, 2H, $^3J_{H-H}$ = 8.22 Hz, CH). $^{13}C\{^1H\}$ NMR ($CDCl_3$): $\delta_C$ -4.42 (s, $SiMe_2$), 29.9 (s, $CH_2Cl$), 124.29 (q, $^1J_{C-F}$ = 272 Hz, $CF_3$), 124.65 (q, $^3J_{C-F}$ =3.8 Hz, CH), 131.9 (q, $^2J_{C-F}$ = 30 Hz, $C(CF_3)$), 134.25 (s, CH), 141.24 (s, *ipso*-C). $^{19}F$ NMR ($CDCl_3$): $\delta_F$ -63.12 (s). $^{29}Si\{^1H\}$ NMR ($CDCl_3$): $\delta_{Si}$ -2.63.

**Synthesis of (2,5-$CF_3$-$C_6H_3$)$Me_2SiCH_2Cl$ (46)**

Made in similar fashion to *p*-$CF_3$-$C_6H_4SiMe_2CH_2Cl$ (**45**) from the addition of 2,5-$CF_3$-$C_6H_3MgBr$ (0.044 mol in diethyl ether) to $ClSiMe_2CH_2Cl$ (5 g, 0.035 mol). Distilled (54 ˚C, $9.3x10^{-1}$ mbar) Yield: 11%. Spectroscopic data were compared to the limited reported data.

$^{1}$H NMR ($CDCl_3$): $\delta_H$ 0.50 (s, 6H, $SiMe_2$), 2.98 (s, 2H, $CH_2Cl$), 7.90 (s, 1H, CH), 7.96 (s, 2H, CH). $^{13}C\{^{1}H\}$ NMR ($CDCl_3$): δ -4.5 (s, $SiMe_2$), 29.3 (s, **C**$H_2Cl$), 123.54 (q, $^{1}J_{C\text{-}F}$ = 237 Hz, **C**$F_3$), 123.7 (sept, *J*=3.8 Hz, p-**C**), 131.2 (q, *J* = 32.9 Hz, **C**($CF_3$)), 133.7 (m, **C**H), 140.0 (s, Si**C**). $^{19}$F NMR ($CDCl_3$) $\delta_F$ -62.94 (s). $^{29}Si\{^{1}H\}$ NMR ($CDCl_3$): $\delta_{Si}$ -1.4.

**Synthesis of (PhC≡C)$Me_2SiCH_2Cl$ (47)**

Phenylacetylene (7.2 $cm^3$, 0.065 mol) was dissolved in diethyl ether (50 $cm^3$) and cooled to −78 ˚C before $^{n}$BuLi (32.0 $cm^3$, 2.5M in hexanes) was added *via* syringe. The yellow solution was stirred for 1 h. to warm to ambient temperature, before being cooled to −78 °C for the addition of neat Chloro(chloromethyl)dimethylsilane (10.0 $cm^3$, 0.076 mol), the mixture was left to stir for 1 hour before warming to ambient temperature and stirring for a further 2 hours. The lithium salts were removed by filtration, and the solvent removed under reduced pressure. The colourless oil was then distilled ($4.0x10^{-2}$ mbar, 55 °C to yield (chloromethyl)dimethyl(phenylethynyl)silane (11.67 g, 0.056 mol, 86%. Spectroscopic data was comparative to the literature data reported.[306]

$^{1}$H NMR ($CDCl_3$) $\delta_H$ 0.37 (s, 6H, $SiMe_2$), 2.94 (s, 2H, $^{1}J_{H\text{-}Si}$ = 59 Hz, $CH_2Cl$), 7.33 (m, 3H, CH), 7.47 (m, 2H, CH). $^{13}$C NMR ($CDCl_3$): $\delta_C$ -3.01 (s, $Si(CH_3)_2$), 30.26 (s, $CH_2Cl$), 90.38 (s, Si-C≡C), 107.12 (s, C≡CPh), 122.64 (s, *ipso*CH), 128.42 (s, Ar-CH, 129.11 (s, Ar-CH), 132.25 (s, Ar-CH). $^{29}$Si NMR ($CDCl_3$): $\delta_{Si}$ -17.3.

**Synthesis of ($Me_3SiC$≡C)$Me_2SiCH_2Cl$ (48)**

$^{n}$BuLi (16 $cm^3$, 2.5 M in hexanes, 0.04 mol) was added to a solution of $Me_3SiC$≡CH (5.4 $cm^3$, 0.038 mol) in diethyl ether (20 $cm^3$) cooled to −78 ˚C. After stirring for 1 hour $Me_2SiCH_2Cl$ (5.0 $cm^3$, 0.038 mol) was added and stirred at −78 ˚C for 1 h., before allowing to warm to ambient temperature over 1 h. The white suspension was filtered to a colourless solution. The solvent was removed under partial vacuum (5 mbar) and the product was distilled to purity ($5x10^{-2}$ mbar, 45 °C) Yield: 6.2 g, 0.31 mol, 80%.

$^{1}$H NMR ($C_6D_6$): $\delta_H$ 0.13 (s, 9H, $SiMe_3$), 0.17 (s, 6H $SiMe_2$), 2.61 (s, 2H, $CH_2$). $^{13}$C NMR ($C_6D_6$) $\delta_C$ -3.2 (s, $SiMe_2$), 0.2 (s, $SiMe_3$), 29.8 (s, $CH_2$), 110.2 (s, $SiMe_2$**C**C), 116.7 (s, $SiMe_3$**C**C). $^{29}$Si NMR ($C_6D_6$) $\delta_{Si}$ -17.83 ($SiMe_3$), -19.58 ($SiMe_2$).

**Synthesis of $^{n}$BuMe$_2$SiCH$_2$Cl (49)**

$^{n}$BuLi (55 $cm^3$, 2.5 M in hexanes, 0.14 mol) was added to a cold (−78 °C) solution of $ClMe_2SiCH_2Cl$ (15.6 g, 0.10 mol) in diethyl ether (80 $cm^3$) resulting in the formation of a white

precipitate. After the addition, the mixture was allowed to warm to ambient temperature and stirred for 3 h. The solvent was reduced to ~50 $cm^3$ and was filtered away from the white precipitate to afford a straw-coloured solution. The diethyl ether was removed under reduced pressure and the product was distilled (9.0x10 mbar, 58 °C) to reveal colourless oil (10.2g, 0.062 mol). Spectroscopic data was comparative to the literature data reported.[307]

$^1$H NMR ($CDCl_3$): $\delta_H$ 0.10 (s, 6H, $Si(CH_3)_2$), 0.66 (m, 2H, $Si\text{-}CH_2$), 0.89 (t, 3H, $^3J_{H\text{-}H}$ = 7.0 Hz, $CH_3$), 1.32 (m, 4H, 2x$CH_2$), 2.78 (s, 2H, $CH_2Cl$). $^{13}$C NMR ($CDCl_3$): $\delta_C$ -4.4 (s, $Si(CH_3)_2$), 13.6 (s, $Si\text{-}CH_2$), 13.9 (s, $CH_3$), 25.9 (s, $CH_2$), 26.6 (s, $CH_2$), 30.6 (S, $CH_2Cl$). $^{29}$Si NMR ($CDCl_3$): $\delta_{Si}$ 3.9.

### 5.4.2 Synthesis of compounds $RMe_2SiCH_2PCl_2$ (50-54)

#### Synthesis of $Me_3SiCH_2PCl_2$ (50)

Made as per literature procedures.[138] A solution of $Me_3SiCH_2Cl$ (21.75 g, 0.18 mol) in diethyl ether (60 $cm^3$) was added dropwise to a suspension of magnesium (8.0 g, 0.3 M) in diethyl ether (80 $cm^3$). The reaction self-initiated after 3/4 of the solution had been added and the remaining solution was added at such a rate as to maintain reflux. The mixture was left to cool to ambient temperature before the solution was filtered into a solution of $PCl_3$ (22 g, 0.16 mol) in diethyl ether (60 $cm^3$) at -78 ˚C. The resulting suspension was left to warm to room temperature and stirred for 18 h., before the colourless solution was filtered from the white solid. The diethyl ether was removed and the product purified by distillation (35 ˚C, 2.5 mbar) to afford a colourless liquid. Yield: 60%.

$^1$H NMR ($CDCl_3$): $\delta_H$ 0.21 (s, 9H, $SiMe_3$), 2.04 (d, 2H, *J* = 15.8 Hz, $CH_2$). $^{31}$P NMR ($CDCl_3$): $\delta_P$ 205.1 (s). $^{13}$C NMR ($CDCl_3$): $\delta_C$ 0.1 (d, $^3J_{C\text{-}P}$ = 5.0 Hz, $SiMe_3$), 35.6 (d, $^1J_{C\text{-}P}$ = 61.2 Hz, $CH_2$).

#### Synthesis of $PhMe_2SiCH_2PCl_2$ (51)

Made as per literature procedures,[138] and **50** from $PhMe_2SiCH_2Cl$, an excess of activated magnesium and $PMe_3$. Colourless liquid was distilled at 0.6 mbar, 94 ˚C.

$^1$H NMR ($CDCl_3$): $\delta_H$ 0.50 (s, 6H, $SiMe_3$), 2.26 (d, 2H, *J* = 15.8 Hz, $CH_2$), 7.41 (m, 3H Ar-H), 7.54 (m, 2H, Ar-H). $^{31}$P NMR ($CDCl_3$): $\delta_P$ 202.9 (s). $^{13}$C NMR ($CDCl_3$): $\delta_C$ -1.4 (d, $^3J_{C\text{-}P}$ = 4.6 Hz, $SiMe_2$), 35.1 (d, $^1J_{C\text{-}P}$ = 62.0 Hz, $CH_2$), 128.3 (s, CH), 130.0 (s, CH), 133.7 (d, *J* = 1Hz, CH), 136.9 (d, *J* = 4 Hz, ipso-CH).

**Synthesis of (*p*-tolyl)$Me_2SiCH_2PCl_2$ (52)**

An ethereal (15 $cm^3$) solution of *p*-tolyl$Me_2SiCH_2Cl$ (6.6 g, 0.033 mol) was added dropwise to a stirring suspension of activated magnesium (2.0 g, 0.08 mol) in diethyl ether (20 $cm^3$). The reaction self-initiated and after allowing to cool to room temperature, was left to stir for 2 h., before it was filtered. The magnesium turning were rinsed with diethyl ether (10 $cm^3$) with the washings added to the filtrate. This solution was added to a stirring solution of $PCl_3$ (4.5 $cm^3$, 0.05 mol) in diethyl ether (20 $cm^3$) cooled to -78 °C, and was left to stir for 30 min, before allowing to warm to ambient temperature for 18 h. The solution was filtered, the solid magnesium halides washed with diethyl ether (3 x 15 $cm^3$) and the washings combined with the filtrate. The diethyl ether was removed by distillation, to leave the product as a colourless liquid. (5.92 g, 0.020 mol, 67%).

$^1$H NMR ($CDCl_3$): $\delta_H$ 0.48 (s, 6H $SiMe_2$), 2.24 (d, $^2J_{H\text{-}P}$ = 15.2 Hz, $CH_2$), 2.37 (s, 3H, $CH_3$), 7.22 (d, $^3J_{C\text{-}H}$ = 7.4 Hz, Ar-H), 7.44 (d, $^3J_{C\text{-}H}$ = 7.4 Hz, Ar-H). $^{31}C\{^1H\}$ NMR ($CDCl_3$): $\delta_C$ -1.33 (s, $SiMe_2$), 21.6 (s, $CH_3$), 35.2 (d, $^1J_{C\text{-}P}$ = 61 Hz, $CH_2$), 129.1 (s, Ar-H), 133.1 (d, $^3J_{C\text{-}P}$ = 4 Hz, Si-C), 133.7 (Ar-H), 140.0 (s, C-Me). $^{29}Si\{^1H\}$ NMR ($CDCl_3$): $\delta_{Si}$ -6.7. $^{31}P\{^1H\}$ NMR ($CDCl_3$) $\delta_P$ 203.3.

**Synthesis of (*p*-$CF_3C_6H_4$)$Me_2SiCH_2PCl_2$ (53)**

To a slurry of magnesium (0.8 g, 0.032 mol) in diethyl ether (50 $cm^3$) was added an ethereal solution of **45** (4.8 $cm^3$, 0.019 mol) in diethyl ether (50 $cm^3$). The mixture was heated to reflux for 5 hours before being allowed to cool. The solution was filtered directly into a cold (−78 °C) solution of $PCl_3$ (1.7 $cm^3$, 0.019 mol) in diethyl ether (30 $cm^3$). The yellow, turbid suspension was stirred cold for 1 hour, before being allowed to warm to ambient temperature and stir for a further 18 hours. The pale yellow solution was filtered from the white solid, and the solid washed with diethyl ether. The washings were combined with the solution and the diethyl ether was removed *via* distillation. The yellow liquid was then distilled under partial vacuum (55 °C, 5.0 x$10^{-2}$ mbar) to yield *p*-$CF_3$-$C_6H_4SiMe_2CH_2PCl_2$ as a colourless liquid. (Yield 3.52g, 58%)

$^1$H NMR ($CDCl_3$): $\delta_H$ 0.51 (d, 6H, $^4J_{H\text{-}P}$ = 1 Hz, $SiMe_2$), 2.24 (d, 2H, $^2J_{H\text{-}P}$ = 15.6 Hz, $CH_2PCl$), 7.63 (m, 4H, CH). $^{19}$F NMR ($CDCl_3$) δ -63.13 (s, $CF_3$).$^{13}C\{^1H\}$ NMR ($CDCl_3$): $\delta_C$ -1.5 (d, $^3J_{C\text{-}P}$ = 4Hz, $SiMe_2$), 34.5 (d, $^1J_{C\text{-}P}$ = 61.7 Hz, $CH_2P$), 124.8 (q, *J* = 3.8 Hz, $CF_3$) 125.6 (s, **C**$CF_3$), 131.8 (s, CH) 132.1 (s, CH ) 134.0 (d *J* = 1.2 Hz, Si**C**). $^{31}P\{^1H\}$ NMR ($CDCl_3$): $\delta_P$ 200.8. $^{29}Si\{^1H\}$ NMR ($CDCl_3$): $\delta_{Si}$ -4.6. Anal. Found: C, 37.75; H, 3.84; Calcd for $C_{10}H_{12}Cl_2F_3PSi$: C, 37.65; H, 3.79.

**Synthesis of $^{n}$BuMe$_2$SiCH$_2$PCl$_2$ (54)**

To a slurry of magnesium (2.0 g, 0.083 mol) in diethyl ether (40 cm$^3$) was added an ethereal solution of **49** (5.0g, 0.030 mol) in diethyl ether (60 cm$^3$). The mixture was heated to reflux for 6 hours before the grey mixture was allowed to cool. The solution was filtered directly into a cold (-78 °C) solution of $PCl_3$ (2.7 cm$^3$, 0.031 mol) in diethyl ether (20 cm$^3$). The resulting turbid suspension was stirred cold for 1 hour, before being allowed to warm to ambient temperature and stirred for a further 18 hours. The pale yellow solution was filtered from the white solid, and the solid washed with diethyl ether before the diethyl ether was removed by distillation to yield $^{n}$BuSiMe$_2$CH$_2$PCl$_2$ as a colourless liquid. (Yield 6.4 g, 90%)

$^1$H NMR ($CDCl_3$): $\delta_H$ 0.18 (s, 6H, Si($CH_3$)$_2$), 0.67 (m, 2H, Si-$CH_2$), 0.90 (t, 3H, $^3J_{H-H}$ = 6.8 Hz, $CH_2$**C**H$_3$), 1.33 (m, 4H, 2x$CH_2$), 2.03 (d, 2H, $^3J_{H-P}$ = 15.37 $CH_2$P). $^{31}$C{$^1$H} NMR ($CDCl_3$): $\delta_C$ -1.6 (d, *J* = 6Hz, Si$Me_2$), 13.8 (s, $CH_2$**C**H$_3$), 25.9 (s, 2 x $CH_2$), 26.5 (s, Si-$CH_2$) 34.5 (d, *J* = 62Hz, $CH_2$P). $^{31}$P{$^1$H} NMR ($CDCl_3$) $\delta_P$ 205.6.$^{29}$Si{$^1$H} NMR ($CDCl_3$): $\delta_{Si}$ 1.2.

### 5.4.3 Synthesis of phosphaalkynes (36, 37, 55-57)

**Synthesis of Me$_3$SiC≡P (36)**

P≡CSi$Me_3$ was prepared by a modified literature procedure.[138] A solution of Me$_3$SiCH$_2$PCl$_2$ (0.75 g, 3.9 mmol) in toluene (5 cm$^3$) was added to a suspension of AgOTf (1.0 g, 8.7 mmol) in toluene (10 cm$^3$). After 5 mins a solution of DABCO (2.25 g, 8.7 mmol) in toluene (10 cm$^3$) was added to the white suspension. The mixture was stirred for 1 h. before an orange/red solution was filtered from the beige mixture. This solution was kept at 5 ˚C in a Youngs' Ampoule. The solution was calibrated before each use using a known volume of Me$_3$SiC≡P (~ 0.50 cm$^3$) which was spiked with an accurately known mass of $PPh_3$ (~ 0.03 g) in $C_6D_6$. The concentration of the solution was determined by integration of the P≡CSi$Me_3$ and $PPh_3$ phosphorous resonances from the $^{31}$P{$^1$H} NMR spectrum recorded at d1 = 40 s.

$^{31}$P NMR ($C_6D_6$) $\delta_P$ 98.8 (s).

**Synthesis of PhMe$_2$SiC≡P (37)**

Prepared in a similar fashion to Me$_3$SiC≡P, from PhMe$_2$SiCH$_2$PCl$_2$ with 2.2 equivalents of AgOTf and DABCO in toluene.

$^{31}$P NMR ($C_6D_6$): $\delta_P$ 104.1 (s).

**Synthesis of (*p*-tolyl)$Me_2SiC{\equiv}P$ (55)**

Made and calibrated in similar fashion to $Me_3SiC{\equiv}P$ from (*p*-tolyl)$Me_2SiCH_2PCl_2$ with 2.2 equivalents of AgOTf and DABCO in toluene.

$^{31}P\{^1H\}$ NMR ($C_6D_6$): $\delta_P$ 103.3 (s).

**Synthesis of (*p*-$CF_3$-$C_6H_4$)$Me_2SiC{\equiv}P$ (56)**

Made and calibrated in similar fashion to $Me_3SiC{\equiv}P$ from (*p*-$CF_3$-$C_6H_4$)$Me_2SiCH_2PCl_2$ with 2.2 equivalents of AgOTf and DABCO in toluene .

$^{31}P$ NMR ($C_6D_6$): $\delta_P$ 106.7 (s).

**Synthesis of $^n$BuMe$_2$SiC≡P (57)**

Made and calibrated in similar fashion to $Me_3SiC{\equiv}P$ from *p*-tolyl$Me_2SiCH_2PCl_2$ with 2.2 equivalents of AgOTf and DABCO in toluene .

$^{31}P\{^1H\}$ NMR ($C_6D_6$): $\delta_P$ 101.2 (s).

**5.4.4 Synthesis of ruthenaphosphaalkenyls (38, 39, 59-61)**

In each case, alkenic protons were assigned from 2D spectra.

**Synthesis of Ru(CO)Cl(P=CHSiMe$_3$)(PPh$_3$)$_2$ (38)**

An excess of $Me_3SiC{\equiv}P$ as a solution in toluene was added to a stirring suspension of [RuHCl(CO)($PPh_3$)$_3$] (1.0 g, 1.0 mmol) in $CH_2Cl_2$ (10 $cm^3$). After stirring the mixture for one hour, the solution was filtered and the solvent was removed under vacuum. The resulting orange solid was vigorously washed with hexanes before being isolated as a yellow orange powdered solid. Yield 93%

$^1H$ NMR ($CDCl_3$): $\delta_H$ 7.98–7.31 (30 H, m, $PPh_3$), 7.28 (1 H, br, P=C*H*), −0.04 (9 H, s, $SiMe_3$). $^{31}P\{^1H\}$ NMR ($CDCl_3$): $\delta_P$ 548.5 (t, $^2J_{P\text{-}P}$ = 8.18 Hz), 34.1 (d, $^2J_{P\text{-}P}$ = 8.18 Hz).

Crystal data for **38**: $C_{41}H_{40}ClOP_3RuSi.C_4H_{10}O$, Mw = 954.49, monoclinic, $P2_1/c$ (no. 14), a = 9.7961(5), b = 34.2580(17), c = 14.8457(7) Å, β = 95.201(5) °, V = 4961.6(4) $A^3$, Z = 4, $D_c$ = 1.278 Mg $m^{-3}$, μ(Cu- Kα) = 4.491 $mm^{-1}$, T = 173(2) K, 9180 independent reflections, full-matrix $F^2$ refinement $R_1$ = 0.0876, $wR_2$ = 0.2864 on 6502 independent absorption corrected reflections [I > 2σ(I); $2\theta_{max}$ = 141.8 °], 473 parameters, CCDC 1036624.

**Synthesis of Ru(CO)Cl(P=CHSiMe$_2$Ph)(PPh$_3$)$_2$ (39)**

Prepared in a similar fashion to that described for Ru(CO)Cl(P=CHSiMe$_3$)(PPh$_3$)$_2$ from an excess of Me$_2$PhSiC≡P in toluene with [RuHCl(CO)(PPh$_3$)$_3$] (1.0 g, 1.0 mmol) in $CH_2Cl_2$ (10 cm$^3$). Yield: 57%

$^1$H NMR ($CDCl_3$): $\delta_H$ 7.93–7.11 (m, 35H, P($C_6H_5$), ($C_6H_5$)), 7.40 (br. 1H, P=C*H*), 0.24 (s, 6H, $SiMe_2$). $^{31}P\{^1H\}$ NMR ($CDCl_3$): $\delta_P$ 553.8 (t, $^2J_{P\text{-}P}$ = 7.98 Hz), 33.8 (d, $^2J_{P\text{-}P}$ = 7.98 Hz).

Crystal data for **39**: $C_{44}H_{42}ClOP_3RuSi$, Mw = 868.37, monoclinic, $P2_1/c$ (no. 14), a = 19.6355(5), b = 11.9196(2), c = 19.5933(5) Å, β = 116.565(3) °, V = 4101.6(2) A$^3$, Z = 4, Dc = 1.406 Mg m$^{-3}$, μ(Cu-Kα) = 5.346 mm$^{-1}$, T = 173(2) K, 7897 independent reflections, full-matrix $F^2$ refinement $R_1$ = 0.0267, $wR_2$ = 0.0714 on 7237 independent absorption corrected reflections [I > 2σ(I); 2θmax = 143.6 °], 479 parameters, CCDC 1036625.

**Synthesis of [Ru(CO)Cl(P=CHSiMe$_2$*p*-tolyl)(PPh$_3$)$_2$] (59)**

Excess (*p*-$CH_3C_6H_4$)$Me_2$SiC≡P as a solution in toluene (27 cm$^3$ of 7.39x10$^{-5}$ mol/cm$^3$) was added to a stirring suspension of [RuHCl(CO)(PPh$_3$)$_3$] (1.5 g, 1.53x10$^{-3}$ mol ) in $CH_2Cl_2$ (15 cm$^3$) for 1 h. The resulting orange red solution was mixture then freed of volatiles in vacuo, before the orange/brown solid was vigorously washed with n-hexane (3 x 10 cm$^3$) affording a yellow suspension. The solvent was removed by filter cannula and the yellow/orange solids dried under partial vacuum. Yield 0.8 g, 9.0x10$^{-4}$ mol, 59 %.
Note: Aromatics signals associated with tolyl group, and the alkenic proton were assigned from 2D spectra.

$^1$H NMR ($CD_2Cl_2$): $\delta_H$ 0.20 (s, 6H, $Si(CH_3)_2$), 2.31 (s, 3H, $CH_3$), 6.9-7.46, 7,55-7.61 (2 x m, 30H $C_6H_5$, 4H $C_6H_4$, 1H P=CH) -7.39 (m, 2H, m-CH), 7.61 (m, 2H, o-CH), 7.41 (m, 1H, P=CH)). $^{13}C\{^1H\}$ NMR ($CD_2Cl_2$): $\delta_C$ 1.4 (s, $Si(CH_3)_2$ ), 21.7 (s, $CH_3$), 127.3 (dd, $J_{C\text{-}P}$ = 7 Hz, 9 Hz, CH), 128.0, (t, $J_{C\text{-}P}$ = 5 Hz, CH), 128.8 (t, $J_{C\text{-}P}$ = 5 Hz, CH), 130.1 (*ipso*-CH) 129.8 (s, CH), 129.5 (s, CH), 130.9 (s, CH), 132.8 (t, $J_{C\text{-}P}$ = 23 Hz, CH),134.3 (s, *o*-CH),135.0 (m, CH), 135.7 (m, CH), 136.5 (t, $J_{C\text{-}P}$ = 23 Hz, CH), 138.3 (*para*-CH), 165.2 (br. C=P), 202.5 (br, CO). $^{31}P\{^1H\}$ NMR ($CD_2Cl_2$): $\delta_P$ 33.7 (d, $^2J_{P\text{-}P}$ = 8 Hz, $PPh_3$), 552.6 (t, $^2J_{P\text{-}P}$ = 8 Hz, P=C). $^{29}Si\{^1H\}$ NMR ($CD_2Cl_2$): $\delta_{Si}$ -14.4. $\nu_{CO}$ = 1936 cm$^{-1}$. Anal. Found: C, 64.02; H, 5.14; Calcd for $C_{47}H_{44}ClOP_3RuSi$: C, 63.98; H, 5.03.
Crystal data: $C_{47}H_{44}ClOP_3RuSi$, $M_w$ = 882.34, monoclinic, $P2_1/c$ (no. 14), a = 19.6947(6), b = 12.0013(2), c = 19.7876(5) Å, γ = 90, β = 116.762(4) °. V= 4176.0(2) A$^3$, Z = 4 Mg/m$^3$. $\mu$(Cu-Kα) =

5.259 $mm^{-1}$, T = 173.0 K, 6511 independent reflections. Full-matrix *F2* refinement $R_1$ = 0.0384, w$R_2$ = 0.1118 on 6511 independent absorption corrected reflections F(000) = 1816.0. A yellow rod crystal with dimensions 0.1 x 0.1 x 0.1 mm was used.

**Synthesis of Ru(CO)Cl{P=CHSiMe$_2$(*p*-CF$_3$-C$_6$H$_4$)}(PPh$_3$)$_2$ (60)**

Prepared in a similar fashion to **59** from an excess of **56** added to [RuH(CO)Cl(PPh$_3$)$_3$] (**58**). Yield 75%.

$^1$H NMR ($CD_2Cl_2$): $\delta_H$ 0.27 (s, 6H, Si($CH_3$)$_2$), 7.32 (br, CHSi), 7.34-7.38 (m, 12H, $PPh_3$), 7.42-7.48 (m, 10H, CH), 7.55-7.60 (m, 12H, CH). $^{19}$F NMR ($CD_2Cl_2$): δ -63.13 (s, $CF_3$). $^{13}$C{$^1$H} NMR ($CD_2Cl_2$): $\delta_C$ -0.8 (d, $^3J_{C\text{-}P}$ = 7.7 Hz, $SiMe_2$), 124.5 (q, $J_{C\text{-}F}$ = 4 Hz, Ar), 124.5 (q, $J_{C\text{-}F}$ = 4 Hz, Ar), 125.0 (q, $^1J_{C\text{-}F}$ = 273 Hz, $CF_3$), 128.8 (t, $J_{C\text{-}P}$ = 5 Hz, Ar), 130.7 (q, $^2J_{C\text{-}F}$ = 32 Hz, $CCF_3$), 131.0 (s, Ar), 132.6 (t, $J_{C\text{-}P}$ = 23 Hz, Ar), 134.5 (m, Ar), 134.9 (t, $J_{C\text{-}P}$ = 5.6 Hz, Ar), 146.2 (d, $J_{C\text{-}P}$ = 5Hz, Ar), 162.9 (dt, *J* = 3, 77 Hz, C=P), 202.5 (t, $^2J_{C\text{-}P}$ = 14 Hz, CO). $^{31}$P{$^1$H} NMR ($CD_2Cl_2$): $\delta_P$ 33.8 (d, $^2J_{P\text{-}P}$ = 8.3 Hz, $PPh_3$), 559.7 (t, $^2J_{P\text{-}P}$ = 8.3 Hz, P=C). $^{29}$Si{$^1$H} NMR ($CD_2Cl_2$): $\delta_{Si}$ -14.03. $\nu_{CO}$ = 1939 $cm^{-1}$. Anal. Found: C, 60.45; H, 4.57; Calcd for $C_{47}H_{41}F_3ClOP_3RuSi$: C, 60.30; H, 4.41.

**Synthesis of [Ru(CO)Cl{P=CHSiMe$_2$$^n$Bu}(PPh$_3$)$_2$] (61)**

Prepared in a similar fashion to **59** from an excess of **57** added to [RuH(CO)Cl(PPh$_3$)$_3$] (**58**). Yield 82%.

$^1$H NMR ($CD_2Cl_2$): $\delta_H$ −0.06 (s, 6H, Si($CH_3$)$_2$), 0.46 (m, 2H, $SiCH_2$), 0.81 (t, 3H, $^3J_{H\text{-}H}$ = 7.11 Hz, $CH_3$), 1.16 (m, 2H, $CH_2$), 1.25 (m, 2H, $CH_2$), 7.10−7.46 (m, 20H, $PPh_3$), 7.32 (br, CHSi), 7.59−7.64 (m, 10H, $PPh_3$). $^{13}$C{$^1$H} NMR ($CD_2Cl_2$): $\delta_C$ −0.8 (d, $^3J_{C\text{-}P}$ = 7.6 Hz, $SiMe_2$), 14.2 (s, $CH_3$), 17.4 (d, $^3J_{C\text{-}P}$ = 5.5 Hz, $SiCH_2$), 26.7 (s, $CH_2$), 27.1 (s, $CH_2$), 128.0 (t, $J_{C\text{-}P}$ = 4.8, CH), 128.7 (t, *J* = 5.1 Hz, CH), 129.8 (s, CH), 130.9 (s, CH), 132.8 (t, *J* = 22.9 Hz, CH), 134.6 (br. CH), 135.0 (t, *J* = 5.6 Hz, CH), 135.1 (t, *J* = 5.7 Hz, CH), 136.4 (t, *J* = 21.6 Hz, CH), 165.9 (dt, $^1J_{P\text{-}C}$ = 76.3, $^3J_{C\text{-}P}$ = 3.0 Hz, P=C) 202.1 (t, $^2J_{C\text{-}P}$ = 14.5 Hz, CO). $^{31}$P{$^1$H} NMR ($CD_2Cl_2$) $\delta_P$ 33.84 (d, $^2J_{P\text{-}P}$ = 8.3 Hz, $PPh_3$), 545.3 (t, $^2J_{P\text{-}P}$ = 8.3 Hz, P=C). $^{29}$Si{$^1$H} NMR ($CD_2Cl_2$): $\delta_{Si}$ -7.33. $\nu_{CO}$ = 1930 $cm^{-1}$. Anal. Found: C, 62.19; H, 5.39; Calcd for $C_{44}H_{46}ClOP_3RuSi$: C, 62.30; H, 5.47.

### 5.4.5 Synthesis of bridging pyrazolyl-η$^2$–phosphaalkene compounds

**Synthesis of [Ru(CO){κ$^3$-N,C,P-P(Pz*)CH(SiMe$_2$*p*-tolyl)}(PPh$_3$)$_2$] (64)**

$^n$BuLi (0.06 cm$^3$, 2.5 M in hexanes) was added dropwise to a solution of HPz* (12.7 mg, 0.13 mmol) in tetrahydrofuran. After allowing the solution to stir for 5 minutes, it was added to a solution of **61** (0.067 g, 0.08 mmol) in tetrahydrofuran at ambient temperature. The mixture was stirred for 1 h before the solvent was removed under reduced pressure and the product was extracted in $CD_2Cl_2$ before spectroscopic analysis.

$^1$H NMR ($CDCl_3$): $\delta_H$ 0.06 (s, 3H, $SiMe_2$), 0.15 (s, 3H, $SiMe_2$), 0.42 (s, 3H, Pz*-Me), 1.75 (m, 1H, CHSi ($^1J_{C\text{-}H}$ = 135.31 Hz), 1.95 (s, 3H, Pz*-Me), 2.34 (s, 3H, $CH_3$), 5.04 (s, 1H, Pz*-H4), 7.08-7.42 (m, 35H, Ar-H). $^{13}C\{^1H\}$ NMR ($CDCl_3$): $\delta_C$ -0.9 (d, $^3J_{C\text{-}P}$ = 7.6 Hz, $SiCH_3$), 0.16 (d, $^3J_{C\text{-}P}$ = 8.5 Hz, $SiCH_3$), 9.6 (d, $^3J_{C\text{-}P}$ = 5.3 Hz, Pz-$CH_3$), 11.9 (s, Pz-$CH_3$), 21.6 (s, $CH_3$), 41.8 (ddd, $J_{C\text{-}P}$ = 4.5, 31.3, 78.6 Hz, CHSi ($^1J_{C\text{-}H}$ = 136.3 Hz)), 105.0 (d, $J_{C\text{-}P}$ = 2.7 Hz, Pz*C4), 127.6 (d, $J_{C\text{-}P}$ = 8.87 Ha, Ar-C), 127.8 (d, $J_{C\text{-}P}$ = 8.87 Hz, ArC), 128.2 (s, ArC), 128.6 (m, ArC), 128.9 (d, $J_{C\text{-}P}$ = 6.7 Hz, ArC), 130.4 (d, $J_{C\text{-}P}$ = 13.0 Hz, ArC), 133.8 m, ArC), 133.6-134.4 (m, ArC), 137.4 (s, ArC), 138.2 (d, $J_{C\text{-}P}$ = 30.7 Hz, ArC), 138.4 (d, $J_{C\text{-}P}$ = 31.8 Hz, ArC), 145.2 (s, Pz*-C5), 152.4 (s, Pz*-C3), 209.5 (br, CO). $^{31}P\{^1H\}$ NMR ($CDCl_3$): $\delta_P$ 46.7 (d, $J_{P\text{-}P}$ = 16.9 Hz), 39.1 (dd, $J_{P\text{-}P}$ = 50.1, 16.7 Hz), 32.6 (d, $J_{P\text{-}P}$ = 50.4 Hz, P=C). $^{29}Si\{^1H\}$ NMR ($CDCl_3$): $\delta_{Si}$ -5.3.

**Synthesis of [Ru(CO){κ$^3$-N,C,P-P(Pz*)CH(SiMe$_2$*p*-CF$_3$-C$_6$H$_4$)}(PPh$_3$)$_2$] (65)**

Prepared in a similar fashion to **64** from an excess of LiPz* added to [Ru(CO)Cl(P=CHSiMe$_2$C$_6$H$_4$*p*-$CF_3$)($PPh_3$)$_2$] (**60**).

$^1$H NMR ($CDCl_3$): $\delta_H$ -0.02 (s, 3H, $SiCH_3$), 0.18 (s, 3H, $SiCH_3$), 0.42 (s, 3H, Pz*-Me), 1.66 (m, 1H, CHSi ($^1J_{C\text{-}H}$ = 135.3 Hz), 1.95 (s, 3H, Pz*-Me), 5.07 (s, 1H, Pz*-H4), 7.09-7.34 (m, 35H, Ar-H), 7.45-7.56 (m, 4H, $C_6H_4CF_3$). $^{19}$F NMR ($CDCl_3$): δ -63.06 (s). $^{13}C\{^1H\}$ NMR ($CDCl_3$): $\delta_C$ -1.3 (d, $^3J_{C\text{-}P}$ = 8 Hz, $SiCH_3$), 0.3 (d, $^3J_{C\text{-}P}$ = 8 Hz, $SiCH_3$), 9.6 (d, $^3J_{C\text{-}P}$ = 5.3 Hz, Pz-$CH_3$), 11.9 (s, Pz-$CH_3$), 39.8 (br. ($^1J_{C\text{-}H}$ = 135.3 Hz) CHSi), 105.2 (d, $J_{C\text{-}P}$ = 2.9 Hz, Pz*C4), 123.8 (q, $^2J_{C\text{-}F}$ = 3.9 Hz, $CCF_3$), 130.9 (q, $^1J_{C\text{-}F}$ = 240.0 Hz, $CF_3$), 127.6-129.1, 134.1-135.5, 137.2-138.1 (3 x m, $PPh_3$, $C_6H_4$), 145.3 (d, $^2J_{C\text{-}P}$ = 1.5 Hz, Pz*-C5), 152.7 (s, Pz*-C3), 209.7 (br, CO). $^{31}P\{^1H\}$ NMR ($CDCl_3$): $\delta_P$ 46.6 (d, $^2J_{P\text{-}P}$ = 16.2 Hz, $PPh_3$), 38.6 (dd, $^2J_{P\text{-}P}$ = 54.4, 16.2 Hz, $PPh_3$), 32.1 (d, $^2J_{P\text{-}P}$ = 51.4 Hz, P=C). $^{29}Si\{^1H\}$ NMR ($CDCl_3$): $\delta_C$ -4.5. $\nu_{CO}$ = 1913 cm$^{-1}$. Anal. Found: C, 62.90; H, 5.01; N, 2.90; Calcd for $C_{52}H_{48}F_3N_2OP_3RuSi$: C, 62.71; H, 4.86; N, 2.81.

Crystal data for **65**: $C_{52}H_{48}P_3F_3N_2OSi•CHCl_3$, $M_w$=1115.42, triclinic, P-1 (no. 2), a = 10.5494(5), b = 11.5375(6), c=21.871(1) Å, α = 76.877(4), β = 82.084(4), γ = 85.941(4) °. V= 2565.6(2) $A^3$, Z = 2, Dc = 1.444 $Mg/m^3$, μ(Cu-Ka) = 5.439 $mm^{-1}$, T = 173(2) K, 9464 independent reflections. Full-matrix *F2* refinement *R*1 = 0.0567, w*R*2 = 0.1894 on 8126 independent absorption corrected reflections, F(000) = 1147.3883. A clear yellow block crystal with dimensions 0.15 x 0.15 x 0.05 mm was used. CCDC 1502285.

**Synthesis of [Ru(CO){κ$^3$-N,C,P-P(Pz*)CH(SiMe$_2$$^n$Bu)}(PPh$_3$)$_2$] (66)**

Prepared in a similar fashion to **64** from an excess of LiPz* added to [Ru(CO)Cl(P=CHSiMe$_2$$^n$Bu)(PPh$_3$)$_2$] (**61**).

$^1$H NMR ($CDCl_3$): $\delta_H$ -0.31 (s, 3H, $SiMe_2$), -0.17 (s, 3H, $SiMe_2$), 0.37 (m, 2H, $SiCH_2$), 0.43 (s, 3H, Pz*-Me), 0.85 (t, 3H, $J_{H-H}$ = 6.58 Hz, $CH_3$), 1.25 (m, 4H, 2 x $CH_2$), 1.52 (m, 1H, CHSi), 1.95 (s, 3H, Pz*-Me), 5.06 (s, 1H, Pz*-H4), 7.09-7.33 (m, 30H, Ar-H). $^{13}$C NMR ($CDCl_3$): $\delta_C$ -1.28 (d, J = 8Hz, $SiCH_3$), 0.3 (d, J = 8Hz, $SiCH_3$) 10.8 (br. Pz*-Me), 11.0 (br. Pz*-Me), 13.9 (br. $CH_2$), 14.8 (s, $CH_2$), 42.9 (br. ($^1J_{C-H}$ = 136.3 Hz), CHSi), 106.3 (br. Pz*C4), 127.4-128.1 (m, CH), 128.6 (d, *J* = 7 Hz, CH), 128.9 (s, CH), 133.8 (s, CH), 134.0 (s, CH), 134.1-134.4 (m, CH), 135.0 (d, *J* = 9 Hz, CH), 137.2 (d, *J* = 9 Hz, CH). Remaining resonances not resolved. $^{31}$P{$^1$H} NMR ($CDCl_3$): $\delta_P$ 46.5 (d, $J_{P-P}$ = 17.0 Hz, $PPh_3$), 39.3 (dd, $J_{P-P}$ = 50.3, 17.0 Hz, $PPh_3$), 34.3 (d, $J_{P-P}$ = 50.3 Hz, P=C). $^{29}$Si{$^1$H} NMR ($CDCl_3$): $\delta_{Si}$ -0.8. $\nu_{CO}$ = 1913 $cm^{-1}$. Anal. Found: C, 65.02; H, 5.90; N, 3.19; Calcd for $C_{49}H_{53}N_2OP_3RuSi$: C, 64.82; H, 5.88; N, 3.08.

**Synthesis of [Ru(CO){κ$^3$-N,C,P-P(Pz$^{CF3}$)CH(SiMe$_2$*p*-tolyl)}(PPh$_3$)$_2$] (68)**

Prepared in a similar fashion to **64** from an excess of LiPz$^{CF3}$ added to [Ru(CO)Cl(P=CHSiMe$_2$*p*-tolyl)(PPh$_3$)$_2$] (**59**).

$^1$H NMR ($CDCl_3$) $\delta_H$ -0.1 (s, 3H, $SiCH_3$), 0.1 (s, 3H, $SiCH_3$), 1.90 (m, 1H, CHSi), 2.35 (m, 3H, $CH_3$), 5.30 (s, 1H, Pz-H3), 5.57 (1 H, s, Pz-H4), 7.04-7.48 (m, 35H, $C_6H_5$). $^{19}$F NMR ($CDCl_3$) $\delta_F$ −60.4 (d ($^4J_{F-P}$ = 17.6 Hz)).$^{13}$C{$^1$H} NMR ($CDCl_3$) $\delta_C$ -0.9 (d, $^3J_{C-P}$ = 10 Hz, $SiCH_3$), -0.25 (d, $^3J_{C-P}$ = 5 Hz, $SiCH_3$), 21.9 (s, $CH_3$), 45.6 (ddd, $J_{C-P}$ = 80.5, 31.0, 4.8 Hz, ($^1J_{C-H}$ = 134 Hz), SiCH), 105.2 (s, Pz-C4), 119.5 (q, $^1J_{C-F}$ = 273 Hz, $CF_3$), 128.2–128.6, 128.7-129.2, 133.7-134.4, 137.6-138.0 (4 x m, CH), 140.9 (s, Pz-C3), 210.5 (t, $^2J_{C-P}$ = 13 Hz, C≡O). *Remaining resonances not resolved*. $^{31}$P{$^1$H} NMR ($CDCl_3$) $\delta_P$ 41.3 (dd, $^2J_{P-P}$ = 44.5, 17.5 Hz, $PPh_3$), 47.9 (d, $^2J_{P-P}$ = 17.5 Hz, $PPh_3$), 75.0 (dq, $^2J_{P-P}$ = 44.5 Hz, $^4J_{P-F}$ = 17.50 Hz, P=CH). $^{29}$Si{$^1$H} NMR ($CDCl_3$) $\delta_{Si}$ −5.6. Anal. Found: C, 62.10; H, 4.85; N, 2.91; Calcd for $C_{51}H_{46}F_3N_2OP_3RuSi$: C, 62.39; H, 4.72; N, 2.85.

**Synthesis of [Ru(CO){κ$^3$-N,C,P-P(Pz$^{CF3}$)CH(SiMe$_2$*p*-CF$_3$-C$_6$H$_4$)}(PPh$_3$)$_2$] (69)**

Prepared in a similar fashion to **64** from an excess of LiPz$^{CF3}$ added to [Ru(CO)Cl(P=CHSiMe$_2$C$_6$H$_4$*p*-CF$_3$)(PPh$_3$)$_2$] (**60**).

$^1$H NMR ($CDCl_3$) $\delta_H$ -0.06 (s, 3H, $SiCH_3$), 0.14 (s, 3H, $SiCH_3$), 1.85 (m, 1H, CHSi), 5.32 (s, 1H, Pz-H3), 5.60 (s, 1H, Pz-H4), 7.05-7.39 (m, 30H, $C_6H_5$), 7.5 (d, 2H, $J_{H-F}$ = 8.0 Hz, $C_6H_4$), 7.63 (d, 2H, $J_{H-F}$ = 7.6 Hz, $C_6H_4$). $^{19}$F NMR ($CDCl_3$) $\delta_F$ −60.1 (d ($^4J_{F-P}$ = 19.4 Hz)), -62.7 (s, $C_6H_4CF_3$). $^{13}$C{$^1$H} NMR ($CDCl_3$) $\delta_C$ 1.2 (s, $SiCH_3$), 43.8 (br. ($^1J_{C-H}$ = 134 Hz), SiCH), 104.9 (s, Pz-C$^4$), 128.0 (t, $J_{C-F}$ = 4.3 Hz, CH), 128.7 (d, $J_{C-F}$ = 7.3 Hz, CH), 128.9 (s, CH), 129.5 (s, CH), 132.2-132.6, 133.5-134.1 (2 x m, CH), 142.8 (s, Pz-C5), 145.4 (br. Pz-C3). *Remaining resonances not resolved*. $^{31}$P{$^1$H} NMR ($CDCl_3$) $\delta_P$ 37.8 (dd, $^2J_{P-P}$ = 47.4, 15.8 Hz), 47.1 (d, $^2J_{P-P}$ = 15.8 Hz, $PPh_3$), 62.0 (dq, $^2J_{P-P}$ = 47.4 Hz, $^4J_{P-F}$ = 19.40 Hz, P=CH). $^{29}$Si{$^1$H} NMR ($CDCl_3$) $\delta_{Si}$ −4.2. $\nu_{CO}$ = 1913 cm$^{-1}$.

**Synthesis of [Ru(CO){κ$^3$-N,C,P-P(Pz$^{CF3}$)CH(SiMe$_2$$^n$Bu)}(PPh$_3$)$_2$] (70)**

Prepared in a similar fashion to **64** from an excess of LiPz$^{CF3}$ added to [Ru(CO)Cl(P=CHSiMe$_2$$^n$Bu)(PPh$_3$)$_2$] (**61**).

$^1$H NMR ($CDCl_3$) $\delta_H$ -0.35 (s, 3H, $SiCH_3$), -0.16 (s, 3H, $SiCH_3$), 0.86, 1.27 (2 x m, 9H, $^n$Bu) 1.77 (m, 1H, CHSi), 5.30 (s, 1H, Pz-H3), 5.59 (1 H, s, Pz-H4), 7.18-7.62 (m, 30H, $C_6H_5$). $^{19}$F NMR ($CDCl_3$) $\delta_F$ −60.0 (d, $^4J_{F-P}$ = 17.6 Hz, **70-P-N-CCF$_3$**), -60.5 (s, **70-Ru-N-CCF$_3$**). $^{13}$C{$^1$H} NMR ($CDCl_3$) $\delta_C$ 1.2 (s, $SiCH_3$), 14.0 (s, $^n$Bu), 25.8 (s, $^n$Bu), 26.7 (s, $^n$Bu), 42.8 (br. $^1J_{C-H}$ = 135 Hz, SiCH), 127.9–128.1, 128.6-128.7, 128.9, 129.5-129.6, 133.6-134.2 (5 x m, CH), 142.8 (s, Pz-C3). *Pz-C3 and SiCH assigned on the basis of 2D spectra, remaining resonances not resolved*. $^{31}$P{$^1$H} NMR ($CDCl_3$) $\delta_P$ 38.5 (dd, $^2J_{P-P}$ = 46.2, 17.8 Hz, $PPh_3$), 47.0 (d, $^2J_{P-P}$ = 17.8 Hz, $PPh_3$), 65.0 (dq, $^2J_{P-P}$ = 46.2 Hz, $^4J_{P-F}$ = 19.50 Hz, P=CH). $^{29}$Si{$^1$H} NMR ($CDCl_3$) $\delta_{Si}$ 1.74. Anal. Found: C, 60.70; H, 5.19; N, 3.04; Calcd for $C_{48}H_{48}F_3N_2OP_3RuSi$: C, 60.82; H, 5.10; N, 2.95

**Synthesis of [Ru(CO){κ$^3$-N,C,P-P(Pz$^{MeCF3}$)CH(SiMe$_2$*p*-tolyl)}(PPh$_3$)$_2$] (71)**

Prepared in a similar fashion to **64** from an excess of LiPz$^{Me,CF3}$ added to [Ru(CO)Cl(P=CHSiMe$_2$*p*-tolyl)(PPh$_3$)$_2$] (**59**).

$^1$H NMR ($CDCl_3$): $\delta_H$ -0.03 (s, 3H, $SiCH_3$), 0.17 (s, 3H, $SiCH_3$), 0.55 (s, 3H, Pz-$CH_3$) 1.97 (br, 1H, CHSi), 2.36 (s, 3H, $CH_3$), 5.52 (br. Pz-H4), 7.12-7.50 (m, 34 H, 2x$PPh_3$, $C_6H_4$). $^{19}$F NMR ($CDCl_3$): $\delta_F$ -59.9 (d, $J_{F-P}$ = 19.4 Hz). $^{13}$C{$^1$H} NMR ($CDCl_3$): $\delta_C$ -1.1 (d, $^3J_{C-P}$ = 7.8 Hz, $SiCH_3$), 0.14 (d, $^3J_{C-P}$ = 8.8 Hz, $SiCH_3$), 11.85 (s, Pz-$CH_3$), 21.6 (m, $CH_3$), 42.1 (br. ddd, $J_{C-P}$ = 28.2, 78.8 Hz, $^1J_{C-H}$ = 137 Hz,

SiCH), 105.7 (br m, Pz-C4), 119.5 (br, $^{1}J_{C\text{-}F}$ = 269 Hz, $CF_3$), 127.6-130.3 (m, $PPh_3$), 133.5-135.1 (m, $PPh_3$, $C_6H_4$) 137.6 (dd, *J* = 1.49, 30.1 Hz, Pz-C5), 152.6 (br, Pz-C3), 209.0 (m, CO). $^{31}P\{^{1}H\}$ NMR ($CDCl_3$): $\delta_P$ 38.4 (ddd, $^{2}J_{P\text{-}P}$ = 45.7, 16.4, $J_{P\text{-}F}$ = 1.4 Hz, $PPh_3$), 47.2 (d, $^{2}J_{P\text{-}P}$ = 16.4 Hz, $PPh_3$), 61.62 (dq, $^{2}J_{P\text{-}P}$ = 45.7, $^{4}J_{P\text{-}F}$ = 19.3 Hz, P=C). $^{29}Si\{^{1}H\}$ NMR ($CDCl_3$): $\delta_{Si}$ -5.7. $\nu_{CO}$ = 1918 $cm^{-1}$. Anal. Found: C, 62.42; H, 5.05; N, 2.89; Calcd for $C_{52}H_{48}F_3N_2OP_3RuSi$: C, 62.71; H, 4.86; N, 2.81.

**Synthesis of [Ru(CO){κ$^3$-N,C,P-P(Pz$^{Me,CF3}$)CH(SiMe$_2$*p*-CF$_3$-C$_6$H$_4$)}(PPh$_3$)$_2$] (72)**

Prepared in a similar fashion to **64** from an excess of $LiPz^{MeCF3}$ added to [Ru(CO)Cl(P=CHSiMe$_2$C$_6$H$_4$*p*-$CF_3$)($PPh_3$)$_2$] (**60**).

$^{1}H$ NMR ($CDCl_3$): $\delta_H$ 0.01 (s, 3H, $SiCH_3$), 0.21 (s, 3H, $SiCH_3$), 0.56 (s, 3H, Pz-$CH_3$) 1.85 (br, 1H, CHSi), 5.54 (s, 1H, Pz-H4), 7.13-7.38, 7.4, 7.5, 7.6 (4 x m, 34H, $PPh_3$, $C_6H_4$). $^{19}F$ NMR ($CDCl_3$): $\delta_F$ -59.9 (d, *J* = 20.3 Hz, Pz-CF3), -62.7 (s, $CF_3$-*p*). $^{13}C\{^{1}H\}$ NMR ($CDCl_3$): $\delta_C$ -1.4 (d, $^{3}J_{C\text{-}P}$ = 7.4 Hz, $SiCH_3$), 0.16 (d, $^{3}J_{C\text{-}P}$ = 8.0 Hz, $SiCH_3$), 11.9 (s, Pz-$CH_3$), 40.7 (ddd, $J_{C\text{-}P}$ = 32.9, 79.8, 5.0 Hz, $^{1}J_{C\text{-}H}$ = 137 Hz, SiCH), 105.9 (br m, Pz-C4), 119.5 (q, $^{1}J_{C\text{-}F}$ = 271 Hz, $CF_3$), 124.3 (q, $^{1}J_{C\text{-}F}$ = 272 Hz, $CF_3$), 127.6-128.0 (m, CH), 128.6 (d, *J* = 7 Hz, CH), 128.5-129.1 (m, CH), 133.6-134.3 (m, CH), 137.6 (dd, *J* = 1.3, 3.2 Hz, Pz-C5), 152.8 (br, Pz-C3), 209.1 (m, CO). Remaining resonances not resolved. $^{31}P\{^{1}H\}$ NMR ($CDCl_3$): $\delta_P$ 37.8 (dd, $^{2}J_{P\text{-}P}$ = 47.0, 15.9, P=C), 47.1 (d, $^{2}J_{P\text{-}P}$ = 15.8 Hz, $PPh_3$), 61.99 (dq, $^{2}J_{P\text{-}P}$ = 57.0, $^{4}J_{P\text{-}F}$ = 18.8 Hz, $PPh_3$). $^{29}Si\{^{1}H\}$ NMR ($CDCl_3$): $\delta_{Si}$ -4.16. νCO 1917 $cm^{-1}$.

**Synthesis of [Ru(CO){κ$^3$-N,C,P-P(Pz$^{Me,CF3}$)CH(SiMe$_2$$^n$Bu)}(PPh$_3$)$_2$] (73)**

Prepared in a similar fashion to **64** from an excess of $LiPz^{Me,CF3}$ added to [Ru(CO)Cl(P=CHSiMe$_2$$^n$Bu)($PPh_3$)$_2$] (**61**).

$^{1}H$ NMR ($CDCl_3$) $\delta_H$ -0.35 (s, 3H, $SiCH_3$), -0.16 (s, 3H, $SiCH_3$), 0.40 (m, 2H, $SiCH_2$), 0.49 (s, 3H, Pz-$CH_3$) 0.80 (m, 4H, $CH_2$), 1.22 (m, 3H, $CH_3$), 1.68 (m, 1H, CHSi), 5.53 (s, 1H, Pz-H3), 7.03-7.40 (m, 30H, CH). $^{19}F$ NMR ($CDCl_3$): δ -59.9 (d, *J* = 19.8 Hz, **73-P-N-CCF$_3$**), 60.52 (s, **73-Ru-N-CCF$_3$**). $^{13}C\{^{1}H\}$ NMR ($CDCl_3$): $\delta_C$ -1.5 (s, $SiCH_3$), -0.7 (s, $SiCH_3$), 11.0 (br, $SiCH_2$), 11.9 (s, Pz-$CH_3$), 43.4 (br. $^{1}J_{C\text{-}H}$ = 137 Hz, SiCH), 105.43 (br m, Pz-C4), 121.20 (q, $J_{C\text{-}F}$ = 268 Hz, $CF_3$), 121.25 (q, $J_{C\text{-}F}$ = 267 Hz, $CF_3$) 127.6- 127.9 (t, *J* = 5 Hz, Ar), 128.2 (q, $J_{C\text{-}F}$ = 5 Hz, Pz-C3), 128.6-130.7 (m, Ar), 132.1 (d, *J* = 3H, CH), 132.3 (d, *J* = 10 Hz, CH), 133.6 (t, *J* = 12Hz, Ar), 133.7-135.2 (m, Ar), 137.0 (d, *J* = 9 Hz, Ar), 149.6 (s, Ar), 150.1 (s, CH), 152.5 (s, Pz-5). $^{31}P\{^{1}H\}$ NMR ($CDCl_3$): $\delta_P$ 38.5 (ddd, $^{2}J_{P\text{-}P}$ = 46.2, 17.8, $^{4}J_{P\text{-}F}$ = 1.4 Hz Hz, $PPh_3$), 47.0 (d, $^{2}J_{P\text{-}P}$ = 17.8 Hz, $PPh_3$), 65.0 (dq, $^{2}J_{P\text{-}P}$ = 46.2, $^{4}J_{P\text{-}F}$ = 19.3 Hz, P=C). possible assignment is limited because of the coincidence of most of the skeleton between the

two isomers. $\nu_{CO}$ = 1920 $cm^{-1}$. Anal. Found: C, 61.08; H, 5.12; N, 3.05; Calcd for $C_{49}H_{50}F_3N_2OP_3RuSi$: C, 61.19; H, 5.24; N, 2.91.

**Synthesis of [Ru(CO){κ$^3$-N,C,P-P(Pz$^{Ph}$)CH(SiMe$_3$)}(PPh$_3$)$_2$] (74)**

Prepared in a similar fashion to **64** from an excess of $LiPz^{Ph}$ added to [Ru(CO)Cl(P=CHSiMe$_3$)(PPh$_3$)$_2$] (**38**).

$^1$H NMR ($CDCl_3$): $\delta_H$ 0.15 (s, 9H, Si($CH_3$)$_3$), 1.74 (m, 1H, CHSi), 5.39 (s, 1H, Pz-H3), 5.56 (br. Pz-H4), 7.05-7.55 (m, 35H, $PPh_3$, $C_6H_5$,). $^{13}C\{^1H\}$ NMR ($CDCl_3$): $\delta_C$ 1.4 (d, $^3J_{C\text{-}P}$ = 5.5 Hz, Si($CH_3$)), 47.5 (ddd, $^2J_{P\text{-}P}$ = 4.4, 31.0, 80.2 Hz, $^1J_{C\text{-}H}$ = 135.9 Hz, SiCH), 103.3 (d, $J_{C\text{-}P}$ = 3.2 Hz, PzC4), 127.4 (d, $J_{C\text{-}P}$ = 6.6 Hz, CH), 127.7 (d, $J_{C\text{-}P}$ = 8.7Hz, CH), 128.1 (d, $J_{C\text{-}P}$ = 8.6 Hz, CH), 128.6 (s, CH), 128.8 (d, $J_{C\text{-}P}$ = 19.0 Hz, CH), 129.1 (s, CH), 133.9 (m, CH), 137.3 (d, $J_{C\text{-}P}$ = 9.7 Hz, *ipso*-C), 137.7 (d, $J_{C\text{-}P}$ = 32.0 Hz, *ipso*-C), 138.0 (d, $J_{C\text{-}P}$ = 32.0 Hz, *ipso*-CH), 141.0 (s, Pz-C3), 147.7 (br, Pz-C5), 210.7 (m, CO). $^{31}P\{^1H\}$ NMR ($CDCl_3$): $\delta_P$ 64.4 (d, $J_{P\text{-}P}$ = 46.2 Hz, P=C), 47.4 (d, $J_{P\text{-}P}$ = 18.5 Hz, $PPh_3$), 41.8 (dd, $J_{P\text{-}P}$ = 46.2, 18.4 Hz, $PPh_3$). $^{29}Si\{^1H\}$ NMR ($CDCl_3$): $\delta_{Si}$ -0.5. $\nu_{CO}$ = 1908 $cm^{-1}$. Anal. Found: C, 65.71; H, 5.18; N, 3.03; Calcd for $C_{46}H_{47}N_2OP_3RuSi$: C, 65.62; H, 5.33; N, 2.99.

**Synthesis of [Ru(CO){κ$^3$-N,C,P-P(Pz$^{Ph}$)CH(SiMe$_2$Ph)}(PPh$_3$)$_2$] (75)**

Prepared in a similar fashion to **64** from an excess of $LiPz^{Ph}$ added to [Ru(CO)Cl(P=CHSiMe$_2$Ph)(PPh$_3$)$_2$] (**39**).

$^1$H NMR ($CDCl_3$): $\delta_H$ -0.06 (s, 3H, $SiCH_3$), 0.19 (s, 3H, $SiCH_3$), 1.86 (m, 1H, CHSi), 5.40 (1H, s, Pz-H3), 5.51 (br. Pz-H4), 7.03-7.57 (m, 40H, 2x$PPh_3$, 2x$C_6H_5$). $^{13}C\{^1H\}$ NMR ($CDCl_3$): $\delta_C$ -1.7 ($SiCH_3$), -0.9 ($SiCH_3$), 41.6 ($^1J_{C\text{-}H}$ = 134.5 Hz, SiCH), 103.1 (Pz-C4), 126.0-135.8 ($PPh_3$, $C_6H_5$), 141.0 (Pz-C3), 147.9 (Pz-C5) *assignments based on 2D spectra*. $^{31}P\{^1H\}$ NMR ($CDCl_3$): $\delta_P$ 41.6 (dd, $^2J_{P\text{-}P}$ = 46.9, 17.5 Hz, $PPh_3$), 47.9 (d, $^2J_{P\text{-}P}$ = 17.5 Hz, $PPh_3$), 61.1 (d, $^2J_{P\text{-}P}$ = 46.9 Hz, P=C). $^{29}Si\{^1H\}$ NMR ($CDCl_3$): $\delta_{Si}$ -5.4. $\nu_{CO}$ = 1912 $cm^{-1}$.

**Synthesis of [Ru(CO){κ$^3$-N,C,P-P(Pz$^{Ph}$)CH(SiMe$_2$*p*-tolyl)}(PPh$_3$)$_2$] (76)**

Prepared in a similar fashion to **64** from an excess of $LiPz^{Ph}$ added to [Ru(CO)Cl(P=CHSiMe$_2$*p*-tolyl)(PPh$_3$)$_2$] (**59**).

$^1$H NMR ($CDCl_3$): $\delta_H$ -0.04 (s, 3H, $SiCH_3$), 0.21 (s, 3H, $SiCH_3$), 1.91 (m, 1H, CHSi), 2.37 (s, 3H, $CH_3$), 5.43 (1H, s, Pz-H4), 5.55 (br. Pz-H5), 7.07-7.50 (m, 39 H, 2x$PPh_3$, $C_6H_5$, $C_6H_4$). $^{13}C\{^1H\}$ NMR ($CDCl_3$): $\delta_C$ -1.5 (d, $^3J_{C\text{-}P}$ = 10 Hz, $SiCH_3$), -0.5 (d, $^3J_{C\text{-}P}$ = 6 Hz, $SiCH_3$), 21.6 (s, $CH_3$), 45.3 (ddd, $J_{C\text{-}P}$ = 4.3, 31.1, 80.1 Hz, SiCH), 103.3 (d, $J_{C\text{-}P}$ = 3.2 Hz, Pz-C4), 127.5-135.2 (2 x m, $PPh_3$, $C_6H_5$, $C_6H_4$),

141.0 (s, Pz-C3), 147.7 (s, Pz-C5), 210.7 (m, CO). $^{31}P\{^{1}H\}$ NMR ($CDCl_3$): $\delta_P$ 41.6 (dd, $^{2}J_{P\text{-}P}$ = 45.8, 18.2 Hz, $PPh_3$). 47.8 (d, $^{2}J_{P\text{-}P}$ = 18.2 Hz, $PPh_3$), 61.25 (d, $^{2}J_{P\text{-}P}$ = 45.8 Hz, P=C). $^{29}Si\{^{1}H\}$ NMR ($CDCl_3$): $\delta_{Si}$ -5.7. $\nu_{CO}$ = 1910 $cm^{-1}$.

Additional species - $^{31}P\{^{1}H\}$ NMR ($CDCl_3$): $\delta_P$ 293.0 (t, $J_{P\text{-}P}$ = 35 Hz), 18.0 (d, $J_{P\text{-}P}$ = 35 Hz).

**Synthesis of [Ru(CO){κ³-N,C,P-P(Pz$^{Ph}$)CH(SiMe$_2$*p*-CF$_3$-C$_6$H$_4$)}(PPh$_3$)$_2$] (77)**

Prepared in a similar fashion to **64** from an excess of $LiPz^{Ph}$ added to [Ru(CO)Cl(P=CHSiMe$_2$*p*-$CF_3$-$C_6H_4$)($PPh_3$)$_2$] (**59**).

$^{1}H$ NMR ($CDCl_3$): $\delta_H$ -0.03 (s, 3H, $SiCH_3$), 0.27 (s, 3H, $SiCH_3$), 1.86 (m, 1H, CHSi), 5.56 (1H, s, Pz-H4), 5.60 (s, 1H, Pz-H5), 7.11-7.68 (m, 39 H, 2x$PPh_3$, $C_6H_5$, $C_6H_4$). $^{19}F$ NMR ($CDCl_3$): $\delta_F$ 62.62 (s, $CF_3$). $^{13}C\{^{1}H\}$ NMR ($CDCl_3$): $\delta_C$ -1.3 (d, $^{3}J_{C\text{-}P}$ = 8 Hz, $SiCH_3$), -0.9 (d, $^{3}J_{C\text{-}P}$ = 5 Hz, $SiCH_3$), 45.6 (ddd, $J_{C\text{-}P}$ = 5.1, 31.4, 79.5 Hz, $^{1}J_{C\text{-}H}$ = 133.9 Hz, SiCH), 103.5 (d, $J_{C\text{-}P}$ = 3.3 Hz, Pz-C4), 124.5 (q, $^{1}J_{C\text{-}P}$ = 272 Hz, $CF_3$), 126.8 (q, *J* = 168 Hz, $CF_3$), 127.4-130.2, 133.7-134.5 (2 x m, $PPh_3$, $C_6H_5$, $C_6H_4$), 141.2 (s, Pz-C3), 147.9 (br. Pz-C5), 210.5 (m, CO). *The $CCF_3$ carbon could not be resolved due to the quality of the spectrum.* $^{31}P\{^{1}H\}$ NMR ($CDCl_3$): $\delta_P$ 41.3 (dd, $^{2}J_{P\text{-}P}$ = 46.9, 17.4 Hz, $PPh_3$). 47.72 (d, $^{2}J_{P\text{-}P}$ = 17.4 Hz, $PPh_3$), 60.56 (d, $^{2}J_{P\text{-}P}$ = 46.9 Hz, P=C). $^{29}Si\{^{1}H\}$ NMR ($CDCl_3$): $\delta_{Si}$ -4.9. $\nu_{CO}$ = 1912. Anal. Found: C, 64.02; H, 4.69; N, 2.71; Calcd for $C_{53}H_{48}F_3N_2OP_3RuSi$: C, 64.11; H, 4.77; N, 2.80.

**Synthesis of [Ru(CO){κ³-N,C,P-P(Pz$^{Ph}$)CH(SiMe$_2$$^{n}$Bu)}(PPh$_3$)$_2$] (78)**

Prepared in a similar fashion to **64** from an excess of $LiPz^{Ph}$ added to [Ru(CO)Cl(P=CHSiMe$_2$$^{n}$Bu)($PPh_3$)$_2$] (**61**).

$^{1}H$ NMR ($CDCl_3$): $\delta_H$ -0.27 (s, 3H, $SiCH_3$), 0.10 (s, 3H, $SiCH_3$), 0.47 (m, 3H, $CH_3$), 0.90 (m, 4H, $^{n}$Bu), 1.76 (m, 1H, CHSi), 5.42 (s, 1H, Pz-H4), 5.58 (d, 1H, $^{3}J_{C\text{-}P}$ = 5Hz, Pz-H5), 7.06-7.93 (m, 35 H, 2x$PPh_3$, $C_6H_5$). *Due to mixture of products, other resonances could not be resolved*. $^{31}P\{^{1}H\}$ NMR ($CDCl_3$): $\delta_P$ 41.8 (dd, $^{2}J_{P\text{-}P}$ = 45.9, 18.6 Hz, $PPh_3$). 47.6 (d, $^{2}J_{P\text{-}P}$ = 18.6 Hz, $PPh_3$), 64.5 (d, $^{2}J_{P\text{-}P}$ = 45.9 Hz, P=C). $^{29}Si\{^{1}H\}$ NMR ($CDCl_3$): $\delta_{Si}$ -0.3. $\nu_{CO}$ = 1913 $cm^{-1}$.

Additional species $^{31}P\{^{1}H\}$ NMR ($CDCl_3$): $\delta_P$ 18.5 (d, *J* = 34.8 Hz, $PPh_3$), 291.1 (t, *J* = 34.8, P=C). $^{29}Si\{^{1}H\}$ NMR ($CDCl_3$): $\delta_{Si}$ -4.1.

**Reaction between Ru(CO)Cl(P=CHSiMe$_2$$^{n}$Bu)(PPh$_3$)$_2$ (61) and LiPz$^{(CF3)2}$ (79)**

Prepared in a similar fashion to **64** from an excess of $LiPz^{(CF3)2}$ added to [Ru(CO)Cl(P=CHSiMe$_2$$^{n}$Bu)($PPh_3$)$_2$] (**61**).

$^{1}$H NMR ($CDCl_3$): $\delta_H$ -0.02 (s, 6H, $SiCH_3$), 0.43 (m, 2H, $SiCH_2$), 0.87 (t, 6H, *J* = 7Hz), 1.15 (m, 7H), 1.2 (m, 7H), 2.75 (s, 2H), 7.05-7.90 (2 x m, 30H, $PPh_3$), 7.73 (br. 1H, PzC4), $^{13}C\{^{1}H\}$ NMR ($CDCl_3$): $\delta_C$ 195. 7 (m, CO), 154.2 (d, *J* = 34 Hz, Pz-C4), 127.2-137.1 (3 x m, Ar), 47.0 (br, CHSi), 26.4 (s), 25.7 (s), 17.0 (d, *J* = 5 Hz), 13.36 (s), -0.58 (d, *J* = 4 Hz, $SiMe_2$), *other resonances could not be resolved*. $^{31}P\{^{1}H\}$ NMR ($CDCl_3$): $\delta_P$ 291.1 (t, $^{2}J_{P-P}$ = 35 Hz), 18.5 (d, $^{2}J_{P-P}$ = 35 Hz). $^{6}Li\{^{1}H\}$ NMR ($CDCl_3$): $\delta_{Li}$ 2.5 (s), 1.72 (s), 1.3 (s), 0.6 (br. s). $\nu_{CO}$ = 1936 $cm^{-1}$

### 5.4.6 Synthesis of ruthenium complex [RuHCl(CO)($PMe_3$)($PPh_3$)$_2$] (80)

An excess of $PMe_3$ (1.5 $cm^3$, 14.5 mmol) was added to a solution of **58** (1.0 g, 1.0 mmol) in dichloromethane (30 $cm^3$) and the pale yellow solution was left to stir for 16 h. The solvent was then removed to leave a yellow solid, which was washed with pentane (20 $cm^3$) to reveal a white solid. Yield: 0.45 g, 54%

$^{1}$H NMR ($CDCl_3$): $\delta_H$ -5.91 (dt, $J_{H-P}$ = 23.0, 103.3 Hz, 1H, Ru-H), 1.0 (d, $J_{H-P}$ = 6.94 Hz, 9H, $PMe_3$), 7.31, 7.69 (2 x m, 30H, 2 x $PPh_3$). $^{31}P\{^{1}H\}$ NMR ($CDCl_3$): $\delta_P$ -23.6 (m, $PMe_3$), 41.0 (m, $PPh_3$).

### 5.4.7 Synthesis of ruthenium vinyls RuCl(CO)(HC=CHR)($PPh_3$)$_2$

General literature procedure for compounds of the type [RuCl(CO)($PPh_3$)$_2$(HC=CHR)] (**79**, **82**, **83**) following literature precedure.[323,324] Excess alkyne was added to a stirring suspension of [RuHCl(CO)($PPh_3$)$_3$] in $CH_2Cl_2$ (20 $cm^3$) to give a colour change (R = Ph; red, $SiMe_3$; orange, $^{t}$Bu; orange), after 30 min to an hour, the solution was concentrated and product precipitated with $Et_2O$ to reveal orange / red solid.

### Synthesis of [RuCl(CO)(HC=CHPh)($PPh_3$)$_2$] (81)

An excess of phenylacetylene (0.25 $cm^3$, 2.2 mmol) was added to a stirring solution of [RuHCl(CO)($PPh_3$)$_3$] (1.0 g, 1.0 mmol) in $CH_2Cl_2$ (20 $cm^3$) to form a red colouration. After 15 mins the solvent was removed *in vacuo* and the solid washed with diethyl ether (5 $cm^3$) to yield a fine red solid, spectroscopic data of which was compared to literature data.[323] Yield 90%.

$^{1}$H NMR ($CDCl_3$): $\delta_H$ 5.59 (d, 1H, *J* = 13 Hz, HC=), 6.78 (d, 2H, *J* = 7.68 Hz, $C_6H_5$), 6.96 (t, 1H, *J* = 7.39 Hz, $C_6H_5$), 7.11 (t, 2H, *J* = 7.39 Hz, $C_6H_5$), 7.39-7.59 (3 x m, 30H, $P(C_6H_5)_3$), 8.40 (dt, 1H, *J* = 13.02, 1.96, Hz, =CH). $^{31}P\{^{1}H\}$ NMR ($CDCl_3$): $\delta_P$ 33.9.

**Synthesis of [RuHCl(CO)(HPz*)($PPh_3$)$_2$] (82)**

Prepared following literature procedures.[346] From an ethereal suspension of [RuHCl(CO)($PPh_3$)$_3$] (2.0g, 2.0 mmol) and HPz* (0.20 g, 2.0 mmol) heated to 50 ˚C for 1 hour and stirred for 18 hours. The impurities were removed by filtration and the resulting grey/white solid was washed with ethanol and *n*-hexanes.

$^1$H NMR ($CDCl_3$): $\delta_H$ -13.46 (t, 1H, $^2J_{H-P}$ = 19.1 Hz, Ru-H), 1.55 (s, 3H, $CH_3$) 1.73 (s, 3H, $CH_3$), 5.23 (s, 1H, Pz-H4), 6.95-7.70 (3 x m, 30H, $C_6H_5$), 11.48 (s, 1H, NH). $^{31}P\{^1H\}$ NMR ($CDCl_3$): $\delta_P$ 44.1.

**Synthesis of [RuHCl(CO)(HPz)($PPh_3$)$_2$] (83)**

Prepared following literature procedures.[347] From an ethereal suspension of RuHCl(CO)($PPh_3$)$_3$ (1.0 g, 1.0 mmol) and HPz (0.070 g, 1.0 mmol) heated to reflux for 8 hours. After allowing to cool, the yellow solution was removed from the white solid which was washed in hexanes. The impurities were removed by filtration and the resulting grey/white solid was washed with absolute ethanol and *n*-hexanes. Yield 0.50 g, 66%.

$^1$H NMR ($CDCl_3$): $\delta_H$ -13.69 (t, *J* = 19.2 Hz, 1H, Ru-H), 5.63 (q, $^3J_{H-H}$ = 2.3 Hz, Pz-H4), 6.71 (d, 2H, $^3J_{H-H}$ = 6.1 Hz, Pz-H3, Pz-H5), 7.22-7.59 (2 x m, 30H, C6$H_5$), 11.76 (br, 1H, Pz-H). $^{31}P\{^1H\}$ NMR ($CDCl_3$): $\delta_P$ 44.4.

**Synthesis of [RuCl(CO)(HC=CH$^t$Bu)($PPh_3$)$_2$] (84)**

Prepared in a similar fashion to **81** from an excess of $^t$BuC≡CH added to RuHCl(CO)($PPh_3$)$_3$ (**58**) and identified by comparison to literature spectroscopic data.[324] Yield: 54%.

'H NMR ($CDCl_3$): $\delta_H$ 0.78 (s, 9 H), 4.68 (d, 1H, *J* = 11.7 Hz, =CH), 6.96 (d, *J* = 13.0 Hz, HC=), 7.19-7.64 (2 x m, 30H, $C_6H_5$). $^{31}P\{'H\}$ NMR ($CDCl_3$): $\delta_P$ 30.0.

**Synthesis of [RuCl(CO)(HC=CHSi$Me_3$)($PPh_3$)$_2$] (85)**

Prepared in a similar fashion to **81** from an excess of $Me_3SiC$≡CH added to RuHCl(CO)($PPh_3$)$_3$ (**58**) and identified by comparison to literature spectroscopic data.[324] Yield: 63%.

$^1$H NMR ($CDCl_3$): $\delta_H$ 0.24 (s, 6H, $SiMe_2$), 0.78 (s, 3H, SiMe), 5.15 (dt, 1H, *J* = 12.9, 2.0 Hz, HC= ) 7.34-7.42 (m, 18H, Ar-H), 7.53-7.59 (m, 12H, Ar-H), 8.23 (dt, 1H, *J* = 2 Hz, 12.8 Hz, =CH). $^{31}P\{^1H\}$ NMR ($CDCl_3$): $\delta_P$ 30.71 (s).

### 5.4.8 Reactions of ruthenaphosphaalkenyls with electrophiles

**Synthesis of $[RuCl_2(P(H)ClCH_2SiMe_3)(CO)(PPh_3)_2]$ (88)**

An excess of HCl solution (1.0 $cm^3$, 1M in $Et_2O$) was added to a stirring solution of **38** (0.30 g, $3.72x10^{-4}$ mol) in $CH_2Cl_2$ (5 $cm^3$), upon addition the solution immediately decolourised to colourless/pale-yellow. After 1 hour, the solvent was removed under reduced pressure and the product washed with $Et_2O$ and hexanes before being dried *in vacuo* to a pale yellow solid. Isolated yield: 0.285 g, 87%.

$^1$H NMR ($CDCl_3$): $\delta_H$ −0.26 (s, 9H, $SiMe_3$), -0.04 (dm, 1H, $^2J_{P-H}$ = 26 Hz, $PCH_2$), 1.40 (dm, 1H, $^2J_{H-P}$ = 14.80 Hz, $PCH_2$), 5.27 (dt, 1H, $^3J_{H-H}$ = 10.8, $^1J_{PH}$ = 424.5 Hz, PH), 7.37 (m, 20H, CH(, 7.83 (t, 5H, *J* = 8Hz, CH), 8.0 (m, 5H, CH). $^{13}C\{^1H\}$ NMR ($CDCl_3$): $\delta_C$ -1.0 (s, $SiMe_3$), 16.7 (d, $J_{C-P}$ = 20.5 Hz, $PCH_2$), 127.8 (m, Ar-CH), 128.6 (s, CH), 130.0 (m, Ar-CH), 131.1 (s, CH), 131.6 (s, CH), 133.2 (s, CH), 132.9 (s, CH), 133.8 (d, $J_{C-P}$ = 18.5 Hz, CH), 134.3 (s, CH), 135.1 (m, CH), 198.9 (m CO). $^{31}P\{^1H\}$ NMR ($CDCl_3$): $\delta_P$ 84.2 (overlapping dd, $^2J_{P-P}$ = 24.3 Hz, P-C), 26.5 (signposted dd $^2J_{P-P}$ = 27.2, *J* = 343.6 Hz, $PPh_3$), 22.4 (signposted dd, $^2J_{P-P}$ =23.6, 343.6 Hz, $PPh_3$). $^{29}Si\{^1H\}$ NMR ($CDCl_3$): $\delta_{Si}$ 3.43. $\nu_{CO}$ = 1970 $cm^{-1}$. Anal. Found: C, 55.98; H, 4.73; Calcd for $C_{41}H_{42}Cl_3OP_3RuSi$: C, 56.02; H, 4.81.

Crystal data: $C_{41}H_{42}Cl_3OP_3RuSi.CH_2Cl_2$, $M_w$ = 964.09, triclinic, P-1 (no. 2), a = 12.5318(8), b = 13.0932(11), c = 15.9653(10) Å, α = 99.390(6), β = 101.138(5), γ = 116.048(7) °. V= 2215.9(3) $A^3$, Z = 2 $Mg/m^3$. $\mu$(Cu-Kα) = 1.54184 $mm^{-1}$, T = 173.0 K, 8091 independent reflections. Full-matrix *F2* refinement $R_1$ = 0.0754, w$R_2$ = 0.2294 on 8091 independent absorption corrected reflections F(000) = 984.0. A yellow block crystal with dimensions 0.2 x 0.15 x 0.05 mm was used.

**Synthesis of $[RuCl_2(P(H)ClCH_2SiMe_2Ph)(CO)(PPh_3)_2]$ (89)**

Prepared in a similar fashion to **88** from an excess of HCl added to $[Ru(CO)Cl(P{=}CHSiMe_2Ph)(PPh_3)_2]$ (**39**), on a analytical scale, after solvent and excess HCl were removed, sample was re-dissolved in $CDCl_3$ to obtain spectroscopic data, then solvent removed and cream solid dried *in vacuo*.

$^1$H NMR ($CDCl_3$): $\delta_H$ 0.01 (s, 3H, $SiMe_2$), 0.04 (s, 3H, $SiMe_2$), 0.15 (dm, 1H, $^2J_{H-P}$ = 26 Hz, $PCH_2$), 1.41 (d, 1H, $^2J_{H-P}$ = 15.2 Hz, $PCH_2$), 5.28 (dtd, 1H, $^3J_{H-H}$ = 2, 10.7, $^1J_{PH}$ = 427.8 Hz PH), 7.32 (m, 25H, CH), 7.79 (t, 5H, *J* = 8.40 Hz, CH), 7.90 (t, 5H, *J* = 8.30 Hz, CH). $^{13}C\{^1H\}$ NMR ($CDCl_3$): $\delta_C$ 1.18 (s, $SiMe_2$), 16.76 (d, $^1J_{C-P}$ = 20.8 Hz, $PCH_2$), 126.8 (m, CH), 127.9 (s, CH), 128.0 (t, $J_{C-P}$ = 8.2 Hz, CH), 129.4 (s, CH), 130.2 (m, CH), 131.3 (d, *J* = 4.4 Hz, CH), 131.7 (d, *J* = 4.5 Hz, CH), 132.4 (m, CH),

132.9 (d, $J_{C\text{-}P}$ = 5.1 Hz, CH), 133.4 (d, $J_{C\text{-}P}$ = 3.2 Hz, CH), 133.7 (s, CH), 133.9 (s, CH), 134.0 (s, CH), 134.7 (m, CH), 135.3 (t, $J_{C\text{-}P}$ = 7.7Hz, CH), 199.3 (m, CO). $^{31}P\{^{1}H\}$ NMR ($CDCl_3$): $\delta_P$ 81.5 (overlapping dd $J$ = 26.3 Hz, C-P), 27.0 (signposted dd $^{2}J_{P\text{-}P}$ =28.5, 342.5 Hz, $PPh_3$), 22.7 (signposted dd, $^{2}J_{P\text{-}P}$ =23.4, $J$ = 343.8 Hz, $PPh_3$). $^{29}Si\{^{1}H\}$ NMR ($CDCl_3$): $\delta_{Si}$ -2.7. $\nu_{CO}$ = 1968 $cm^{-1}$. Anal. Found: C, 58.62; H, 4.63; Calcd for $C_{46}H_{44}Cl_3OP_3RuSi$: C, 58.70; H, 4.71.

**Synthesis of $[RuCl_2(P(H)ClCH_2SiMe_2$*p*-tolyl)(CO)$(PPh_3)_2]$ (90)**

Prepared in a similar fashion to **88** from an excess of HCl added to [Ru(CO)Cl(P=CHSi$Me_2$*p*-tolyl)$(PPh_3)_2$] (**59**) on an analytical scale. After solvent and excess HCl were removed, the sample was re-dissolved in $CDCl_3$ to obtain spectroscopic data, then solvent removed and cream solid dried *in vacuo*.

$^{1}H$ NMR ($CDCl_3$): $\delta_H$ 0.05 (d, 6H, $^{4}J_{H\text{-}P}$ = 12.4 Hz, $SiMe_3$), 0.15 (dm, 1H, $^{2}J_{H\text{-}P}$ = 27 Hz, $PCH_2$), 1.41 (dd, 1H, $^{2}J_{H\text{-}P}$ = 2, 15.1 Hz, $PCH_2$), 2.36 (s, 3H, $CH_3$) 5.31 (dtm, 1H, $^{3}J_{H\text{-}H}$ = 10.6, $^{1}J_{PH}$ = 425.6 Hz, PH), 7.04 (m, 4H, CH), 7.38 (m, 20H, CH), 7.79 (t, 5H, $J$ = 8.36 Hz, CH), 7.89 (t, 5H, $J$ = 8.36 Hz, CH). $^{13}C\{^{1}H\}$ NMR ($CDCl_3$): $\delta_C$ 1.36 (s, $SiMe_2$). 17.0 (d, $^{1}J_{C\text{-}P}$ = 20.9 Hz, $CH_2$), 21.8 (s, $CH_2$), 182.5 (t, $J_{C\text{-}P}$ = 8.9 Hz, CH), 129.0 (s, CH), 130.8 (m, CH), 131.6 (t, $J_{C\text{-}P}$ = 2.1 Hz, CH), 131.7 (d, $J_{C\text{-}P}$ = 6.2 Hz, CH), 132.1 (d, $J_{C\text{-}P}$ = 6.2 Hz, CH), 133.5 (d, $J_{C\text{-}P}$ = 6.23 Hz, CH), 133.8 (d, $J_{C\text{-}P}$ = 6.4 Hz, CH), 134.1 (s, CH), 134.9 (m, CH), 135.6 (dd, $J_{C\text{-}P}$ = 8.3, 1.6 Hz, CH), 135.7 (dd, $J_{C\text{-}P}$ = 8.6, 1.6 Hz, CH), 139.9 (s, CH), 200.1 (m, CO). $^{31}P\{^{1}H\}$ NMR ($CDCl_3$): $\delta_P$ 82.5 (overlapping dd $J$ = 24.5 Hz, C-P), 26.4 (signposted dd $^{2}J_{P\text{-}P}$ =26.5, $J$ = 343.5 Hz, $PPh_3$), 22.7 (signposted dd, $^{2}J_{P\text{-}P}$ =24.9, $J$ = 343.5 Hz, $PPh_3$). $^{29}Si\{^{1}H\}$ NMR ($CDCl_3$): $\delta_{Si}$ -2.8. $\nu_{CO}$ = 1969 $cm^{-1}$. Anal. Found: C, 58.98; H, 4.81; Calcd for $C_{47}H_{46}Cl_3OP_3RuSi$: C, 59.10; H, 4.85.

**Synthesis of $[RuCl_2(P(H)ClCH_2SiMe_2$*p*-$CF_3$-$C_6H_4)(CO)(PPh_3)_2]$ (91)**

Prepared in a similar fashion to **88** from an excess of HCl added to [Ru(CO)Cl(P=CHSi$Me_2$*p*-$CF_3$-$C_6H_4$)$(PPh_3)_2$] (**60**), on an analytical scale. After solvent and excess HCl were removed, the sample was re-dissolved in $CDCl_3$ to obtain spectroscopic data, then solvent removed and cream solid dried *in vacuo*..

$^{1}H$ NMR ($CDCl_3$): $\delta_H$ 0.04 (d, 6H, $^{4}J_{H\text{-}P}$ = 11.4 Hz, $SiMe_2$), 0.19 (dm, 1H, $^{2}J_{H\text{-}P}$ = 25 Hz, $PCH_2$), 1.43 (dd, 1H, $^{2}J_{P\text{-}H}$ = 14.8 Hz, $^{2}J_{H\text{-}H}$ = 2.87 Hz, $CH_2P$), 5.21 (dtd, 1H, $^{3}J_{H\text{-}H}$ = 11.4, $J_{H\text{-}F}$ = 2.3 Hz, $^{1}J_{H\text{-}P}$ = 428 Hz, PH), 7.52 (s, 4H, CH), 7.35 (m, 20H, CH), 7.80 (t, 5H, $J_{H\text{-}P}$ = 8.7 Hz, CH), 7.90 (t, $J$ = 8.4 Hz, CH). $^{19}F$ NMR ($CDCl_3$): $\delta_F$ -63.0 (s). $^{13}C\{^{1}H\}$ NMR ($CDCl_3$): $\delta_C$ 1.2 (s, $SiMe_2$), 16.5 (d, $^{1}J_{C\text{-}P}$ = 21.0 Hz, C-P), 124.3 (q, $J_{C\text{-}F}$ = 134 Hz, $CF_3$) 124.3 (q, $J$ = 3.8, $CCF_3$) 128.0 (dd, $J_{C\text{-}P}$ = 11.0, 9.3 Hz, Ar), 130.3 (dd, $J$ = 1.9, 6.8 Hz, Ar), 131.1 (d, $J$ = 4.3 Hz, Ar), 131.5 (d, $J$ = 4.5 Hz, Ar), 132.9 (d, $J$ = 5.3 Hz, Ar),

133.3 (d, *J* = 5.2 Hz, Ar), 134.0 (s, Ar), 134.9 (m, Ar), 135.2 (td, *J* = 8.6, 1.2 Hz, Ar), 142.0 (m, Ar), 199.2 (m, CO). $^{31}P\{^{1}H\}$ NMR ($CDCl_3$): $\delta_P$ 79.86 (overlapping dd, $^{2}J_{P\text{-}P}$ = 25.7 Hz, CP), 27.3 (dd, $^{2}J_{P\text{-}P}$ = 27.9, *J* = 342.4 Hz, $PPh_3$), 22.6 (dd, $^{2}J_{P\text{-}P}$ = 23.4, *J* = 343.3 Hz, $PPh_3$). $^{29}Si\{^{1}H\}$ NMR ($CDCl_3$): $\delta_{Si}$ -1.9. $\nu_{CO}$ = 1968 $cm^{-1}$. MS[ESI]: m/z 983.15 [M-Cl].

**Synthesis of $[RuCl_2(P(H)ClCH_2SiMe_2{}^{n}Bu)(CO)(PPh_3)_2]$ (92)**

Prepared in a similar fashion to **86** from an excess of HCl added to $[Ru(CO)Cl(P{=}CHSiMe_2{}^{n}Bu)(PPh_3)_2]$ (**61**), on a analytical scale. After solvent and excess HCl were removed, the sample was re-dissolved in $CDCl_3$ to obtain spectroscopic data, then solvent removed and cream solid dried *in vacuo*.

$^{1}H$ NMR ($CDCl_3$): $\delta_H$ −0.3 (d, 6H, $^{4}J_{H\text{-}P}$ = 2.7 Hz, $SiMe_2$), −0.03, (dm, 1H, $^{2}J_{H\text{-}P}$ = 24 Hz, $PCH_2$) 0.21 (m, 2H, $SiCH_2$), 0.85 (t, 4H, $J_{H\text{-}H}$ = 7.22 Hz, 2 x $CH_2$) 0.98 (m, 3H, $CH_3$), 1.42 (dd, 1H, *J* = 15.0, 2.4 Hz, $CH_2P$), 5.24 (dtd, 1H, *J* = 426.1 10.46 Hz, PH), 7.36 (m, 20H, CH), 7.82 (m, 5H, CH), 7.95 (m, 5H, CH). $^{13}C\{^{1}H\}$ NMR ($CDCl_3$): $\delta_C$ -2.7 (dd, *J* = 39.5, 2.3 Hz, $SiMe_2$), 13.9 (s, $CH_2$), 15.5 (m, $SiCH_2$), 16.3 (d, $J_{C\text{-}P}$ = 21.3 Hz, $PCH_2$), 25.7 (s, $CH_2\mathbf{C}H_3$), 128.0 (d, $J_{C\text{-}P}$ = 9.1 Hz, CH), 128.1 (d, $J_{C\text{-}P}$ = 9.1 Hz, CH), 130.20 (d, $J_{C\text{-}P}$ = 4.5 Hz, CH), 130.23 (d, $J_{C\text{-}P}$ = 4.5 Hz, CH), 131.4 (d, $J_{C\text{-}P}$ = 4.2 Hz, CH), 131.8 (d, $J_{C\text{-}P}$ = 4.5 Hz, CH), 132.2 (d, $J_{C\text{-}P}$ = 9 Hz, CH), 133.0 (d, $J_{C\text{-}P}$ = 4.5 Hz, CH), 133.4 (d, $J_{C\text{-}P}$ = 4.7 Hz, CH), 133.9 (d, $J_{C\text{-}P}$ = 18.83 Hz, CH), 134.5 (m, CH), 135.3 (dd, *J* = 8.9, 4.8 Hz, CH), 199.4 (m, CO). $^{31}P\{^{1}H\}$ NMR ($CDCl_3$): $\delta_P$ 83.3 (dd, $^{2}J_{P\text{-}P}$ = 25.5 Hz, P=C), 26.8 (dd, $^{2}J_{P\text{-}P}$ = 27.6, *J* = 343.3 Hz), 22.7 (dd, $^{2}J_{P\text{-}P}$ = 23.1, *J* = 343.3 Hz). $^{29}Si\{^{1}H\}$ NMR ($CDCl_3$): $\delta_{Si}$ 4.1. $\nu_{CO}$ = 1970 $cm^{-1}$. Anal. Found: C, 57.50; H, 5.16; Calcd for $C_{44}H_{48}Cl_3OP_3RuSi$: C, 57.37; H, 5.25.

**Synthesis of $[RuCl_2(P(H)ClCH_2{}^{t}Bu)(CO)(PPh_3)_2]$ (94)**

An excess of HCl (3-4 equivalents, 1M in diethyl ether) was added to an NMR sample of $[Ru(P{=}CH{}^{t}Bu)Cl_2(CO)(PPh_3)_2]$ in $CDCl_3$. The resulting crude pale yellow solution was analysed by NMR.

$^{31}P\{^{1}H\}$ NMR ($CDCl_3$): $\delta_P$ 84.1 (overlapping dd, $^{2}J_{P\text{-}P}$ = 24 Hz, CP), 26.3 (dd, $^{2}J_{P\text{-}P}$ = 29, *J* = 344 Hz, $PPh_3$), 22.3 (dd, $^{2}J_{P\text{-}P}$ = 25, *J* = 344 Hz, $PPh_3$).
Traces of **35** present in NMR spectra: $^{31}P\{^{1}H\}$ NMR ($CDCl_3$): $\delta_P$ 350.5 (t, $^{2}J_{P\text{-}P}$ = 16 Hz).

# 6. References


1 G. Bouhadir and D. Bourissou, *Chem. Soc. Rev.*, 2016, **45**, 1065–1079.

2 D. L. Grimmett, J. A. Labinger, J. N. Bonfiglio, S. T. Masuo, E. Shearin and J. S. Miller, *J. Am. Chem. Soc.*, 1982, **104**, 6858–6859.

3 H. H. Karsch, A. Appelt, F. H. Koehler and G. Mueller, *Organometallics*, 1985, **4**, 231–238.

4 F.-G. Fontaine and D. Zargarian, *J. Am. Chem. Soc.*, 2004, **126**, 8786–8794.

5 M.-H. Thibault, J. Boudreau, S. Mathiotte, F. Drouin, O. Sigouin, A. Michaud and F.-G. Fontaine, *Organometallics*, 2007, **26**, 3807–3815.

6 J. S. Jones and F. P. Gabbaï, *Acc. Chem. Res.*, 2016, **49**, 857–867.

7 I. Kuzu, I. Krummenacher, J. Meyer, F. Armbruster and F. Breher, *Dalton Trans.*, 2008, **35**, 5836–65.

8 F.-G. Fontaine, J. Boudreau and M.-H. Thibault, *Eur. J. Inorg. Chem.*, 2008, **2008**, 5439–5454.

9 A. Amgoune, G. Bouhadir and D. Bourissou, in *Reactions of Phosphine-Boranes and Related Frustrated Lewis Pairs with Transition Metal Complexes*, Springer Berlin Heidelberg, 2012, pp. 281–311.

10 G. N. Lewis, *Valence and The Structure of Atoms and Molecules*, Chemical Catalogue Company, New York, New York, 1923.

11 H. C. Brown, H. I. Schlesinger and S. Z. Cardon, *J. Am. Chem. Soc.*, 1942, **64**, 325–329.

12 H. C. Brown and B. Kanner, *J. Am. Chem. Soc.*, 1966, **88**, 986–992.

13 G. Wittig and A. Rückert, *Justus Liebigs Ann. Chem.*, 1950, **566**, 101–113.

14 G. Wittig and E. Benz, *Chem. Ber.*, 1959, **92**, 1999–2013.

15 W. Tochtermann, *Angew. Chem. Int. Ed. Engl.*, 1966, **5**, 351–371.

16 S. Döring, G. Erker, R. Fröhlich, O. Meyer and K. Bergander, *Organometallics*, 1998, **17**, 2183–2187.

17 D. W. Stephan, *Org. Biomol. Chem.*, 2008, **6**, 1535–9.

18 D. W. Stephan and G. Erker, *Angew. Chem. Int. Ed.*, 2010, **49**, 46–76.

19 D. W. Stephan, *Dalton Trans.*, 2009, **17**, 3129–36.

20 T. Voss, T. Mahdi, E. Otten, R. Fro, G. Kehr, D. W. Stephan, G. Erker, R. Fröhlich, G. Kehr, D. W. Stephan and G. Erker, *Organometallics*, 2012, **31**, 2367–2378.

21 A. G. Massey and J. Park, *J. Organomet. Chem.*, 1964, **2**, 245–250.

22 A. G. Massey and J. Park, *J. Organomet. Chem.*, 1966, **5**, 218–225.

23 W. E. Piers and T. Chivers, *Chem. Soc. Rev.*, 1997, **26**, 345–354.

24 D. J. Parks, R. E. von H. Spence and W. E. Piers, *Angew. Chem. Int. Ed. Engl.*, 1995, **34**,

809–811.

25 E. F. Knights and H. C. Brown, *J. Am. Chem. Soc.*, 1968, **90**, 5280–5281.

26 H. C. Brown and G. Zweifel, *J. Am. Chem. Soc.*, 1960, **82**, 3222–3223.

27 D. J. Parks, W. E. Piers and G. P. A. Yap, *Organometallics*, 1998, **17**, 5492–5503.

28 P. Spies, S. Schwendemann, S. Lange, G. Kehr, R. Fröhlich and G. Erker, *Angew. Chem. Int. Ed.*, 2008, **47**, 7543–7546.

29 M. Ullrich, A. J. Lough and D. W. Stephan, *J. Am. Chem. Soc.*, 2009, **131**, 52–53.

30 Y.-X. (Eugene) Chen, M. V. Metz, L. Li, C. L. Stern and T. J. Marks, *J. Am. Chem. Soc.*, 1998, **120**, 6287–6305.

31 S. C. Binding, H. Zaher, F. Mark Chadwick and D. O'Hare, *Dalton Trans.*, 2012, **41**, 9061–9066.

32 C. Appelt, H. Westenberg, F. Bertini, A. W. Ehlers, J. C. Slootweg, K. Lammertsma and W. Uhl, *Angew. Chem. Int. Ed.*, 2011, **50**, 3925–3928.

33 D. W. Stephan, *Org. Biomol. Chem.*, 2012, **10**, 5740–5746.

34 D. W. Stephan and G. Erker, *Angew. Chem. Int. Ed.*, 2015, **54**, 6400–6441.

35 P. Laszlo, *Organic Reactions: Simplicity and Logic*, Wiley, New York, 1995.

36 P. Atkins and J. De Paula, *Atkins Physical Chemistry*, Oxford University Press, New York, 8th edn., 2006.

37 G. H. Spikes, J. C. Fettinger and P. P. Power, *J. Am. Chem. Soc.*, 2005, **127**, 12232–12233.

38 H.-J. Himmel and J. Vollet, *Organometallics*, 2002, **21**, 5972–5977.

39 J. G. de Vries and C. J. Elsevier, *The handbook of homogeneous hydrogenation*, Wiley-VCH, 2007.

40 G. C. Welch, R. R. S. Juan, J. D. Masuda and D. W. Stephan, *Science*, 2006, **314**, 1124–1126.

41 D. W. Stephan, *J. Am. Chem. Soc.*, 2015, **137**, 10018–32.

42 H. Wang, R. Fröhlich, G. Kehr and G. Erker, *Chem. Commun.*, 2008, 5966–5968.

43 G. C. Welch and D. W. Stephan, *J. Am. Chem. Soc.*, 2007, **129**, 1880–1881.

44 V. Sumerin, F. Schulz, M. Nieger, M. Leskelä, T. Repo and B. Rieger, *Angew. Chem. Int. Ed.*, 2008, **47**, 6001–6003.

45 H.-U. Blaser, C. Malan, B. Pugin, F. Spindler, H. Steiner and M. Studer, *Adv. Synth. Catal.*, 2003, **345**, 103–151.

46 C. Walling and L. Bollyky, *J. Am. Chem. Soc.*, 1964, **86**, 3750–3752.

47 A. Berkessel, T. J. S. Schubert and T. N. Müller, *J. Am. Chem. Soc.*, 2002, **124**, 8693–8698.

48 B. Chan and L. Radom, *J. Am. Chem. Soc.*, 2005, **127**, 2443–54.

49 P. A. Chase, T. Jurca and D. W. Stephan, *Chem. Commun.*, 2008, 1701–1703.

50 P. A. Chase, G. C. Welch, T. Jurca and D. W. Stephan, *Angew. Chem. Int. Ed.*, 2007, **46**, 8050–8053.

51 P. A. Chase and D. W. Stephan, *Angew. Chem. Int. Ed.*, 2008, **47**, 7433–7.

52 D. Holschumacher, T. Bannenberg, C. G. Hrib, P. G. Jones and M. Tamm, *Angew. Chem. Int. Ed.*, 2008, **47**, 7428–7432.

53 X. Yin and J. R. Moss, *Coord. Chem. Rev.*, 1999, **181**, 27–59.

54 A. E. Ashley, A. L. Thompson and D. O'Hare, *Angew. Chem. Int. Ed.*, 2009, **48**, 9839–9843.

55 A. E. Ashley, T. J. Herrington, G. G. Wildgoose, H. Zaher, A. L. Thompson, N. H. Rees, T. Krämer and D. O'Hare, *J. Am. Chem. Soc.*, 2011, **133**, 14727–14740.

56 R. Dobrovetsky and D. W. Stephan, *J. Am. Chem. Soc.*, 2013, **135**, 4974–4977.

57 A. M. Chapman, M. F. Haddow and D. F. Wass, *J. Am. Chem. Soc.*, 2011, **133**, 18463–78.

58 J. Boudreau, M.-A. Courtemanche and F.-G. Fontaine, *Chem. Commun.*, 2011, **47**, 11131–11133.

59 G. Ménard and D. W. Stephan, *Angew. Chem. Int. Ed.*, 2011, **50**, 8396–8399.

60 G. Ménard and D. W. Stephan, *J. Am. Chem. Soc.*, 2010, **132**, 1796–1797.

61 S. Roters, C. Appelt, H. Westenberg, A. Hepp, J. C. Slootweg, K. Lammertsma and W. Uhl, *Dalton Trans.*, 2012, **41**, 9033–9045.

62 M. A. Dureen and D. W. Stephan, *J. Am. Chem. Soc.*, 2010, **132**, 13559–13568.

63 T. W. Bentley, *J. Org. Chem.*, 1982, **47**, 60–64.

64 A. B. Burg and H. I. Schlesinger, *J. Am. Chem. Soc.*, 1937, **59**, 780–787.

65 M. Sajid, L.-M. Elmer, C. Rosorius, C. G. Daniliuc, S. Grimme, G. Kehr and G. Erker, *Angew. Chem. Int. Ed.*, 2013, **52**, 2243–6.

66 D. W. Stephan, S. Greenberg, T. W. Graham, P. Chase, J. J. Hastie, S. J. Geier, J. M. Farrell, C. C. Brown, Z. M. Heiden, G. C. Welch and M. Ullrich, *Inorg. Chem.*, 2011, **50**, 12338–12348.

67 A. Berkefeld, W. E. Piers and M. Parvez, *J. Am. Chem. Soc.*, 2010, **132**, 10660–10661.

68 G. Erker, *Dalton Trans.*, 2011, **40**, 7475–7483.

69 K. V. Axenov, G. Kehr, R. Fröhlich and G. Erker, *Organometallics*, 2009, **28**, 5148–5158.

70 A. M. Chapman, M. F. Haddow and D. F. Wass, *J. Am. Chem. Soc.*, 2011, **133**, 8826–8829.

71 O. J. Metters, S. J. K. Forrest, H. A. Sparkes, I. Manners and D. F. Wass, *J. Am. Chem. Soc.*, 2016, **138**, 1994–2003.

72 A. T. Normand, C. G. Daniliuc, B. Wibbeling, G. Kehr, P. Le Gendre and G. Erker, *J. Am. Chem. Soc.*, 2015, **137**, 10796–10808.

73 A. T. Normand, C. G. Daniliuc, G. Kehr, P. Le Gendre and G. Erker, *Dalton Trans.*, 2016, **45**, 3711–3714.

74 A. M. Chapman and D. F. Wass, *Dalton Trans.*, 2012, **41**, 9067–9072.

75 A. T. Normand, P. Richard, C. Balan, C. G. Daniliuc, G. Kehr, G. Erker and P. Le Gendre, *Organometallics*, 2015, **34**, 2000–2011.

76 W. H. Harman and J. C. Peters, *J. Am. Chem. Soc.*, 2012, **134**, 5080–5082.

77 M. Rakowski DuBois and D. L. DuBois, *Acc. Chem. Res.*, 2009, **42**, 1974–1982.

78 A. Berkefeld, W. E. Piers, M. Parvez, L. Castro, L. Maron and O. Eisenstein, *J. Am. Chem. Soc.*, 2012, **134**, 10843–10851.

79 M. J. Sgro and D. W. Stephan, *Chem. Commun.*, 2013, **49**, 2610–2.

80 G. J. Kubas, *Science*, 2006, **314**, 1096–1097.

81 T. J. Tague and L. Andrews, *J. Am. Chem. Soc.*, 1994, **116**, 4970–4976.

82 T. A. Rokob, A. Hamza, A. Stirling, T. Soós and I. Pápai, *Angew. Chem. Int. Ed.*, 2008, **47**, 2435–2438.

83 A. Moroz, R. L. Sweany and S. L. Whittenburg, *J. Phys. Chem.*, 1990, **94**, 1352–1357.

84 A. Hamza, A. Stirling, T. András Rokob and I. Pápai, *Int. J. Quantum Chem.*, 2009, **109**, 2416–2425.

85 S. Grimme, H. Kruse, L. Goerigk and G. Erker, *Angew. Chem. Int. Ed.*, 2010, **49**, 1402–1405.

86 L. Zhao, H. Li, G. Lu and Z.-X. Wang, *Dalton Trans.*, 2010, **39**, 4038–4047.

87 R. Ponec and P. Beran, *J. Phys. Chem. A*, 2013, **117**, 2656–2663.

88 D. M. Camaioni, B. Ginovska-Pangovska, G. K. Schenter, S. M. Kathmann and T. Autrey, *J. Phys. Chem. A*, 2012, **116**, 7228–37.

89 T. Soós, *Pure Appl. Chem.,* 2011, **83**, 667.

90 A. Fischbach, P. R. Bazinet, R. Waterman and T. D. Tilley, *Organometallics*, 2008, **27**, 1135–1139.

91 H. Schmidbaur, M. Sigl and A. Schier, *J. Organomet. Chem.*, 1997, **529**, 323–327.

92 P. Spies, R. Fröhlich, G. Kehr, G. Erker and S. Grimme, *Chem. - A Eur. J.*, 2008, **14**, 333–343.

93 P. Spies, G. Erker, G. Kehr, K. Bergander, R. Fröhlich, S. Grimme and D. W. Stephan, *Chem. Commun.*, 2007, **2**, 5072–5074.

94 M. Erdmann, C. Rösener, T. Holtrichter-Rößmann, C. G. Daniliuc, R. Fröhlich, W. Uhl, E.-U. Würthwein, G. Kehr and G. Erker, *Dalton Trans.*, 2013, **42**, 709–718.

95 P. Spies, G. Kehr, K. Bergander, B. Wibbeling, R. Fröhlich and G. Erker, *Dalton Trans.*, 2009, 1534–1541.

96 G. Kehr, S. Schwendemann and G. Erker, *Top. Curr. Chem.*, 2013, **332**, 45–83.

97 P. Binger and R. Köster, *J. Organomet. Chem.*, 1974, **73**, 205–210.

98 A. M. Chapman, S. R. Flynn and D. F. Wass, *Inorg. Chem.*, 2016, **55**, 1017–1021.

99 J. Bauer, H. Braunschweig, R. D. Dewhurst and K. Radacki, *Chem. - A Eur. J.*, 2013, **19**, 8797–8805.

100 J. Grobe, K. Lütke-Brochtrup, B. Krebs, M. Läge, H. H. Niemeyer and E. U. Würthwein, *Z. Naturforsch. B.*, 2006, **61**, 882–895.

101 P. K. Byers, A. J. Canty and R. T. Honeyman, *Adv. Organomet. Chem.*, 1992, **34**, 1–65.

102 C. Slugovc, R. Schmid and K. Kirchner, *Coord. Chem. Rev.*, 1999, **185-186**, 109–126.

103 S. Trofimenko, *Scorpionates: The Coordination Chemistry of Polypyrazolylborate Ligands*, World Scientific, 1999, vol. 3.

104 C. Slugovc, I. Padilla-Martínez, S. Sirol and E. Carmona, *Coord. Chem. Rev.*, 2001, **213**, 129–157.

105 I. R. Crossley, *Adv. Organomet. Chem.*, 2008, 56, 199–321.

106 C. Pettinari, *Scorpionates II : chelating borate ligands*, Imperial College Press, London, 2008.

107 I. R. Crossley, *Advances in Organometallic Chemistry Volume 58*, Elsevier, 2010, vol. 58.

108 A. F. Hill, G. R. Owen, A. J. P. White and D. J. Williams, *Angew. Chem. Int. Ed.*, 1999, **38**, 2759–2761.

109 I. R. Crossley and A. F. Hill, *Dalton Trans.*, 2008, 201–203.

110 N. Tsoureas, Y.-Y. Kuo, M. F. Haddow and G. R. Owen, *Chem. Commun.*, 2011, **47**, 484–486.

111 I. R. Crossley, A. F. Hill and A. C. Willis, *Organometallics*, 2007, **26**, 3891–3895.

112 S. Mummadi, D. K. Unruh, J. Zhao, S. Li and C. Krempner, *J. Am. Chem. Soc.*, 2016, **138**, 3286–3289.

113 A. G. Brook, F. Abdesaken, B. Gutekunst, G. Gutekunst and R. K. Kallury, *J. Chem. Soc. Chem. Commun.*, 1981, **4**, 191.

114 R. West, M. J. Fink and J. Michl, *Science*, 1981, **214**, 1343–1344.

115 J. Waluk, H. P. Klein, A. J. Ashe and J. Michl, *Organometallics*, 1989, **8**, 2804–2808.

116 R. J. P. Corriu, G. F. Lanneau and D. Leclercq, *Tetrahedron*, 1989, **45**, 1959–1974.

117 J. F Nixon, K. B Dillon and F. Mathey, *Phosphorus: The Carbon Copy*, Wiley, Chichester.

118 R. Appel., *Pure Appl. Chem*, **59**, 977–982.

119 K. S. Pitzer, *J. Am. Chem. Soc.*, **70**, 2140–2145.

120 T. E. Gier, *J. Am. Chem. Soc.*, 1961, **83**, 1769–1770.

121 H. W. Kroto, *Chem. Soc. Rev.*, 1982, **11**, 435–491.

122 W. Ensslin, H. Bock and G. Becker, *J. Am. Chem. Soc.*, 1974, **96**, 2757–2762.

123 D. C. Frost, S. T. Lee and C. A. McDowell, *Chem. Phys. Lett.*, 1973, **23**, 472–475.

124 P. Atkins and L. Jones, *Chemical Principles: The Quest for Insight*, W. H Freeman and Company, 3rd Ed., 2004.

125 M. J. Hopkinson, H. W. Kroto, J. F. Nixon and N. P. C. Simmons, *J. Chem. Soc., Chem. Commun.*, **13**, 513–515.

126 G. Becker, G. Gresser and W. Uhl, *Z. Naturforsch. B.*, 1981, **36**, 16–19.

127 M. Y. Antipin, A. N. Chernega, K. A. Lysenko, Y. T. Struchkov and J. F. Nixon, *J. Chem. Soc., Chem. Commun.*, 1995, **5**, 505–506.

128 J. E. Huheey, E. A. Keiter and R. L. Keiter, in *SpringerReference*, Springer-Verlag, Berlin/Heidelberg, 1993, pp. A25–A33.

129 J. C. T. R. Burckett St. Laurent, M. A. King, H. W. Kroto, J. F. Nixon and R. J. Suffolk, *J.*

*Chem. Soc., Dalt. Trans.*, 1983, **4**, 755–759.

130 M. Regitz and P. Binger, *Angew. Chem. Int. Ed. Engl.*, 1988, **27**, 1484–1508.

131 J. C. T. R. Burckett St. Laurent, T. A. Cooper, H. W. Kroto, J. F. Nixon, O. Ohashi and K. Ohno, *J. Mol. Struct.*, 1982, **79**, 215–220.

132 N. P. C. Westwood, H. W. Kroto, J. F. Nixon and N. P. C. Simmons, *J. Chem. Soc. Dalton. Trans.*, 1979, 1405.

133 H. W. Kroto, J. F. Nixon and N. P. C. Simmons, *J. Mol. Spectrosc.*, 1979, **77**, 270.

134 H. W. Kroto, N. P. C. Simmons and N. P. C. Westwood, *J. Am. Chem. Soc.*, 1978, **100**, 446–448.

135 H. W. Kroto, J. F. Nixon and N. P. C. Simmons, *J. Mol. Spectrosc.*, 1980, **82**, 185–192.

136 J. Guillemin, T. Janati and J. Denis, *J. Org. Chem.*, 2001, 7864–7868.

137 J. G. Cordaro, D. Stein, H. Rüegger and H. Grützmacher, *Angew. Chem. Int. Ed.*, 2006, **45**, 6159–6162.

138 C. E. Averre, M. P. Coles, I. R. Crossley and I. J. Day, *Dalton Trans.*, 2012, **41**, 278–284.

139 J. C. Guillemin, T. Janati, J. M. Denis, P. Guenot and P. Savignac, *Angew. Chem. Int. Ed. Engl.*, 1991, **30**, 196–198.

140 R. Appel, G. Maier, H. P. Reisenauer and A. Westerhaus, *Angew. Chem. Int. Ed. Engl.*, 1981, **20**, 197–197.

141 J.-C. Guillemin, T. Janati and J.-M. Denis, *J. Chem. Soc. Chem. Commun.*, 1992, 415–416.

142 S. Haber, P. Le Floch and F. Mathey, *J. Chem. Soc. Chem. Commun.*, 1992, 1799–1800.

143 V. Greenacre, MChem. Dissertation, University of Sussex, 2012.

144 S. M. Mansell, M. Green, R. J. Kilby, M. Murray and C. A. Russell, *C. R. Chim.*, 2010, **13**, 1073–1081.

145 G. Märkl and H. Sejpka, *Tetrahedron Lett.*, 1986, **27**, 171–174.

146 C. Jones and M. Waugh, *J. Organomet. Chem.*, 2007, **692**, 5086–5090.

147 K. Toyota, S. Kawasaki and M. Yoshifuji, *J. Org. Chem.*, 2004, **69**, 5065–5070.

148 M. Brönstrup, J. Gottfriedsen, I. Kretzschmar, S. J. Blanksby, H. Schwarz and H. Schumann, *Phys. Chem. Chem. Phys.*, 2000, **2**, 2245–2250.

149 M. Westerhausen, S. Schneiderbauer, H. Piotrowski, M. Suter and H. Nöth, *J. Organomet. Chem.*, 2002, **644**, 189–193.

150 M. Brym and C. Jones, *Dalton Trans.*, 2003, 3665–3667.

151 F. Brodkorb, M. Brym, C. Jones and C. Schulten, *J. Organomet. Chem.*, 2006, **691**, 1025–1029.

152 G. Becker, W. Schwarz, N. Seidler and M. Westerhausen, *Zeitschrift für Anorg. und Allg. Chemie*, 1992, **612**, 72–82.

153 F. F. Puschmann, D. Stein, D. Heift, C. Hendriksen, Z. A. Gal, H.-F. Grützmacher and H. Grützmacher, *Angew. Chem. Int. Ed.*, 2011, **50**, 8420–8423.

154 I. Krummenacher and C. C. Cummins, *Polyhedron*, 2012, **32**, 10–13.

155 A. R. Jupp and J. M. Goicoechea, *Angew. Chem. Int. Ed.*, 2013, **52**, 10064–10067.

156 A. M. Tondreau, Z. Benkő, J. R. Harmer and H. Grützmacher, *Chem. Sci.*, 2014, **5**, 1545–1554.

157 T. P. P. Robinson, M. J. J. Cowley, D. Scheschkewitz and J. M. M. Goicoechea, *Angew. Chem. Int. Ed.*, 2015, **54**, 683–686.

158 M. Regitz, *Chem. Rev.*, 1990, **90**, 191–213.

159 F. Hahn, L. Wittenbecher, Le Van D, R. Fröhlich and B. Wibbeling, *Angew. Chem. Int. Ed.*, 2000, **39**, 2307–2310.

160 M. Weidenbruch, S. Olthoff, K. Peters and H. G. von Schnering, *Chem. Commun.*, 1997, 1433–1434.

161 A. H. Cowley, S. W. Hall, C. M. Nunn and J. M. Power, *J. Chem. Soc. Chem. Commun.*, 1988, 753–754.

162 O. Wagner, M. Ehle and M. Regitz, *Angew. Chem. Int. Ed. Engl.*, 1989, **28**, 225–226.

163 G. M. Jamison, R. S. Saunders, D. R. Wheeler, M. D. McClain, D. A. Loy and J. W. Ziller, *Organometallics*, 1996, **15**, 16–18.

164 A. H. Cowley, S. W. Hall, C. M. Nunn and J. M. Power, *Angew. Chem. Int. Ed. Engl.*, 1988, **27**, 838–839.

165 B. Wrackmeyer and U. Klaus, *J. Organomet. Chem.*, 1996, **520**, 211–226.

166 E. P. O. Fuchs, W. Rösch and M. Regitz, *Angew. Chem. Int. Ed. Engl.*, 1987, **26**, 1011–1012.

167 F. Mathey, *Angew. Chem. Int. Ed.*, 2003, **42**, 1578–1604.

168 J. F. Nixon, *Chem. Rev.*, 1988, **88**, 1327–1362.

169 P. B. Hitchcock, M. J. Maah and J. F. Nixon, *J. Chem. Soc., Chem. Commun.*, 1986, **10**, 737–738.

170 P. Binger, R. Milczarek, R. Mynott, M. Regitz and W. Rösch, *Angew. Chem. Int. Ed. Engl.*, 1986, **25**, 644–645.

171 P. B. Hitchcock, M. J. Maah, J. F. Nixon and C. Woodward, *J. Chem. Soc. Chem. Commun.*, 1987, 844–845.

172 J. Malberg, T. Wiegand, H. Eckert, M. Bodensteiner and R. Wolf, *Chem. A Eur. J.*, 2013, **19**, 2356–2369.

173 P. Binger, J. Stannek, B. Gabor, R. Mynott, J. Bruckmann, C. Krüger and S. Leininger, *Angew. Chem. Int. Ed. Engl.*, 1995, **34**, 2227–2230.

174 F. Tabellion, A. Nachbauer, S. Leininger, C. Peters, F. Preuss and M. Regitz, *Angew. Chem. Int. Ed.*, 1998, **37**, 1233–1235.

175 S. B. Clendenning, P. B. Hitchcock and J. F. Nixon, *Chem. Commun.*, 1999, 1377–1378.

176 S. B. Clendenning, P. B. Hitchcock, G. A. Lawless, J. F. Nixon and C. W. Tate, *J. Organomet. Chem.*, 2010, **695**, 717–720.

177 P. L. Arnold, F. G. N. Cloke, P. B. Hitchcock and J. F. Nixon, *J. Am. Chem. Soc.*, 1996, **118**, 7630–7631.

178 R. L. Falconer and C. A. Russell, *Coord. Chem. Rev.*, 2015, **297-298**, 146–167.

179 J. C. T. R. Burckett St. Laurent, P. B. Hitchcock, H. W. Kroto and J. F. Nixon, *J. Chem. Soc. Chem. Commun.*, 1981, 1141–1143.

180 S. I. Al-Resayes, P. B. Hitchcock, M. F. Meidine and J. F. Nixon, *J. Chem. Soc. Chem. Commun.*, 1984, **4**, 1080–1082.

181 P. Binger, B. Biedenbach, A. T. Herrmann, F. Langhauser, P. Betz, R. Goddard and C. Krüger, *Chem. Ber.*, 1990, **123**, 1617–1623.

182 P. B. Hitchcock, M. J. Maah, J. F. Nixon, J. A. Zora, G. J. Leigh and M. A. Bakar, *Angew. Chem. Int. Ed. Engl.*, 1987, **26**, 474–475.

183 P. B. Hitchcock, M. Amélia, N. D. A. Lemos, M. F. Meidine, J. F. Nixon and A. J. L. Pombeiro, *J. Organomet. Chem.*, 1991, **402**, C23–C26.

184 D. Carmichael, S. I. Al-Resayes and J. F. Nixon, *J. Organomet. Chem.*, 1993, **453**, 207–210.

185 J. C. T. R. Burckett St. Laurent, P. B. Hitchcock, H. W. Kroto, M. F. Meidine and J. F. Nixon, *J. Organomet. Chem.*, 1982, **238**, C82–C84.

186 H. Jun, V. G. Young and R. J. Angelici, *J. Am. Chem. Soc.*, 1992, **114**, 10064–10065.

187 H. Jun and R. J. Angelici, *Organometallics*, 1994, **13**, 2454–2460.

188 A. Ehlers, J. G. Cordaro, D. Stein and H. Grützmacher, *Angew. Chem. Int. Ed.*, 2007, **46**, 7878–81.

189 S. M. Mansell, M. Green and C. A. Russell, *Dalton Trans.*, 2012, **41**, 1–9.

190 N. Trathen, *Ph.D Thesis, University of Sussex*, 2014.

191 N. Trathen, M. C. Leech, I. R. Crossley, V. K. Greenacre and S. M. Roe, *Dalton Trans.*, 2014, **43**, 9004–9007.

192 R. Appel, C. Casser and F. Knoch, *Chem. Ber.*, 1984, **117**, 2693–2702.

193 A. J. Saunders, *Ph.D Thesis, University of Sussex*, 2014.

194 S. Lacombe, D. Gonbeau, J. L. Cabioch, B. Pellerin, J. M. Denis and G. Pfister-Guillouzo, *J. Am. Chem. Soc.*, 1988, **110**, 6964–6967.

195 K. Issleib, E. Leißring, M. Riemer and H. Oehme, *Zeitschrift für Chemie*, 2010, **23**, 99–100.

196 O. Kühl, *Phosphorus-31 NMR spectroscopy: A Concise Introduction for the Synthetic Organic and Organometallic Chemist*, 2009.

197 E. P. O. Fuchs, H. Heydt, M. Regitz, W. W. Schoeller and T. Busch, *Tetrahedron Lett.*, 1989, **30**, 5111–5114.

198 J. Grobe, D. Le Van and J. Nientiedt, *Z. Naturforsch., B.*, 1986, **41b**, 149–161.

199 J. Grobe, D. Le Van, J. Nientiedt, B. Krebs and M. Dartmann, *Chem. Ber.*, 1988, **121**, 655–664.

200 L. Weber, *Eur. J. Inorg. Chem*, 2000, 2425–2441.

201 V. A. Wright, B. O. Patrick, C. Schneider and D. P. Gates, *J. Am. Chem. Soc.*, 2006, **128**, 8836–8844.

202 V. B. Gudimetla, A. L. Rheingold, J. L. Payton, H.-L. Peng, M. C. Simpson and J. D. Protasiewicz, *Inorg. Chem.*, 2006, **45**, 4895–901.

203 G. Recker, *Zeitschrift für Anorg. und Allg. Chemie*, 1976, **423**, 242–254.

204 R. Appel and B. Laubach, *Tetrahedron Lett.*, 1980, **21**, 2497–2500.

205 R. Appel and W. Paulen, *Tetrahedron Lett.*, 1983, **24**, 2639–2642.

206 K. Issleib, H. Schmidt and H. Meyer, *J. Organomet. Chem.*, 1978, **160**, 47–57.

207 K. Issleib, H. schmidt and H. Meyer, *J. Organomet. Chem.*, 1980, **192**, 33–39.

208 T. C. Klebach, R. Lourens and F. Bickelhaupt, *J. Am. Chem. Soc.*, 1978, **100**, 4886–4888.

209 A. Jouaiti, M. Geoffroy and G. Bernardinelli, *Tetrahedron Lett.*, 1992, **33**, 5071–5074.

210 M. Yoshifuji, K. Toyota and N. Inamoto, *Tetrahedron Lett.*, 1985, **26**, 1727–1730.

211 H. Oehme, E. Leissring and H. Meyer, *Tetrahedron Lett.*, 1980, **21**, 1141–1144.

212 S. Shah and J. D. Protasiewicz, *Chem. Commun.*, 1998, 1585–1586.

213 P. Le Floch, A. Marinetti, L. Ricard and F. Mathey, *J. Am. Chem. Soc.*, 1990, **112**, 2407–2410.

214 C. C. Cummins, R. R. Schrock and W. M. Davis, *Angew. Chem. Int. Ed. Engl.*, 1993, **32**, 756–759.

215 T. L. Breen and D. W. Stephan, *J. Am. Chem. Soc.*, 1995, **117**, 11914–11921.

216 L. Weber, *Angew. Chem. Int. Ed.*, 2002, **41**, 563–572.

217 D. Gudat, M. Nieger, K. Schmitz and L. Szarvas, *Chem. Commun.*, 2002, 1820–1821.

218 T. C. Klebach, R. Lourens, F. Bickelhaupt, C. H. Stam and A. Van Herk, *J. Organomet. Chem.*, 1981, **210**, 211–221.

219 H. Eshtiagh-Hosseini, H. W. Kroto, J. F. Nixon, M. J. Maah and M. J. Taylor, *J. Chem. Soc. Chem. Commun.*, 1981, 199–200.

220 S. I. Al-Resayes, S. I. Klein, H. W. Kroto, M. F. Meidine and J. F. Nixon, *J. Chem. Soc., Chem. Commun.*, 1983, 930–932.

221 T. A. Van der Knaap, F. Bickelhaupt, H. Van der Poel, G. Van Koten and C. H. Stam, *J. Am. Chem. Soc.*, 1982, **104**, 1756–1757.

222 S. Holand, C. Charrier, F. Mathey, J. Fischer and A. Mitschler, *J. Am. Chem. Soc.*, 1984, **106**, 826–828.

223 W. Schnurr and M. Regitz, *Tetrahedron Lett.*, 1989, **30**, 3951–3954.

224 T. Allspach, M. Regitz, G. Becker and W. Becker, *Synthesis*, 1986, 31–36.

225 A. J. Ashe, *J. Am. Chem. Soc.*, 1971, **93**, 3293–3295.

226 J. Grundy and F. Mathey, *Angew. Chem. Int. Ed.*, 2005, **44**, 1082–1084.

227 C. Müller, L. E. E. Broeckx, I. de Krom and J. J. M. Weemers, *Eur. J. Inorg. Chem.*, 2013, **2013**, 187–202.

228 C. Müller and D. Vogt, *Dalton Trans.*, 2007, 5505–5523.

229 L. Weber and K. Reizig, *Angew. Chem. Int. Ed. Engl.*, 1985, **24**, 53–54.

230 S. Ito, K. Toyota and M. Yoshifuji, *Chem. Commun.*, 1997, 1637–1638.

231 M. Yoshifuji, T. Niitsu and N. Inamoto, *Chem. Lett.*, 1988, 1733–1734.

232 M. van der Sluis, J. B. M. Wit and F. Bickelhaupt, *Organometallics*, 1996, **15**, 174–180.

233 E. Niecke, M. Nieger, O. Schmidt, D. Gudat and W. W. Schoeller, *J. Am. Chem. Soc.*, 1999, **121**, 519–522.

234 J. Renner, U. Bergsträßer, P. Binger and M. Regitz, *Eur. J. Inorg. Chem.*, 2000, 2337–2340.

235 S. Aldridge, C. Jones, P. C. Junk, A. F. Richards and M. Waugh, *J. Organomet. Chem.*, 2003, **665**, 127–134.

236 C. Jones and A. F. Richards, *J. Organomet. Chem.*, 2001, **629**, 109–113.

237 L. Weber, S. Uthmann, B. Torwiehe and R. Kirchhoff, *Organometallics*, 1997, **16**, 3188–3193.

238 L. Weber, S. Kleinebekel, A. Rühlicke, H. Stammler and B. Neumann, *Eur. J. Inorg. Chem.*, 2000, **2000**, 1185–1191.

239 R. B. Bedford, A. F. Hill and C. Jones, *Angew. Chem. Int. Ed. Engl.*, 1996, **35**, 547–549.

240 A. S. Balueva and O. A. Erastov, *Russ. Chem. Bull.*, 1988, **37**, 151–153.

241 A. S. Balueva and G. N. Nikonov, *Russ. Chem. Bull.*, 1993, **42**, 341–343.

242 A. S. Balueva, G. N. Nikonov, S. G. Vul'fson, N. N. Sarvarova and B. A. Arbuzov, *Russ. Chem. Bull.*, 1990, **39**, 2367–2370.

243 A. S. Balueva, Y. Y. Efremov, V. M. Nekhoroshkov and O. A. Erastov, *Bull. Russ. Acad. Sci. Div. Chem. Sci.*, 1990, **38**, 2793–2796.

244 O. Ekkert, G. Kehr, R. Fröhlich and G. Erker, *J. Am. Chem. Soc.*, 2011, **133**, 4610–4616.

245 I. P. Beletskaya, V. V. Afanasiev, M. A. Kazankova and I. V. Efimova, *Org. Lett.*, 2003, **5**, 4309–4311.

246 H. D. Empsall, E. M. Hyde, E. Mentzer and B. L. Shaw, *J. Chem. Soc. Dalton. Trans.*, 1977, 2285–2291.

247 V. V. Afanasiev, I. P. Beletskaya, M. A. Kazankova, I. V. Efimova and M. U. Antipin, *Synthesis*, 2003, 2835–2838.

248 B. Liu, K. K. Wang and J. L. Petersen, *J. Org. Chem.*, 1996, **61**, 8503–8507.

249 A. Kondoh, H. Yorimitsu and K. Oshima, *J. Am. Chem. Soc.*, 2007, **129**, 4099–4104.

250 W. Siebert, W. E. Davidsohn and M. C. Henry, *J. Organomet. Chem.*, 1968, **15**, 69–75.

251 O. Ekkert, G. Kehr, R. Fröhlich and G. Erker, *Chem. Commun.*, 2011, **47**, 10482–10484.

252 T. L. Breen and D. W. Stephan, *Organometallics*, 1997, **16**, 365–369.

253 F. H. Allen, *Acta Crystallogr. Sect. B Struct. Sci.*, 2002, **58**, 380–388.

254 J. P. Perdew, K. Burke and M. Ernzerhof, *Phys. Rev. Lett.*, 1996, **77**, 3865–3868.

255 R. F. W. Bader, *Acc. Chem. Res*, 1985, **18**, 9–15.

256 B. M. Barry, D. A. Dickie, L. J. Murphy, J. A. C. C. Clyburne and R. A. Kemp, *Inorg. Chem.*, 2013, **52**, 8312–8314.

257 T. Strassner, C. Rosorius, C. G. Daniliuc, R. Fröhlich, G. Kehr and G. Erker, *J. Organomet. Chem.*, 2013, **744**, 149–155.

258 B.-H. Xu, G. Kehr, R. Fröhlich, B. Wibbeling, B. Schirmer, S. Grimme and G. Erker, *Angew. Chem. Int. Ed.*, 2011, **50**, 7183–7186.

259 T. Wiegand, H. Eckert, O. Ekkert, R. Fröhlich, G. Kehr, G. Erker and S. Grimme, *J. Am. Chem. Soc.*, 2012, **134**, 4236–4249.

260 P. Feldhaus, B. Schirmer, B. Wibbeling, C. G. Daniliuc, R. Fröhlich, S. Grimme, G. Kehr and G. Erker, *Dalton Trans.*, 2012, **41**, 9135–9142.

261 R. Luck and R. H. Morris, *Inorg. Chem.*, 1984, **23**, 1489–1491.

262 A. J. Saunders, *Unpublished Results*, 2014.

263 A. J. Saunders and I. R. Crossley, *Dalton Trans.*, 2016, **45**, 2148–2155.

264 J. Vergnaud, M. Grellier, G. Bouhadir, L. Vendier, S. Sabo-Etienne and D. Bourissou, *Organometallics*, 2008, 1140–1146.

265 M. B. Ansell, University of Sussex, 2013.

266 G. W. Kramer and H. C. Brown, *J. Organomet. Chem.*, 1974, **73**, 1–15.

267 A. Stute, G. Kehr, R. Fröhlich and G. Erker, *Chem. Commun.*, 2011, **47**, 4288–4290.

268 Y. Hasegawa, G. Kehr, S. Ehrlich, S. Grimme, C. G. Daniliuc and G. Erker, *Chem. Sci.*, 2014, **5**, 797–803.

269 J. Heinicke and R. Kadyrov, *J. Organomet. Chem.*, 1996, **520**, 131–137.

270 J. E. Nycz, *Phosphorus. Sulfur. Silicon Relat. Elem.*, 2009, **184**, 2605–2612.

271 EU, EP1688424 (A1), *EP1688424 (A1)*, 2006.

272 S. G. Thangavelu, K. E. Hocker, S. R. Cooke and C. N. Muhoro, *J. Organomet. Chem.*, 2008, **693**, 562–566.

273 S. R. Flynn and D. F. Wass, *ACS Catal.*, 2013, **3**, 2574–2581.

274 L. J. Hounjet and D. W. Stephan, *Org. Process Res. Dev.*, 2014, **18**, 385–391.

275 J. Paradies, *Angew. Chem. Int. Ed.*, 2014, **53**, 3552–3557.

276 N. G. Connelly and W. E. Geiger, *Chem. Rev.*, 1996, **96**, 877–910.

277 R. Bertani, M. Biasiolo, K. Darini, R. A. Michelin, M. Mozzon, F. Visentin and L. Zanotto, *J. Organomet. Chem.*, 2002, **642**, 32–39.

278 J. A. Mcleverly and G. Wilkinson, *Inorg. Synth.*, 1966, **8**, 211–214.

279 Á. Álvarez, R. Macías, M. J. Fabra, F. J. Lahoz and L. A. Oro, *J. Am. Chem. Soc.*, 2008, **130**, 2148–2149.

280 R. V. Parish, *NMR, NQR, EPR, and Mössbauer Spectroscopy in Inorganic Chemistry*, E. Horwood, 1990.

281 H. L. M. van Gaal and F. L. A. van den Bekerom, *J. Organomet. Chem.*, 1977, **134**, 237–248.

282 D. Hanh Nguyen, N. Lassauque, L. Vendier, S. Mallet-Ladeira, C. Le Berre, P. Serp and P. Kalck, *Eur. J. Inorg. Chem.*, 2014, **2014**, 326–336.

283 J. Grimblot, J. P. Bonnelle, A. Mortreux and F. Petit, *Inorg. Chim. Acta*, 1979, **34**, 29–36.

284 K. Wang, M. E. Goldman, T. J. Emge and A. S. Goldman, *J. Organomet. Chem.*, 1996,

**518**, 55–68.

285 S. Serron, S. P. Nolan and K. G. Moloy, *Organometallics*, 1996, **15**, 4301–4306.

286 J. M. Kessler, J. H. Nelson, J. S. Frye, A. DeCian and J. Fischer, *Inorg. Chem.*, 1993, **32**, 1048–1052.

287 M. Bressan and A. Morvillo, *J. Organomet. Chem.*, 1989, **361**, 249–254.

288 V. K. Greenacre, M. B. Ansell, S. M. Roe and I. R. Crossley, *Eur. J. Inorg. Chem.*, 2014, **2**, 5053–5062.

289 M. B. Ansell, *JRA Report, University of Sussex*, 2012.

290 R. B. Bedford, A. F. Hill, C. Jones, A. J. P. White, D. J. Williams and J. D. E. T. Wilton-ely, *Organometallics*, 1998, **7333**, 4744–4753.

291 A. F. Hill, J. D. E. T. Wilton-Ely, C. Jones and R. B. Bedford, *Chem. Commun.*, 1999, **35**, 451–452.

292 R. B. Bedford, D. E. Hibbs, A. F. Hill, M. B. Hursthouse, K. M. A. Malik and C. Jones, *Chem. Commun.*, 1996, 1895–1896.

293 R. B. Bedford, A. F. Hill, C. Jones, A. J. P. White, D. J. Williams and J. D. E. T. Wilton-Ely, *Chem. Commun.*, 1997, **2**, 179–180.

294 R. B. Bedford, A. F. Hill, C. Jones, A. J. P. White and J. D. E. T. Wilton-Ely, *J. Chem. Soc. Dalton. Trans.*, 1997, 139–140.

295 A. F. Hill, A. J. P. White, D. J. Williams, J. D. E. T. Wilton-Ely and C. Jones, *Chem. Commun.*, 1998, 367–368.

296 A. F. Hill, C. Jones, A. J. P. White, J. Williams, J. D. E. T. Wilton-ely, D. J. Williams and J. D. E. T. Wilton-ely, *Dalton Trans.*, 1998, **2**, 1419–1420.

297 N. Trathen, V. K. Greenacre, I. R. Crossley and S. M. Roe, *Organometallics*, 2013, **32**, 2501–2504.

298 V. K. Greenacre, N. Trathen and I. R. Crossley, *Organometallics*, 2015, **34**, 2533–2542.

299 G. E. Maciel, J. W. McIver, N. S. Ostlund and J. A. Pople, *J. Am. Chem. Soc.*, 1970, **92**, 1–11.

300 B. Prabhakaran, N. Santhi and M. Emayavaramban, *Int. Lett. Chem. Phys. Astron.*, 2013, **8**, 53–66.

301 C. Hu, J. He, D. H. O'Brien and K. J. Irgolic, *J. Organomet. Chem.*, 1984, **268**, 31–38.

302 J. W. Wilt, F. G. Belmonte and P. A. Zieske, *J. Am. Chem. Soc.*, 1983, **105**, 5665–5675.

303 M. Fujio, M. Uchida, A. Okada, M. A. Alam, R. Fujiyama, H.-U. Siehl and Y. Tsuno, *Bull. Chem. Soc. Jpn.*, 2005, **78**, 1834–1842.

304 L. S. Zakharov, G. N. Molchanova, T. M. Shcherbina, P. V. Petrovskii and M. I. Kabachnik, *Russ. Chem. Bull.*, 1998, **47**, 1718–1724.

305 J. Heinicke, E. Nietzschmann and A. Tzschach, *J. Organomet. Chem.*, 1983, **243**, 1–8.

306 D. Blackwell, W. Galloway and D. Spring, *Synlett*, 2011, 2140–2144.

307 G. J. D. Peddle, *J. Organomet. Chem.*, 1967, **9**, 171–174.

308 M. G. Assadi, M. Mahkam and Z. Tajrezaiy, *Heteroat. Chem.*, 2007, **18**, 414–420.

309 J. W. Bruno, G. M. Smith, T. J. Marks, C. K. Fair, A. J. Schultz and J. M. Williams, *J. Am. Chem. Soc.*, 1986, **108**, 40–56.

310 J. G. Lee and D. S. Ha, *Synthesis*, 1988, **1988**, 318–319.

311 J. S. Figueroa and C. C. Cummins, *J. Am. Chem. Soc.*, 2004, **126**, 13916–13917.

312 M. S. Lupin and B. L. Shaw, *J. Chem. Soc. A*, 1968, **0**, 741–749.

313 P. Chutia, N. Kumari, M. Sharma, J. Woollins, Derek, A. M. Z. Slawin and D. Kumar Dutta, *Polyhedron*, 2004, **23**, 1657–1661.

314 A. Takaoka, A. Mendiratta and J. C. Peters, *Organometallics*, 2009, **28**, 3744–3753.

315 A. M. Arif, A. H. Cowley and S. Quashie, *J. Chem. Soc. Chem. Commun.*, 1985, 428.

316 A. H. Cowley, N. C. Norman and S. Quashie, *J. Am. Chem. Soc.*, 1984, **106**, 5007–5008.

317 D. Gudat, E. Niecke, W. Malisch, U. Hofmockel, S. Quashie, A. H. Cowley, A. M. Arif, B. Krebs and M. Dartmann, *J. Chem. Soc. Chem. Commun.*, 1985, 1687–1689.

318 A. M. Arif, A. H. Cowley, C. M. Nunn, S. Quashie, N. C. Norman and A. G. Orpen, *Organometallics*, 1989, **8**, 1878–1884.

319 M. Tafazzoli and H. P. Ebrahimi, *Phosphorus. Sulfur. Silicon Relat. Elem.*, 2011, **186**, 1491–1500.

320 J. B. Foresman and Æ. Frisch, *Exploring Chemistry with electronic structure methods (2nd ed.)*, 1996.

321 M. P. Waugh and R. J. Mawby, *J. Chem. Soc. Dalt. Trans*, 1996, 21–33.

322 X.-H. Wu, J. H. Liang, J.-L. Xia, S. Jin, G.-A. Yu and S. H. Liu, *Organometallics*, 2010, **29**, 1150–1156.

323 M. R. Torres, A. Vegas, A. Santos and J. Ros, *J. Organomet. Chem.*, 1986, **309**, 169–177.

324 M. R. Torres, A. Vegas and A. Santos, *J. Organomet. Chem.*, 1987, **326**, 413–421.

325 M. R. Torres, A. Santos, A. Perales and J. Ros, *J. Organomet. Chem.*, 1988, **353**, 221–228.

326 R. B. Bedford, D. E. Hibbs, A. F. Hill, M. B. Hursthouse, K. M. A. Malik and C. Jones, *Chem. Commun.*, 1996, **352**, 1895–1896.

327 G. Jia, F. W. Wan, R. C. Y. Yeung and H. P. Xia, *J. Organomet. Chem.*, 1997, **539**, 53–59.

328 A. Santos, J. Lopez, J. Montoya, P. Noheda, A. Romero and A. M. Echavarren, *Organometallics*, 1994, **13**, 3605–3615.

329 K. R. Grundy, *Inorg. Chim. Acta*, 1981, **53**, L225–L226.

330 S. Shinoda, H. Itagaki and Y. Saito, *J. Chem. Soc. Chem. Commun.*, 1985, 860–861.

331 S. M. Maddock, C. E. F. Rickard, W. R. Roper and L. J. Wright, *Organometallics*, 1996, **15**, 1793–1803.

332 M. R. Torres, A. Perales, H. Loumrhari and J. Ros, *J. Organomet. Chem.*, 1990, **384**, C61–C64.

333 M. Karplus, *J. Chem. Phys.*, 1959, **30**, 11–15.

334 E. S. F. Ma, S. J. Rettig and B. R. James, *Chem. Commun.*, 1999, **69**, 2463–2464.

335 G. M. Sheldrick, *Acta Crystallogr.*, 2008, **A64**, 112–122.

336 O. V. Dolomanov, L. J. Bourhis, R. J. Gildea, J. A. K. Howard and H. Puschmann, *J. Appl. Crystallogr.*, 2009, **42**, 339–341.

337 J. Cartwright, A. Harman and A. F. Hill, *J. Organomet. Chem.*, 1990, **396**, 31–34.

338 C. White, A. Yates, P. M. Maitlis and D. M. Heinekey, *Inorg. Synth.*, 1992, **29**, 228–234.

339 S. Jasimuddin and D. G. Thakurata, *Transit. Met. Chem.*, 2009, **34**, 937–942.

340 L. Vaska and E. M. Sloane, *J. Am. Chem. Soc.*, 1960, **82**, 1263–1263.

341 M. J. Frisch, *Gaussian 09, Revis. C.01*, 2009.

342 E. D. Glendening, C. R. Landis and F. Weinhold, *J. Comput. Chem.*, 2013, **34**, 1429–1437.

343 R. F. W. Bader, *Atoms in molecules: A Quantum Theory*, 1990.

344 T. Lu and F. Chen, *J. Comput. Chem.*, 2012, **33**, 580–592.

345 S. F. Sousa, P. A. Fernandes and M. J. Ramos, *J. Phys. Chem. A*, 2007, **111**, 10439–10452.

346 A. Romero, A. Vegas, A. Santos and A. M. Cuadro, *J. Chem. Soc. Dalton. Trans.*, 1987, 183–186.

347 M. P. García, A. M. López, M. A. Esteruelas, F. J. Lahoz and L. A. Oro, *J. Organomet. Chem.*, 1990, **388**, 365–377.

# 7. Appendices

## 7.1 Structural characterisation of *trans*-[Ru(dppe)$_2$(C≡CC$_6$H$_4$OMe)(C≡P)]

Crystal was grown by M. C. Leech by the vapour diffusion of hexane into a $CH_2Cl_2$ solution of *trans*-[Ru(dppe)$_2$(C≡CC$_6$H$_4$OMe)(C≡P)].[191]

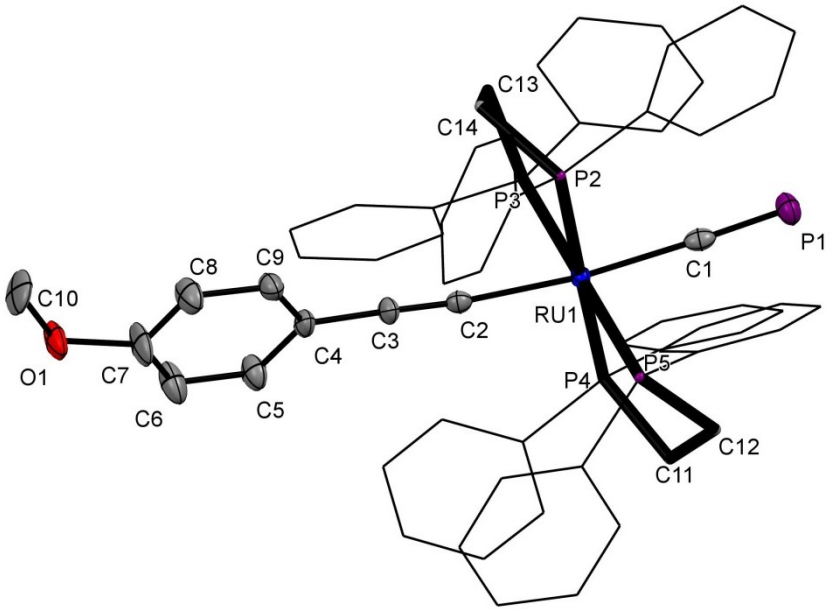


Structure of cyaphide (Ellipsoids set to 30%, and dppe bridges have been reduced for clarity).

Crystal data (CCDC 990881): $C_{62}H_{55}OP_5Ru$, Mw = 1071.98, triclinic, P -1 (no 2), a = 9.9951(7) Å, b = 11.9374(6) Å, c = 21.7684(13) Å, α = 85.981(5) °, β = 86.336(5), ° γ = 85.461(5) °. V = 2578.3(3) Å$^3$ . Z = 2. $D_c$ 1.381 Mg m$^{-3}$, μ(Cu-Kα) = 4.252 mm$^{-1}$, T = 173 K, 9644 independent reflections, full-matrix $F^2$ refinement. $R_1$ = 0.0458 $wR_2$ = 0.1365 on 7915 independent absorption corrected reflections F(000) = 1108.0 A yellow square crystal with dimensions 0.05, 0.1, 0.25 mm was used.

Selected bond distances (Å) and angles (°): C1–P1 1.544(4), Ru1–C1 2.065(4), Ru1–C2 2.084(3), C2–C3 1.205(5), Ru1–C1–P1 172.3(2), Ru1–C2–C3 174.4(3), C1–Ru1–C2 171.91(14), C2–C3–C4 178.5(4).

## 7.2 Academic papers published

Trathen, Nicola; Leech, Matthew C; Crossley, Ian R; Greenacre, Victoria K and Roe, S Mark

**Dalton Transactions, 2014, 43 (24) 9004-9007**

"*Synthesis and electronic structure of the first cyaphide-alkynyl complexes.*"

Greenacre, Victoria K; Ansell, Melvyn; Roe, S Mark and Crossley, Ian R

***Eur. J. Inorg. Chem.*, 2014 (29) 5053-5062**

"*Synthesis, structures and coordination chemistry of singly bridged phosphane-boranes with coordinately unsaturated platinum group metals.*"

Greenacre, Victoria K; Trathen, Nicola and Crossley, Ian R

***Organometallics*, 2015, 34, (11), 2533-2542**

"*Ruthenaphosphaalkenyls: synthesis, structures, and their conversion to* $\eta^2$ *phosphaalkene complexes*."

Greenacre, Victoria K and Crossley Ian R

***Inorganics,* 2016, *4*, (4), 30-40**

*"*$\eta^1$*:*$\eta^2$*-P-pyrazolylphosphaalkene Complexes of Ruthenium(0)"*

Greenacre, Victoria K; Day, Iain J and Crossley, Ian R

***Organometallics*, 2017, *36* (2), 435–442**

*"Hydrochlorination of Ruthenaphosphaalkenyls: Unexpectedly Facile Access to Alkylchlorohydrophosphane Complexes."*